

# U.S. ARMY FOREIGN SCIENCE AND TECHNOLOGY CENTER

AD 684596



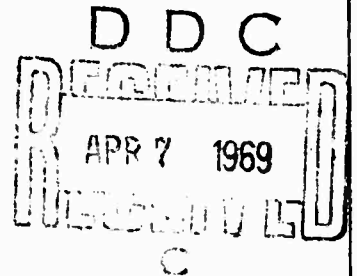
STRENGTH OF SHIPS SAILING IN ICE

COUNTRY: USSR

## TECHNICAL TRANSLATION

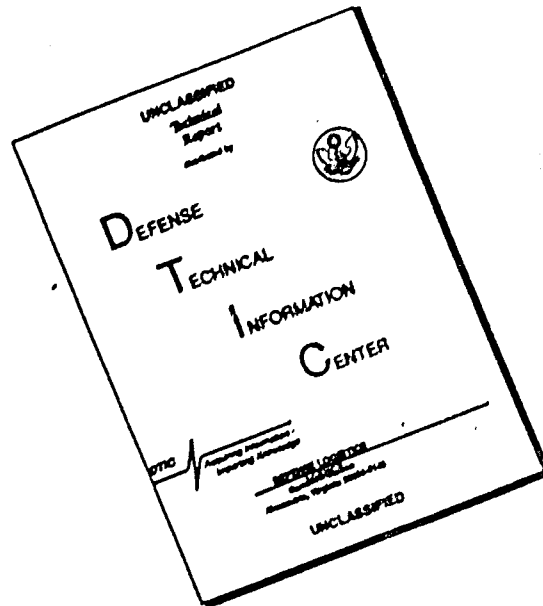
Distribution of this document is unlimited. It may be released to the Clearinghouse, Department of Commerce, for sale to the general public.

Reproduced by the  
CLEARINGHOUSE  
for Federal Scientific & Technical  
Information Springfield Va 22151



232

# DISCLAIMER NOTICE



THIS DOCUMENT IS BEST QUALITY AVAILABLE. THE COPY FURNISHED TO DTIC CONTAINED A SIGNIFICANT NUMBER OF PAGES WHICH DO NOT REPRODUCE LEGIBLY.

TECHNICAL TRANSLATION

FSTC-HT-23-96-68

STRENGTH OF SHIPS SAILING IN ICE

by

Yu. N. Popov, O. V. Faddeyev, D. Ye.  
Kheysin, A. A. Yakovlev

Source: STRENGTH OF SHIPS SAILING IN ICE  
Sudostroyeniye Publishing House  
Leningrad. 1967  
pp. 1-223  
USSR

Translated for FSTC by ACSI

This translation is a rendition of the original foreign text without any analytical or editorial comment. Statements or theories advocated or implied are those of the source and do not necessarily reflect the position or opinion of the US Army Foreign Science and Technology Center. This translation is published with a minimum of copy editing and graphics preparation in order to expedite the dissemination of information. Requests for additional copies of this document should be addressed to the Defense Documentation Center, Cameron Station, Alexandria, Virginia, ATTN: CSR-2

## STRENGTH OF SHIPS SAILING IN ICE

Yu. N. Popov, O. V. Faddeyev,  
D. Ye. Kheysin, A. A. Yakovlev

Sudostroyeniye Publishing House  
Leningrad, 1967

### Author's Foreword

Intensive construction of ships able to sail in ice and of icebreakers, as well as a systematic study of the ice qualities of ships sailing in ice, was begun in the Soviet Union in the 1930's in connection with the mastery of the Northern Sea Route and the expansion in the volume of shipping in frozen seas.

In 1933-1934, work was carried out under the leadership of A. K. Osmolovskiy [35] in which an attempt was made to evaluate the magnitude of ice stresses which damaged cargo ships in the Gulf of Finland. The evaluation was based on analysis of the ice damage. A simplified theory of the elastic-plastic bending of beams was used to determine the magnitude of the ice loads. However, this work did not relate the magnitude of the internal stresses to the physical and mechanical characteristics of ice, so results could not be used to study other frozen basins. Moreover, this method could not be used to determine the ice loads on icebreakers, which have a high safety factor.

Attempts to experimentally establish the nature and magnitude of ice loads by investigating strain on the hull joints in the icebreaking steamship Sadke were also a part of the prewar period. Experimental work was continued with the icebreaker Yermak and the icebreaking steamship Sibiryakov in 1935. Gugenberger strain gages, slide deflectometers, Geiger strain micrographs, and similar instruments were used to take the measurements. As tests proceeded, it became evident that none of these instruments were suitable for investigating dynamic ice pressures under natural conditions. Therefore, during the expedition aboard the icebreaker Yermak in 1936, a contact deflectometer, which made remote synchronous recording of deformations at various points on the hull possible, was used. Investigation of the ice strength of the icebreaker Krasin and of the icebreaking steamship Sadke was made during this same year. These tests established the dynamic, local nature of ice loads and approximate ice load magnitudes for various ships.\*

---

\* A. K. Osmolovskiy, F. V. Yakovskiy, V. V. Davydov, G. O. Taubin, L. M. Nogid, and others took part in the experiments.

Conventional Measurements of the Ice Qualities of Ships, by Yu.

A. Shimanskiy [53], published in 1938, was the first scientific work to make note of the improved method of making a comparative evaluation of the strength of ships, taking into consideration their operational experiences. For a long time this work served as the only guide for designers.

However, rational designing of icebreakers and ships which sail in the ice makes it necessary to know not only the relative (conditional) values, but also the true values of ice loads. A. I. Maslov devoted his work [32] to this problem. He was the first to consider the strength of the ice as one of the factors determining the magnitude of ice loads which act on a ship's hull.

V. V. Davydov [12, 13] investigated the process involved when a ship hits the ice, and proceeded from the general solution for eccentric impact from theoretical mechanics, taking into consideration the yielding of the side and the elastic strain of ice compression. However, V. V. Davydov did not consider such very important factors as crumpling of the ice edge, its deflection by the sloping side of the ship, and the effect of the adjoining water masses.

N. A. Zobotkin devoted his work [19] to investigating the dynamics of an icebreaker's movements when breaking ice by gaining momentum and hitting the ice.

In the early 1940's, V. I. Neganovyy, L. M. Nogid, and A. S. Fisher conducted important experimental and theoretical research on the process involved in breaking the ice cover and in the nature of the interaction between the icebreaker's hull and the ice. A little later, Yu. A. Shimanskiy and L. M. Nogid developed the basis of a theory for modeling ships' movements in ice.

I. V. Vinogradov's monograph [10], published in 1946, presents an analysis of icebreaker operations in ice and discusses the influence of a ship's basic elements on its ice qualities. In addition, interesting factual material concerning the design and construction of the hulls of cargo ships for ice use and of icebreaker hulls is assembled and generalized.

In 1954-1957, Yu. I. Voskresenskiy and A. Ya. Sukhorukov (under the direction of Yu. A. Shimanskiy) developed, and made more precise, the "conventional gage" method. Specifically, instead of the previously considered strip bending, the solution for a plate resting on a flexible foundation was used. At the same time, a determination of the reduced kinetic energy was made on a basis of the results of Yu. N. Popov's work [38]. He considered the spatial problem of the eccentric impact of two bodies (ship and ice), taking into consideration the adjoining water masses. Yu. I. Voskresenskiy investigated the behavior of hull structures in the plastic zone to evaluate the magnitude of real ice loads by measuring non-elastic strain.

N. F. Yershov [17] investigated the strength of the external plating in the elastic-plastic zone for ships sailing in the ice. In his consideration of ice compression for cargo ships, N. F. Yershov assumed that the ice cover was broken by shear stresses, and that cracks perpendicular to the side, are formed after which strips of ice break off.

M. K. Tarshis also made a theoretical determination of ice loads. He considered the process of eccentric impact of a ship against the ice and took the carrying capacity of the ice cover into consideration in his analysis of ice compression.

In 1959, L. M. Nogid's work [33], devoted to the determination of impact loads on a ship's hull when it contacts ice, was published. The author solved this problem by the energy method, taking into consideration the crumpling of the edge and buckling of the ice. L. M. Nogin took the indeterminacy of the solution, connected with the impossibility of making a strict selection of ice floe configuration and of the physical and mechanical properties of the ice, into consideration and introduced a correction factor in the final formulas used for the calculations. A shortcoming common to the work done by M. K. Tarshish and L. M. Nogid is that the ice edge crumples throughout its thickness, and this is not so under natural conditions.

The use of electrical resistance strain gages, which make possible synchronous recordings of readings of sensors installed at several points, must be considered a new stage in experimental research on the strength of hulls under ice conditions. Tests such as these were made aboard the diesel-electric ships Lena (1956), Baykal (1957), Dneproges (1958), Penzhina (1963), the motorships Bobruyskies (1964), Ivan Moskvina (1965), and the new icebreakers (1965-1966). Valuable data on the magnitude and nature of the application of dynamic ice loads were obtained from these tests.

The works of N. M. Shchapov [55], B. V. Zylev [20], K. N. Korzhavin [22, 23], and I. P. Butyagin [7], devoted to the study of the action of ice on hydraulic engineering structures, as well as the works of S. S. Golushkevich and P. A. Kuznetsov [27], which present the results of the investigation of the physical and mechanical properties of ice, and the strength characteristics of the ice cover, are of definite interest.

Scientific-research papers devoted to questions of the ice strength of cargo ships and icebreakers are rarely published abroad. The article by Simpson [58], which considers the selection of the bow lines for Wind class icebreakers can be included among known foreign papers. Jansson's paper [56] studied the physical and mechanical properties of ice, defined the forces which act on an icebreaker when it is breaking ice, and investigated how the ice cover is broken. This paper also considered questions concerned with overall and local strength of icebreakers. The paper by Milano [57], which appeared in 1962, is devoted to an investigation of the process of breaking ice with an icebreaker. It is of interest only from the standpoint of its use of experimental data on the

strength characteristics of ice and of empirical coefficients obtained from operational experience of American icebreakers.

This book, which is devoted to the ice strength of ships, takes the basic positions developed by the above-mentioned Soviet researchers into consideration. Widely used as well are the results of recent research, experimental work, and the voluminous factual material from the operational experience of cargo ships and icebreakers.

The book has two sections. The first section presents a method for determining ice loads acting on the hull of a ship sailing in ice. Determining the magnitudes of the ice loads is an extremely complex problem in view of the diversity of ice conditions. Therefore, a method for computing ice loads is taken which, while reflecting the physical sense of the phenomenon considered as a whole, allows the basic factors which stipulate it to be calculated. The proposed method is universal in the sense that it is used for merchant ships for any purpose and any ice class.

The second section presents the basis for, and choice of, calculation systems for determining internal stresses and strains arising in hull structures under the influence of ice loads, and makes recommendations for the rational designing of these structures.

The book, while calling the reader's attention to these questions, does not pretend to be an exhaustive treatment of all questions concerned with the ice strength of ships. Many of these questions need further development and clarification. The authors set themselves the modest task of helping designers more soundly approach the selection of calculated ice pressures and the determination of the strength dimensions of hull structures for ships sailing in ice.

We ask that remarks and comments concerning the book be sent to the following address: Leningrad, D-65, ul. Gogolya, 8, "Sudostroyeniye" Publishing House.

## SECTION ONE

### DETERMINING ICE LOADS WHICH ACT ON A SHIP'S HULL

#### CHAPTER I

### NAVIGATIONAL CONDITIONS AND AN ANALYSIS OF INTERACTION BETWEEN A SHIP'S HULL AND THE ICE

#### 1. Classification of Sea Ice and Its Physical and Mechanical Properties.

Ice conditions in the Arctic and other frozen seas are unstable because of the large variety of ices caused by such natural factors as wind, current, ice-freezing and-thawing temperature conditions, etc.

In the present classification system, sea ice is categorized according to age, formation, susceptibility to erosion, mobility and floe size. In addition, drift (mobile) ice, is categorized according to compactness.

The age classifications of ice are: new ice (candle ice, frazil, grease ice); black ice (pancake ice, glass ice); gray ice; white ice; one-year ice; young polar ice and old ice (Arctic pack), more than two years old which is characteristic of high Arctic latitudes.

Ice cover is subdivided by formation into level ice, rafted ice and hummocked ice. The degree of hummocking is rated on a five-point scale according to the area covered by hummocks relative to the entire visible area.

Ice erosion is characterized by external indications of thawing such as puddles on the ice, thawing, holes in the ice, lakes, etc. Ice erosion is rated on a five-point scale.

Sea ice is divided according to mobility into fast ice, the basic form of which is shore ice -- a compact ice cover connected to the shore and drift ice which moves as a result of wind and current action. Shore ice can extend up to several hundred kilometers.

Drift ice is subdivided into two basic groups according to size -- ice fields and open pack ice which are formed as a result of the erosion of shore ice and subsequent breaking up of the ice, accretion of ice and freezing of small floes.

The condition of drift ice is defined, aside from erosion, according

to compactness which is rated according to the ration of the floe area to the visible sector area (compactness is rated on a ten-point scale); and by compression which results from ice motion caused by wind and current. The degree of compression is rated on a three-point scale.

From what has been said, it follows that an extremely wide variety of ice conditions, difficult to breakdown into strict classifications, can be encountered on shipping lanes. Therefore, when determining ice loads which act on a ship's hull, basic factors which substantially influence the magnitude of these loads should be taken into consideration. These include, first of all, the ice thickness and strength as well as floe size.

Ice is a hard crystalline substance having a number of specific properties. The elastic and plastic properties of ice develop in various ways depending on age, presence of snow cover, duration of load application, state of stress, temperature, texture and chemical composition. Its physical and mechanical characteristics also change correspondingly.

The duration of load application exerts a substantial influence on ice behavior. Therefore, when studying the physical and mechanical properties of ice, the more characteristic forms of loads which occur when there is interaction between a ship's hull and ice should be considered at length. These should include impact loads acting on the hull when a ship is moving in ice and static loads when a ship is under ice compression.

When there is dynamic interaction between a ship's hull and ice, the latter behaves as a completely elastic, solid body [4, 29, 37]. Natural ice cover is a polycrystalline body and in directions parallel to its freezing surface, can be considered as isotropic. Some change in physical and mechanical characteristics resulting from a temperature drop and change in relationship between the crystal and liquid (brine) phases, is usually observed throughout the thickness. With this type of anisotropy, the ice cover can be considered as an isotropic plate [26], the elastic characteristics of which are described by some average modulus of normal elasticity  $E$  and Poisson's ratio  $\mu$ .

The most widespread methods for determining these characteristics at the present time are acoustic and seismic methods, as well as tests on small ice samples [4, 29]. The most reliable method is to determine the modulus of normal elasticity  $E$  by the magnitude of the resonant (critical) frequency of flexular waves propagated in the ice cover.

Calculations obtained by using data from these measurements have shown that the modulus of elasticity of solid Arctic, salty ice, changes with the range

$$E = (2 \text{ to } 5) \times 10^5 \text{ t/m}^2.$$

The magnitude of the modulus of elasticity determined in such a way, provides its average value for a large area. Heterogeneities in the

ice cover do not affect the magnitude  $E$  since their dimensions are practically incommensurable with the critical wavelength which reaches 100 to 200 m. Proceeding further from these considerations, an average value for the modulus of elasticity  $E = 3 \cdot 10^5 \text{ t/m}^2$  is assumed for dynamic conditions for solid, Arctic, salty ice. For fresh ice, the design value of the modulus should be increased to  $E = 5 \cdot 10^5 \text{ t/m}^2$ .

The magnitude of the modulus of shearing  $G$ , is also unstable, however, the ratio  $E/G$  remains practically constant in the majority of cases ( $E/G \approx 2.6$ ). Therefore, an average value of Poisson's ratio for ice  $\mu = 0.34$  can be obtained.

When there is prolonged load application, for example during ice compression, the plastic properties of ice appear. In this case, the relationship between the strain velocity and the magnitude of stress may be nonlinear. According to K. F. Voytkovskiy's data [11], a quadratic relationship exists between the established velocity of deflection of ice beams and the magnitude of a design load. Deflection of floating ice slabs is relatively well-described by a linear model, viscous elastic body [50]. In this case, the modulus of constant resistance should be taken as a computed value. As some academic calculations and experimental data show, the magnitude of this modulus is approximately eight to nine times smaller than the dynamic modulus. In the future, when there is prolonged load action,  $E = 4 \times 10^4 \text{ t/m}^2$  will be taken as the computed value of the modulus of elasticity for sea ice.

The maximum value for loads acting on a ship's hull in ice cannot exceed the magnitude of stresses which break ice covers. Therefore, when determining ice loads, it is necessary to know the magnitudes of the ice's ultimate local crushing (breaking) strength  $\sigma_c$ , bending strength  $\sigma_b$  and shearing strength  $\tau_s$ .

According to K. N. Korzhavin's data [22], the magnitude of the ultimate local crushing strength of ice is  $\sigma_c = (2.5 \text{ to } 2.7) \sigma_{c,un}$ , where  $\sigma_{c,un}$  is the ultimate strength of ice against uniaxial compression, determined on samples.

With static loading (ice compression), a magnitude of  $\sigma_{c,un}$  within the range  $\sigma_{c,u} = 50 \text{ to } 100 \text{ t/m}^2$  can be assumed, then  $\sigma_c = 125^c \text{ to } 270 \text{ t/m}^2$ .

When there is static load action, it is recommended that  $\sigma_c = 200 \text{ t/m}^2$  be assumed as an average value for the ultimate crushing strength of ice for ice-strengthened classes of cargo ships. This corresponds to average strength Arctic ices. For icebreakers, a value near to the upper limit is assumed as the design value:  $\sigma_c = 250 \text{ t/m}^2$ . This corresponds to solid Arctic fresh ice and shore ice.

When there is dynamic load action, the magnitude of ice crushing stresses is considerably greater than the static value, reaching 800 to 1000  $\text{t/m}^2$  and greater. In essence, pressure in the contact zone between

a ship's hull and ice cannot be identified with the ultimate crushing strength of ice  $\sigma_c$ . In this case, an effective value for  $\sigma_c$ , depending primarily on the velocity of the collision, should be introduced.

A method for determining the magnitude of contact stresses when a ship strikes ice is described in detail below (see number 6). In order to calculate these stresses, the design values for  $\sigma_{c2}$  which can be assumed as 500 to 600 t/m<sup>2</sup> for icebreakers and 300 to 400 t/m<sup>2</sup> for ice cargo ships, must be known. We note that values for  $\sigma_c$  greater than 600 t/m<sup>2</sup> comprise less than 5% of the total number of feasible measurements for the crushing strength of Arctic seas [37].

According to experimental data, the magnitude of the ultimate bending strength of ice  $\sigma_b$  depends only slightly on the period of load application [21, 23]. However, the magnitude of  $\sigma_b$  changes within a wide range as a result of the salinity of ice and its temperature. Thus, according to B. P. Veyberg's data [9],  $\sigma_b = (44 \text{ to } 162) \text{ t/m}^2$  for fresh ice.

The bending strength of Arctic, salty ice is considerably less and varies in range from 30 to 120 t/m<sup>2</sup>.

V. I. Kashtelyan [21] notes that the reason for such wide variation in the magnitude of  $\sigma_b$  is evidently, not only that there are differences in ice properties but also differences in experimental methods. In this work, near maximum values for  $\sigma_b$  are assumed as design values:  $\sigma_b = 100 \text{ t/m}^2$  for salty ice and  $\sigma_b = 125 \text{ t/m}^2$  for fresh ice. These values for  $\sigma_b$  are assumed as design values in the case of a ship's striking ice as well as a ship under ice compression.

The ultimate shearing strength of ice is considerably less than its ultimate bending and crushing strengths. According to data of K. N. Korzhavin [22], this magnitude does not exceed  $\tau_s = 60 \text{ t/m}^2$  for fresh ice. The magnitude of  $\tau_s$  is considerably less for salty, sea ice and in the future, will be assumed as 30 t/m<sup>2</sup>.

The strength of ice depends on its composition, temperature, age, porosity, etc., and changes within a rather wide range. Under natural conditions, sectors of ice with great strength exist side by side with sectors having extremely little strength. In the future, a near maximum value of ice strength will be assumed for calculations. Accordingly, the density of fresh ice is assumed as  $\gamma = \rho g = 0.91 \text{ to } 0.92 \text{ t/m}^3$ , and the density of salty ice in wintertime,  $\gamma = 0.87 \text{ to } 0.90 \text{ t/m}^3$  [37]. For Arctic, salty ice in the summertime,  $\gamma = 0.85 \text{ to } 0.87 \text{ t/m}^3$ .

In conclusion, we shall present some data concerning the coefficient of friction of ice against steel.

According to V. I. Arnol'd-Alyab'yev's data [1], the coefficient of static friction of ice against smooth steel varies within the range  $f_f = 0.15 \text{ to } 0.20$  and the coefficient of kinetic friction  $f_k = 0.10 \text{ to } 0.15$ . The coefficient of static friction depends on the magnitude of the load. When the specific pressure increases to 1.3 t/m<sup>2</sup>, this coefficient

becomes equal to the coefficient of kinetic friction and does not vary with any subsequent load increases. The coefficient of friction depends substantially on the condition of the ship's plating: it increases to  $f_f = 0.35$  to  $0.40$  for painted steel. Inasmuch as side plating in the effective waterline area is practically always glazed with ice and pressure is greater than  $1.3 \text{ t/m}^2$  as a rule, we shall assume  $f_f = 0.15$  as the value of the coefficient of friction in the future.

Table 1 presents the values of physical and mechanical characteristics of ice which will be assumed as initial design magnitudes in future discussion of the material.

Table 1

Physical and mechanical characteristics of ice.

1 Виды льда	2 Характер приложения нагрузки	3 Характеристики льда				
		4 $E, \frac{\text{t}}{\text{m}^2}$	5 $\sigma_c, \frac{\text{t}}{\text{m}^2}$	6 $\sigma_p, \frac{\text{t}}{\text{m}^2}$	7 $\tau_p, \frac{\text{t}}{\text{m}^2}$	$\mu$
8 Арктический Соленый	9 Сжатие во льдах	$4 \cdot 10^6$	125-270	90-100	-30	0,34
	10 Удар о льдину	$3 \cdot 10^6$	350-600	90-100	—	0,34
11 Пресный	12 Сжатие во льдах	$6 \cdot 10^6$	—	120-130	60	0,34
	13 Удар о льдину	$5 \cdot 10^6$	—	120-130	—	0,34

1-types of ice; 2-nature of load application; 3-ice characteristics; 4- $E \text{ t/m}^2$ ; 5- $\sigma_c, \text{tm}^2$ ; 6- $\sigma_p, \text{t/m}^2$ ; 7- $\tau_p, \text{t/m}^2$ ; 8-Arctic salty; 9-compressed in ice; 10-impact against floe; 11-fresh; 12-compressed in ice; 13-impact against floe.

## 2. Sailing Conditions for Ships in Ice.

Characteristic sailing conditions for ships in ice are:

- continuous movement in compact ice;
- breaking ice by charging;
- movement in a lane behind an icebreaker;
- movement in drift ice;
- compressed in ice.

Continuous movement in compact ice. This is a characteristic condition for icebreakers and partially, for ships active in sailing in ice. The stability of continuous movement for each specific ship depends on the thickness and strength of the ice cover. During continuous movement, the ship's hull contacts the ice and due to the icebreaker form of bow lines, crushes the ice by bending which results from vertical stresses.

Absence of ice damages to ships' hulls during continuous movement in compact ice, testifies to the fact that the ice loads are relatively small and cannot be used as design loads when designing hull structures.

Breaking ice by charging. Breaking ice by charging is a characteristic operating condition for an icebreaker when it is unable to pass through the ice with continuous movement. The greatest ice loads occur when an icebreaker which has hit the ice does not fracture it and only local crushing of the edge of the ice field occurs. With all other conditions equal, the magnitude of ice loads will depend on the speed of the icebreaker at the moment it hits the ice.

Movement in a lane behind an icebreaker. This is one of the basic conditions for ships being led by an icebreaker. In this situation the ship's hull is subjected to impacts against broken-off pieces of ice floes which fill the lane as well as against the sides of the lane. In the latter case, ice stresses will be great. This is confirmed by the damage suffered by ships in contact with the edge of an unbroken ice field.

Ship's movement in drift ice. This sailing condition is characteristic for icebreakers and all categories of ice ships. When ships are sailing in large fields of drift ice, ice loads will be similar to those which occur when a ship hits an ice field. Sailing in open pack ice is accompanied by periodic impacts of the hull against individual floes. The magnitude of ice loads in this case, will depend on the floe size, the ice thickness and strength and the ship's speed.

Ship under ice compression. A ship can undergo ice compression during which the midsection of a ship having a relatively small slope to its side or a vertical side, experiences considerable pressure from the ice. Icebreakers and ice cargo ships may be subjected to compression. The intensity of compressive stresses depends on the slope of the ship's side, as well as on the thickness and strength characteristics of the ice.

Thus, when calculating design ice loads which act on a hull, the following cases of interaction between a ship and ice which are characteristic for all ships sailing in ice, should be considered:

- ship striking an individual ice floe;
- ship striking the edge of an ice field (impact when breaking ice by charging and contact with edge of lane);
- ship under ice compression.

The magnitude of ice loads in each of the cases considered will depend on the ship's speed, displacement and hull lines and the physical and mechanical characteristics of the ice. Moreover, the ice load occurring as a result of a ship's striking ice, should be used as the design load for the bow and stern and the load resulting from ice compression on a ship, should be used for the midsection.

### 3. Interaction between a Ship's Hull and the Ice.

Considerable stresses causing straining and failure of ice, can occur in the contact zone between a ship's side and ice. The magnitude of these stresses varies substantially for dynamic and static conditions. The interaction between a ship's hull and ice is investigated in this work on the basis of the general theory of tangency of two solid bodies [25]. The surface hardness of ice is considerably less than the surface hardness of steel. Therefore, the shell plating can be considered to be a smooth, absolutely rigid surface when it contacts ice. The surface of the ice's edge is usually uneven. These irregularities can be broken down into three groups according to size.

Small projections of a floe's edge, on the order of several hundred centimeters high, come into contact with the ship's side first. Thus, at first, the ship's side comes into contact with the ice in separate sectors. The total area of these sectors, the so-called contour area  $F_c$ , is considerably smaller than area  $F_n$  which is defined as the locus of all of the possible contact spots. The average pressure on the side  $P_{av}$  is considerably less than the contour pressure  $p_c$  and in this case, cannot be considered as the design pressure for external shell plates.

In the second stage, relatively large irregularities on the order of one to two frame spacings, come into contact. In this case, the edge crumples over the entire contact area, i.e.,  $F_c = F_n$  and the average pressure equals the contour pressure and is the design pressure for the shell plating.

In the third stage, after all of the irregularities of the edge have been crushed, the area of the contact zone depends primarily on the general outline of the ice's edge in the plane and the shape of the ship's waterline in the contact area. The total contact stresses proportional to this area are the design stresses for the side framing, transverse bulkheads, decks and platforms. These stresses, besides causing local failure of the edge, induce a general strain in the ice cover. The ice can also fail from bending or shearing or by the ice plate losing its stability before the contact pressure reaches its maximum.

Thus, either the value of the stresses which fracture ice covers or an individual floe, or the maximum contact pressure value, if general failure of the ice does not occur, should be assumed as design ice loads.

When analyzing the process of a collision of a ship with ice, one can proceed from the proposition concerning the equality of contact pressures to the local ultimate crushing strength of ice as the majority of researchers, and specifically L. M. Nogid [33], do. An effective value for  $\sigma_c$ , depending primarily on the speed of collision, should be assumed for high speeds of interaction. When there is short-term interaction between a ship and ice, the magnitude of the ultimate crushing strength of the ice is not maximum and can be considerably exceeded [15].

As is known, if a solid body penetrates a crystalline substance upon impact, movement will continue until the contact pressure  $p$  exceeds the ultimate pressure  $p_b$ , necessary to fracture that substance

$$p \geq p_b = k\rho\epsilon_f,$$

where  $\rho$  is compactness;

$\epsilon_f$  is specific failure energy;

$k$  is a numeral coefficient, depending on the physical and mechanical characteristics of the failing substance.

The penetrating body stops when  $p = p_b$ . The magnitude of  $p_b$  can be assumed to equal the local ultimate crushing strength of the ice, in the first approximation.

The magnitude of specific failure energy can be written in the form  $\epsilon_f = a_{cr}^2/2$  where  $a_{cr}$  is the critical penetration speed. Consequently, fracturing will have already ceased before the body comes to a complete stop, at the moment when the penetration speed becomes equal to the critical penetration speed

$$a_{cr} = \sqrt{\frac{2\sigma_c}{k\rho}}.$$

A moving body with mass  $M$  maintains a certain momentum  $Ma_{cr}$  before coming to a stop. This will be transmitted to the ice in the form of elastic strains. Thus, an impact with penetration cannot be considered as a completely plastic impact. The last phase of the impact is always the elastic phase. Therefore, the coefficient of restitution must differ from zero somewhat. When there is an elastic impact, pressure in the contact zone is determined by the formula

$$p = \rho S_s \dot{\zeta}^s, \quad (3.1)$$

where  $\rho$  is the ice compactness;

$S_s$  is the speed of sound in the ice;

$\dot{\zeta}^s$  is the speed of surface displacement (side of the ship) in the zone of contact with the ice.

At the initial moment of the elastic phase of the impact

$$\sigma_c = \rho S_s a_{cr},$$

from which, considering that  $S_s = \sqrt{\frac{E}{\rho}}$ ,

$$a_{cr} = \frac{\sigma_c}{\sqrt{E\rho}}, \quad k = \frac{2E}{\sigma_c},$$

where  $E$  is the modulus of normal ice elasticity.

Giving heed to all of the aforesaid, the contact pressure magnitude can be found from a physically tenable collision model. Actual observations show that the impact of a ship against the ice's edge causes crushing to a considerable depth (up to several tens of centimeters) and fractured ice presses up to the surface in the form of finely broken crumbs.

The pressing-up of the broken ice in the contact zone, makes it possible to assume that some interstitial layer of finite thickness, formed between the absolutely rigid compactness of the side and the unfractured mass of crystalline ice, exists. Three sequentially disposed zones can be isolated by analyzing the structure of this layer.

In solid bodies, failure is associated with the formation of discontinuity surfaces along one side of which the material is still an elastic solid body and along the other side, it can be considered as a viscous fluid. A similar situation evidently takes place when a ship hits the ice. A discontinuity surface moves in front of the compactness of the side of the ship, penetrating the ice. All other conditions being equal, (mass of the impacting body, its speed, etc.), the distance between these surfaces depends on the physical and mechanical properties of the ice. The thickness of the transition zone is small [29]. Therefore, in the future, it can be considered as a two-dimensional bounding surface. Elastic compression can be disregarded in the plastic phase of impact; then, particles disposed on the bounding surface will not move along the normal to the surface. As a second boundary condition, the tangential speed component can be assumed to equal zero.

A zone filled with fractured and melted ice crystals follows this surface and can be interpreted as a viscous fluid layer. The thickness of this layer  $\epsilon$  must be sufficiently large for the fractured material to press up to the sides. The magnitude of the coefficient of internal friction  $\eta$  in the layer, depends on the ice composition, structure and temperature. This coefficient can be considered as a physical and mechanical constant, subject to experimental determination.

Complex friction processes develop in the layer directly adjoining the side of the ship. The structure of this layer depends on the direction of impact. When there is a central impact, friction between the side and the broken layer can be considered "dry." When there is a glancing impact, the boundary layer is in a melted state, primarily because the work of the driving forces overcoming the friction is converted to heat (self-lubrication of ice, see [48]). This layer can also be considered as a two-dimensional bounding surface on which the normal velocity component of the ice particles will equal the velocity of displacement of the side  $\zeta$  in the direction of the normal, regardless of the presence or absence of frictional forces. The second boundary condition will be different for glancing and central impacts. With a glancing impact and formation of a fluid layer, the coefficient of friction is small ( $f_f = 0.03$  to  $0.06$ , [5]). In this case, it can be assumed that ice particles

will not adhere to the surface of the side and consequently, shear stress will equal zero.

When there is a central impact without sliding, a fluid layer does not form. This provides basis for assuming the tangential speed component equal to zero.

The process of pressing out the fractured ice can be mathematically described by considering the movement of the interstitial viscous layer, taking into account the above-established conditions on bounding surfaces. For this, the problem of convergence of two surfaces with expulsion of a thin layer of viscous fluid from the space between them, one of the surfaces being a discontinuity surface, should be solved. At each considered moment of time, the velocity of their convergence must be assumed to be constant and equal to  $\zeta$ .

Reynolds has already obtained the solution to an analogous problem. For simplicity, we shall also consider a two dimensional problem, i.e., we shall assume that motion occurs only in a plane normal to the surface of the side at the point of impact (Figure 1).

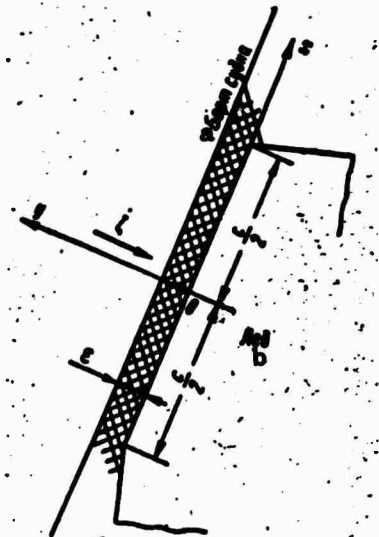


Figure 1. Formation of interstitial layer when a ship's side contacts ice. a-ship's side; b-ice (remainder as is).

In the first approximation, the thickness of the interstitial layer  $\epsilon$  may be considered as being independent of coordinate  $x$ . Motion of the particles in this layer is symmetric relative to axis  $Oy$ , and in view of the small thickness of the layer, is basically directed along axis  $Ox$ , i. e.,  $v_x \gg v_y$ . In this case, Reynold's generalized equation for a thin layer can be used [44]:

$$\frac{\partial^2 v_x}{\partial y^2} = \frac{1}{\eta} \cdot \frac{\partial p}{\partial x} + \frac{\rho}{\eta} w_{av}, \quad (3.2)$$

$$\frac{\partial p}{\partial y} = 0$$

and the discontinuity equation

$$\frac{\partial v_x}{\partial x} + \frac{\partial v_y}{\partial y} = 0.$$

Here,  $w_{av}$  is the average acceleration throughout the thickness of the layer,

$$w_{av} = \frac{1}{\epsilon} \int_0^{\epsilon} (v_x \frac{\partial v_x}{\partial y} + v_y \frac{\partial v_y}{\partial x}) dy.$$

The solution of these equations for conditions corresponding to the adhesion of particles to both bounding surfaces is known [44]. On surface  $y = 0$   $v_x = v_y = 0$ , and on the surface of the ship's side  $y = \epsilon$   $v_x = 0$  and  $v_y = -\dot{\zeta} \cdot y$ . This corresponds to an impact against ice without shearing strain. In this case, pressure in the layer will be

$$p = \frac{6}{\epsilon^3} \zeta \left( \frac{c^3}{4} - x^3 \right) (\eta + 0.2\rho\epsilon\dot{\zeta}), \quad (3.3)$$

where  $c$  is the width of the crushing zone.

In this expression, the term  $0.2 \rho \epsilon \dot{\zeta}$  takes the quadratic inertial terms into consideration and does not depend on viscosity. When the values of  $\epsilon$  are small, the effect of this term on the final result is small. Therefore, it can be assumed

$$p = \frac{6\eta\zeta}{\epsilon^3} \left( \frac{c^3}{4} - x^3 \right). \quad (3.4)$$

If the fluid lubricating layer is taken into consideration, Reynold's generalized equation should be solved, giving attention to the zero value of shear stresses along the bounding surface  $y = \epsilon$ . Then, pressure in the layer

$$p = \frac{3}{2} \cdot \frac{\zeta}{\epsilon^3} (\eta + 0.3\rho\epsilon\dot{\zeta}) \times \left( \frac{c^3}{4} - x^3 \right).$$

Without considering the quadratic term

$$p = \frac{3}{2} \cdot \frac{\eta}{\epsilon^3} \zeta \left( \frac{c^3}{4} - x^3 \right). \quad (3.5)$$

Comparing (3.5) with (3.4), we note that the fluid lubricating layer reduces the contact pressure four times, In general, it can be assumed

$$p = k\zeta\left(\frac{c^2}{4} - x^2\right), \quad (3.6)$$

where  $k$  is a numerical coefficient determined by experimentation.

Integrating (3.6) along coordinate  $x$  in a range from  $-\frac{c}{2}$  to  $\frac{c}{2}$ , we obtain an expression for the intensity of the linear ice load, set to the unit of contact zone length,

$$q = \frac{k}{6}\zeta c^3. \quad (3.7)$$

The width of the crushing zone  $c$  depends on the depth to which the edge crushes  $\zeta$  and the shape of the floe cross section (Figure 2). Inasmuch as the second and third stages of impact are being considered, when small protrusions are already crushed, the outline of the floe edge can be considered to be formed by straight lines. In a general case, the generating line of the floe's lateral face can be vertically inclined at an arbitrary angle  $\alpha$ .

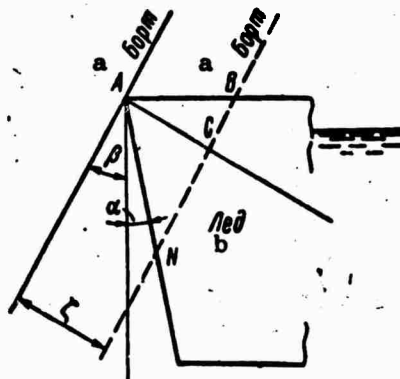


Figure 2. Ship's side crushing the ice's edge. a-ship's side; b-ice.

As follows from Figure 2,

$$c = BN = \frac{\zeta \cos \alpha}{\cos \beta \sin(\alpha + \beta)}, \quad (3.8)$$

where  $\beta$  is the vertical slope of the ship's side.

Sometimes, crushing can occur throughout the entire thickness of the ice's edge  $h$ . The maximum depth of crushing in this situation is determined by the formula

$$\zeta_{\max} = h \frac{\sin(\alpha + \beta)}{\cos \alpha}.$$

Observations show that crushing over the entire thickness of the ice, practically never occurs. The magnitude of angle  $\alpha$  is usually small and in future calculations will be disregarded. Contact of a ship's side over the entire thickness of the ice can take place when there is a glancing impact of the midsection of a ship having vertical sides against the ice. However, such a case of impact is not computed for this area; therefore, in the future, we shall consider crushing of the edge through only part of the floe's thickness, not examining the condition  $\zeta < \zeta_{\max}$ .

Setting value  $c$ , determined by (3.8) in expression (3.7), and assuming angle  $\alpha = 0$ , we obtain a formula for computing the intensity of a linear ice load

$$q = \frac{k}{6} \frac{\zeta^3}{\sin^3 \beta \cos^3 \beta} \quad (3.9)$$

Coefficient  $k$ , depending on thickness  $\epsilon$  and viscosity  $\eta$  of the interstitial layer is entered in expression (3.6) and (3.9). The numerical values of  $\eta$  and  $\epsilon$  can be determined by actual experiment results. In doing this, it is necessary to measure the average values of these parameters for various ice types corresponding to the characteristic ice conditions for the given navigation area. Until such experiments are formulated, use of the obtained dependencies for estimating contact pressure will have a conditional nature.

Expressions (3.6) and (3.9) are valid when the velocity of interaction of the ship's side with the ice is greater than the critical speed, i.e.,  $\zeta \geq \alpha_{cr}$ . With lesser velocities, contact pressures equal the ultimate crushing strength of ice. The velocity of penetration of the ship's side into the edge of the ice cannot exceed  $v_0 l_1$ , where  $v_0$  is the ship's forward motion and  $l_1$  is the cosine of the angle between the normal to the side at the point of impact and the direction of the ship's movement. The value  $\alpha_{cr}$  is within the range 0.8 to 1.0 m/sec., and the magnitude  $l_1$  usually does not exceed 0.2 to 0.3. Thus, for actual velocity of ships in ice, a simplified hypothesis, assuming contact pressures to equal the effective value of the ice's ultimate crushing strength, will be used in most cases. (See 1.).

It should be noted that determination of the design magnitude of total contact stresses depends little on the nature of the statements accepted concerning the magnitude of contact pressures. Actually, regardless of the impact nature, the total contact stress  $P$  is determined from the condition

$$M_{red} \Delta v = Pt,$$

where  $M_{red}$  - is the ship's reduced mass;  
 $\Delta v$  - is the loss of velocity in the direction of impact;  
 $t$  - is collision time.

Any hypothesis which reduces to a physically probable collision time, makes it possible to determine the total stress value  $P$  with a sufficient degree of accuracy.

#### 4. Nature of Ice Cover Strains.

In the process of interaction between a ship's hull and ice, a general strain occurs in the ice cover, determined by the magnitude and nature of distribution of contact stresses. If the ice field fails at this time, the maximum magnitude of contact stress acting on the hull will equal the force fracturing the ice cover. If the ice cover does not fail, the magnitude of the contact stress is determined not only by local crushing of the edge, but also by bending of the ice.

The ice cover's state of stress depends on the vertical slope of the ship's side  $\beta$ . If the ship's side is vertical, contact stresses act in the plane of the ice cover. In this case, the ice plate's plane state of stress should be considered. If the side is inclined, the vertical component of contact stress,  $P_z = P \sin\beta$ , and the horizontal component,  $P_x = P \cos\beta$ , cause unsymmetrical<sup>z</sup> bending of the ice cover (Figure 3).

Ice cover is usually considered as a plate resting on a hydraulic-type flexible foundation when computing bending of an ice cover. When doing this, the strains and stresses in the ice cover are determined by applying the theory for bending of thin plates, i.e., the following equation is considered

$$D\nabla^4 w + \rho g w = q + q^*, \quad (4.1)$$

where  $D$  - is the flexural stiffness of the plate;

$\rho g$  - is the density of water;

$w(x,y)$  - is deflection of the plate;

$q(x,y)$  - is an external load, directed along a normal to the ice surface;

$q^*(x,y)$  - is the effective load caused by axial forces  $T_x$  and  $T_y$  and tangential forces  $S_{xy} = S_{yx}$ , acting on the middle of<sup>y</sup> the plate's surface:

$$q^* = - \left( T_x \frac{\partial^2 w}{\partial x^2} + 2S_{xy} \frac{\partial^2 w}{\partial x \partial y} + T_y \frac{\partial^2 w}{\partial y^2} \right). \quad (4.2)$$

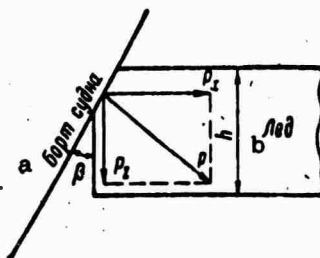


Figure 3. Resolution of contact stresses in vertical and horizontal components. a-ship's side; b-ice.

When determining flexural stiffness of an ice plate  $D$ , reduced values of the physical and mechanical characteristics of ice, defined as integrals, according to the thickness of the plate  $h$  [26, 30], should be assumed as design values. For ice in which Poisson's ratio  $\mu$  changes little, the usual formula is valid

$$D = \frac{Eh^3}{12(1-\mu^2)}$$

where  $E$  - is the reduced value of the modulus of elasticity.

Equation (4.1) is only valid when there are average (moderate) velocities of interaction. If the external load action time is great, the ice plate should be considered as a viscous-elastic plate. If the load action time is small, for example during an impact, it is necessary to take the inertia of the ice mass and the hydrodynamic water pressure field into consideration.

When there is prolonged external load action, ice manifests its plastic properties to a significant degree and deflection of the ice slab increases with the passage of time, the velocity of the deflection increases, being a linear function of the magnitude of force  $P$  [50]. At the same time, the magnitude of ultimate fracturing stress depends little on time in actual cases of interaction of a ship's hull and ice. As V. I. Kashtelyan [21] showed, the ultimate concentrated, vertical stress applied to the edge of a semi-infinite ice plate is determined by the formula

$$P_{\text{frac}} = 0.52 \sigma_b h^2, \quad (4.3)$$

where  $\sigma_b$  - is the ice's ultimate bending strength;  
 $h$  - is the thickness of the ice cover.

Actually, contact stress is applied for some finite length  $b$  along the edge of the ice cover. When  $b \leq (5 \text{ to } 7) h$ , the total fracturing stress is practically independent of the length to which the load is applied. In connection with this, ice fracturing stress can be written in the following form for hull areas where the length of the contact zone between the ship and ice is relatively small (areas outside of the parallel middle body):

$$P_{\text{frac}} = \int_{(b)} q db.$$

When there is brief ice load action, when a ship's extremities hit the ice for example, calculation of the inertial mass forces of ship and ice, as well as the hydrodynamic pressure of the water, become quite significant. In this case, the equation for dynamic bending of a plate and the Laplace equation for liquid velocity potential must be solved concurrently. Moreover, it is necessary to satisfy consistency of conditions

at the surface where ice and water separate and at the bottom of the water expanse, and the boundary conditions at the edge of the plate.

The exact solution to this problem for concentrated stress which depends arbitrarily on the time, was obtained in work [49]. Elastic deflection of a plate is determined by the formula  $\omega = \omega_{st} - \omega_d$ , where the dynamic component of deflection  $\omega_d \rightarrow 0$  for sufficiently long actions and  $\omega_d \rightarrow \omega_{st}$  when  $t \rightarrow 0$ . Thus, when there is dynamic load action, the flexural yielding of a floating ice plate decreases.

As actual observations show, the shapes of floes broken off by a hull are practically the same as those occurring when a semi-infinite floating plate which is loaded with a concentrated stress, or a stress on some length of its edge, fails. When a ship travels at low speed in ice or when there is ice compression, the sizes of broken-off segments will correspond to the sizes of segments computed by the theory of plastic bending of a plate on a flexible foundation [see equation (4.1)]. Observations show that when a ship is traveling at high speed and ice loads take on a dynamic nature, the size of these segments is considerably reduced. This gives evidence of a change in the general nature of ice cover strain.

Maximum contact stresses during impact will be attained if the ice plate does not fail, i.e., when its thickness and strength are adequate. At the same time, deflection of the plate will be small in comparison with the crushing of the edge because of the dynamic nature of the load on one hand, and the high degree of rigidity of the plate on the other. Thus, when determining the magnitude of design impact loads, erring on the side of providing a margin of safety, may not take into consideration the flexural yielding of the ice plate by assuming the plate's thickness to be extremely great.

When there is ice compression on ships with vertical sides and a parallel middle body, strain in an ice cover loaded with horizontal stresses should be considered as being distributed along the edge of the ice plate. Observations bear this out. A picture of relatively thin ice failing in this case, gives witness to the loss of the ice plate's stability.

For elastic plates lying on a flexible foundation, Euler's load for a concentrated force is

$$P_{EU} = 4.23 \sqrt[4]{\gamma D^3} \quad (4.4)$$

and for a load distributed along a considerable length of the edge,

$$q_{EU} = \sqrt{\gamma D}, \quad (4.5)$$

where  $\gamma$  - is the density of water;  
 $D$  - is flexural stiffness of the ice plate.

For prolonged loads, which include ice compression loads, the plastic properties of ice should be taken into consideration. As indicated above, the relationship between strain velocity and ice stresses is non-linear. In this case, the relation  $P_{cr}/P_{EU}$  depends on the effective period of the load [51]. If it is short, the magnitude of the critical stress  $P_{cr}$  equals Euler's stress. For prolonged ice load action, the ratio  $P_{cr}/P_{EU}$  decreases. Subsequently, we shall allow for the decrease in the magnitude of critical stress by substituting the conditional static values for the modulus of elasticity  $E \ll E_{ela}$  presented in 1., into formulas (4.4) and (4.5) for Euler's loads.

## CHAPTER II

### CALCULATING THE MAGNITUDE OF STRESSES OCCURRING WHEN A SHIP STRIKES ICE AND DURING ICE COMPRESSION

#### 5. Calculating Momentum and Reduced Masses When a Ship Strikes the Ice.

To calculate the magnitude of stresses which occur when a ship strikes ice, it is necessary to make a preliminary calculation of the values of the reduced (to the line of impact) masses and velocities of the ship and ice floe. These values can be determined by solving the problem of the collision of two bodies [38], for which we shall make the following assumptions:

1. the ship shall be considered as a solid body, symmetric relative to the longitudinal plane and transverse plane of the ship's center of gravity. Coordinate axes  $O_1x_1, O_1y_1$  and  $O_1z_1$  which are relative to the ship and disposed so that their origin coincides with the center of gravity  $O_1$  (axis  $O_1x_1$  points to the bow, axis  $O_1y_1$  points starboard and axis  $O_1z_1$  points upward), will be the principal central axes of the ship's inertia (Figure 4);
2. the ice floe shall be assumed to be circular and its thickness small in comparison with its expanse; coordinate axes  $O_2x_2, O_2y_2$  and  $O_2z_2$  are the principal central axes of inertia relative to the ice floe. The shape of the floe is taken as circular for sake of simplicity in computing its apparent masses;
3. water resistance forces resulting from translation of the ship and ice floe during the impact are small in comparison with contact stresses. This is confirmed by results of theoretical research;

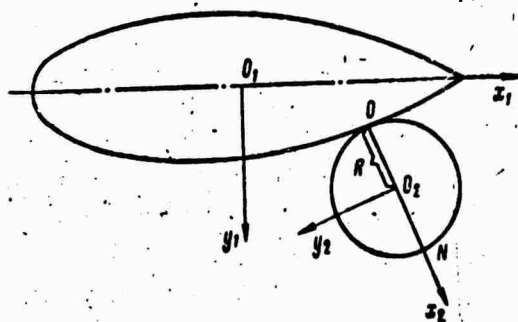


Figure 4. Diagram of a ship's striking an ice floe.

4. translations of the ship and ice floe during the impact process are small and only a change in velocities of the ship and ice floe occur as a result of the collision;

5. frictional forces do not exert a substantial influence on the magnitude of ice loads and can be disregarded. In this case, the direction of the momentum effect coincides with the direction of the normal  $N$  to the surface of the colliding bodies;

6. yielding of the ship's side is disregarded and the impact of a ship against an ice floe is considered as an inelastic impact inasmuch as crushing of the ice occurs during impact. In consequence, the coefficient of restitution  $\epsilon = 0$ .

With an elastic-plastic impact which is accompanied not only by crushing of the ice but also by bending of the floe, the coefficient of restitution  $\epsilon$  also equals zero during the first half of the impact when the contact stress grows from zero up to its maximum value -- the initial value for determining ice loads;

7. before striking against an ice floe or the edge of an ice field, the ship moves forward at a speed of  $v_0$  in the direction of axis  $O_1x_1$  and the ice floe is immobile.

The following symbols will be used when solving the problem:

- $L$  - length of ship;
- $B$  - breadth of ship;
- $T$  - draft of ship;
- $H$  - height of ship's side;
- $\delta$  - block coefficient;
- $\alpha$  - coefficient of fineness of waterline;
- $\alpha_B$  - coefficient of fineness of bow section of waterline;
- $\beta$  - slope of ship's side at impact point;
- $l$  - length of bow section of parallel body;
- $M^p$  - mass of ship;
- $M_1^1$  - mass of ice floe;
- $M_2^1$  - mass of ice floe;
- $R$  - radius of ice floe;
- $S$  - impact momentum;
- $x_1, y_1, z_1$  - coordinates of impact point on ship;
- $x_2, y_2, z_2$  - coordinates of impact point on ice floe;
- $I_{x_1}, I_{y_1}, I_{z_1}$  - moments of inertia of ship's mass relative to main central axes  $O_1x_1, O_1y_1, O_1z_1$ ;
- $I_{x_2}, I_{y_2}, I_{z_2}$  - moments of inertia of ice floe's mass relative to axes  $O_2x_2, O_2y_2, O_2z_2$ ;
- $v_1, u_1, \omega_1$  - projections of velocity of ship's center of gravity along coordinate axes  $O_1x_1, O_1y_1, O_1z_1$  after impact;

- $v_2, \omega_2$  - projections of velocity of center of gravity of ice floe along coordinate axes  $O_2x_2, O_2z_2$  after impact ( $u_2 = 0$ );  
 $P_1, p_1, r_1$  - projections of angular velocity vector of ship along coordinate axes after impact;  
 $q_2$  - angular velocity of ice floe after impact ( $p_2=r_2=0$ );  
 $l_1, m_1, n_1$  - cosines of angles formed by a normal to the surface of the ship's side and axes of coordinates  $O_1x_1, O_1y_1, O_1z_1$ ;  
 $l_2, m_2, n_2$  - cosines of angles formed by a normal to the surface of the ship's side and axes of coordinates  $O_2x_2, O_2y_2, O_2z_2$ ;

$$\lambda_1 = y_1 n_1 - z_1 m_1$$

$$\mu_1 = z_1 l_1 - x_1 n_1 \quad - \text{ are moment arms of impact momentum for the ship;}$$

$$v_1 = x_1 m_1 - l_1 z_1$$

$$\mu_2 = R n_2 \quad - \text{ is the moment arm of impact momentum for the ice floe;}$$

$$\lambda_{ij} \quad - \text{ are coefficients of reduced masses and moments of inertia of adjoining water masses.}$$

Considering the movement of each body in the impact process to be forward along with the center of gravity and rotating around the momentary axis passing through the center of gravity and making use of laws of momentum and angular momentum, we obtain:

for the ship

$$\left. \begin{aligned} M_1(1 + \lambda_{11})v_1 - v_0 &= -l_1 S, \\ M_1(1 + \lambda_{22})u_1 &= -m_1 S, \\ M_1(1 + \lambda_{33})\omega_1 &= -n_1 S, \\ I_{x_1}(1 + \lambda_{23})p_1 &= -\lambda_1 S, \\ I_{y_1}(1 + \lambda_{13})q_1 &= -\mu_1 S, \\ I_{z_1}(1 + \lambda_{12})r_1 &= -v_1 S, \end{aligned} \right\} \quad (5.1)$$

for the ice floe

$$\left. \begin{aligned} M_2(1 + \lambda'_{11})v_2 &= l_2 S, \\ M_2(1 + \lambda'_{33})\omega_2 &= n_2 S, \\ I_{y_2}(1 + \lambda'_{13})q_2 &= n_2 R S. \end{aligned} \right\} \quad (5.2)$$

Considering that the coefficient of restitution  $\epsilon$ , the characteristic elastic properties of colliding bodies, equals zero, we write in expanded form a supplementary equation from the condition of equality of the normal (at the point of impact) velocities of a ship and ice floe at

the end of an impact  $v_{1red} = v_{2red}$ ,

$$I_1 v_1 + m_1 u_1 + n_1 w_1 + (q_1 x_1 - r_1 y_1) l_1 + (r_1 x_1 - p_1 z_1) m_1 + \\ + (p_1 y_1 - q_1 z_1) n_1 = I_2 v_2 + n_2 w_2 - q_2 x_2 n_2. \quad (5.3)$$

Solving the system of equations (5.1), (5.2), (5.3) jointly and keeping in mind that  $n_1 = n_2$ , an expression for impact momentum can be obtained

$$S = \frac{M_1}{C'} \cdot \frac{v_{01}}{1 + \frac{M_1}{C'} \cdot \frac{C''}{M_2}}, \quad (5.4)$$

where  $C'$  - is a coefficient allowing for the ship's reduced mass;

$$C' = \left( \frac{I_1^2}{1 + \lambda_{11}} + \frac{m_1^2}{1 + \lambda_{22}} + \frac{n_1^2}{1 + \lambda_{33}} \right) + \\ + \left[ \frac{\lambda_1^2}{I_{x_1}(1 + \lambda_{33})} + \frac{\mu_1^2}{I_{y_1}(1 + \lambda_{33})} + \frac{v_1^2}{I_{z_1}(1 + \lambda_{33})} \right] M_1; \quad (5.5)$$

$C''$  is a coefficient allowing for the ice floe's reduced mass,

$$C'' = \left( \frac{I_2^2}{1 + \lambda'_{11}} + \frac{n_2^2}{1 + \lambda'_{33}} \right) + \frac{R^2 n_2^2}{I_{y_2}(1 + \lambda'_{33})} M_2. \quad (5.6)$$

From equating formula (5.4) with the expression for momentum during a central impact

$$S = M_1 \frac{v}{1 + \frac{M_1}{M_2}} \quad (5.7)$$

obviously, the reduced masses and velocities for an eccentric impact of a ship against an ice floe of infinite dimensions are determined in the following manner:

the reduced velocity of the ship which is a projection of the ship's velocity in the direction of the outward normal to the surface of the hull at the impact point

$$v_{red} = v_{01}^i;$$

reduced mass of the ship

$$M_{1 red} = \frac{M_1}{C'};$$

reduced mass of the ice floe

$$M_2 \text{ red} = \frac{M_2}{C^n}.$$

When a ship strikes an infinitely large ice flow  $M_1/M_2 \rightarrow 0$ , and the formula for impact momentum takes the form

$$S = \frac{v_{O_1}^1 M_1}{C'} = v \text{ red} M_1 \text{ red} \quad (5.8)$$

The magnitude  $l_1$  of the cosine of the angle between the normal at the point of impact and the direction of the ship's movement can be computed with sufficient accuracy for practice by the formula

$$l_1 = 0,01\alpha(1,6 \cos \beta + 0,11), \quad (5.9)$$

where  $\alpha$  - is the angle between a tangent to the waterline at the impact point and the longitudinal plane, in degrees;

$\beta$  - is the vertical slope of the frame at the impact point, in degrees.

By entering this into (5.5) and (5.6), expressions for moments of inertia and adjoining masses can be computed:

$I_{x_1}$  - according to Yu. A. Shimanskiy's formula

$$I_{x_1} = M_1 \left( \frac{a^3 B^3}{11,4\beta} + \frac{H^3}{12} \right);$$

$I_{y_1}$  - according to the generally accepted formula

$$I_{y_1} = 0,07\alpha M_1 L^3;$$

$I_{z_1}$  - as an average for an ellipsoid and parallelepiped

$$I_{z_1} = \frac{M_1 L^3}{16}.$$

The moment of inertia of a circular ice floe relative to axis  $O_2 y_2$ :

$$I_{y_2} = M_2 \left( \frac{R^3}{4} + \frac{h^3}{3} \right) \approx \frac{M_2 R^3}{4},$$

where  $h$  is the ice thickness, which can be ignored in comparison with the expanse of the floe.

The following values for coefficients of adjoining water masses and the floe are assumed on the basis of theoretical and experimental data:

$$\lambda_{11} = 0;$$

$$\lambda_{22} = \frac{2T}{B};$$

$$\lambda_{33} = 0,667 \frac{a^2}{8(1+a)} \cdot \frac{B}{T};$$

$$\lambda_{23} = 0,25^{***};$$

$$\lambda_{13} = \frac{B}{T} \cdot \frac{1}{3-2a} \cdot \frac{1}{3-a}.$$

---

\* As for an ellipsoid with semiaxes L/2, B/2, T.

\*\* G. Ye. Pavlenko's formula.

\*\*\* According to experimental data.

---

Values of  $\lambda_{12}$  for various L/B (when B/T = 2.5) are presented below:

$\frac{L}{B}$	$\lambda_{12}$	$\frac{L}{B}$	$\lambda_{12}$
3,5	0,45	6	0,63
4,5	0,53	7	0,65
5,5	0,60	8	0,68

We take a coefficient of adjoining mass for an ice floe as for an oblate ellipsoid, assuming that the thickness of the floe is small in comparison with its expanse. Then

$$\lambda_{11} = 0,$$

$$\lambda_{33} = 1,$$

$$\lambda_{13} = 1.$$

As formulas (5.5) and (5.6) show, the coefficients C' and C'' entered in expression (5.4) for impact impulse will depend on the contour of the ship's lines, the relationships of its main dimensions and the coordinates of the impact point. However, numerous calculations have shown that coefficients C' and C'' are practically independent of ship's parameters such as the relationship of its main dimensions (L/B, B/T, L/H), coefficients of fineness ( $\alpha$  and  $\beta$ ) and length of the parallel middle body.

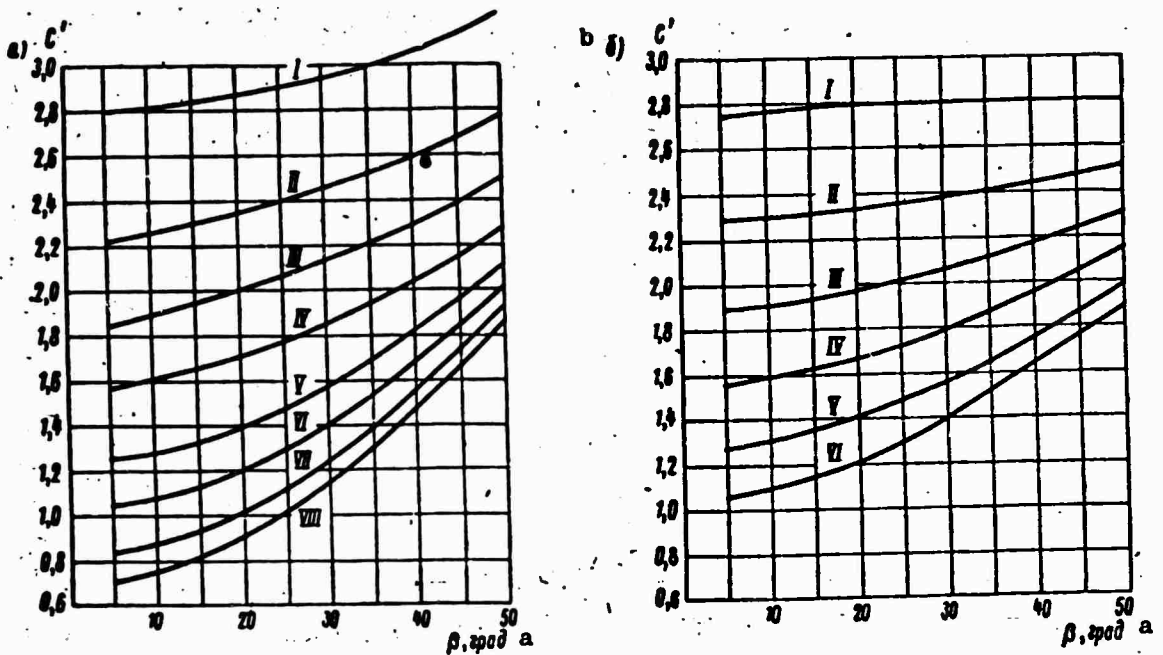


Figure 5. Values of coefficients  $C'$ : a - for icebreakers; b - for cargo ships. I - VIII are frame line reference numbers. a - degrees.

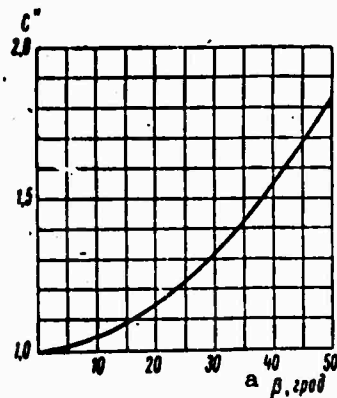


Figure 6. Values of coefficients  $C''$ . a - degrees.

To simplify computing contact stresses occurring when a ship strikes an ice floe, values of  $C'$  for various frame lines and vertical slopes  $\beta$  of frames at the impact point are presented in Figure 5. Figure 6 presents values for coefficient  $C''$ . Numerous calculations have shown that the magnitude of this coefficient is practically independent of the coordinates of the impact point and is only a function of the vertical slope of the ship's side at the impact point.

## 6. Contact Stresses When a Ship Strikes a Floating Ice Floe.

Let the ship be moving prior to impact uniformly at a velocity of  $v_0$  in the direction of axis  $O_1x_1$ . At the moment of time,  $t = 0$ , the side of the ship came into contact with an initially immobile ice floe of finite dimensions. We shall assume that the impact took place at point  $O$ , and straight line  $ON$  is normal to the side of the ship (Figure 7). We shall consider the ship's side at the place of contact as being flat and vertically inclined at an angle  $\beta_1$ , which is determined by the expression

$$\beta_1 = \text{arctg} \left( \frac{\text{tg } \beta}{\cos \alpha} \right), \quad (6.1)$$

where  $\beta$  - is the vertical slope of the frame;  
 $\alpha$  - is the angle between the tangent to the waterline and the longitudinal plane.

In subsequent calculations, we shall assume that  $\beta_1 = \beta$ , inasmuch as the maximum value of angle  $\alpha$  does not usually exceed 20 to 25°.

Let us investigate the movement of a ship and an ice floe during the impact process, using all the assumptions taken in the preceding paragraph. Moreover, we shall disregard stresses expended on submerging (breaching) of the ice floe as well as its rotation relative to its horizontal axis. The breaching and rotation of an ice floe near its horizontal axis assume significance only when a ship strikes an ice floe of relatively small dimensions but in this case, contact stresses are small and are not calculated.

The relative translation of a ship and ice floe during the impact process is the algebraic sum of the inelastic crushing strain of the ice floe's edge and the elastic strains of the ice and the ship's side. The magnitude of elastic strains is considerably smaller than the depth of crushing of the edge which reaches several tens of centimeters. Therefore, we shall subsequently disregard elastic strains, assuming the ship's side to be absolutely rigid and not considering the elastic compression of the ice. It should be noted that elastic strain of an ice floe and yielding of the side structure soften the impact, decreasing the magnitude of contact stresses. Thus, by disregarding elastic strains, we increase the magnitude of calculated stresses somewhat.

Let us consider movement of a ship and ice floe during the impact process (Figure 8). Figure 8 depicts:  $ON$  - the normal to the ship's side at the point of impact;  $x_1$  is the translation of the side in the direction of impact;  $x_2$  is the translation of the ice in that same direction;  $\zeta$  is the inelastic crushing strain of the ice floe's edge:

$$\zeta = x_1 - x_2. \quad (6.2)$$

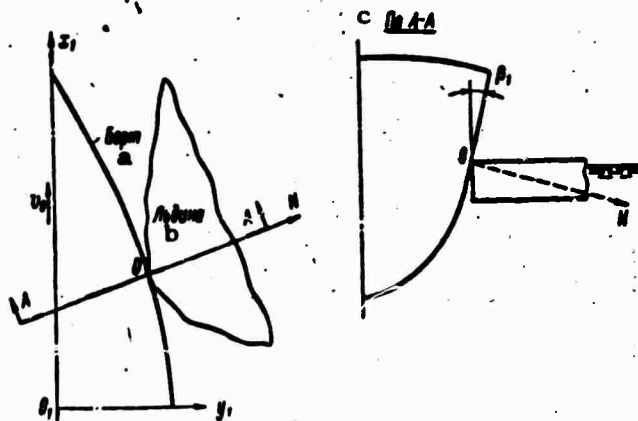


Figure 7. Impact of a ship against an ice floe. a-ship's side; b-ice floe; c-along A-A.

At impact, the kinetic energy of the ship, reduced toward the line of impact ON, will be partially converted into kinetic energy of the moving ice floe and will partially be expended in crushing the edge. We shall designate:

$$T_{1 \text{ red}} = \frac{M_{1 \text{ red}} v_{\text{red}}^2}{2} \quad \text{- is the kinetic energy of the ship, reduced toward the line of impact;}$$

$$T_{2 \text{ red}} = \frac{M_{2 \text{ red}} v_{2 \text{ red}}^2}{2} \quad \text{- is the reduced kinetic energy of the ice floe;}$$

$$U = \int_0^{\zeta} P d\zeta \quad \text{- is the work of contact forces which cause crushing of the ice floe,}$$

where  $M_{1 \text{ red}}$  and  $M_{2 \text{ red}}$  are the reduced masses of the ship and ice floe, determined by formulas 5;

$v_{\text{red}}$  - is the reduced velocity of the ship;  
 $v_{2 \text{ red}}$  - is the reduced velocity of the ice floe;  
 $P$  - is the combined contact crushing stress.

According to the principle of least action, the integral from the Lagrangian function,  $L = T_{1 \text{ red}} + T_{2 \text{ red}} - U$  of the ship-ice floe system under consideration - must be minimum. Taking equation (6.2) into consideration, we obtain

$$I(\zeta, x_1) = \int_0^t \left[ \frac{M_{1 \text{ red}} x_1^2}{2} + \frac{M_{2 \text{ red}} (x_1 - \zeta)^2}{2} - \int_0^{\zeta} P d\zeta \right] dt = \min. \quad (6.3)$$

If the functional I reaches minimum, Euler's equations must be satisfied

$$\frac{\partial L}{\partial \alpha} - \frac{d}{dt} \frac{\partial L}{\partial \dot{\alpha}} = 0;$$

$$\frac{\partial L}{\partial x_1} - \frac{d}{dt} \frac{\partial L}{\partial \dot{x}_1} = 0.$$

From this we obtain a system of differential equations which describe the movement of the ship-ice floe system during the impact process:

$$\left. \begin{aligned} M_2 \text{ red } \ddot{\zeta} &= \ddot{x}_1 (M_1 \text{ red} + M_2 \text{ red}), \\ M_2 \text{ red } (\ddot{x}_1 - \ddot{\zeta}) &= P. \end{aligned} \right\} \quad (6.4)$$

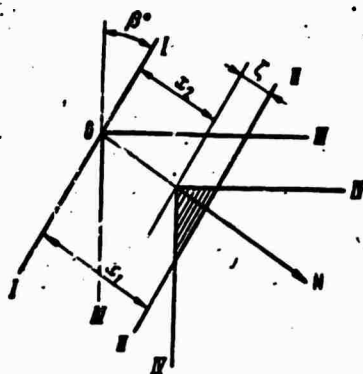


Figure 8. Translation of ship's side during impact against an ice floe.

- I - I - side at start of impact ( $t = 0$ );
- II - II - side during impact;
- III-III - ice floe at start of impact;
- IV - IV - ice flow during impact.

Excluding the unknown acceleration  $\ddot{x}_1$  from this system, we obtain a basic differential equation for determining the depth of crushing of the ice floe's edge  $\zeta$  and consequently, also for determining the contact stress

$$M_1 \text{ red } \ddot{\zeta} = -P \left( 1 + \frac{M_1 \text{ red}}{M_2 \text{ red}} \right). \quad (6.5)$$

The initial conditions when  $t = 0$ , will be

$$\dot{\zeta}(0) = 0 \text{ и } \zeta(0) = 0$$

where  $v_{01}$  is the reduced velocity of the ship at the initial moment of impact.

Conditions at the termination of the impact, when  $t = t_1$ , will be

$$\zeta(t_1) = \zeta_{\max} \text{ and } \dot{\zeta}(t_1) = 0,$$

where  $t_1$  - is the duration of the impact;

$\zeta_{\max}$  - is the maximum depth of crushing.

The magnitude of the combined contact stress  $P$  is defined as an integral from the contact pressures  $p$  taken over the entire actual area  $F$  of the contact zone,

$$P = \int p dF. \quad (6.6)$$

The magnitude of area  $F$  will depend on the configuration of the ice floe's edge and the depth of penetration of the ship's side into the ice. In an ordinary situation, it can be assumed that

$$F = A\zeta^a, \quad (6.7)$$

where  $A'$  - is a coefficient depending on the geometric parameters of the ship and ice floe;

$a$  - is an exponent depending only on the configuration of the ice floe's edge at the impact point.

Taking (6.7) into consideration and considering that the magnitude of contact pressure is also a function of the depth and velocity of penetration, in place of (6.6) we can write:

$$P = aA \int_0^{\zeta} p(\zeta, \dot{\zeta}) \zeta^{a-1} d\zeta. \quad (6.8)$$

Substituting expression (6.8) into formula (6.5) and substituting variables  $\zeta = z$ , we obtain a first order differential equation

$$\frac{M_{1 \text{ red}}}{1 + \frac{M_{1 \text{ red}}}{M_{2 \text{ red}}}} z \frac{dz}{d\zeta} = - aA \int_0^{\zeta} p(\zeta, z) \zeta^{a-1} d\zeta. \quad (6.9)$$

Assuming the proposition of equality of contact pressures with the value of ultimate crushing strength of ice, i.e.,  $p(\zeta, z) = \sigma_c$  (see 3.) and integrating the right side (6.9), we obtain a differential equation with separable variables

$$M_{\text{red}} dz = - a\sigma_c \zeta^a d\zeta, \quad (6.10)$$

where  $M_{\text{red}} = \frac{M_{1 \text{ red}} M_{2 \text{ red}}}{M_{1 \text{ red}} + M_{2 \text{ red}}}$  is the reduced mass of the system of colliding

bodies.

Let us integrate both sides of expression (6.10):

$$\int_{v_{01}}^z z dz = \frac{A\sigma_c}{M_{red}} \int_0^{\zeta} \zeta^a d\zeta.$$

After integrating, we obtain

$$z^2 - (v_{01})^2 = -\frac{2A\sigma_c}{M_{red}} \frac{\zeta^{a+1}}{a+1}. \quad (6.11)$$

At the termination of impact, when  $\dot{\zeta} = z = 0$ , the depth of crushing will be maximum and will be determined by the expression

$$\zeta = \zeta_{max} = \left[ \frac{(a+1) M_{red} (v_{01})^2}{2A\sigma_c} \right]^{\frac{1}{1+a}} \quad (6.12)$$

The maximum contact stress, corresponding to  $\zeta = \zeta_{max}$ ,

$$P_{max} = A\sigma_c \left[ \frac{(1+a) M_{red} (v_{01})^2}{2A\sigma_c} \right]^{\frac{a}{1+a}} \quad (6.13)$$

From (6.11), we can obtain

$$z = \frac{d\zeta}{dt} = v_{01} \sqrt{1 - \left( \frac{\zeta}{\zeta_{max}} \right)^{a+1}}.$$

Integrating this equation, we obtain an expression for impact time:

$$t_1 = \frac{\zeta_{max} \sqrt{\pi}}{v_{01} (a+1)} \cdot \frac{\Gamma\left(\frac{1}{1+a}\right)}{\Gamma\left(\frac{3+a}{2+2a}\right)}. \quad (6.14)$$

The values of the  $\Gamma$ -function depending on parameter  $a$  can be determined from reference book tables.

Formulas (6.12) to (6.14) give general expressions for determining the maximum depth of crushing of the edge, the maximum contact stress during impact and the impact time. No assumptions concerning the shape of the ice floe and geometry of the contact zone which are allowed for by parameters  $A$  and  $a$  are made in the conclusion of these formulas. Average values of these parameters can be determined experimentally by measuring the maximum contact stress  $P_{max}$  and the duration of impact  $t_1$ . However, there is presently a little research data which is available until the

values of parameters  $A$  and  $a$  can be determined experimentally. Therefore, two practically possible cases are considered below: impact against an ice floe with a rounded edge and impact against a projecting corner of an ice floe.

7. Contact Stresses During Impact of a Ship Against an Ice Floe With a Rounded and an Angular Edge.

Impact against an ice floe with a rounded edge (Figure 9). Let the edge of the floe in the area of contact with the ship's side have a smooth outline and let it be fixed by the equation  $x = f(y)$ , axis  $y$  coinciding with the line of intersection of the plane of the ship's side and the upper surface of the floe.

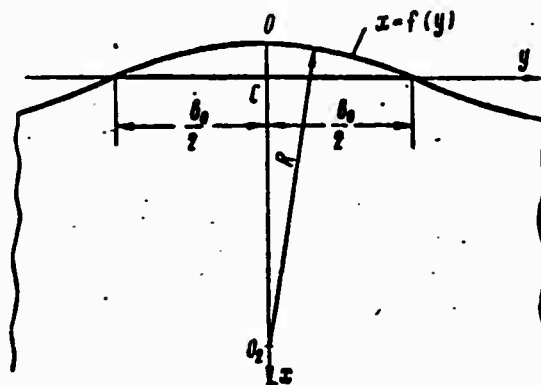


Figure 9. Parameters of an Ice Floe with a Rounded Edge.

The magnitude of the radius of curvature  $R$ , within the range of the length of the contact zone, can be assumed to be significantly changing and is taken as a design or its average value, or the value at point  $O$ . Then, for the length of the contact zone

$$b_0 = 2\sqrt{2Rh_1 - h_1^2}, \quad (7.1)$$

where  $h_1 = CO = \frac{c}{\cos \beta}$ , as follows from Figure 10.

The magnitude of the radius of the edge curvature is usually rather large. The inequality  $h_1 \ll 2R$  is nearly always observed. Therefore, in formula (7.1), the member  $h_1^2$  can be disregarded. Thus we obtain

$$b_0 = 2\sqrt{2Rh_1} = 2\sqrt{\frac{2Rc}{\cos \beta}}, \quad (7.2)$$

from which

$$R = \frac{b_0^2}{8h_1}. \quad (7.3)$$

The function  $x = f(y)$  can be considered to be symmetric relative to axis  $x$  within the limits of the length of the crushing zone and can be presented in the form of a Fourier series. Being limited by the first member of the series and determining the radius of curvature at point  $O$  ( $x = h_1$ ), we obtain

$$R = \frac{b_0^2}{8h_1}$$

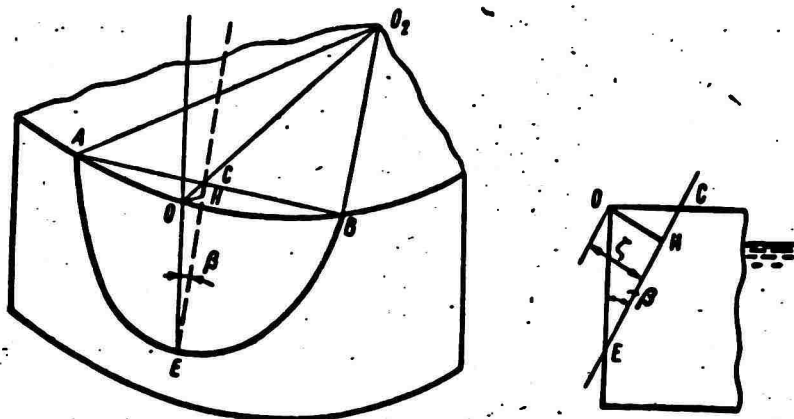


Figure 10. Diagram of crushing of a rounded edge of an ice floe.

$$AB = b, CE = c, OH = l, OO_2 = R, OC = h.$$

Setting function  $x = f(y)$  in the form of a quadratic parabola and averaging the radius of curvature by formula

$$\bar{R} = \frac{2}{b_0} \int_0^{b_0/2} R dy,$$

we have

$$\bar{R} = \frac{b_0^2}{8h_1}$$

Thus, the average value of the radius of curvature changes within an extremely narrow range. Therefore, formula (7.3) can subsequently be used, assuming that the inaccuracy of the magnitude of the numerical coefficient will be compensated for when selecting the mean statistical parameter  $R$ .

The contact zone formed by the intersection of the floe's edge with the plane of the ship's side is a parabolic segment (Figure 10), the area of which can be approximately determined by formula

$$F = \frac{2}{3} b_0 c = \frac{2}{3} \frac{b_0^2}{\sin \beta \cos \beta}$$

Taking expression (7.2) into consideration, we obtain, for an ice floe with a vertical edge

$$F = \frac{4}{3} \cdot \frac{\zeta^{3/2} \sqrt{2R}}{\cos^{3/2} \beta \sin \beta}. \quad (7.4)$$

Equating function (7.4) with the general expression (6.7) for the area of the contact zone, we have

$$\left. \begin{aligned} a &= \frac{3}{2}, \\ A &= \frac{4}{3} \cdot \frac{\sqrt{2R}}{\cos^{3/2} \beta \sin \beta}. \end{aligned} \right\} \quad (7.5)$$

Substituting the obtained expression for  $a$  into formula (6.12), we determine the maximum depth of crushing of the edge

$$\zeta_{\max} = \left( \frac{5}{4} \cdot \frac{M_{\text{red}}^2 v_{\text{red}}^2}{\sigma_c A} \right)^{1/2}. \quad (7.6)$$

The maximum contact stress

$$P_{\max} = 1.14 (M_{\text{red}} v_{\text{red}}^2)^{3/5} (\sigma_c)^{2/5}; \quad (7.7)$$

impact time

$$t_1 = 1.61 (\sigma_c)^{-2/5} (M_{\text{red}} v_{\text{red}}^2)^{2/5} v_{\text{red}}^{-1/5}. \quad (7.8)$$

As follows from expression (7.8), the impact time is proportional to  $v_{\text{red}}^{-1/5}$ , which qualitatively satisfies a realistic picture of an impact. Actually, when the ship's velocity is small  $v_{\text{red}} \rightarrow 0$ , impact time will be greater ( $t_1 \rightarrow \infty$ ). With an increase in velocity, the duration of impact decreases.

Impact against an Ice Floe with an Angular Edge (Figure 11). In this case, the ship's side comes into contact with the edge of the floe taking the form of a protruding angle. The area of crushing  $F$  is a triangle and is determined by the formula

$$F = \frac{b \varphi}{2} = \frac{\text{tg} \frac{\psi}{2}}{\sin \beta \cos^2 \beta} \zeta^2, \quad (7.9)$$

where  $\psi$  is the magnitude of the angle at center of the edge projection.

Comparing (7.9) with the general expression (6.7), we find

$$\left. \begin{aligned} a &= 2, \\ A &= \frac{\operatorname{tg} \frac{\psi}{2}}{\sin \beta \cos^2 \beta}. \end{aligned} \right\} \quad (7.10)$$

Substituting the obtained value for  $a$  into general solution formulas, we determine:

the maximum depth of crushing of the edge

$$c_{\max} = 1.15 \left( \frac{M_{\text{red}} v_{\text{red}}^2}{\sigma_c A} \right)^{1/3}, \quad (7.11)$$

maximum contact stress

$$P_{\max} = 1.31 (M_{\text{red}} v_{\text{red}}^2)^{2/3} (A \sigma_c)^{1/3}, \quad (7.12)$$

impact time

$$t_1 = 1.61 (A \sigma_c)^{-1/3} M_{\text{red}}^{1/3} v_{\text{red}}^{-1/3}. \quad (7.13)$$

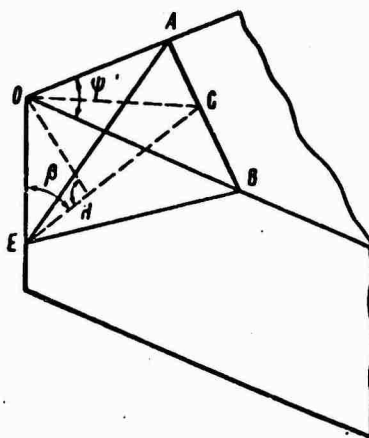


Figure 11. Diagram of crushing of a protruding angle of the edge of an ice floe.

$AB=b$ ,  $CE=c$ ,  $OH=l$ .

Comparing formulas (7.6) through (7.8) with (7.11) through (7.13), we see that their structure is identical.

We shall attempt to estimate the magnitude of protruding angle  $\psi$  of the edge of the ice field. An impact against the edge of a channel in a compact ice field is the most dangerous when a ship is moving in a canal behind an icebreaker. In this case, the magnitude of the protruding angle will be calculated by the dimensions of the segments broken off by the icebreaker (Figure 12). Academic calculations and data from experiments in fracturing floating ice plates show that the dimensions of a

segment broken off from a semi-infinite ice plate depend on the thickness of the ice and the relationship of the height of the segment to its width, fluctuates within a narrow range. These conclusions well agree with data from actual observations.

Let the height of the segment equal  $nh$ , where  $h$  is the thickness of the ice and  $n$  is a coefficient depending, when all other conditions are equal, on the reduced velocity of the icebreaker. As a rule, the magnitude of this coefficient fluctuates within the range  $n = 1.5$  to  $3.0$  for floes broken off by the bow and  $n = 5$  to  $7$  for floes of the latter series of breaking (conditions close to static). The width of the segment equals  $2knh$ , where  $k$  is a coefficient characterizing the relationship of the dimensions of the broken off segment in a plane. It can usually be assumed that  $k = 3$ .

The magnitude of the angle at center  $\psi$  of the protruding edge of the floe is determined from the simple geometric constructions shown in Figure 12. The unknown radius,  $R$ , will be

$$R = nh \frac{k^2 + 1}{2}.$$

Then

$$\psi = 2 \operatorname{arctg} \frac{k^2 - 1}{2k}. \quad (7.14)$$

It is obvious from expression (7.14), that the magnitude of angle  $\psi$  depends neither on the thickness of the ice  $h$ , nor on coefficient  $n$ , which changes within a wide range. For the above-indicated value,  $k = 3$ , angle  $\psi = 106^\circ$ .

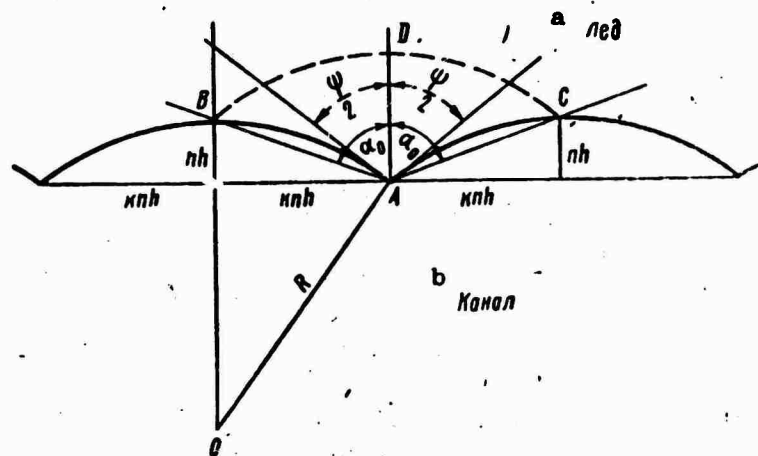


Figure 12. Geometric characteristics of a protrusion of the channel edge in a channel opened by an icebreaker. a-ice; b-channel.

The maximum value of the angle at center cannot exceed  $2\alpha_0$  (Figure 12). Thus,

$$\psi_{\max} = 2\alpha_0 = 2 \operatorname{arctg} k.$$

When  $k = 3$ , angle  $\psi_{\max} = 145^\circ$ .

Another extreme value of this angle can be determined, taking in formula (7.4), the minimum value observed under natural conditions  $k = 1.5$ . Then,  $\psi_{\min} = 45^\circ$ . Consequently, possible values of the angle at center fluctuate over a wide range from 45 to 145°. The average value of this angle which can be used for calculations is 90 to 100°.

As an example, we shall calculate contact stress  $P_{\max}$ , depth of crushing  $\zeta_{\max}$  and impact time  $t_1$  during impact of a ship displacing  $D_1 = 12,000$  t at various speeds against an ice floe weighing  $D_2 = 3000$  t. The impact takes place at the third frame line which has a vertical slope of  $\beta = 29^\circ$ . The cosine of the angle between a normal to the ship's side at the impact point and the direction of the ship's movement  $\lambda_1 = 0.219$ . With an impact against an ice floe with a rounded edge, we assume  $R = 25$  m as the radius of the curve and with an impact against a floe with an angular edge, we consider  $\psi = 90^\circ$ , as the tip angle. The ultimate crushing strength of the ice  $\sigma_c = 400$  t/m<sup>2</sup>.

The values of  $P_{\max}$ ,  $\zeta_{\max}$ ,  $b_0$  and  $t_1$  in an impact of a ship against a rounded edge and against a protruding corner of an ice floe's edge are presented in Tables 2 and 3 respectively. From the tables, it is obvious that the magnitude of combined stress is considerably greater during impact against a floe with a rounded edge. In this situation, the contact stress is distributed over a considerable length along the side of the ship. Contact stresses during impact against a protruding corner of the edge are of a local nature, embracing no more than two or three frame-spacings.

Table 2

Values of  $P_{\max}$ ,  $\zeta_{\max}$ ,  $b_0$  and  $t_1$  during impact of a ship against an ice floe with a rounded edge.

$v_0$ , узлы a	$P_{\max}$ , т b	$\zeta_{\max}$ , м	$b_0$ , м	$t_1$ , сек. c
2	162	0,066	3,90	0,430
4	372	0,114	5,13	0,375
6	608	0,159	6,05	0,346
8	856	0,200	6,78	0,327
10	1124	0,239	7,41	0,319

a-knots; b-t; c-sec.

Table 3

Values of  $P_{\max}$ ,  $\zeta_{\max}$ ,  $b_0$  and  $t_1$  during impact of a ship against an angular edge.

$v_0$ , узлы a	$P_{\max}$ , т b	$\zeta_{\max}$ , м	$b_0$ , м	$t_1$ , сек. c
2	56	0,232	0,532	1,414
4	142	0,368	0,845	1,123
6	244	0,482	1,103	0,985
8	358	0,584	1,336	0,892
10	460	0,678	1,553	0,829

a-knots; b-t; c-sec.

### 8. Impact of a Ship Against the Edge of an Ice Field.

When a ship strikes the edge of an ice field, the edge of the ice crushes and the ice field bends as a result of the vertical component of the contact stress. The effect that the crushing of the edge and bending have on the magnitude of the contact stresses primarily depends on the thickness of the ice and the vertical slope of the ship's side.

Let us consider a general case of impact, allowing for crushing of the ice's edge and bending of the ice field. Extreme cases of this problem are the impact of a ship against an ice cover of great thickness (hummock, stamukh, iceberg), when bending of the ice field can be disregarded and impact against an ice cover of relatively small thickness, when crushing of the ice's edge can be disregarded.

The problem of determining contact stresses occurring when a ship strikes against the edge of an ice field is solved with the same assumptions and premises as those used in solving the problem of a ship's impact against an ice floe of finite dimensions.

Determining Contact Stresses during Impact of a Ship against the Edge of an Ice Field, Taking Bending into Account. The process of a ship's impact against a non-failing ice field can be divided into two stages. In the first stage, at the start of the impact, crushing of the edge takes place. With this, the vertical component  $P_v = P \sin \beta$  causes bending of the field (Figure 13). Contact stress increases from zero to maximum. At the end of the first stage, the velocity of the ship in the direction of impact (reduced velocity) becomes zero. In the second stage, the potential bending energy of the ice field, built up in the strain process is converted into kinetic energy of the reverberating ship. Thus, the impact of a ship against a non-failing ice field should be considered as an elastic-plastic impact.

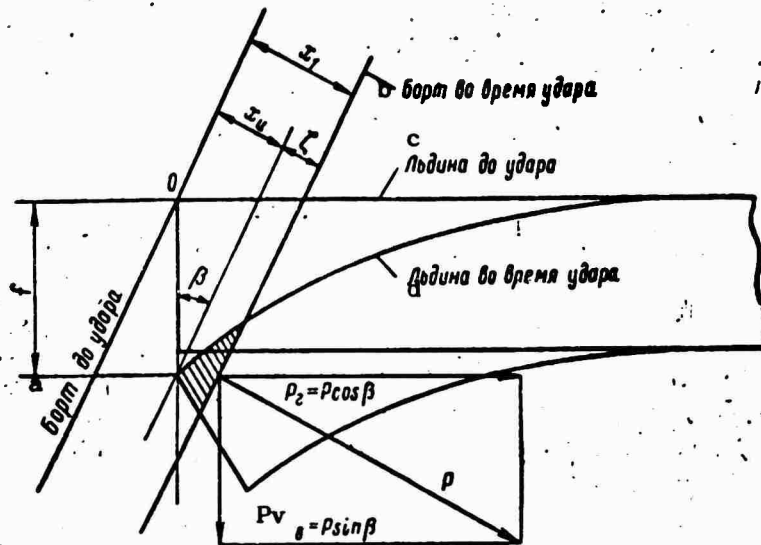


Figure 13. Diagram of impact, taking bending of the floe into account.

a-ship's side before impact; b-ship's side during impact; c-ice floe before impact; d-ice floe during impact.

When a ship strikes against a failing ice field, only the first stage takes place during which the contact stress increases from zero to a magnitude which causes the field to fail from bending.

Thus, in the process of impact against the edge of an ice field, the ship's kinetic energy is expended in crushing and bending the ice field. An energy balance equation for this situation can be presented in the form

$$T = U + V,$$

where  $T = \frac{M_{red} v_{red}^2}{2}$  - is the kinetic energy of the ship in the direction of impact;

U - is the work of crushing forces, defined as an integral:

$$U = \int_0^{\zeta_{max}} P d\zeta = \sigma_c A \frac{\zeta_{max}^{a+1}}{a+1};$$

V - is the potential bending strain energy of a semi-infinite ice plate at the end of the first stage:

$$V = \frac{1}{2} f P_{max} \sin \beta = \frac{P_{max}^2 \sin^2 \beta}{4 \sqrt{\gamma D}}.$$

Then

$$\frac{M_{red} v_{red}^2}{2} = \sigma_c A \frac{\zeta_{max}^{a+1}}{a+1} + \frac{P_{max}^2 \sin^2 \beta}{4 \sqrt{\gamma D}}. \quad (8.1)$$

Keeping in mind that in the general case  $P = \sigma_c A \zeta^a$ , we obtain a formula for determining the maximum depth of crushing of the ice's edge

$$\zeta_{\max} = \left( \frac{M_{1\text{red}} v_{\text{red}}^2}{\frac{2\sigma_c A}{a+1} + \frac{\sigma_c^2 A^2 \sin^2 \beta}{2\sqrt{\gamma D}} \zeta_{\max}^{a-1}} \right)^{\frac{1}{a+1}}. \quad (8.2)$$

The magnitude  $\zeta_{\max}$  should be determined by formula (8.2), using the successive approximations method. The value  $\zeta_{\max}$ , computed without taking bending into account, i.e., assuming at first that  $\zeta_{\max}$  (in a denominative fraction) equals zero, must be taken as the first approximation.

The depth of crushing of the edge, as well as the impact time can be determined by solving a differential equation of the ship's movement in the direction of impact. We obtain this equation by using the principle of least action as was done in 6., i.e., by assuming

$$\int_0^t \left[ \frac{M_{1\text{red}} \dot{x}_1^2}{2} - \sigma_c A \frac{\zeta^{a+1}}{a+1} - \frac{P^2 \sin^2 \beta}{4\sqrt{\gamma D}} \right] dt = \min. \quad (8.3)$$

As seen in Figure 13, translation  $x_1$  of point O, on the side where the impact occurs, will be computed from the elastic translation  $x_b$  which is caused by bending of the ice field and from the inelastic crushing strain of the floe's edge  $\zeta$ , i.e.,

$$x_1 = \zeta + x_b.$$

Translation  $x_b$  and the amount of deflection of the edge of an ice plate  $f$  are related to the function  $x_b = f \sin \beta$ . The amount of deflection of a floating semi-infinite ice plate under the influence of vertical stress  $P_v = P \sin \beta$  which is applied to the edge is,

$$f = \frac{P \sin \beta}{2\sqrt{\gamma D}}.$$

Noting that  $P = \sigma_c A \zeta^a$ , we obtain

$$x_1 = \frac{\sigma_c A \sin^2 \beta}{2\sqrt{\gamma D}} \zeta^a + \zeta.$$

Then the integral (8.3) will be written in the following form:

$$\int_0^t \left[ \frac{M_{1\text{red}}}{2} \left( \frac{\sigma_c a A \sin^2 \beta}{2\sqrt{\gamma D}} \zeta^{a-1} \dot{\zeta} + \dot{\zeta} \right)^2 - \frac{\sigma_c A}{a+1} \zeta^{a+1} - \frac{\sigma_c^2 A^2 \sin^2 \beta}{4\sqrt{\gamma D}} \zeta^{2a} \right] dt = \min. \quad (8.4)$$

Euler's equation for this function takes the form

$$\ddot{\zeta}(1 + B\zeta^{a-1}) + B(a-1)\zeta^{a-2}\dot{\zeta}^2 + A_1\zeta^a = 0,$$

where

$$A_1 = \frac{\sigma_c A}{M_{1red}}, \quad B = \frac{\sigma_c A \sin^2 \beta}{2V_{red}^2 D}.$$

The obtained equation is reduced to a linear substitution of variable  $\zeta^2 = \eta$ .

Finally, we have

$$\frac{d\eta}{d\zeta} + 2f_1(\zeta)\eta + 2f_2(\zeta) = 0, \quad (8.5)$$

where

$$f_1(\zeta) = \frac{B(a-1)\zeta^{a-2}}{1+B\zeta^{a-1}}; \quad f_2(\zeta) = \frac{A_1\zeta^a}{1+B\zeta^{a-1}}.$$

Equation (8.5) has an integrating factor

$$\mu = e^{2 \int_0^{\zeta} f_1(\zeta) d\zeta}.$$

Taking into account the initial conditions  $\zeta = 0$ ;  $\dot{\zeta} = v_{red}$ ;  $\dot{x}_b = 0$ , when  $t = 0$ , we obtain a general integral of equation (8.5)

$$\eta = e^{-2 \int_0^{\zeta} f_1(\zeta) d\zeta} \left[ -2 \int_0^{\zeta} f_2(\zeta) e^{2 \int_0^{\zeta} f_1(\zeta) d\zeta} d\zeta + v_{red}^2 \right] \quad (8.6)$$

At the end of the impact, when  $t = t_1$ , the ship's velocity in the direction of impact equals zero, i.e.,  $\dot{\zeta} = \sqrt{\eta} = 0$ , and the depth of crushing is maximum  $\zeta = \zeta_{max}$ . From this, we obtain the condition for determining the maximum depth of crushing of the ice's edge:

$$2 \int_0^{\zeta_{max}} f_2(\zeta) \exp\left(2 \int_0^{\zeta} f_1(\zeta) d\zeta\right) d\zeta = v_{red}^2$$

If integration is performed, it is possible to obtain an expression for  $\zeta_{max}$ , coinciding with formula (8.2) which was obtained by the energy method. We determine the value of the maximum contact stress at the end of the impact by substituting  $\zeta_{max}$  into formula  $P_{max} = A\sigma_c \zeta_{max}^a$ . We shall find the impact time by integrating the right side of equation  $d\zeta/\sqrt{\eta} = dt$  from 0 to  $t_1$  and the left side, correspondingly, from 0 to  $\zeta_{max}$ . Then

$$t_1 = \int_0^{\zeta_{max}} \frac{d\zeta}{\sqrt{\exp\left(-2 \int_0^{\zeta} f_1(\zeta) d\zeta\right) \left[ -2 \int_0^{\zeta} f_2(\zeta) \exp\left(2 \int_0^{\zeta} f_1(\zeta) d\zeta\right) d\zeta + v_{red}^2 \right]}}$$

If the impact occurs against an ice field with a rounded or angular edge, all expressions are substantially simplified.

Let us consider an impact against an ice field with a rounded edge with a radius  $R$ . In this case, the maximum depth of crushing of the edge should be determined by formula (8.2), substituting in it the values of coefficients  $a$  and  $A$  according to (7.5).

$$\zeta_{\max} = \left( \frac{v_{\text{red}}^2}{\frac{4}{8} A_1 + \frac{2}{3} A_1 B c_{\max}^2} \right)^{1/5} \quad (8.7)$$

where

$$\left. \begin{aligned} A_1 &= \frac{4}{3} \frac{c_c \sqrt{2R}}{M_{\text{lred}} \sin \beta \cos^{3/2} \beta}; \\ B &= c_c \frac{\sin \beta}{\cos^2 \beta} \sqrt{\frac{2R}{\gamma D}} \end{aligned} \right\} \quad (8.8)$$

As indicated above, the first approximation will give the value  $\zeta_{\max}$ , computed without allowing for bending

$$\zeta_{\max} = \left( \frac{15}{16} \right)^{2/5} \left( \frac{M_{\text{lred}} v_{\text{red}}^2}{\sigma_c} \right)^{2/5} \frac{\sin^{2/5} \beta \cos^{3/5} \beta}{(2R)^{1/5}} = \left( \frac{5v_{\text{red}}^2}{4A_1} \right)^{2/5} \quad (8.9)$$

this concurs with expression (7.6), if we set  $M_{2\text{red}} = \infty$  in it and take functions (7.5), (8.8) and (6.10) into consideration.

Inasmuch as  $P = \sigma_c A_c^a$  in a general situation, by using dependence (7.5), we obtain an expression for the maximum contact stress which occurs during the impact of a ship against the edge of an ice field, allowing for bending of the ice cover

$$P_{\text{max}} = \frac{4}{3} \frac{c_c \sqrt{2R}}{\sin \beta \cos^{3/2} \beta} \zeta_{\max}^2 \quad (8.10)$$

where  $\zeta_{\max}$  is computed by expression (8.7).

During impact of a ship against the edge of an ice field, the greatest contact stress  $P_{\text{max}}$  and impact time  $t_1$ , without taking bending of the ice into consideration, can be determined by formulas (7.7) and (7.8) if we set  $M_1/M_2 = 0$  into them, inasmuch as the mass of the ice floe  $M_2 = \infty$ . In this case,  $P_{\text{max}}$  can also be computed directly by formula (8.10), if we substitute  $\zeta_{\max}$  from expression (8.9) into it.

Let us consider the impact of a ship against an ice field with an angular edge. In this case, the depth of crushing is computed by formula (8.2) which, giving consideration to (7.10), can be written in form

$$\zeta_{\max} = \left( \frac{v_{\text{red}}^2}{\frac{2}{3} A_1 + \frac{1}{2} A_1 B \zeta_{\max}} \right)^{1/3}, \quad (8.11)$$

where

$$\left. \begin{aligned} A_1 &= \frac{\sigma_c \operatorname{tg} \frac{\psi}{2}}{M_{1\text{red}} \sin \beta \cos^2 \beta}; \\ B &= \frac{\sigma_c \sin \beta \operatorname{tg} \frac{\psi}{2}}{\cos^2 \beta \sqrt{\gamma D}}. \end{aligned} \right\} \quad (8.12)$$

Assuming in the first approximation that  $\zeta_{\max} = 0$  in the denominator of expression (8.11), we obtain the depth of crushing, computed without considering bending of the field

$$\zeta_{\max} = \left( \frac{3}{2} \cdot \frac{v_{\text{red}}^2}{A_1} \right)^{1/3} = 1.15 \left( \frac{M_{1\text{red}} v_{\text{red}}^2 \sin \beta \cos^2 \beta}{\sigma_c \operatorname{tg} \frac{\psi}{2}} \right)^{1/3}, \quad (8.13)$$

this coincides with expression (7.11), if we set  $M_{2\text{red}} = \infty$  and take relationships (7.10) and (8.12) into consideration.

Maximum contact stress

$$P_{\max} = \frac{\operatorname{tg} \frac{\psi}{2}}{\sin \beta \cos^2 \beta} \sigma_c \zeta_{\max}^2, \quad (8.14)$$

where  $\zeta_{\max}$  is determined by expression (8.11), if bending of the ice field is taken into consideration or by formula (8.13) without allowing for bending of the ice field.

**Example.** We shall determine contact stresses occurring during impact of a ship displacing  $D_1 = 12,000$  t against an ice field with a rounded and with an angular edge. The velocity of the ship at the moment of impact  $v = 3$  knots ( $v_0 = 1.545$  m/sec). The impact occurs at the third frame line, the vertical slope of which forms an angle of  $\beta = 29^\circ$ , and the cosine of the angle between a normal to the side at the point of impact and the direction of movement  $l_1 = 0.219$ . The radius of the rounded ice field at the point of impact  $R = 25$  m, the angle of the point of the edge  $\psi = 90^\circ$ . The thickness of the ice  $h = 1.3$  m, the ultimate crushing strength  $\sigma_c = 400$  t/m<sup>2</sup>, the modulus of elasticity of the ice  $E = 3 \cdot 10^5$  t/m<sup>2</sup>, the Poisson coefficient  $\mu = 0.34$  and the specific weight of the ice  $\gamma = 0.85$  t/m<sup>3</sup>.

Impact against an ice floe with a rounded edge.

The flexural stiffness of the ice field

$$D = \frac{Eh^3}{12(1-\mu^2)} = \frac{3 \cdot 10^9 \cdot 1,3^3}{12(1-0,34^2)} = 8,20 \cdot 10^8 \text{ t m.}$$

The reduced mass of the ship

$$M_{\text{lred}} = \frac{D_1}{gC'} = \frac{12000}{9,81 \cdot 2,06} = 594 \text{ t} \cdot \text{cex}^2/\text{m.}$$

The value of coefficient  $C'$  is determined according to Figure 5 for the third frame line where  $\beta = 29^\circ$ .

The reduced velocity of the ship  $v_{\text{red}} = v_{01} = 0,338 \text{ m/sec.}$

Coefficients  $A_1$  and  $B$  are computed by formula (8.8):

$$A_1 = \frac{4}{3} \frac{\sigma_c \sqrt{2R}}{M_{\text{lred}} \sin \beta \cos^{3/2} \beta} = \frac{4 \cdot 400 \sqrt{2 \cdot 25}}{3 \cdot 594 \cdot 0,485 \cdot 0,810} = 16,1 \text{ m}^{1/2} \text{ cex}^{-2}.$$

$$B = \frac{\sigma_c \sin \beta \sqrt{2R}}{\cos^{3/2} \beta \sqrt{\gamma D}} = \frac{400 \cdot 0,485 \sqrt{2 \cdot 25}}{0,810 \sqrt{0,85 \cdot 8,20 \cdot 10^8}} = 6,4 \text{ m}^{-1/2}.$$

The depth of crushing in the first approximation, determined by formula (8.9),

$$\zeta_{\text{max } 1} = \left( \frac{5}{4} \frac{v_{\text{red}}^2}{A_1} \right)^{1/5} = \left( \frac{5 \cdot 0,338^2}{4 \cdot 16,1} \right)^{1/5} = 0,151 \text{ m.}$$

We substitute the obtained value  $\zeta_{\text{max } 1}$  in the right side of formula (8.7) and compute the depth of crushing in a second approximation

$$\zeta_{\text{max } 2} = \left( \frac{v_{\text{red}}^2}{\frac{4}{5} A_1 + \frac{2}{3} A_1 B \zeta_{\text{max } 1}^{1/5}} \right)^{1/5} = \left( \frac{0,338^2}{\frac{4}{5} 16,1 + \frac{2}{3} 16,1 \cdot 6,4 \cdot 0,151^{1/5}} \right)^{1/5} = 0,0963 \text{ m.}$$

Substituting the obtained value  $\zeta_{\text{max } 2}$  into the right side of formula (8.7), we find the depth of crushing in a third approximation

$$\zeta_{\text{max } 3} = \left( \frac{0,338^2}{\frac{4}{5} 16,1 + \frac{2}{3} 16,1 \cdot 6,4 \cdot 0,0963^{1/5}} \right)^{1/5} = 0,103 \text{ m.}$$

We shall not make further approximations.

The maximum contact stress, taking bending into consideration, is determined by formula (8.10)

$$P_{\max} = \frac{4\sigma_c \sqrt{2R}}{3 \sin \beta \cdot \cos^{2/3} \beta} \zeta_{\max}^{2/3} = \frac{4 \cdot 400 \sqrt{2 \cdot 25} \cdot 0.103^{2/3}}{3 \cdot 0.485 \cdot 0.81} = 327.5 \text{ t.}$$

We obtain the maximum contact stress without considering bending of the ice by formula (8.10), substituting the maximum depth of crushing obtained in the first approximation, i.e., without considering bending, into the formula,

$$P_{\max} = \frac{4\sigma_c \sqrt{2R}}{3 \sin \beta \cos^{2/3} \beta} \zeta_{\max 1}^{2/3} = \frac{4 \cdot 400 \sqrt{2 \cdot 25} \cdot 0.151^{2/3}}{3 \cdot 0.485 \cdot 0.81} = 562 \text{ m.}$$

Thus, reduction of the maximum contact stress because of bending of the ice comprises  $\frac{562 - 327.5}{562} \cdot 100 = 41.7\%$ .

Impact against an ice floe with an angular edge.

We determine coefficients  $A_1$  and  $B$  by formulas (8.12):

$$A_1 = \frac{\sigma_c \operatorname{tg} \frac{\psi}{2}}{M_{1\text{red}} \sin \beta \cos^2 \beta} = \frac{400 \cdot 1}{594 \cdot 0.485 \cdot 0.875^2} = 1.825 \text{ m}^{-1} \cdot \text{сек}^{-2};$$

$$B = \frac{\sigma_c \sin \beta \operatorname{tg} \frac{\psi}{2}}{\cos^2 \beta \sqrt{\gamma D}} = \frac{400 \cdot 0.485 \cdot 1}{0.875^2 \cdot \sqrt{0.85 \cdot 8 \cdot 20 \cdot 10^4}} = 0.915 \text{ m}^{-1}.$$

We compute the depth of crushing in a first approximation by formula (8.13)

$$\zeta_{\max 1} = \left( \frac{3}{2} \frac{v_{\text{red}}^2}{A_1} \right)^{1/3} = \left( \frac{3 \cdot 0.338^2}{2 \cdot 1.825} \right)^{1/3} = 0.456 \text{ m.}$$

We substitute the obtained value  $\zeta_{\max 1}$  into the right side of formula (8.11) and find the depth of crushing in a second approximation

$$\begin{aligned} \zeta_{\max 2} &= \left( \frac{v_{\text{red}}^2}{\frac{2}{3} A_1 + \frac{1}{2} A_1 B \zeta_{\max 1}} \right)^{1/3} = \\ &= \left( \frac{0.338^2}{\frac{2}{3} \cdot 1.825 + \frac{1}{2} \cdot 1.825 \cdot 0.915 \cdot 0.456} \right)^{1/3} = 0.416 \text{ m.} \end{aligned}$$

The depth of crushing in a third approximation

$$c_{\max} = \left( \frac{v_{\text{red}}^2}{\frac{2}{3} A_1 + \frac{1}{2} A_1 B c_{\max}} \right)^{1/4} =$$

$$= \left( \frac{0,338^2}{\frac{2}{3} 1,825 + \frac{1}{2} 1,825 \cdot 0,915 \cdot 0,416} \right)^{1/4} = 0,433 \text{ m.}$$

We shall not make further approximations.

The maximum contact stress, taking bending into consideration, is determined by formula (8.14)

$$P_{\max} = \frac{1g \frac{\psi}{2} v_{\text{red}}^2 c_{\max}^3}{\sin \beta \cos^2 \beta} = \frac{1,400 \cdot 0,433^3}{0,485 \cdot 0,875^2} = 202 \text{ t.}$$

We obtain the maximum contact stress without taking bending of the ice into consideration by this same formula, substituting into the formula the value  $c_{\max} = 1$ , which was determined in the first approximation, i.e., without considering bending,

$$P_{\max} = \frac{1,400 \cdot 0,456^3}{0,485 \cdot 0,875^2} = 224 \text{ t.}$$

Decrease of the maximum contact stress because of bending of the ice  $\frac{224 - 202}{224} \cdot 100 = 9.8\%$ .

Determining contact stresses during an impact of a ship against the edge of an ice field having a small thickness. We shall consider the impact of a ship against the edge of a relatively thin ice field when crushing of the edge plays a secondary role in comparison with bending. This can be considered as a design situation when determining external stresses for river and sea vessels destined to sail in relatively thin ice. We shall disregard the work of crushing forces of the edge of the ice floe and, assuming that all of the reduced kinetic energy of the ship is converted into potential bending strain energy of the ice plate, we obtain

$$\frac{M_{\text{ired}} v_{\text{red}}^2}{2} = \frac{P_{\max}^2 \sin^2 \beta}{4 \sqrt{\gamma D}}.$$

From this, we find the maximum contact stress

$$P_{\max} = \frac{v_{\text{red}}}{\sin \beta} \sqrt{2 M_{\text{ired}} \sqrt{\gamma D}}. \quad (8.15)$$

Assuming for fresh ice  $E = 6 \cdot 10^5 \text{ T/m}^2$ ,  $\gamma = 1 \text{ T/m}^3$  and the Poisson coefficient  $\mu = 0.34$ , we obtain

$$P_{\max} = \frac{21.9 v_{\text{red}} M_{\text{ired}}^{1/2} h^{3/4}}{\sin \beta} \quad (8.16)$$

For sea ice  $E = 3 \cdot 10^5 \text{ t/m}^2$ , therefore

$$P_{\max} = \frac{18.4 v_{\text{red}} M_{1\text{red}}^{1/2} h^{3/4}}{\sin \beta} \quad (8.17)$$

Using the principle of least action, we obtain a differential equation for the ship's movement

$$M_{1\text{red}} \ddot{x}_1 = -\frac{2x_1 \sqrt{\gamma D}}{\sin^3 \beta} \quad (8.18)$$

and, satisfying the initial conditions where  $t = 0$ ,  $x_1 = 0$ ,  $\dot{x}_1 = v_{\text{red}} = v_{01}$ , we find the solution to equation (8.18)

$$x_1 = v_{\text{red}} \sin \beta \sqrt{\frac{M_{1\text{red}}}{2\sqrt{\gamma D}}} \sin \left( t \sqrt{\frac{2\sqrt{\gamma D}}{M_{1\text{red}} \sin^2 \beta}} \right) \quad (8.19)$$

The maximum value for  $x_1$  will occur when

$$t \sqrt{\frac{2\sqrt{\gamma D}}{M_{1\text{red}} \sin^2 \beta}} = \frac{\pi}{2},$$

from which, the impact time

$$t_1 = \frac{\pi}{2} \sqrt{\frac{M_{1\text{red}} \sin^2 \beta}{2\sqrt{\gamma D}}} \quad (8.20)$$

It should be kept in mind that the vertical component of contact stress  $P_{\max}$ , determined by formula (8.16) or (8.17), equal to  $P_{\max} \sin \beta$ , cannot be greater than the vertical stress  $P_{\text{frac}}$  which fractures ice covers of the specified thickness. Thus formulas (8.16) to (8.20) are valid in a case when

$$P_{\max} \sin \beta \leq P_{\text{frac}},$$

where  $P_{\text{frac}}$  is determined by formula (4.3).

$$P_{\text{frac}} = 0.52 \sigma_b h^2;$$

$h$  - is the thickness of the ice;  
 $\sigma_b$  - is the ultimate bending strength of the ice.

Determining contact stresses during an impact of a ship against a failing ice field. When a ship impacts against an ice field which is failing in bending, the contact stress grows from zero to the value  $P = P_{\text{frac}}$ , with which failure of the field occurs. The failure condition of an ice cover can be written in the form

$$P_{\max} \sin \beta = P_{\text{frac}}.$$

For realistic conditions of interaction between a ship's hull and ice, the magnitude of combined stress which causes ice failure is practically independent of the length of the contact stress distribution. Therefore, by replacing the distributed stress which causes ice failure with a concentrated load which is determined by formula (4.3), we obtain the failure condition of the ice cover

$$P_{\max} \sin \beta = 0,52 \sigma_c h^2.$$

From this, we find the magnitude of the contact stress which causes ice of a given strength and thickness to fail,

$$P_{\max} = \frac{0,52 \sigma_c h^2}{\sin \beta}. \quad (8.21)$$

If the thickness and strength of an ice field are given, the minimum velocity at which a ship will crush the ice with a determined sector of its side can be calculated by use of formula (8.21). For this, the magnitude  $P_{\max}$  should be computed by formula (8.21). Then, substituting it into expression (8.10),  $\zeta_{\max}$  should be computed and according to its value, the reduced velocity and velocity of the ship should be found by using formula (8.7).

#### 9. Relationship of the Magnitude of Contact Stresses to the Length of the Crushing Zone of the Ice.

The formulas presented in 7. and 8. for determining contact stresses are somewhat simplified if, instead of the edge configuration of the ice floe in the zone of contact with the ship, the length of crushing of the edge of the ice field is taken as an initial parameter. Consider, for example, the impact of a ship against an ice floe with a rounded edge, taking its bending into consideration. As follows from formula (7.2), the length of the zone of crushing  $b_0$  corresponding to the maximum contact stress  $P_{\max}$  equals

$$b_0 = 2 \sqrt{\frac{2R \zeta_{\max}}{\cos \beta}},$$

from which

$$\sqrt{2R} = \frac{b_0}{2} \sqrt{\frac{\cos \beta}{\zeta_{\max}}}. \quad (9.1)$$

Substituting the value  $\sqrt{2R}$  in formula (8.7), we determine the depth of crushing

$$\zeta_{\max} = \sqrt{\frac{M_{\text{ired}}^2 v_{\text{red}}^2}{\frac{16}{15} \frac{\sigma_c b_0}{\sin 2\beta} + \frac{2}{9} \frac{\sigma_c^2 b_0^2}{\cos^2 \beta \sqrt{\gamma D}}}}. \quad (9.2)$$

The formula for maximum contact stress (8.10), after substituting  $\sqrt{2R}$  and  $\zeta_{\max}$  into it, which were determined by expressions (9.1) and (9.2), can be presented in the form

$$P_{\max} = \frac{v_{\text{red}}}{\sin \beta} \sqrt{\frac{M_{\text{lred}} \sigma^b c^0}{\frac{6}{5} \text{ctg} \beta + \frac{1}{2} \frac{c_c b_0}{\sqrt{\gamma D}}}} \quad (9.3)$$

An analogous expression may also be obtained for a floe with an angular edge. As seen from Figure 11,

$$\text{tg} \frac{\psi}{2} = \frac{b_0 \cos \beta}{2x_{\max}} \quad (9.4)$$

Substituting the value  $\text{tg} \frac{\psi}{2}$  in formula (8.11), we determine the depth of crushing

$$\zeta_{\max} = \sqrt{\frac{M_{\text{lred}} v_{\text{red}}^2}{\frac{2}{3} \frac{c_c b_0}{\sin 2\beta} + \frac{1}{8} \frac{c_c^2 b_0^2}{\cos^2 \beta \sqrt{\gamma D}}}} \quad (9.5)$$

Formula (8.14) for maximum contact stress, taking expressions (9.4) and (9.5) into account, can be reduced to form

$$P_{\max} = \frac{v_{\text{red}}}{\sin \beta} \sqrt{\frac{M_{\text{lred}} \sigma^b c^0}{\frac{4}{3} \text{ctg} \beta + \frac{1}{2} \frac{c_c b_0}{\sqrt{\gamma D}}}} \quad (9.6)$$

When the ice thickness is relatively great, the second term in the denominator of the radicand which takes the bending of the ice into account, can be disregarded inasmuch as the primary part of the energy in this case is expended on crushing the ice. Then formulas (9.3) and (9.6) take the form:

for an ice floe with a rounded edge

$$P_{\max} = 1.29 v_{\text{red}} \sqrt{\frac{M_{\text{lred}} \sigma^b c^0}{\sin 2\beta}} \quad (9.7)$$

for an ice floe with an angular edge

$$P_{\max} = 1.23 v_{\text{red}} \sqrt{\frac{M_{\text{lred}} \sigma^b c^0}{\sin 2\beta}} \quad (9.8)$$

The obtained formulas for contact stresses are practically the same even though they were derived for essentially different forms of ice field

edges in the zone of contact with a ship. This indicates that both formulas can be used to determine the magnitude of contact stress when a ship strikes against ice having an arbitrary outline. Moreover, the solution to the problem under consideration is presented in closed form, not requiring subsequent approximations to determine the magnitude of contact stress.

Formulas (9.3) and (9.6) coincide in structure with the formula obtained by L. M. Nogid [33]. Such coincidence is a consequence of identical assumptions for the nature of interaction between a ship's hull and ice.

It must be noted that for practical calculations, it is more rational to use formulas expressing contact stresses in relation to the configuration of the edge of the ice floe and not to the length of the crushing zone  $b_0$ . The unknown parameters  $R$  and  $\psi$ , which characterize the configuration of the edge in the contact zone, do not depend on elements of the ship and physical and mechanical characteristics of the ice. The average values of these parameters which are necessary to determine ice loads can be computed on a basis of processed materials concerning ice damage to ships' hulls and an evaluation of their construction strengths. The unknown parameter  $b_0$  essentially depends on elements of the ship and physical and mechanical characteristics; this makes it difficult to determine its average values which are necessary for computing ice loads. However, in individual situations, formulas (9.3) and (9.6) allow the magnitude of the ice load along a given length of its distribution to be found. Rearranging this expression, it is possible to obtain an equation for an impact against a protruding angle of the edge of a field

$$\frac{M_{\text{ired}} v_{\text{red}}^2}{2} = \frac{P_{\text{max}}^2 \sin^2 \beta}{4\sqrt{\gamma D}} + \frac{1}{3} \frac{P_{\text{max}}^2 \sin 2\beta}{b_0 \sigma_c},$$

and for impact against a rounded edge

$$\frac{M_{\text{ired}} v_{\text{red}}^2}{2} = \frac{P_{\text{max}}^2 \sin^2 \beta}{4\sqrt{\gamma D}} + \frac{1}{3.33} \frac{P_{\text{max}}^2 \sin 2\beta}{b_0 \sigma_c}.$$

The obtained expressions are energy balance equations. In contrast to general expression (8.1), length  $b_0$  appears in them instead of the depth of crushing of the edge  $\zeta$ . Obviously, here also, the configuration of the ice's edge has no essential value.

Substituting in these expressions the ice fracturing stress according to (8.21), we obtain a design equation for determining the minimum velocity of a ship at which failure of the ice cover will occur

$$v_0 = \frac{0.52 \sigma_c h^3}{l_1} \sqrt{\frac{\frac{6}{5} \text{ctg} \beta + \frac{1}{2} \frac{\sigma_c b_0}{\sqrt{\gamma D}}}{b_0 \sigma_c M_{\text{ired}}}} \quad (9.9)$$

With a reduction in thickness and an increase in the ice's ultimate crushing strength  $\sigma_c$ , crushing of the edge will have little effect on the magnitude of ice loads. In view of this, by disregarding the first member of the numerator of the radicand in expression (9.9), which allows for crushing, we obtain

$$v_0 = \frac{0.52\sigma_b h^2}{l_1} \cdot \frac{1}{\sqrt{2M_{lred} \sqrt{\gamma D}}} \quad (9.10)$$

Solving this expression for  $h$ , we obtain

$$h = 1.79 \sqrt[5]{\frac{\gamma E (M_{lred} v_{red}^2)^2}{4(1-\mu^2)\sigma_b^4}} \quad (9.11)$$

Formula (9.11) allows the thickness of the ice being forced to be estimated in the first approximation for a given velocity. This problem relates to questions of the passability of ice which directly touch upon the problem of external forces.

#### 10. Impact of a Ship Against Ice, Accompanied by Wedging and a Reverberated Impact.

During movement of a ship in ice, a situation is possible in which both sides simultaneously come into contact with an ice cover and the ship, not fracturing the cover, comes to a stop. This situation of interaction between a ship and ice is called a wedging impact. Let us consider the process of a wedging impact of a ship into an ice field, assuming that the points of contact are symmetrically located, relative to the longitudinal plane (Figure 14).

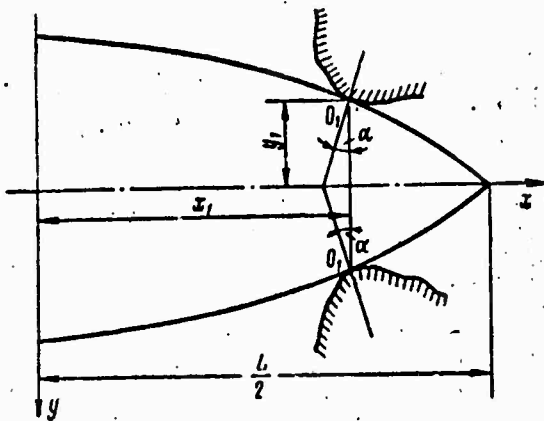


Figure 14. Diagram of an impact with wedging.

During a wedging impact, a ship can have three translations:

translation in the direction of axis Ox, accompanied by crushing of the edge of the ice;

trim, brought about by the vertical components of the contact stresses;

broaching, caused by these same components.

Using the same assumptions and specifications as were used in 5., we shall write the following equations for momentum and angular momentum

$$\left. \begin{aligned} M_1(1 + \lambda_{11})v_1 - v_0 &= -2l_1S, \\ M_1(1 + \lambda_{22})\omega_1 &= -2n_1S, \\ I_{y_1}(1 + \lambda_{13})q_1 &= 2x_1n_1S. \end{aligned} \right\} \quad (10.1)$$

The numerical coefficient, 2, is introduced because the impact occurs simultaneously on both sides. Assuming as was previously done, that the coefficient of restitution  $\epsilon = 0$ , i.e., considering the impact as being inelastic, we obtain a subsidiary condition of the ship's velocity in the direction of the normal to the side at the end of the impact equaling zero:

$$l_1v_1 + n_1\omega_1 - q_1x_1n_1 = 0. \quad (10.2)$$

Solving equations (10.1) and (10.2) jointly, we obtain an expression for impact momentum

$$S = \frac{v_0 l_1 M_1}{2 \left[ \frac{l_1^2}{1 + \lambda_{11}} + \frac{n_1^2}{1 + \lambda_{22}} + \frac{n_1^2 x_1^2}{I_{y_1} (1 + \lambda_{13})} \right]} = v_{\text{red}} M_{\text{ired}}, \quad (10.3)$$

where  $v_{\text{red}} = v_0 l_1$  = is the reduced velocity of the ship;

$M_{\text{ired}} = \frac{M_1}{C'}$  = is the reduced mass of the ship;

$C'$  = is a coefficient of the ship's reduced mass:

$$C' = 2 \left[ \frac{l_1^2}{1 + \lambda_{11}} + \frac{n_1^2}{1 + \lambda_{22}} + \frac{n_1^2 x_1^2}{I_{y_1} (1 + \lambda_{13})} \right].$$

It is not difficult to show that in the case of impact of a ship against an ice floe of finite dimensions, expression (10.3) by analogy with formula (5.4), is written in the form

$$S = \frac{M_1}{C'} \cdot \frac{v_0 l_1}{1 + \frac{M_1}{C'} \cdot \frac{C''}{M_2}},$$

where  $M_2$  - is the mass of the ice floe;

$C''$  - is a coefficient allowing for the reduced mass of the ice floe:

$$C'' = 2 \left[ \frac{I_2}{1 + \lambda'_{11}} + \frac{n_2^2}{1 + \lambda'_{22}} + \frac{R^2 n_2^2}{I_y (1 + \lambda'_{12})} M_2 \right]$$

In this case, the above-obtained equations can be used to determine the magnitude of contact stresses during a wedging impact of a ship, substituting the coefficients of reduced masses  $C'$  and  $C''$  in them.

When a ship is moving through ice, reverberated impacts are also observed when a ship having struck the ice with one side, is sharply deflected in the opposite direction and strikes the ice with its other side. In this case, the projected velocity of the ship on the normal at the point of the second impact, will be greater than with the first impact. Correspondingly, contact stresses also grow and frequently lead to serious damages. Specifically, such damages occurred on the icebreaker Ermak during its first Arctic cruise [31], as well as on several transport vessels of various ice classes. Large dents in the plating and strains in the side framing occurred as a result of reverberated impacts. In several cases, leaks occurred in the ship's hull.

Let us consider a case in which a ship moving at velocity  $v$  has struck an ice field or an ice floe of finite dimensions with its starboard side. The impact took place at a point with coordinates  $x_1, y_1$ . Using the formulas from the preceding paragraphs, it is possible to determine the magnitude of impact momentum and contact stress during this impact. Knowing the magnitude of the impact momentum  $S$ , it is possible to determine all six velocities of the reverberating ship from the system of equations (5.1). If the time interval from the first impact on the starboard side until the reverberated impact on the port side is small, the velocity obtained after the first impact should be used as the initial velocity for the second impact. If the time between impacts is great, then it is necessary to consider only the first impact.

If, during the second (reverberated) impact, a ship strikes the edge of the ice field, the shock impulse for this situation can be written in the following form:

$$S = \frac{M_1}{C'} v_{O1}^{\text{red}} = M_{1\text{red}} v_{\text{red}}$$

where the coefficient of reduced mass  $C'$  is determined by formula (5.5), and the reduced velocity, taking into account the conversion from the left to the right side system of coordinates, is calculated as

$$v_{\text{red}} = v_1 l_2 - u_1 m_2 + w_1 n_2 - p_1 \lambda_2 + q_1 \mu_2 - r_1 \nu_2 \quad (10.4)$$

Subscript 1 refers to the first impact at point  $(x_1, y_1)$ , subscript 2, to the reverberated impact at point  $(x_2, y_2)$ . Velocities  $v_1, u_1, \omega_1, p_1, q_1$  and  $r_1$  can be calculated by expressions (5.1) and (5.7):

$$\left. \begin{aligned} v_1 &= v_0 \left[ 1 - \frac{l_1^2}{C'(1+\lambda_{11})} \right]; & u_1 &= -v_0 \frac{l_1 m_1}{C'(1+\lambda_{11})}; \\ \omega_1 &= -v_0 \frac{l_1 n_1}{C'(1+\lambda_{11})}; & p_1 &= -v_0 \frac{M_1 l_1 (y_1 n_1 - z_1 n_1)}{C' l_{x_1} (1+\lambda_{11})}; \\ q_1 &= -v_0 \frac{M_1 l_1 (z_1 l_1 - x_1 n_1)}{C' l_{y_1} (1+\lambda_{11})}; & r_1 &= -v_0 \frac{M_1 l_1 (x_1 m_1 - y_1 l_1)}{C' l_{z_1} (1+\lambda_{11})}. \end{aligned} \right\} \quad (10.5)$$

We note that translations of the ship at velocities  $v_1$  and  $u_1$ , as well as rotation  $r_1$  around axis Oz are nonperiodic. If the time between the first and second impacts is small, these velocities do not have sufficient time to decrease as a result of resistance of the medium. Thus, their values which are determined by formulas (10.5) can be substituted.

Translations with velocities  $\omega_1, p_1$  and  $q_1$  correspond to the non-stationary modes of heaving, rolling and pitching of the ship. Strictly speaking, velocity values, computed with time between impacts taken into consideration, should be substituted in formula (10.4). When doing this, the resulting reduced velocity  $v_{red}$  will be either increased or decreased, depending on the relationship of the time between impacts to the period of tossing. As observations under ice conditions show, the corresponding translations of the ship are small. Therefore, the velocity of ship's broaching  $\omega_1$  and angular velocities  $p_1$  and  $q_1$ , corresponding to list and trim, can be ignored in expression (10.4). Then:  $v_{red} = v_0^1 red$ , where

$$v_{red}^1 = l_2 - \frac{l_2^2}{C'} + \frac{l_1 m_1 m_2}{C'(1+\lambda_{11})} + \frac{M_1 l_1 (x_1 m_1 - y_1 l_1) (x_2 m_2 - l_2 y_2)}{l_{x_1} C' (1+\lambda_{11})}. \quad (10.6)$$

Calculations show that  $v_{red}^1 > v_0^1 l_2$ . This indicates that contact stresses will be greater during a reverberated impact than during a direct impact. The reduced velocity  $v_{red}^1$  will differ from zero, even for the area of the parallel middle body where  $l_2 = 0$ .

Figure 15 gives values of the coefficient of reduction for  $v_{red}^1$  during a reverberated impact in the area of the first and tenth frame lines computed for a heavy icebreaker. It can be seen from the figure that the maximum value of  $v_{red}^1$  is obtained in the area of the third and fourth frame lines, regardless of where the impact occurs.

Figure 16 presents values for  $v_{red}^1$  for various areas of the hull during a direct impact in the area of the third frame line; the lower curve corresponds to a direct impact, the upper to a reverberated impact. If, for example, for the first frame line,  $v_{red}^1$  and consequently, also  $v_{red}^1$  during a reverberated impact, are 1.5 times greater than  $v_{red}^1$  and  $l_{red}^1$  during a direct impact, this difference increases to more than 2.5 times for the eighth frame line.

2

It is possible to use the relationships shown in Figure 15 for ships having lines similar to the icebreaker Moskva, scaling  $l_{red}$  proportionally to the ratio between the coefficients  $l_1$  for the icebreaker Moskva and the ship being considered. For ships having contours which substantially differ from the hull lines of the icebreaker Moskva, it is necessary to perform preliminary calculations in the method set forth in this paragraph. Finding the value  $l_{red}$  in this way, the magnitude of contact stresses should be determined by formulas 6. to 8.

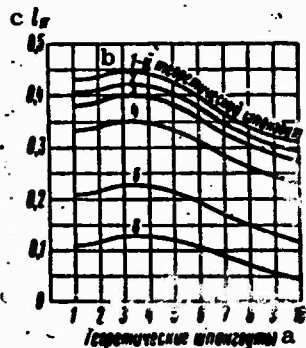


Figure 15. Values of coefficient  $l_{red}$  for a heavy icebreaker. a-frame lines; b-first frame line; c- $l_{red}$ .

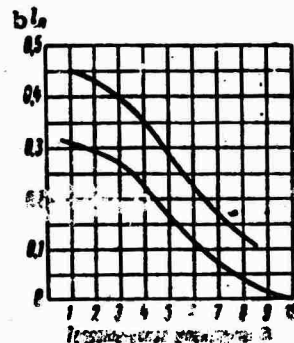


Figure 16. Values of coefficient  $l_{red}$  during direct and reverberated impacts. a-frame lines; b- $l_{red}$ .

#### 11. Magnitude of Stresses Occurring During Ice Compression of A Ship.

Determining loads which act on a ship's hull during ice compression is part of the overall problem of contact stresses experienced by hull structures of a ship sailing in ice.

Ice compression can be considered as a static process. It is most dangerous when a ship is moving in a large, compact, ice field. Taking the static nature of ice compression into consideration, an ice field can be considered as a homogeneous plate resting on a hydraulic-type flexible foundation. In this situation, the problem of static action of the system of vertical and horizontal forces on this plate should be solved.

It is natural to assume the critical load which fractures ice of the given thickness, as the design external loads acting on the ship's hull during compression. If the ship's strength is inadequate, the ship can be damaged or even crushed by the ice.

Observations of compression on icebreakers show that failure of an ice field occurs primarily because of bending; this explains the considerable vertical slope of icebreakers' sides. In view of this, larger ice floes break off at the midsection where the slope of the sides is less

than at the ends and the curvature of the waterline is relatively small. Smaller fractures of the field are observed at the extremities.

If, during movement of the ice, one of the edges of the channel is immobile, local crushing of this edge and minor hummocking occur during compression of a ship. Failure and intensive hummocking of the ice are observed on the moving edge. Ice on this side piles up as high as the main deck in some cases. There have been cases when icebreakers with a significant slope in their sides amidships (15 to 18°) have been pressed up to a height of 1m or more during ice compression.

Ice failure at the extremities of ice cargo ships where slope of the side is great, generally occurs the same as for icebreakers, i.e., because of bending of the ice field. In the midsection of a ship having a parallel middle body, where the side is either vertical or slightly inclined, the nature of ice failure changes somewhat. Initially, irregularities in the walls of the channel break off, then the ice field adjoins the greatest part of the parallel middle body. Failure of the ice field in this area resembles the failure of a plate resulting from loss of stability affiliated with axial compressive stresses. In this case, loads acting on the hull will considerably exceed the stresses which fracture ice because of bending and present a great danger to the side structures, as a whole.

Ice compression can be conditionally divided into two stages. In the first stage (local crushing), protruding sectors which quickly crumple or are broken off, come into contact with the side. Stresses occurring at this time are distributed over comparatively small areas encompassing small segments of the side structures. In the second stage, after protruding sections have broken off, large segments of the side come into contact with the ice. Contact pressures which occur in connection with this are spread over a large part of the ship.

It should be kept in mind that it is extremely difficult to fix boundaries between these two stages of compression, just as it is extremely difficult to determine which of the types of compression are more dangerous to a ship's side structures. However, there is basis to assume that the second stage of compression, in spite of the comparatively smaller magnitude of linear loads, is in some cases more dangerous to a ship as a whole because it can cause grave damages over a large hull area.

The overall compression of a ship in an ice field can be considered as analogous to the impression of a hard stamp (ship) into an elastic half-plane (ice field). Direct application of analytical dependencies of the theory of elasticity contact problem is impossible in this case because of the large number of undetermined factors which cause overall compression of a ship. Therefore, the magnitude of external loads which act on a ship's hull during overall compression shall be determined by starting from the conditional design plans presented below. We shall consider two situations: compression of ships having sloping sides amidships and compression of ships having vertical sides.

Results obtained by theoretical means will subsequently be compared with the actual strength of icebreakers and ice-class cargo ships sailing in the Arctic.

Compression of a ship with sloping sides. When a ship is compressed in an ice field, the edge of the ice crushes until the total contact stress reaches a magnitude which crushes ice covers. When solving the problem of strain on a floating ice plate, it was shown that for the actual ratio of the length of the crushing zone  $b_0$  to the thickness of the ice ( $b_0/h < 10$ ), the magnitude of the total fracturing stress is practically independent of the length  $b_0$ . Therefore, we shall evaluate the strength of the ice field by determining the magnitude of the concentrated stress  $P$ , which fractures the plate.

The magnitude of the ice fracturing stress for a semi-infinite plate can be determined by expression (8.21)

$$P_{\text{frac}} = 0.52 \frac{\sigma_b h^2}{\sin \beta},$$

where  $\sigma_b$  - is the ultimate bending strength of ice;  
 $h$  - is the ice thickness;  
 $\beta$  - is the vertical slope of the side.

A projection of the edge of the ice field comes into contact with the side during compression. Assuming that the side of the ship in the contact zone is flat and that the projection is described as an arc with a radius  $R$ , we shall use formulas presented in 8. to determine the length of the crushing zone and the magnitude of contact stress. The total contact stress is determined by formula (8.10)

$$P_{\text{max}} = \frac{4}{3} \frac{\sigma_b h^2 \sqrt{2R}}{\sin \beta \cos^2 \beta}$$

Equating the right sides of expressions (8.10) and (8.21), we shall determine the maximum depth of crushing from the obtained equation at which failure of the ice field will occur.

$$\zeta_{\text{max}} = 0,534 \left( \frac{\sigma_b}{\sigma_c} \right)^{2/3} \frac{h^{2/3} \cos \beta}{(2R)^{1/3}} \quad (11.1)$$

Using formula (7.2), for the length of the crushing zone corresponding to  $\zeta_{\text{max}}$ , we obtain

$$b_0 = 1,46 \sqrt[3]{2R h^2 \frac{\sigma_b}{\sigma_c}}, \quad (11.2)$$

from which

$$\frac{b_0}{h} = 1,46 \sqrt[3]{\frac{2R}{h} \frac{\sigma_b}{\sigma_c}}$$

Thus, the relative length of the crushing zone of the edge decreases with an increase in ice thickness which is confirmed by natural observations.

Compression of a ship with vertical sides. When there is pressure by an ice cover on a vertical side, contact stresses act in the plane of the ice field. When the slope angles are small, the side may also be considered as vertical. The magnitude of the ultimate slope  $\beta_{ult}$  at which a side is considered to be vertical is evaluated, proceeding from the following considerations.

When there is a sloping side, an ice plate fails when the normal tensile stresses on its external surface (in the extreme fibers of the section) exceed the bending strength of ice  $\sigma_b$ . The horizontal component of the contact stress in this case, increases these stresses on one side and on the other, decreases them (because of crushing). When the slope of the side is greater than 5 to 10°, these factors neutralize each other and the carrying capacity of the plate is determined primarily by the vertical component of the contact stress, i.e., by the bending. This provides basis for using formula (8.21) for calculations.

We arrive at analogous values for the ultimate slope angle by considering the friction of the ice against the side of the ship during compression during which, in all cases where  $\beta \leq \arctg f_f$  (where  $f_f$  is the coefficient of friction of ice against steel), the side can be considered as vertical. Considering that  $f_f = 0.15$ , we obtain  $\beta = 8^\circ$  for an ultimate slope angle.

Failure of an ice cover by action of stresses applied to its plane can occur either as a consequence of loss of stability of the ice plate or under the effect of shear stresses. From the theoretical solution to the problem of stability of a floating, semi-infinite ice plate under the effect of a concentrated force applied to its edge, it follows that the magnitude of critical force causing loss of stability and ice failure, considerably exceeds the magnitude of the stress causing the appearance of radial cracks from shearing. Actual observations also show that ice failure in case of a vertical side, begins with formation of cracks and then losses of stability of the ice cover and breaking off of floes occur. This gives basis to assume that cracks are formed in an ice field as a result of shear stresses,

From the solution of the two-dimensional problem of the theory of elasticity, it is known that maximum shear stresses for load  $q$ , occurring in sections 1 and 2 (figure 17), are determined by the expression

$$\tau = \frac{q}{\pi h}, \quad (11.3)$$

where  $h$  - is the thickness of the plate;  
 $q$  - is the intensity of the linear load on the plate.

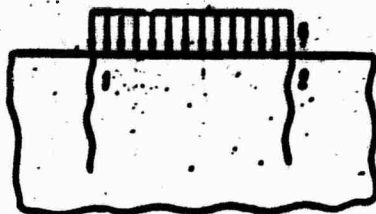


Figure 17. Formation of cracks in an ice cover during compression.

The moment of crack formation corresponds to the advance of shear stresses to the ultimate shearing strength of ice  $\tau$ . For fresh ice, N. F. Yershov (16), assumes  $\tau = 60 \text{ t/m}^2$ . Experimental data shows that  $\tau = 30 \text{ t/m}^2$  can be assumed as the ultimate shearing strength of sea ice. Then, a uniform linear load which causes the appearance of cracks in sea ice is determined by the expression

$$q = \pi \cdot h = 94h \text{ t/m.} \quad (11.4)$$

The segment of the plate in which the cracks are formed loses its stability as being flexible along its cylindrical surface (strip). The magnitude of critical stress for the strip

$$\gamma_{cr} = \sqrt{\gamma D}, \quad (11.5)$$

where  $\gamma$  - is the specific weight of water;

$D$  - is the flexural stiffness of the ice plate (see 4.).

Assuming that with compression which is a static process,  $E = 4 \cdot 10^4 \text{ t/m}^2$  and  $\gamma = 1 \text{ t/m}^3$  and  $\mu = 0.34$ , we obtain

$$\gamma_{cr} = 62h\sqrt{h} \text{ t/m.} \quad (11.6)$$

Comparing the obtained value  $\gamma_{cr}$  with the magnitude  $q$  determined by formula (11.4), it is easy to be convinced that in the range of thicknesses up to  $h = 2.2\text{m}$ , which presents the greatest practical interest,  $q > \gamma_{cr}$ , i.e., loss of stability occurs immediately after cracks are formed.

In the first stage of compression when relatively small irregularities of the edge of the ice are broken off, ice load distribution along the side does not depend on the rigidity of the side structures. As a consequence of the considerable magnitude of the inelastic crushing strain of the ice's edge in comparison with the elastic strain, a different rigidity of side grillage cannot exert a substantial effect on redistribution of the ice load. Otherwise, there is a situation of overall compression of a ship when ice adjoins the side for a considerable length. In this case, the ice cover strains elastically and redistribution of the contact ice loads must take place. This redistribution can be extremely important for ice cargo ships in which transverse bulkheads are placed a considerable distance from each other and there are no frames.

An analysis of the functioning of the side grillage can be made in a first approximation by using the formulas for calculating a wall

beam\*, which is used in construction work. In the case under consideration, the ice field is the wall, the side grillage is the wall beam and the transverse bulkheads are the columns.

\* A beam which bears the load from wall pressure and is supported on columns is called a wall beam.

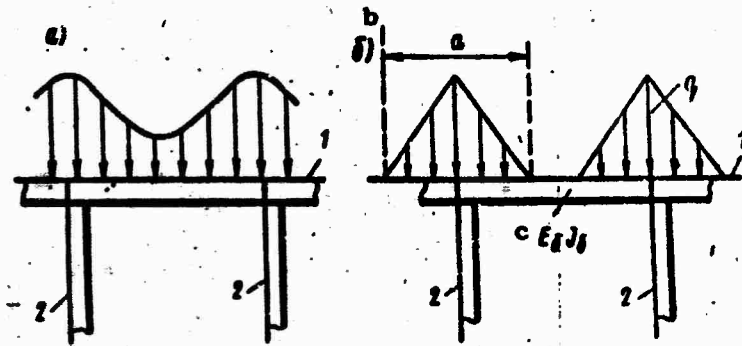


Figure 18. Diagram of the redistribution of contact stresses during ice compression.  
1-side; 2-transverse bulkheads; a-b;  $b-E I_s$ .

The load on the beam increases near the supports (bulkheads) and decreases toward the center of the span. Its curve takes the form depicted in Figure 18a. For practical purposes, a curve consisting of triangles can be assumed (Figure 18b). Failure of ice cover in this case begins with formation of cracks at the maximum load sites, i.e., principal compressive stress in the area of the bulkhead reaches the ultimate static compressive strength of ice. We shall assume the following expression for stress  $q$  which fractures ice covers

$$q = \frac{c_0 h}{\sqrt{2}} \quad (11.7)$$

The total stress, experienced chiefly by the transverse bulkhead and partially borne by the frames,

$$P = \frac{qa}{2} = \frac{c_0 a h}{2\sqrt{2}} \quad (11.8)$$

where  $a$  - is a coefficient determined according to B. N. Zhemochkin's recommendation [18],

$$a = 3,3 \sqrt{\frac{E_s I_s}{E_i h}} \quad (11.9)$$

$E_i$  - is the modulus of elasticity for ice;

$E I_s$  - is the reduced rigidity of the side grillage.

If a load is directly applied to a side stringer, the moment of inertia of the stringer with its attached flange can be taken as  $I$ . For a load applied to the span between stringers, the magnitude  $E I_s$  must be determined by calculating the side grillage.

Taking into consideration that a sector of an ice field bounded by cracks, loses its stability as a plate which is bending along its cylindrical surface, the critical load, determined by expression (11.5) should be taken as the critical design load for side grillage with ice up to 2.2m thick. For ice of greater thickness, the reserve stability of an ice plate is very large and the magnitude of the design load for the grillage, in this case, is determined by the ultimate crushing and shearing strength of the ice.

The formulas presented in this paragraph make it possible to compute design loads for side framing in the midsection of ice ships depending on ice compression conditions as well as to solve the reverse problem: to determine, for the known strength of the side framing, the maximum thickness of ice in which a ship can be compressed without damage.

## CHAPTER III

### CALCULATING MAGNITUDES OF DESIGN ICE LOADS FOR MAIN HULL BRACINGS

#### 12. Loads on Side Framing.

The first stage when planning and designing hull structures of ice ships and icebreakers is to calculate the magnitude of ice loads which act on the side framing and external plating of a ship's hull. This chapter gives a practical method for calculating ice loads, based on previously-cited investigations. Contact stresses which occur during impact of a ship against ice and during ice compression are used as initial data.

Before moving on to the essence of the matter, it is necessary to bring to mind that the magnitude of an ice load basically depends on the configuration of the edge of the ice floe in the area of its contact with the side. Generally speaking, the shape of the edge can be most varied. Therefore, for design ice loads, it is necessary to set the outlines of a floe's edge in the area of contact with the ship's side in such a way that the hull strength calculated according to these loads will guarantee accident-free operation of ships in ice. Investigation of this matter and observations have shown that the most acceptable of the number of possible configurations is an edge of a floe defined as an arc of a circle. Results of comparing the construction strength of ships in operation with design values of the ice load for some certain type and class of ship obtained by the suggested method, are taken into consideration when selecting a numerical value for radius R of this circle.

Calculations have shown that if the magnitude of the radius R is set within the range of 10 to 40m, the value of the impact time and the length of the ice load distribution computed theoretically, well agree with data of actual observations and are confirmed by operating experience of ships in ice. Inasmuch as the magnitude of the radius of the circular ice edge in the contact area has a relatively small effect on the ice load intensity, for example, when changing the radius four times (from 10 to 40 m), the intensity of the ice load changes only by 30%. A radius of 25m was taken as a mean within the indicated range for practical calculations.

An ice load acting on a ship's bow\* is determined for the case of an impact against an individually floating floe or an ice field, with and without, taking its bending into account. The design ice load should be computed by relating the total contact strength  $P_{max}$  to the length of the distribution area b along the ship's side. Magnitude b is defined as the length of the contact area between the hull and the ice, corresponding to

the maximum value of contact stress. The numerical value of  $b$  is determined from the crushing conditions of the ice's edge in the contact area.

---

\* In the given case, bow means that part of the hull where impact loads are larger than the compressive loads in the midsection.

---

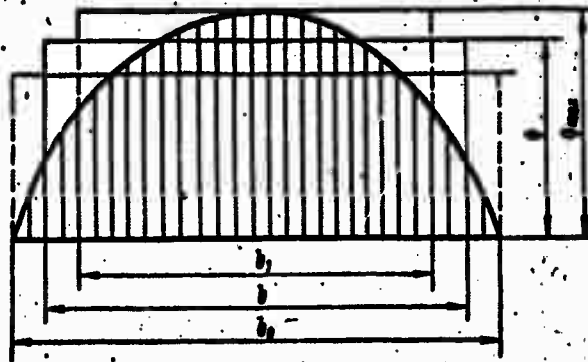


Figure 19. Finding the design length of load distribution.

It is evident from Figure 10 that the area of crushing of the ice's edge has a parabolic segment's form. The length of this area is calculated by formula (7.2). The distribution curve of contact stress along the length also has the form of a parabolic segment (Figure 19), the area of which

$$P_{\max} = \frac{2}{3} b_0 q_{\max},$$

where  $q_{\max}$  - is the maximum ordinate of the curve.

We shall assume that the design contact stress is equally distributed on length  $b$ , which is defined as an arithmetical mean between  $b_0$  and  $b_1$ , where  $b_1$  is found from the condition of equality of areas

$$\frac{2}{3} b_0 q_{\max} = b_1 q_{\max},$$

from which

$$b_1 = \frac{2}{3} b_0, \text{ and } b = \frac{b_0 + b_1}{2} = \frac{5}{6} b_0.$$

In this case, taking (7.2) into account, we can write

$$b = \frac{5}{3} \sqrt{\frac{2R'_{\max}}{\cos \beta}}. \quad (12.1)$$

Using formulas (8.10) and (12.1), we obtain an expression for the intensity of the design ice load during an impact of a ship against an ice floe with a rounded edge

$$q_{\text{bow}} = \frac{P_{\text{max}}}{b} = \frac{4 \cdot c_c' c_{\text{max}}}{5 \sin^2 \beta \cos^2 \beta} \quad (12.2)$$

Substituting the maximum depth of crushing  $c_{\text{max}}$ , calculated by formula (7.6) into this expression and taking (7.5) into consideration, we obtain

$$q_{\text{bow}} = \frac{4}{5} \left( \frac{15}{16} \right)^{1/2} \left( \frac{M_1}{C' + C' \frac{M_1}{M_2}} \right)^{1/2} \frac{\sigma_c'^{1/2} v_{\text{red}}'^{1/2}}{(2R)^{1/2} \sin^{1/2} \beta \cos^{1/2} \beta}$$

Substituting the reduced velocity of the ship in the form of  $v_{\text{red}} = v_0' = 0.514 v_1'$  (where  $v_1'$  is the ship's velocity in knots) and designating  $M_1 = D_1/g$ ,  $M_2 = D_2/g$  (where  $D_1$  is the ship's displacement and  $D_2$  is the weight of the ice floe). For the case of impact of a ship against a floe with a circular edge radius of  $R = 25$  m, we obtain

$$q_{\text{bow}} = 0,084 \left( \frac{D_1}{C' + C' \frac{D_1}{D_2}} \right)^{1/2} \frac{\sigma_c'^{1/2} v_1'^{1/2}}{\sin^{1/2} \beta \cos^{1/2} \beta} \quad (12.3)$$

For an impact of a ship against an infinite ice field when  $D_1/D_2 \rightarrow 0$ , formula (12.3) is simplified and takes the form

$$q_{\text{bow}} = 0,084 \left( \frac{D_1}{C'} \right)^{1/2} \frac{\sigma_c'^{1/2} v_1'^{1/2}}{\sin^{1/2} \beta \cos^{1/2} \beta} \quad (12.4)$$

In formulas (12.3) and (12.4), the displacement of the ship and weight of the ice floe are assumed in tons and the crushing strength of the ice  $\sigma_c'$  in  $t/m^2$ . The magnitude of the cosine of the angle between the normal to the side and axis  $x_1$  can be computed with adequate accuracy by formula

$$l_1 = 0,01 \alpha m, \quad (12.5)$$

where  $\alpha$  - is the angle between a tangent to the waterline at the point of impact and the longitudinal plane, in degrees;

$m = 1.6 \cos \beta + 0.11$  - is a coefficient, calculated in dependence on angle  $\beta$  in Figure 23.

For convenience in calculating, formula (12.3) can be presented in its ultimate form

$$q_{\text{bow}} = 780 \frac{k_D k_\sigma k_v k_\beta}{k_p} \quad (12.6)$$

where  $k_D = \left[ \frac{D_1}{10^4 (C' + C'' \frac{D_1}{D_2})} \right]^{1/2}$  - is a coefficient, allowing for the effect of the reduced masses of the ship and ice floe;

$k_\sigma = \left( \frac{\sigma_c}{400} \right)^{1/2}$  - is a coefficient allowing for the crushing strength of the ice;

$k_v = \left( \frac{v_{v1}}{2.35} \right)^{1/2}$  - is a coefficient allowing for the reduced velocity of the ship;

$k_\beta = \frac{\sin^{3/2} 8^\circ \cos^{3/2} 8^\circ}{\sin^{3/2} \beta \cos^{3/2} \beta}$  - is a coefficient allowing for the effect of the vertical slope of the frame.

Coefficients  $k_D$ ,  $k_\sigma$ ,  $k_v$  and  $k_\beta$  are determined from the graphs in Figures 20 to 23. When computing these coefficients, a ship displacing  $D_1 = 10,000$  t striking against ice having a crushing strength of  $\sigma_c = 1400$  t/m<sup>2</sup> was used as a standard.

When computing the magnitude of an ice load on the side framing of the bow, the following order of calculations must be observed:

1. the values of angles  $\alpha$  and  $\beta$  for each frame line are taken from the line drawing (Figure 24). For ice ships, these angles are taken at the level of the load waterline and for icebreakers, at the level of the designer's waterline. To check the accuracy of assumed angles  $\alpha$  and  $\beta$ , it is necessary to construct a graph of the changes of these angles (Figure 25), and if the curves are not adequately even, smooth them out and introduce corrected angles into the calculations. Particular attention must be given to accuracy in calculating angles  $\alpha$  and  $\beta$  when they are small. If, for any hull sector, angle  $\beta$  is less than  $8^\circ$ , angle  $\beta$  should be taken as equal to  $8^\circ$  for that sector;

2. coefficients  $C'$  and  $C''$  are found on graphs presented in Figures 5 and 6, depending on angle  $\beta$  and the relative coordinate of the point of impact  $x/L$ ;

3. characteristic  $l_1 = 0.01$  cm is calculated by formula (12.5);

4. characteristic  $\frac{D_1}{C' + C'' \frac{D_1}{D_2}}$  is calculated, where  $D_1$  is

displacement, taken for an ice ship at its load waterline and for an icebreaker, its greatest displacement;  $D_2$  is the weight of the ice floe. If an impact against the edge of an infinite field occurs, instead of characteristic  $\frac{D_1}{C' + C'' \frac{D_1}{D_2}}$ , characteristic  $\frac{D_1}{C'}$

as in this situation  $\frac{D_1}{D_2} \rightarrow 0$ . Coefficient  $k_D$  is determined from the graph presented in Figure 20, depending on the relationship  $\frac{D_1}{C' + C'' \frac{D_1}{D_2}}$  or

$$\frac{D_1}{C'}$$

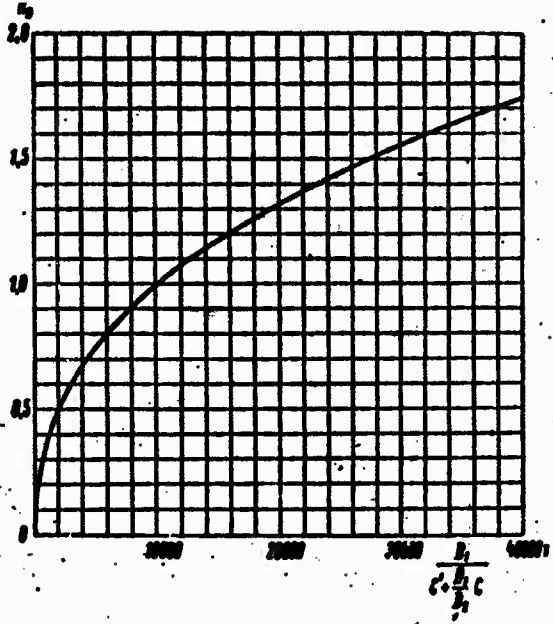


Figure 20. Values of coefficient  $k_D$ .

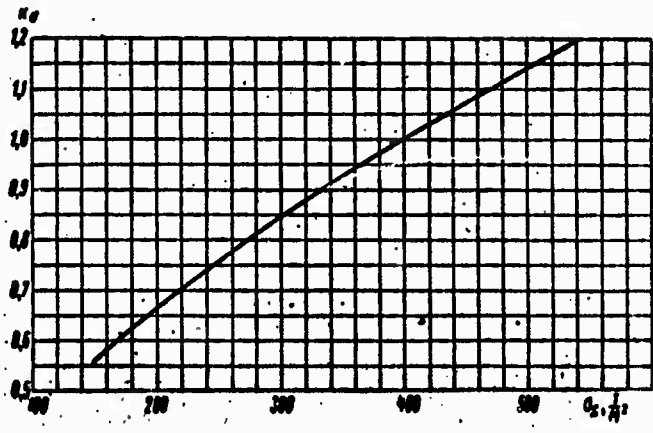


Figure 21. Values of coefficient  $k_G$ .

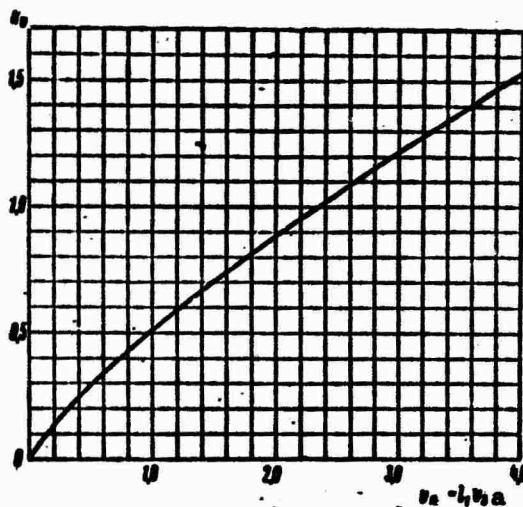


Figure 22. Values of coefficient  $k_v$ .  $a - V_{red} = l_1 V_s$ .

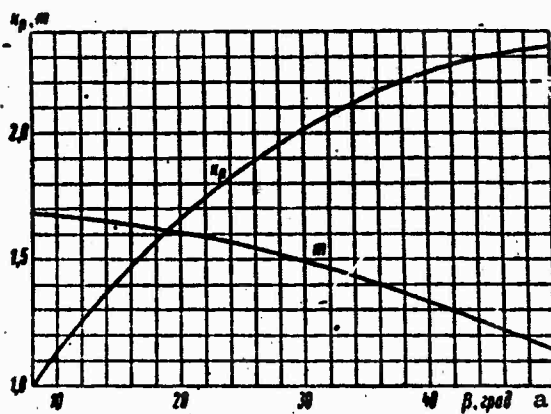


Figure 23. Values of coefficients  $k_\beta$  and  $m$ .  $a - \beta, \text{deg}$ .

5. values of coefficients  $k_\sigma$ ,  $k_v$  and  $k_\beta$  are found on graphs in Figures 21 to 23;

6. the intensity of the ice load is computed by formula (12.6) and results of the calculations are presented in the form of a graph (Figure 26, curve I);

7. a final curve of an ice load on the bow is constructed. It must be drawn on the basis of calculations of the strength of the hull structures. For this, it is necessary to square (according to designing considerations, considering for example, the spacing of lateral bulkheads, etc.) the theoretical loads curve obtained in paragraph 6 for separate sectors so that the number of these sectors will be minimum (two to three). When doing this, it should be kept in mind that the ordinates of the

squared curve must be no less than the ordinates of the load curve obtained in paragraph 6.

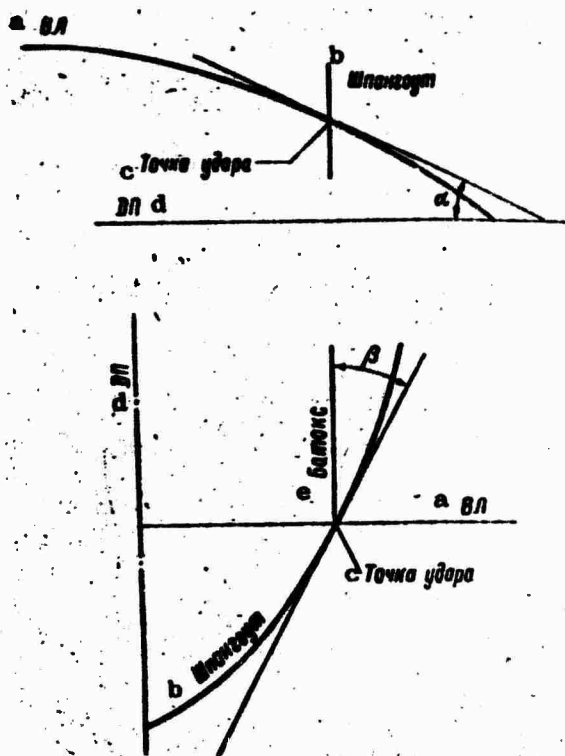


Figure 24. Determining angles  $\alpha$  and  $\beta$ . a-WL; b-frame; c-point of impact; d-LP; e-buttock.

The ice load during impact against an ice field, taking its bending into account, should be determined by formula (8.10) where the depth of crushing  $C_{\max}$  is found by means of successive approximations, as shown in 8. To accommodate practical calculations, the maximum depth of crushing was computed for a series of ships depending on the thickness and ultimate crushing strength of the ice  $\sigma_c$ , vertical slope of the side, velocity and displacement. Results of these calculations were compared with the value of the depth of crushing, computed without taking bending of the ice field into consideration. As a result, a graph of correction factors was constructed, making it possible to recalculate the intensity of an ice load during impact of a ship against an ice field, allowing for bending of the field from a known magnitude of a load calculated without allowing for the bending.

The formula for computing an ice load during impact against the edge of an ice field, taking bending of the latter into account, has the form

$$(q_{\text{bow}})_b = q_{\text{bow}} k_1, k_2, k_3, \quad (12.7)$$

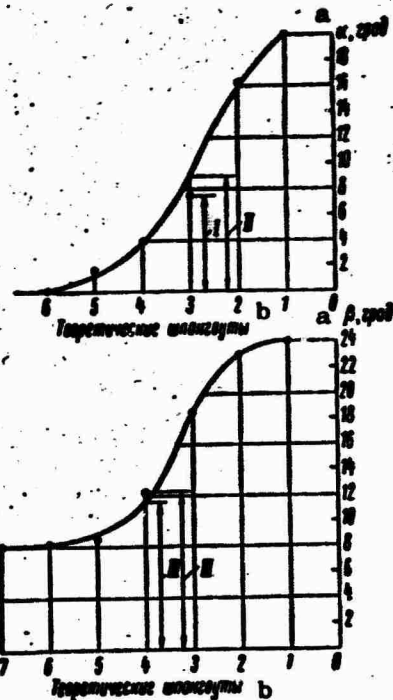


Figure 25. Correcting Values of Angles  $\alpha$  and  $\beta$ . a-deg; b-frame lines.

- I - obtained value  $\alpha$ ; II - corrected value  $\alpha'$ ;
- III - obtained value  $\beta$ ; IV - corrected value  $\beta'$ .

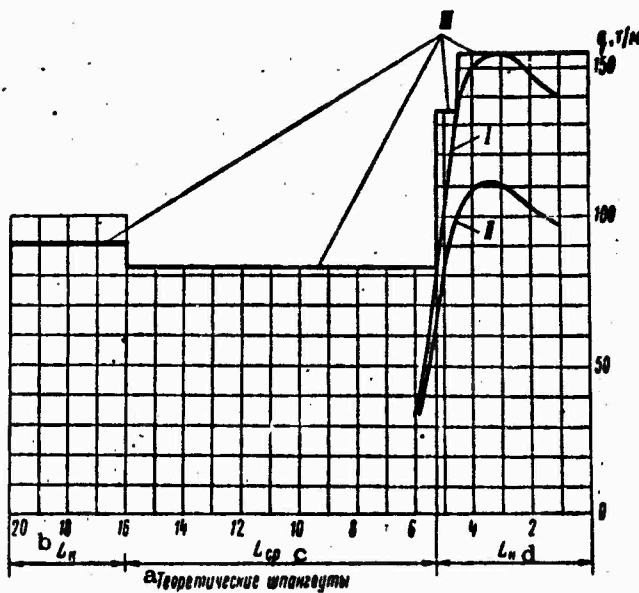


Figure 26. Curve of Ice Load on Plating. a-frame lines; b-L stern; c- L mid; d- L bow.

- I - theoretical load without considering bending;
- II - theoretical load taking bending into consideration;
- III - square curve of the load (design).

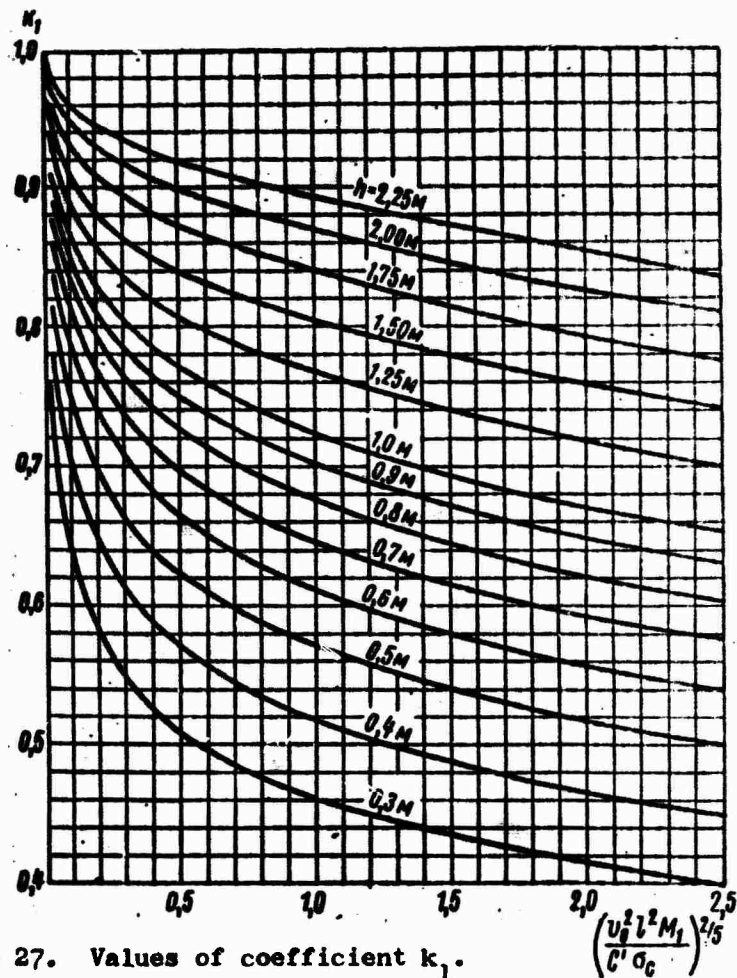


Figure 27. Values of coefficient  $k_1$ .

where  $(q_{\text{bow}})_b$  - is the intensity of an ice load, taking bending of the field into account, t/m;

$q_{\text{bow}}$  - is the intensity of an ice load calculated by formula (12.6) without considering bending of the field, t/m;

$k_1$  - is a coefficient depending on the ice thickness  $h$  and characteristics  $\left(\frac{v_0^2 l^2 M_1}{C' \sigma_c}\right)^{2/5}$  ( $v_0$  - is the velocity of the ship, m/sec) (Figure 27);

$k_2$  - is a coefficient, determined from Figure 28, depending on ice thickness  $h$  and vertical slope of the frame  $\beta$  in the impact area;

$k_3$  - is a coefficient calculated according to Figure 29, depending on the thickness and ultimate crushing strength of the ice.

The procedure for calculating an ice load, allowing for bending of the ice field follows.

The ice load without allowing for bending of the ice field is calculated according to formula (12.6). Then, the characteristic  $\left(\frac{\sigma_c^2 M_1}{C \sigma_b}\right)^{1/2}$  is calculated.

Correction factors  $k_1$ ,  $k_2$  and  $k_3$  are determined on graphs, Figures 27 to 29 and the intensity of the ice load is computed by formula (12.7).

Ice loads are calculated for side framing in the hull midsection on the basis of conditions of static compression on the ship by an ice field. In doing this, cases of compression on ships having an incline ( $\beta \geq 8^\circ$ ) or a vertical side ( $\beta < 8^\circ$ ) in the midsection are considered separately. For ships with a sloping side, considering expression (8.21) and (12.1), we obtain

$$q_{\text{mid}} = \frac{0,312 \sigma_b h^2 \cos^{1/2} \beta}{(2R)^{1/2} \sigma_{\text{max}}^{1/2} \sin \beta}$$

Substituting expression (7.6) for the maximum depth of crushing here, we find

$$q_{\text{mid}} = \frac{0,43}{\sin \beta} \sqrt[3]{\frac{\sigma_c \sigma_b^2 h^4}{2R}} \quad (12.8)$$

Thus, the design load for the hull midsection will depend on the slope of the side  $\beta$ , ice thickness  $h$ , and its strength characteristics  $\sigma_c$  and  $\sigma_b$ , as well as the parameter  $R$ , characterizing the configuration of the ice's edge. To evaluate the correspondence of design loads to real ice loads, empirical data of ships operating in ice should be used, selecting ship prototypes, the strength of which has been proven in the defined compression conditions. A medium power icebreaker and a UL (Arkt.)-Class icebreaker cargo ship active in ice navigation, were taken as these prototypes. The structural strength of these ships in the midsection is 90 and 100 t/m respectively. The thickness of an ice field in which these ships could undergo compression without suffering noticeable hull damage is: for a medium icebreaker  $h = 2.5$  m and for UL (Arkt.) cargo ships, the sides of which have considerably less slope ( $8^\circ$  instead of  $18^\circ$  on the icebreaker),  $h = 1.5$  m. For medium icebreakers and ships of ice-strengthened classes, the design value for the ultimate crushing strength of ice can be taken as  $\sigma_c = 200$  t/m<sup>2</sup> and the design value for ultimate bending strength  $\sigma_b = 100$  t/m<sup>2</sup>. For heavy icebreakers, these values should be increased to 250 and 125 t/m<sup>2</sup> respectively.

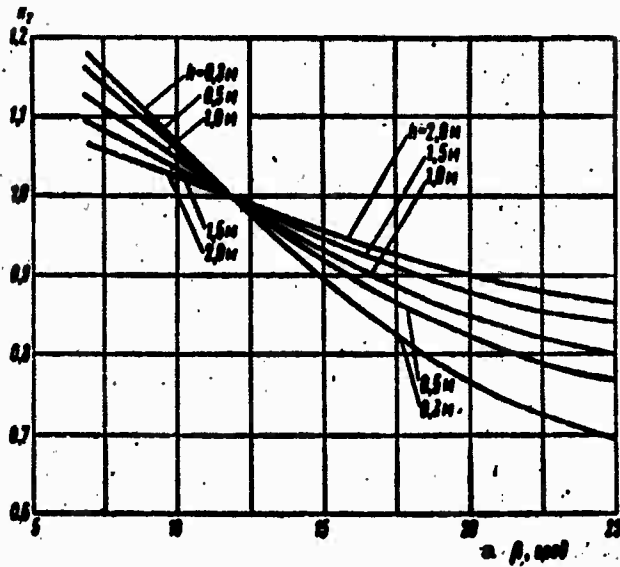


Figure 28. Values of coefficient  $k_2$ .  $\alpha - \beta$ , deg.

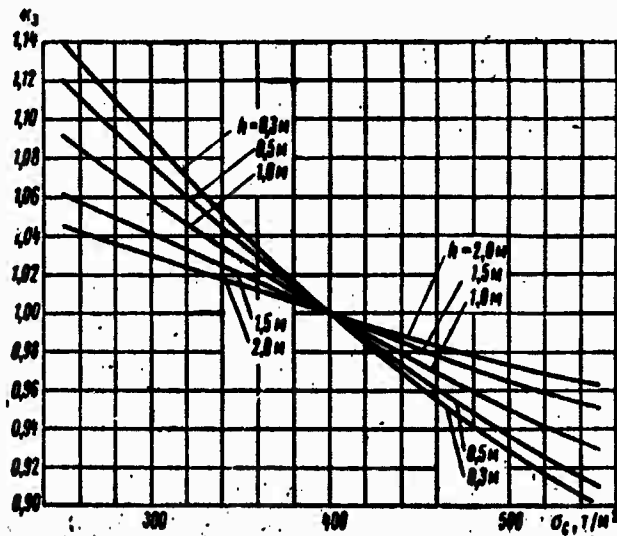


Figure 29. Values of coefficient  $k_3$ .

Assuming that the value of the parameter  $R$  is identical for the prototype ship and the ship under consideration and using the above-presented formula (12.8), we obtain, in a general situation

$$\eta_{mid} = \eta_{mid_0} \frac{\sin \beta_2}{\sin \beta} \sqrt{\frac{c_c}{c_{c_0}} \left(\frac{cb}{cb_0}\right)^3 \left(\frac{h}{h_0}\right)^6}$$

where the terms with a zero index relate to the prototype ship.

The obtained formula can be presented in a form to accommodate practical calculations

$$q_{mid} = 95k_p'k_c k_b k_h \quad (12.9)$$

where  $k_p' = \frac{\sin \beta_0}{\sin \beta}$  - is a coefficient allowing for the effect of the vertical slope of the side (Figure 30);

$k_c = \sqrt[3]{\frac{\sigma_c}{200}}$  - is a coefficient allowing for the effect of ultimate crushing strength of the ice (Figure 31);

$k_b = \sqrt[3]{\frac{\sigma_b^2}{100^2}}$  - is a coefficient allowing for the effect of the ultimate bending strength of the ice (Figure 31);

$k_h = \sqrt[3]{\frac{h^4}{h_0^4}}$  - is a coefficient for the effect of the ice thickness (Figure 32).

The design load  $q_{mid}$  for ships having vertical sides is calculated by formula (11.6), if we place  $\gamma = 1 \text{ t/m}^3$  in it and  $\mu = 0.34$  and  $E = 4 \cdot 10^4 \text{ t/m}^2$  (for salt ice) or  $E = 6 \cdot 10^4 \text{ t/m}^2$  for fresh ice.

Thus, for salt ice

$$q_{mid} = 62h \sqrt{h} \quad \text{t/m,}$$

for fresh ice

$$q_{mid} = 73h \sqrt{h} \quad \text{t/m,}$$

(12.10)

where  $h$  is the design ice thickness during compression, m.

Ice loads which act on the stern can be determined from a condition of an impact of a ship against the ice when moving astern or when the stern piles up on the edge of the ice during yawing. The design diagram does not differ in principle from the design diagram of impact loads taken for the bow. However, it can first be said that conditions for the stern are less severe than for the bow inasmuch as the velocity of a ship moving astern and when piling up on the edge of the field is considerably less than its forward velocity. Moreover, the stern lines of ships which sail in ice are extremely well-suited for absorbing ice stresses in view of the large slope to the side of the afterbody. Therefore, we shall designate the magnitude of ice loads in the stern  $q_{st}$  as fractions of the maximum load acting on the bow,

$$q_{st} = k(q_{bow})_{max} \quad (12.11)$$

where  $k$  - is a coefficient designated depending on the ship type and class.

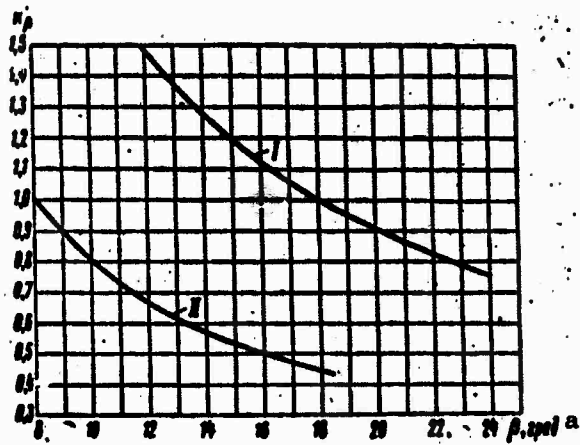


Figure 30. Values of the coefficient  $k_p'$ .

I - for icebreakers; II - for icebreakers - cargo ships.  
α-degrees.

For icebreakers  $k = 0.7$  is used but the load must be at least 30% greater than the load amidships and for UL (Arkt.)-class ice ships  $k = 0.5$  but the load  $q_{st}$  must be at least 10% greater than the load amidships.

The magnitude of coefficient  $k$  is designated on the basis of the condition of an impact by the stern against ice at a velocity of 4 to 5 knots for icebreakers and 1 to 2 knots for ice ships. Experience gained in construction of icebreakers and UL (Arkt.)-class ships, the sterns of which were strengthened by 30 and 10% respectively in comparison with their midsections, was taken into consideration in this. The length of the strengthened area of the stern was taken as 20% of the length of the ship, computed from the stern perpendicular.

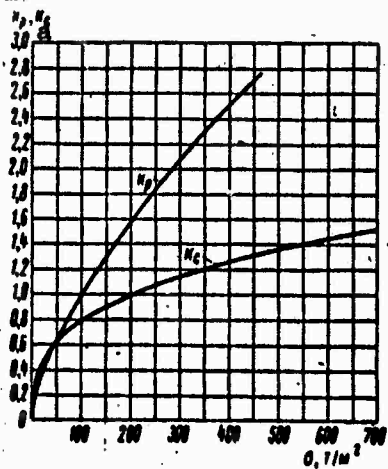


Figure 31. Values of coefficients  $k_c$  and  $k_b$ .  
a -  $k_b$ ,  $k_c$ .

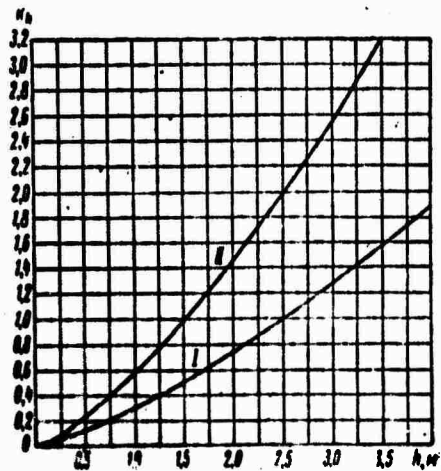


Figure 32. Values of coefficient  $k_h$ . I - for icebreakers; II - for ice cargo ships.

Table 4

Value of angles  $\beta$  and  $\alpha$ 

Угол, град. а	Номера теоретических шпангоутов b									
	1	2	3	4	5	6	7	8	9	10
$\beta$	30	27	23	17	12	8	8	8	8	8
$\alpha$	20	19	16	10	4	1	0	0	0	0

a - angles, deg.; b - frame line numbers.

**Example.** We shall calculate an ice load on the side framing of a UL (Arkt.)-class cargo ship using the following initial data: displacement  $D_1 = 10,000$  t; velocity at the time of impact against ice field  $v_1 = 4$  kts; thickness of ice field  $h = 1.4$  m; ultimate crushing strength of the ice in impact  $\sigma_c = 350$  t/m<sup>2</sup> and in compression  $\sigma = 175$  t/m<sup>2</sup>; ultimate bending strength of the ice in compression  $\sigma_b = 90$  t/m<sup>2</sup>.

The slopes of the side  $\beta$  and angles between the tangent to the waterline and the longitudinal plane  $\alpha$  are presented in Table 4. The ice load for the ship's bow is computed by formula (12.6) in Table 5.

Table 5

Determining the ice load for a ship's bow without considering bending of the ice field.

Параметры а	Номера теоретических шпангоутов b						
	1	2	3	4	5	6	7
c Коэффициент $C'$ (Fig.5)	2,79	2,58	2,00	1,64	1,32	1,07	—
» $m$ (Fig.26)	1,50	1,54	1,58	1,64	1,67	1,68	—
$l_1 = 0,01 \text{ ат}$	0,300	0,293	0,253	0,164	0,067	0,017	0
d Характеристика $D_1/C'$	3580	3960	5000	6100	7580	9350	—
e $v_n = l_1 v_1$	1,20	1,17	1,01	0,65	0,27	0,07	0
f Коэффициент $k_D$ (Fig.20)	0,65	0,675	0,74	0,80	0,88	0,97	—
» $k_1$ (Fig.21)	0,925	0,925	0,925	0,925	0,925	0,925	—
» $k_2$ (Fig.22)	0,60	0,58	0,52	0,37	0,19	0,050	—
» $k_3$ (Fig.23)	2,02	1,93	1,60	1,52	1,22	1,00	—
g Интенсивность нагрузки $q_n = 780 \frac{k_D k_1 k_2}{k_3}$ , т/м	140	147	155	140	99	35	0

a - parameters; b - frame line numbers; c - coefficient  $C'$ ; d - characteristic  $D_1/C'$ ; e -  $v_n = l_1 v_1$ ; f - coefficient  $k_D$ ; g - intensity of load  $q_{\text{bow}} = 780 \frac{k_D k_1 k_2}{k_3}$ , t/m.

The ice load for the hull midsection is computed by formula (12.9) as for a ship with an inclined side:

$$q_{\text{bow}} = 95 \frac{k_b k_c k_d k_h}{\beta}$$

We take the values of coefficients  $k_b$ ,  $k_c$ ,  $k_d$  and  $k_h$  from the graphs presented in Figures 30 to 32:  $k_b = 1$ ,  $k_c = 0.94$ ,  $k_d = 0.92$ ,  $k_h = 0.96$ . Then

$$q_{\text{bow}} = 95 \cdot 0.94 \cdot 0.92 \cdot 0.96 = 80 \text{ t/m.}$$

The ice load in the stern calculated by formula (12.11),  $q_{\text{st}} = 0.5 \cdot 155 = 77.5 \text{ t/m}$ . The ice load in the stern, taken as 10% greater than the load amidships,  $q_{\text{st}} = 1.1 \cdot 80 = 88 \text{ t/m}$ .

We take the larger of the two obtained values:  $q_{\text{st}} = 88 \text{ t/m}$ .

The distribution of the ice load along the length of a ship is presented in the form of a curve (Figure 26, curve III).

The ice load for a ship's bow is computed in Table 6 according to formula (12.7), taking bending of the ice field into consideration, with a given ice thickness of  $h = 1.4 \text{ m}$ . The results of the calculations are presented in Figure 26, curve II.

It is obvious from Table 6 that allowing for bending permits the design loads for the bow to be decreased by nearly 40%.

Table 6

Determining ice load for a ship's bow, taking bending of the ice field into consideration.

a Параметры	b Номера теоретических шпангоутов						
	1	2	3	4	5	6	7
с Нагрузка без учета изгиба (табл. 5)							
$q_{\text{bow}}$ , т/м	140	147	155	140	99	35	0
$\frac{\sigma_0^2 M_1}{C' \sigma_c}$	0,400	0,410	0,395	0,198	0,043	0,043	—
$\left( \frac{\sigma_0^2 M_1}{C' \sigma_c} \right)^{1/2}$	0,693	0,700	0,688	0,522	0,284	0,104	—
Коэффициент $k_1$ (Fig. 27)	0,810	0,810	0,815	0,830	0,856	0,895	—
„ $k_2$ (Fig. 28)	0,84	0,85	0,86	0,92	1,00	1,05	—
„ $k_3$ (Fig. 29)	1,02	1,02	1,02	1,02	1,02	1,02	—
д Нагрузка с учетом изгиба $(q_{\text{st}})_2 = q_{\text{st}} k_1 k_2 k_3$ , т/м	97,5	102	111	109	86,5	33,5	0

a-parameters; b-frame line numbers; c-load without considering bending (Table 5); d-load, taking bending into consideration

$$(q_{\text{bow}})_b = q_{\text{bow}} k_1 k_2 k_3, \text{ t/m.}$$

### 13. Loads on Shell Plating.

The design intensity of an ice load on side plating is calculated depending on the magnitude of contact pressures developing during breaking up of the edge of the ice. The analysis of interaction between a ship's hull and ice performed in 3., shows that the contact pressures depend on the mass, lines and velocity of the ship as well as on the physical and mechanical characteristics of the ice and specifically, on the magnitude of the coefficient of internal friction of the interstitial layer  $f_{\eta}$  and its thickness  $\epsilon$  (see 3.). Adequately reliable data concerning the magnitude of characteristics  $f_{\eta}$  and  $\epsilon$  of natural ice cover is presently not available. Because of this, it is difficult to make a strict determination of the design magnitude of contact pressures. Therefore, when calculating ice loads on plating, we are forced to use the method of converting from a prototype.

Observations show that the distribution area of an external load on shell plating takes the form of a patch stretching along the ship for a distance of several frame spacings. This provides basis to assume that on the sector of the side being considered, the design load on the plating  $p$  is proportional to the design load on the side framing  $q$ , i.e.,

$$\frac{p}{p_0} = \frac{q}{q_0}, \quad (13.1)$$

where the symbols without an index refer to the ship under consideration and the symbols with a zero index refer to the prototype ship.

For ships sufficiently close in size, hull lines and power plant, operating conditions in ice can be considered to be similar. Consequently, parameters characterizing the physical and mechanical properties of ice, the configuration of the ice's edge and the velocity in the ice will be identical for both ships:

$$\frac{c_e}{c_{e0}} = \frac{R}{R_0} = \frac{v}{v_0} = 1.$$

Moreover, we will assume that the intensity of ice stresses acting on the plating depend on the hull shape only to the degree at which it effects the force of impact, i.e., the reduced mass of the ship and reduced velocity. The geometry of the crushing of the ice's edge which is a function of the vertical slope of the side  $\beta$  and the parameter  $R$ , does not have a noticeable effect on the magnitude of the load in the given case. Therefore, using formulas (13.1) and (12.3), we obtain the following expression for intensity of an ice load on plating during an impact against an ice floe

$$p_{\text{bow}} = (p_{\text{bow}})_0 \frac{M_1^{3/4} \left( C' + C'' \frac{M_1}{M_0} \right)^{1/4} v_0 f_{\eta}^2}{(M_1)_0^{3/4} \left( C' + C'' \frac{M_1}{M_0} \right)^{1/4} (v_0)_0^2 (h)_0^2} \quad (13.2)$$

In case of impact against the edge of an ice field, when  $\frac{M_1}{M_2} \rightarrow 0$ ,  
 formula (13.2) is simplified:

$$P_{\text{bow}} = (P_{\text{bow}})_0 \frac{M_1^2 (C')^2 v_1^4 l_1^2}{(M_2)^2 (C')^2 (v_2)^2 (l_2)^2} \quad (13.3)$$

The relationship of the displacement of ships similar in elements can be taken as proportional to the relationship of the linear dimensions to the third power. Then, considering the equality of the velocities  $v_2 = v_1 = (v_2)_0$ , we write formula (13.3) in the following form:

$$P_{\text{bow}} = (P_{\text{bow}})_0 \frac{L^3 (C')^2 l_1^2}{L_0^3 (C')^2 (l_2)_0^2}$$

or

$$P_{\text{bow}} = 10^{-3} k_p^2 L^3 k_p \quad (13.4)$$

where  $\alpha$  - is the angle between the tangent to the waterline and the longitudinal plane, degrees;

$L$  and  $L_0$  - are the lengths of the ships, m;

$k_p$  - is a coefficient allowing for the effect of the vertical slope of the frames;

$$k_p = \frac{(1.6 \cos \beta + 0.11)^{1/5}}{(C')^{1/5}} = \frac{m^{1/5}}{(C')^{1/5}}$$

$m = 1.6 \cos \beta + 0.11$  - is a coefficient determined from the graph in Figure 23;

$k$  - is a coefficient calculated from data on the prototype ship:

$$k = \frac{10^3}{100^{1/5}} \cdot \frac{(P_{\text{bow}})_0 (C')^{2/5}}{[L_0^3 (l_2)_0^2]^{1/5}}$$

Values of coefficient  $k$  for icebreakers and cargo ships of various ice classes are presented in Table 7.

Table 7

Values of coefficient  $k$  for icebreakers and cargo ships of various ice classes\*

а Тип	б Класс судна	к
с Ледокол	и I класс II класс III класс	30,5 24 18
д Транспортные суда	уЛ (Аркт.) суЛ Л	12,2 6,5 4,8
ф Буксиры	суЛ Л	18 9

г Классификация судна см. § 17.

a-type; b-ship class; c-icebreakers; d-cargo ships; e-UL (Arkt) UL L; f-tugboats; g- UL L; h-\*see ship classifications 17; i-I Class, II Class, III Class.

The procedure for determining the ice load on bow plating follows. Angles  $\alpha$  and  $\beta$  for each frame line are taken from the line drawing (Figure 24), graphs are constructed and the corrected values for these angles are found (Figure 25). Coefficient  $C'$  is found on graph, Figure 5, depending on angle  $\beta$  and the relative coordinate of the point of impact  $x/L$ . Coefficient  $m$  is found on the graph in Figure 23, depending on angle  $\beta$ . Then, we determine the coefficient

$$k_p = \frac{m^{1/2}}{(C')^{1/2}}$$

and coefficient  $k$  is selected from Table 7. The intensity of the ice load on the plating is calculated according to formula (13.4) and the results are presented in the form of a graph (Figure 33, curve I). Then a square curve for the ice load on bow plating is constructed similarly as was done for the side framing (Figure 33, curve II).

The intensity of an ice load on the midsection of a ship is determined from conditions of compression of a ship in the ice similarly as done for the bow. Using expressions (12.8) and (13.1), we obtain

$$P_{\text{mid}} = (P_{\text{mid}})_0 \sqrt[3]{\frac{\sigma_c}{(\sigma_c)_0} \cdot \frac{\sigma_b^2}{(\sigma_b)_0^2} \cdot \frac{h^4}{h_0^4}} \quad (13.5)$$

where symbols with a zero index refer to the prototype ship.

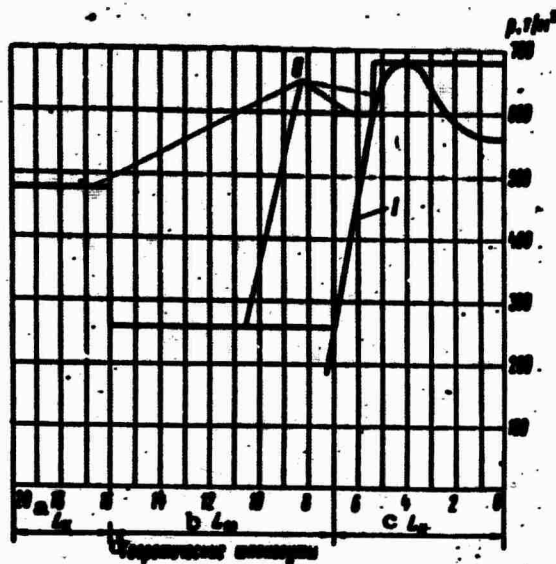


Figure 33. Curve of ice load on plating. a-L<sub>1</sub> stern; b-L<sub>2</sub> mid; c-L<sub>3</sub> bow; d-frame lines.

I - Theoretical load; II - Square curve of load (design).

A heavy icebreaker and an icebreaker-cargo ship which have operated many years in the Arctic were used as prototypes. The maximum ice thickness to which the midsection of an icebreaker-cargo ship was exposed during compression was  $h \approx 1.5$  m; for an icebreaker, it can be assumed as  $h \approx 4$  m. The construction strength\* of the side plating was calculated by the formula

$$(p_{\text{mid}})_0 = 2\sigma_y \left(\frac{\delta}{s}\right)^2, \quad (13.6)$$

where  $\sigma_y$  - is the yield strength of the plating material,  $\text{kg/cm}^2$ ;

$\delta$  - is the plating thickness, mm;

$s$  - is the frame spacing, mm.

---

\* In this case and subsequently, construction strength denotes the magnitude of the external ice load under the influence of which design stresses in the hull members reach their ultimate yield strength.

---

For the icebreaker prototype, when  $\sigma_y = 2600 \text{ kg/cm}^2$ ,  $\delta = 40$  mm and  $s = 400$  mm, we find according to formula (13.6) that  $(p_{\text{mid}})_0 = 52 \text{ kg/cm}^2$  or  $520 \text{ t/m}^2$ . For the ship prototype, when  $\sigma_y = 3600 \text{ kg/cm}^2$  and  $\delta = 18$  mm and  $s = 400$  mm, we obtain  $(p_{\text{mid}})_0 = 150 \text{ t/m}^2$ .

Assuming for icebreakers, the ultimate crushing and bending strength of ice as  $(\sigma_c)_0 = 250 \text{ t/m}^2$  and  $(\sigma_b)_0 = 125 \text{ t/m}^2$  respectively and ice thickness as  $h = 4 \text{ m}$ , and for cargo ships\*  $(\sigma_c)_0 = 200 \text{ t/m}^2$ ,  $(\sigma_b)_0 = 100 \text{ t/m}^2$  and  $h = 1.5 \text{ m}$ , we obtain, according to (13.5), formulas for calculating the intensity of an ice load on midship plating:

icebreakers

$$P_{\text{mid}} = 0,52 \sqrt[3]{\sigma_c \sigma_b^2 h^4}, \text{ t/m}^2; \quad (13.7)$$

cargo ships

$$P_{\text{mid}} = 0,69 \sqrt[3]{\sigma_c \sigma_b^2 h^4}, \text{ t/m}^2; \quad (13.8)$$

---

\* For cargo ships, the strength characteristics of ice are assumed as 25% lower than for icebreakers, which can sail in the early navigation period when the ice is stronger.

---

If changes in the strength characteristics of ice are not taken into consideration when converting from the prototype to the ship being designed,  $\frac{\sigma_c}{(\sigma_c)_0} = \frac{\sigma_b}{(\sigma_b)_0} = 1$  should be set in formula (13.5).

Then, for icebreakers

$$P_{\text{mid}} = (P_{\text{mid}})_0 \sqrt[3]{\frac{h^4}{h_0^4}} = 520 \sqrt[3]{\frac{h^4}{4^4}} = 82h \sqrt[3]{h}; \quad (13.9)$$

for UL (Arkt.) and UL-class cargo ships

$$P_{\text{mid}} = (P_{\text{mid}})_0 \sqrt[3]{\frac{h^4}{h_0^4}} = 150 \sqrt[3]{\frac{h^4}{1,5^4}} = 88h \sqrt[3]{h}. \quad (13.10)$$

It should be noted that on the majority of UL-class ships in operation, the correlation between carrying capacity of bow plating and midship plating is more or less stable and on an average, equals two. According to Regulations of the Register of Shipping of the USSR [40], the thickness of the side plating ice belt for a section, 0.15 L from the stem of UL-class ships is increased 60% above the required thickness for the mid-section of an unstrengthened ship. The thickness of the midship hull plating is assumed 15% greater than the thickness of the plating of a ship not having an ice classification. In this case

$$\frac{P_{\text{bow}}}{P_{\text{mid}}} = \left(\frac{1,60}{1,15}\right)^3 = 1,94.$$

Thus, the load on the midship hull plating of UL-class cargo ships should be fixed either by formula (13.10) or by Regulations of the Registry of Shipping of the USSR, assuming the greater as the design value. L-class cargo ships' hulls are not rated for ice compression and midship plating thickness is designated in accordance with the Registry of Shipping.

The intensity of an ice load on stern plating  $p_{st}$  is calculated the same as for side framing, i.e., in relation to the design value of the load in the bow  $(p_{bow})_{max}$

$$p_{st} = k' (p_{bow})_{max} \quad (13.11)$$

where  $k'$  - is a coefficient of the same magnitude as when calculating the load for side framing.

For icebreakers,  $k' = 0.7$  (the load  $p_{st}$  must be at least 30% greater than the load for the midsection); for UL (Arkt.)-class ice ships,  $k' = 0.5$  (load  $p_{st}$  must be at least 10% greater than the load in the midsection).

The length of the strengthened area of plating in the stern is assumed as 20% of the length of the ship. For L and UL-class ships, the design load for stern plating is assumed the same as for the midsection.

**Example.** Determine the ice load on the plating of an icebreaker from the following initial data: length of ship  $L = 98$  m; ice thickness  $h = 2.5$  m; ultimate crushing strength of the ice in impact  $\sigma = 490$  t/m<sup>2</sup>; ultimate crushing strength of the ice in compression  $\sigma_c = 220$  t/m<sup>2</sup>; ultimate bending strength of the ice in compression  $\sigma_b = 120$  t/m<sup>2</sup>.

The vertical slopes of the frames  $\beta$  and angles  $\alpha$  between a tangent to the waterline and the longitudinal plane are presented in Table 8. The ice load for the bow is computed according to formula (13.4) in Table 9, with  $k = 24$  (see Table 7).

Using formula (13.8), we find for the midsection of a ship

$$p_{mid} = 0.52 \sqrt{h^3 \sigma_c} = 0.52 \sqrt{2.5^3 \cdot 220} = 258 \text{ t/m}^2$$

For the stern, we determine, according to formula (13.11):

$$p_{st} = k' (p_{bow})_{max} = 0.7 \cdot 686 = 480 \text{ t/m}^2$$

The curve for ice loads on plating is presented in Figure 33.

Table 8.

Values of angles  $\alpha$  and  $\beta$ 

Угол, град. a	Номера теоретического шпангоута b									
	1	2	3	4	5	6	7	8	9	10
$\beta$	45	44	41	36	32	28	24	20	18	18
$\alpha$	23	23	23	21	18	13	9	4	1	0

a-angles, deg.; b- frame line numbers.

Table 9.

Determining the ice load on the bow plating of an icebreaker

Параметры a	Номер теоретического шпангоута b							
	1	2	3	4	5	6	7	8
Коэффициент $C'$ c	3,16	2,67	2,30	1,96	1,61	1,37	1,10	0,90
Коэффициент $m$	1,24	2,26	1,31	1,40	1,47	1,52	1,57	1,61
$m^{1/2}$	1,18	1,20	1,24	1,31	1,36	1,40	1,43	1,46
$(C')^{1/2}$	1,58	1,48	1,38	1,28	1,21	1,13	1,03	0,96
$a^{1/2}$	12,25	12,12	12,25	11,40	10,10	7,85	5,80	3,04
$k_p = \frac{m^{1/2}}{(C')^{1/2}}$	0,75	0,81	0,90	1,02	1,12	1,24	1,39	1,63
$R_{bow} 10^{-2} k_a^{1/2} L^{1/2} k_p$	565	585	645	685	665	575	475	273

a-parameters; b-frame line numbers; c-coefficient.

14. Effect of Hull Shape on the Magnitude of Ice Loads.

Basic hull parameters which effect the magnitude of ice loads include:

- the length of the fore parallel middle body  $L_{pbow}$ ;
- relationship of the ship's length and breadth  $L/B$ ;
- fore waterplane coefficient  $\alpha_{bow}$ ;
- vertical slope of frames  $\beta$ .

To analyze the effect of the parameters listed, we use a superposition method and consider the effect of each parameter on the ice load on a series of ships with various bow shapes, displacing  $D_1 = 10,000$  t, and striking an ice field at a speed of two knots.



Figure 34. Line drawing of waterlines. a-y; b- $L_{pbow}$ ; c- $L_{bow}$ .

The bow line of the waterline is expressed by equation in the form

$$y = 0.5B \left[ 1 - \left( \frac{x}{L_{bow}} \right)^2 \right] \left[ 1 - b \left( \frac{x}{L_{bow}} \right)^2 \right]$$

where B - is the breadth of the ship;

b - is a parameter characterizing the bow waterplane;

$L_{bow}$  - is the length of the entrance, equal to  $\frac{L}{2} - L_{pbow}$  (Figure 34).

The forward waterplane coefficient

$$\alpha_{bow} = \frac{0.5BL_{pbow} + \int_0^{L_{bow}} 0.5B \left[ 1 - \left( \frac{x}{L_{bow}} \right)^2 \right] \left[ 1 - b \left( \frac{x}{L_{bow}} \right)^2 \right] dx}{0.5L \cdot 0.5B}$$

$$= \frac{L_{pbow} + L_{bow} \left( \frac{10 - 2b}{15} \right)}{0.5L}$$

Assuming

$$L_{pbow} = k \frac{L}{2} \text{ and } L_{bow} = \frac{L}{2} - L_{pbow} = \frac{L}{2} (1 - k),$$

we obtain

$$\alpha_{bow} = k + \frac{2}{15} (1 - k) (5 - b).$$

The effect of the length of the fore parallel middle body on the ice load was investigated with  $k = 0.3; 0.4$  and  $0.5; L/B = 7$  and  $\alpha_{bow} = 0.804$ ; and the effect of the fore waterplane coefficient was investigated with  $\alpha_{bow} = 0.768$  ( $b = 0.4$ );  $\alpha_{bow} = 0.804$  ( $b = -0.05$ ),  $\alpha_{bow} = 0.840$  ( $b = -0.5$ ), with  $L/B = 7$  and  $L_{pbow} = 0.4 L/2$ .

The effect of the ratio  $L/B$  was investigated for  $L/B = 6, 7$  and  $8$  with  $L_{pbow} = 0.4 L/2$  and  $\alpha_{bow} = 0.804$ .

The ice loads of the variants considered were compared for icebreaker bow shapes with identical vertical slopes of frames  $\beta$  on all variants. Slope angles  $\beta$  are presented in Table 10. For an evaluation of the effect of vertical slope of the frame  $\beta$  on ice loads, the load for a ship with an icebreaker and a non-icebreaker bow shape were considered. The results of the calculations are presented in the form of curves of ice loads in Figures 35 to 38. From Figure 35, it is obvious that with an increase in the length of the parallel middle body and all other conditions being equal, the curve of impact loads is displaced to the forepart of the ship, proportionately to the length of the parallel middle body. With this, there is a growth in the ice load in the area of the first and second frame lines with an increase in the length of the parallel middle body. Curves of loads on ships with various fore waterplane coefficients presented in Figure 36, reveal the substantial effect this parameter has on ice loads. A decrease in the waterplane coefficient  $\alpha_{bow}$  causes a considerable increase in loads in the area of the third and fifth frame lines (the so-called fore shoulders of the waterline). This is explained by the increase in the angles between the tangent to the waterline and the longitudinal plane in this area. For a waterline with a large fore waterplane coefficient, maximum loads move toward the stem and the curve of ice loads has no maximum. Curves of loads for ships with various ratios  $L/B$  with  $L_{pbow} = 0.2 L$  and  $\alpha_{bow} = 0.804$  are presented in Figure 37. From the figure, it follows that the ratio of a ship's length to its breadth has a comparatively small effect on the magnitude of ice loads. So, with  $L/B = 8$ , loads decrease by approximately 20%; this can be explained by the decrease in the angles between the tangent to the waterline and the longitudinal plane with an increase in  $L/B$ . Curves of loads of two ships having different vertical slopes to their sides are presented in Figure 38, (see Table 10). A comparison of these curves shows that the ice load substantially increases (by an average of 50%) when the slope of the bow frames is cut in half.

Table 10

Values for angle  $\beta, ^\circ$

Форма обводов носовой оконечности	Номер теоретического шпангоута					
	1	2	3	4	5	6
Ледокольная	34	30	24	17	12	8
Неледокольная	17	15	12	8,5	5	1,5

a-bow hull lines; b-frame line number; c-icebreaker; d-non-icebreaker.

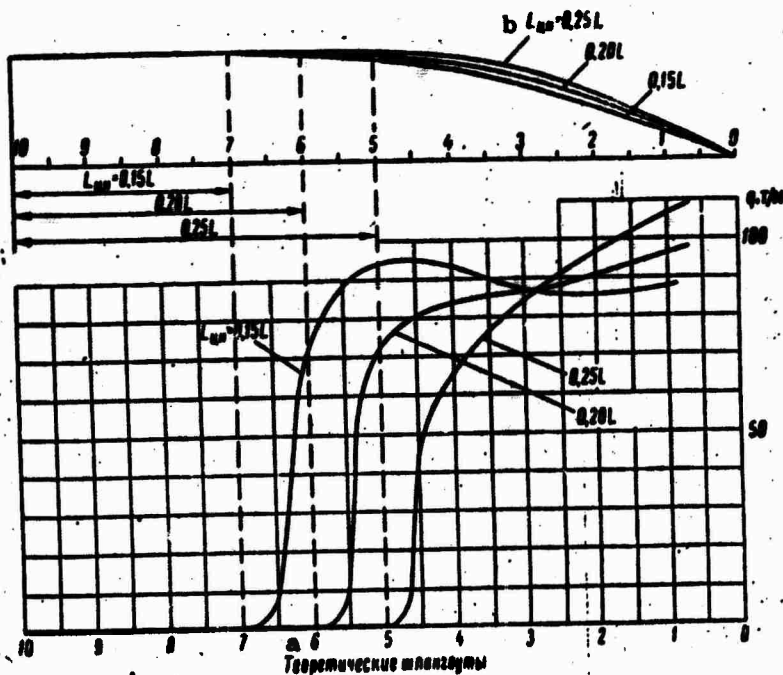


Figure 35. Effect of the length of the parallel middle body on an impact ice load. a-frame lines; b- $L_{\text{пр}}$

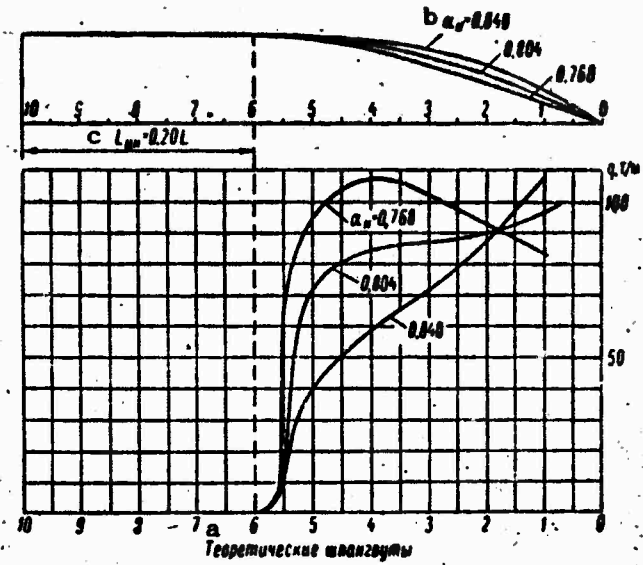


Figure 36. Effect of the coefficient of fineness of waterline on an impact ice load. a-frame lines; b- $\alpha_{DOW}$ ; c- $L_{pp}$ .

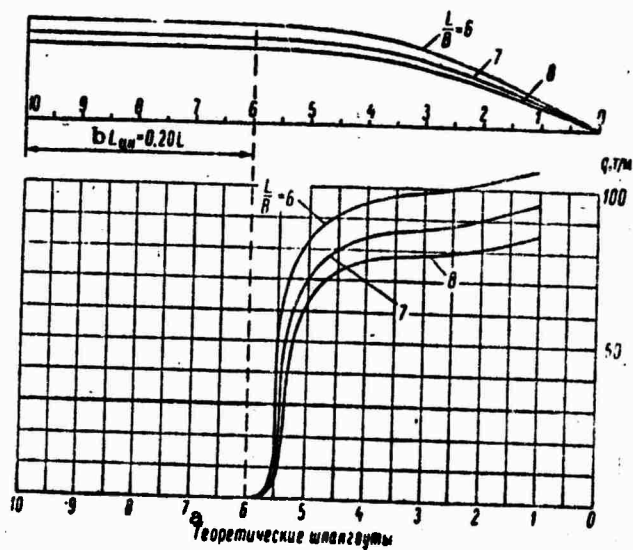


Figure 37. Effect of the ratio  $L/B$  on an impact ice load. a-frame lines; b- $L_{pp}$ .

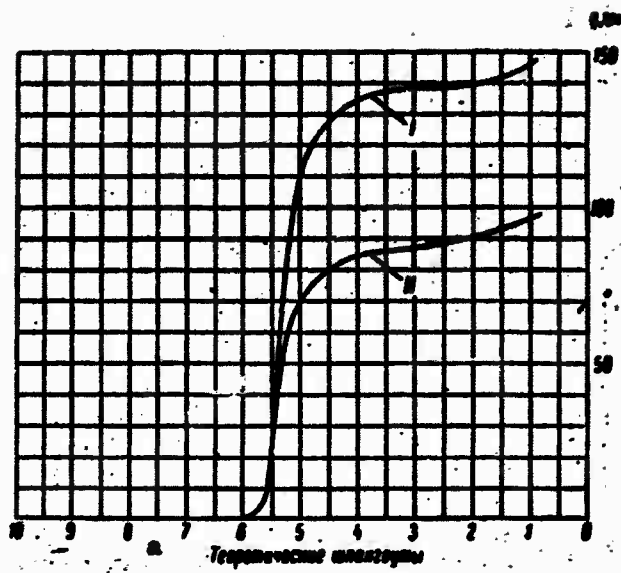


Figure 38. Effect of vertical slopes of frames on an impact ice load. a-frame lines.

I - Non-icebreaker shape; II - Icebreaker shape.

## CHAPTER IV

### DATA ON OPERATIONAL EXPERIENCE OF SHIPS UNDER ICE CONDITIONS.

#### CLASSIFICATION OF SHIPS SAILING IN ICE.

##### 15. Ice Damage to Hull Structures of Icebreakers and Cargo Ships.

Study and analysis of ice damage to hull structures of icebreakers and cargo ships, the construction strength of which is known, make it possible to compare the above recommended design ice loads with ice loads which actually act on a ship's hull. As a result of such comparison, it is possible to determine more accurately a design plan for calculating ice loads for various classes of ice ships. Detailed analysis of ice damage to hull structures with necessary calculations is an independent, large volume task. Therefore, only several conclusions concerning ice damage to ships are cited below. Damages resulting from violations of navigation rules and tactics for sailing in ice are not considered here.

When examining the hulls of several icebreakers, it became clear that they all had ice damages, the amount and nature of which depended considerably on the technical condition of the ship. The usual types of ice damage to icebreakers' hulls are dents and crimps in shell plating, permanent deflections of frames, loss of flexural stability of frames and beams, and disturbance of the strength of riveted joints. Most of the damage was registered in the area of the ice belt as well as on the bottom of the icebreaker's bow. Most of the damage occurs in the bow which takes impact ice loads. Damage to icebreaker midsections resulting from ice compression is insignificant in comparison with bow damage. Most icebreaker hull damage (dents and crimps in shell plating, permanent deflections of frames, etc.) is characterized by an insignificant amount of deflection (up to 50 mm) and does not present a danger to the ship. More severe damage to hull structures with deflections up to 200 mm are observed on old construction icebreakers. This is explained by the considerable wear on the shell plating and framing over a long period of operation.

It should be noted that the hull strength of most icebreakers which have been constructed is adequate and ensures accident-free operation in ice conditions.

Study and analysis of ice damages to various cargo ships make it possible to make the following generalizations.

1. Nearly all cargo ships sailing in ice experience ice damage. The amount and nature of these damages depend on the technical condition of the ships' hulls and their operating conditions.

2. The most characteristic damages to cargo ships include: dents, crimps and less often, cracks and fractures in the shell plating; bending, loss of stability and fracturing of frames, stringers and knees; and much less often, damage to decks, platforms and transverse bulkheads.

3. Ice damage is usually located in the ice belt of the hull as well as beneath it. Most damage occurs on the ship's bow, the most severe damage being observed in the area where the entrance joins the parallel middle body.

4. Bow ice damage is a consequence of impacts of the hull against ice; damage in the midsection of the hull is a result of ice compression. Permanent deflections and damage of hull structures in the bow are usually of a local nature. In the midsection of the hull, damages are spread over considerably larger sectors.

5. The hulls of some cargo ships of various ice classes have inadequate strength. In a number of cases, this is explained by construction and engineering defects. However, as a rule, inadequate ice strength of cargo ships is a consequence of the ice class not actually corresponding to operating conditions, especially in the Arctic, early-navigation period when ice conditions are most severe.

#### 16. Comparison of Construction Strength of Ships with Design Ice Loads.

To evaluate the correspondence of ships' construction strength with their actual operating conditions in ice, it is necessary to select magnitudes for initial parameters determining ice loads and specifically, the ship's speed before striking the ice and their strength and thickness. These parameters must be such that the design ice strength of the hull will ensure accident-free ship operation.

To determine ice loads in the bow, the impact of a ship against an ice field at a given design velocity without allowing for bending of the field should be considered. Loads in the midsection should be calculated from a condition of compression of the hull in ice of a given thickness, taking bending of the field into consideration. From this, it is possible to construct a curve of theoretical loads and to designate design ice loads by squaring curvilinear sections of the curve as indicated in 12. and 13. The velocities obtained as design velocities are the maximum permissible during impact against an ice massif which does not fracture but experiences only local crushing strain in the impact area. In the case under consideration, it is assumed that small-sized ice floes which are usually located between the ship's side and the edge of the ice field and soften the impact, are absent. Bending of the ice field which decreases the magnitude of the ice load, especially during movement in relatively thin ice, is also disregarded. Naturally, with such initial conditions, the actual

operating speeds at which a ship can move in ice without damaging its hull will be greater than the selected conditional design velocities.

Table 11

Design velocities for impact against ice for ships of classes.

Ship type	Ship class	Speed, kts.
Icebreakers	I	12
	II	8
	III	6
Cargo ships	UL (Arkt)	5
	UL	2
	L	0.7
Tugboats	UL	3
	L	1.2

Table 12

Maximum ice thickness during ice compression for ice ships.

Ship type	Ship class	Ice thickness, m
Icebreakers	I	4
	II	3
	III	2
Cargo ships	UL (Arkt)	1.5
	UL	0.9
Tugboats	UL	0.7
	L	0.3

When setting design velocities and ice thicknesses for icebreakers, the purpose and power of the icebreakers are taken into consideration. Practice shows that for I-class, heavy icebreakers (see 17.), 12 knots can be taken as the design velocity of impact against ice. For medium icebreakers (II class) and harbor icebreakers (III class), these velocities

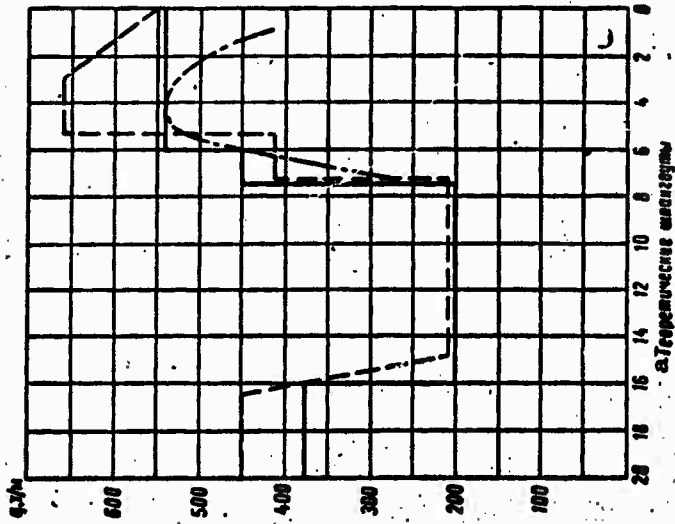


Figure 39. Construction strength and design strength of side framing of heavy icebreakers.  
 — design load; - - - construction strength; - . - . - theoretical ice load. a-frame lines.

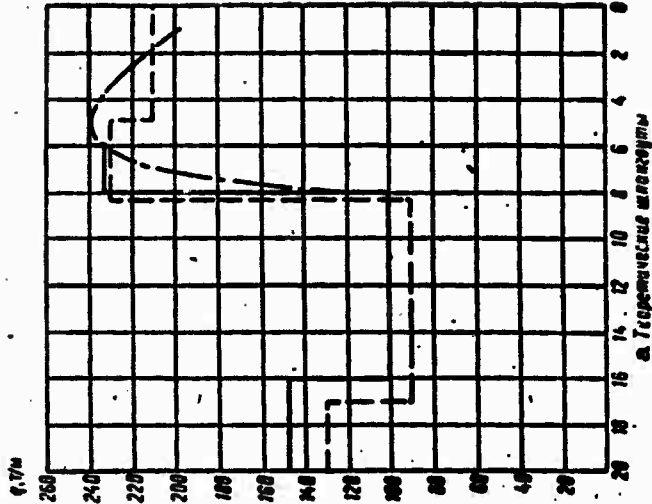


Figure 40. Construction and design strength of side framing of a medium icebreaker.  
 — design load; - - - construction strength; - . - . - theoretical ice load. a-frame lines.

are 8 and 6 knots respectively. Design velocities for cargo ships are designated depending on the ice class of the ships, allowing for their movement in a channel behind a heavy icebreaker. In doing this, attention was given to operating experience of ice ships which proved themselves well, while operating in ice.

Conditional design velocities of impact against ice have been taken for ice ships in accordance with the aforesaid. (Table 11).

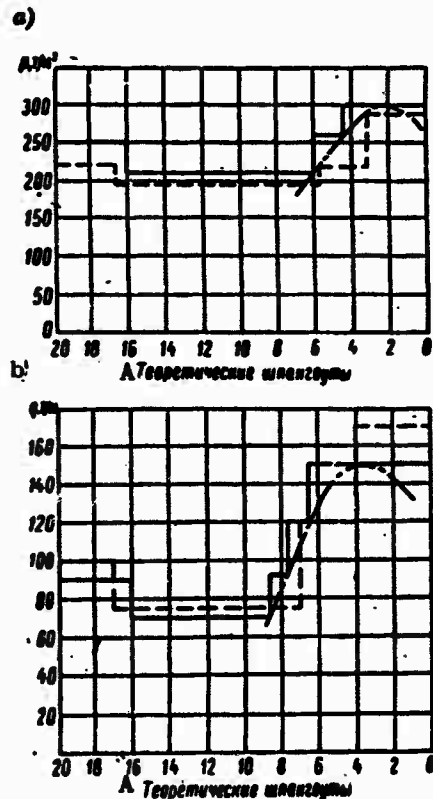


Figure 41. Construction and design strength of a harbor icebreaker: a- plating; b-side framing. — design load; - - - - theoretical ice load; . . . . construction strength. A-frame lines.

When calculating ice loads, the strength characteristics of the ice are assumed in accordance with data presented in 1. for Arctic ice. For cargo ships and tugboats, the ultimate crushing strength of ice in impact is taken as  $\sigma_c = 400 \text{ t/m}^2$ , in compression  $\sigma_c = 200 \text{ t/m}^2$  and in bending  $\sigma_b = 100 \text{ t/m}^2$ . For icebreakers, the indicated strength characteristics are increased by 25% in view of their expeditionary navigation in the early navigational periods. The Poisson coefficient is assumed as  $\mu = 0.34$ ; specific weight of ice  $\gamma = 0.87 \text{ t/m}^3$  and the modulus of normal elasticity in compression  $E = 4 \cdot 10^4 \text{ t/m}^2$ . Values for ice thickness at which the midsection does not undergo serious damages in the process of compression are presented in Table 12.

L-class ice cargo ships must sail during favorable ice conditions when there is no compression.

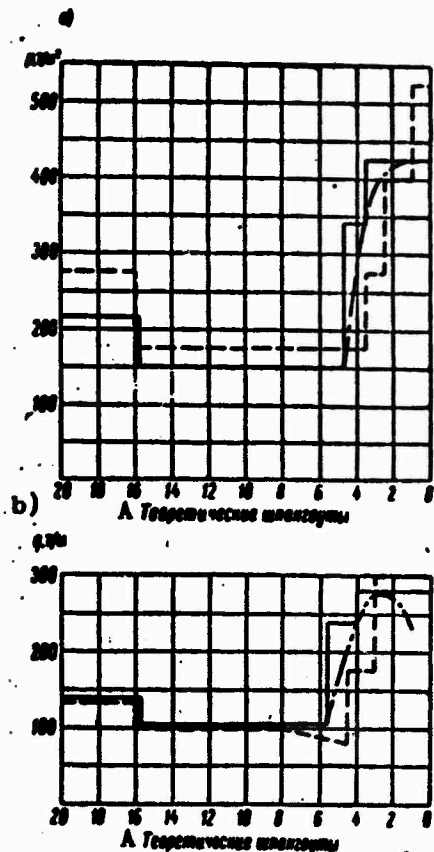


Figure 42. Structural and design strength of prototype: a-shell; b-side framing. — designed load; - - - structural strength; - . . . - theoretical ice load. A-frame lines.

Figures 39 and 40 present graphs of the construction strength of the side framing of a heavy and medium icebreaker, as well as values of ice loads, obtained by calculations for the corresponding ice navigating conditions. Analogous data for side framing and plating for a harbor icebreaker is presented in Figure 41. From these graphs, it is obvious that the construction strength and design ice loads agree with each other as a whole. At the same time, it is known from operating experience that the icebreakers under consideration did not suffer substantial ice damages.

The construction strength of framing at the extremities of a heavy icebreaker proved to be somewhat greater than design ice loads. For a medium icebreaker, the construction strength and ice loads in the bow and midsection were very close. Considering that icebreakers must quite often

move astern in ice, it is necessary to increase the strength of their stern in comparison with their midsection.

From Figure 41, it is seen that in the area of the third to seventh frame lines, the strength of the side framing and plating is somewhat lower than required by calculations. As operating experience shows, insignificant crimping of the shell plating occurred specifically in that area.

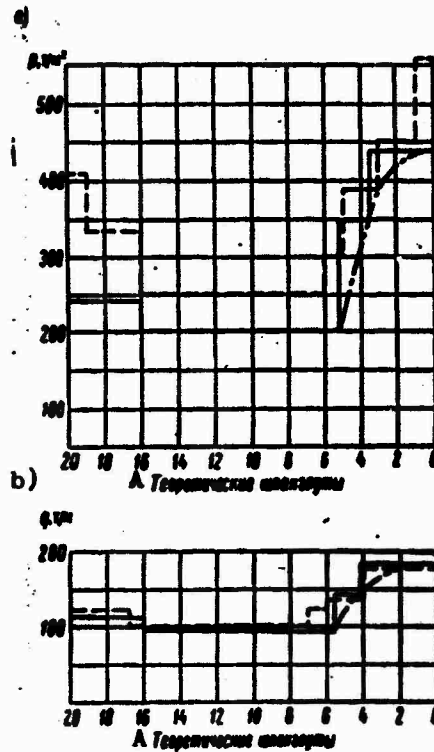


Figure 43. Construction and design strength of a UL (Arkt)-class cargo ship: a - plating; b- side framing. \_\_\_\_\_ design load; - - - - construction strength; - . - . - . - theoretical ice load. A-frame lines.

Further operating experience of icebreakers will permit more accuracy to be introduced when designating their hull strength in the ice belt area.

Figure 42 presents curves of the construction strength of side framing and plating of a UL (Arkt)-class cargo ship; curves of design ice load are also constructed there. From a comparison of these curves, it follows that they are relatively close with the exception of the area of the third and fifth frame lines where construction strength is less than design strength. This situation points to the inadequate strength of the side plating and especially of the framing of the ship in the area under consideration, which is the juncture of the bow with the parallel middle body. Calculations show that ice loads in the area of the third

and fifth frames attain a significant magnitude as a result of the comparatively small slope to the side and sharp transition of the entrance with the parallel middle body. Operating experience in ice completely confirms this conclusion, inasmuch as a large part of ice damage to plating and especially to framing, occurs specifically in that area of the hull.

Curves of construction strength of side framing and plating of one of the ships, also of the UL (Arkt.)-class are compared in Figure 43. As the figure shows, the construction strength and ice loads practically coincide over the entire hull length.

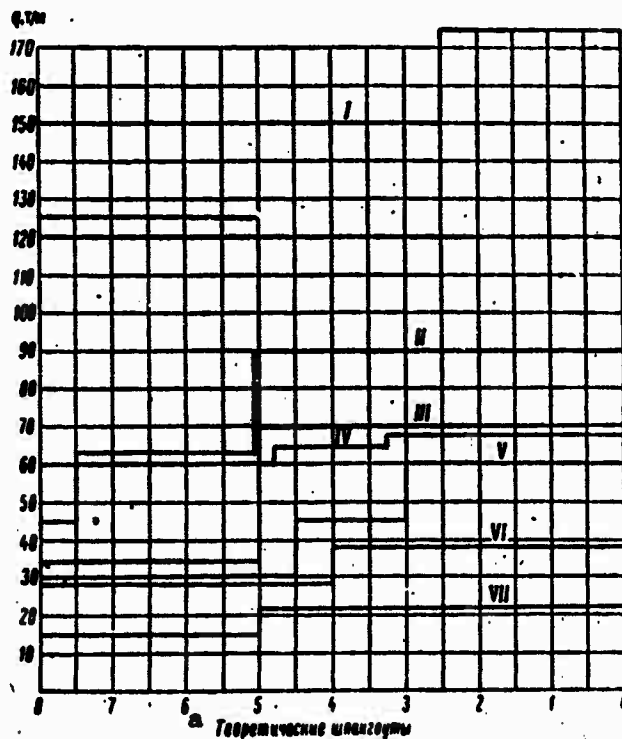


Figure 44. Construction strength of side framing of UL-and L-class cargo ships.

I - UL, D = 11,179 t; II - UL, D = 9,500 t; III - UL, D = 10,450 t;  
 IV - UL, D = 9,050 t; V - UL, D = 11,080 t; VI - L, D = 12,700 t;  
 VII - L, D = 13,500 t. a-frame lines.

Figure 44 presents graphs of the construction strength of side framing of several cargo ships of various ice classes. From the figure, it is obvious that the construction strength of a series of ships of the same ice class and of nearly the same displacement (dimensions) fluctuates over a rather wide range. The excessively high hull strength of several UL-class ships displacing 11,170 t, which practically corresponds to the UL (Arkt.)-ice class, attracts attention. This is a consequence of the present practice of installing ice strengthening on ships which sail in the

ice and cannot be assumed as normal. It should also be noted that UL-ice class light and medium ships, as a rule have less ice strength than larger ships of that same ice class. Therefore, during ice compression, the intensity of which does not depend on a ship's dimensions, light-and medium-cargo ships find themselves under more difficult conditions than heavy ships and naturally receive considerable ice damage. Construction strength and design ice loads of a UL-class, medium, timber carrier are compared in Figure 45. From the figure it is obvious that the strength of the ship's plating as a whole, corresponds to the design ice loads except in the area of the third to fifth frame lines, where it is inadequate. The strength of midship side framing is considerably less than the strength required for ships of the given ice class. This was reflected in this ship's operation. During ice compression, the ship received heavy ice damages in the form of non-elastic strains in the hull framing amidships.

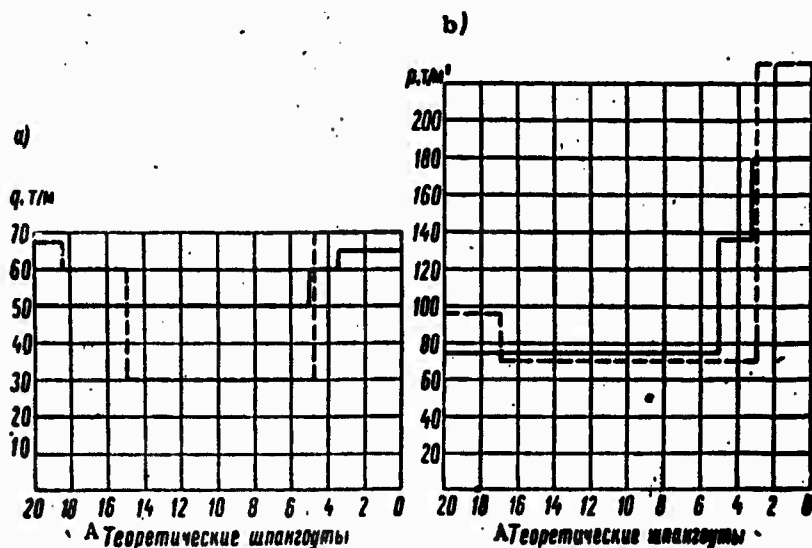


Figure 45. Construction and design strength of a medium, timber carrier: a- strength of framing; b-strength of plating. \_\_\_\_\_ design load; - - - - construction strength. А-frame lines.

Figure 46 presents graphs of ice loads on the side framing of cargo ships displacing 10,000 t, for various hull lines and ice classes in conformity with the classification of ice ships cited in 17.

A number of assumptions were made in the process of computing the magnitude of ice loads when performing the comparative calculations of the strength of icebreakers and ice class cargo ships; therefore, the estimate of the construction strength of ships that sail in ice and the recommendations made should be considered as preliminary, requiring introduction of corrections as additional theoretical and experimental data is accumulated.

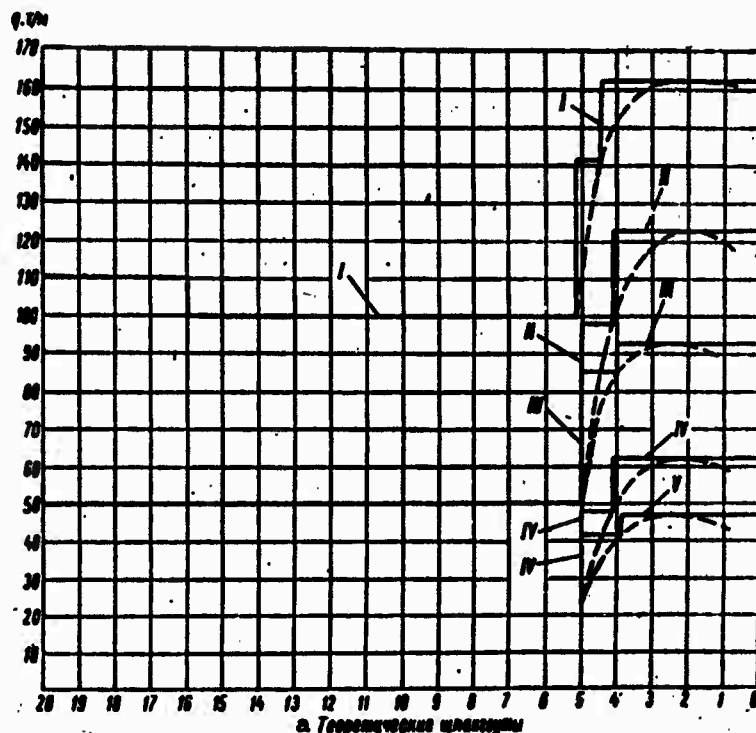


Figure 46. Ice loads on side framing of cargo ships displacing 10,000 t of various ice classes and having various hull lines.

\_\_\_\_\_ design load; - - - - theoretical ice load.  
 I - UL (Arkt.) icebreaker form; II - UL, non-icebreaker form;  
 III- UL semi-icebreaker form; IV - L, non-icebreaker form;  
 V - L, semi-icebreaker form.  
 a- frame lines.

**17. Requirements of Various Shipping Registries for Ice Strengthening of Ships. Proposals for Classifying Ice Ships.**

The hull strength of ice ships is conditioned, to a considerable degree, by special requirements which are compiled in ship classification and construction regulations. These cargo ship construction and strength requirements are in the Rules of the Register of Shipping of the USSR as well as in the rules of the majority of leading foreign shipping registries (British Lloyd's, French Bureau Veritas, Finnish Shipping Council, Norwegian Veritas, American Bureau of Shipping). The basic requirements of the listed shipping registries regarding ice strengthening of the hull are presented in Table 13.

Icebreaker construction rules are not regulated by any of the shipping registries with the exception of the Norwegian Veritas, which for the first time in 1961, published rules containing icebreaker classifications, recommendations concerning hull strength and construction,

selection of lines, designation of the power plant capacity, etc.

It should be noted that in the various rules, the length of strengthened areas is not the same. In connection with this, when making comparisons, it is conditionally assumed that the ratio of length to breadth for ice cargo ships is about seven on the average. It is possible to formulate some concept of the degree of hull strengthening in comparison with the hull of an unstrengthened ship from data in Table 13. However, it is difficult to compare strength of ships constructed according to rules of the various shipping registries on the basis of the presented data inasmuch as they designate ice strengthening on the basis of different operating conditions and technical proposals. Moreover, the shipping registries use different approaches to the determination of scantlings of midship framing and plating of unreinforced ships, on the basis of which supplementary strengthening for ice class ships is designated as a rule. Therefore, Tables 14 and 15 present comparative data on the hull strength of a ship displacing 10,000 t, selected from the Rules of the Registry of Shipping of the USSR, British Lloyd's, and Norwegian Veritas.

A comparison of the requirements of the various shipping registries (Tables 13, 14 and 15) shows that:

1. of the foreign shipping registries, British Lloyd's sets the highest requirements for ice strengthening of ships;
2. the hull strength of I-class ice ships of British Lloyd's corresponds approximately to the hull strength of UL class ships of the Registry of Shipping of the USSR. The strength of the side framing of the fore body according to Lloyd's Regulations is approximately 35% less and in the midsection is 25% higher than according to Regulations of the Registry of Shipping of the USSR. The plating thickness in the fore body (for a length of 0.15 L from the stem) is 1.5 mm greater for the same frame spacings, according to Lloyd's. The hull strength in the bow of a ship of the highest ice class IsA of Norwegian Veritas, is less than the hull strength of UL-class ships of the Registry of Shipping of the USSR and in the midsection and stern, it is approximately the same;
3. the hull strength of II-ice class ships of British Lloyd's and IsB-class of Norwegian Veritas is greater than the hull strength of L-class ships of the Registry of Shipping of the USSR and III-class ships of Lloyd's and IsC-class ships of Norwegian Veritas are close in strength to L-class ships;
4. there is no ice class corresponding to the UL (Arkt.) of the Registry of Shipping of the USSR stipulated in regulations of foreign registries. There are no specific hull strength requirements for ships of that class in Regulations of the Registry of Shipping of the USSR;
5. a general deficiency in the regulations of shipping registries is that when scantlings of hull strength braces are designated, basic factors on which the magnitude of the ice load depends are not considered

at all or are inadequately considered. These include hull lines, ships' speed in ice and ice thickness and strength;

6. requirements for ice strengthening of ships are systematically being improved and made more severe. For example, in Regulations of the Norwegian Veritas issued in 1958, there were instructions concerning strengthening of only one ice class IAIII and in the 1962 edition, three ice classes, IsA, IsB and IsC were stipulated. Moreover, in 1961, Norwegian Veritas published rules for the classification and construction of ice-breakers for the first time.

Considering the above-mentioned defects inherent in effective regulations as well as the existing tendency in the Soviet maritime fleet to extend the Arctic navigation period and to ensure year-round operation of ports in frozen seas outside the Arctic, the authors propose a new, more complete classification of ice ships. The quantity and designations of ice classes of cargo ships and tugboats adopted in effective Regulations of the Registry of Shipping of the USSR are kept under the proposed classification system.

For the first time in Soviet practice, a classification is made of icebreakers which are subdivided into classes according to their purpose and ability to pass through ice, determined by their basic dimensions and power plant capacity, all other conditions being equal. In accordance with the proposed classification, specific recommendations concerning designation of scantlings for hull structures which are subject to ice action are presented in the second section of the book. Results of the latest theoretical research in the field of ice strength as well as experience in design and operation of ice ships were considered when working out these recommendations,

Acceptance of one or another classification for ice ships is doubtlessly the prerogative of the shipping registries. However, the authors hope that their proposals will be of use and will be taken into consideration when the Regulations of the Registry of Shipping of the USSR is corrected and republished.

Classification of icebreakers. The Polyarnyy-Class icebreaker or I-class is the designation for icebreakers with a power plant capacity of more than 20,000 hp, which are intended for making channels; conducting, breaking around and towing ships; and forcing heavy ice dams and hummocked formations in Arctic Seas during the course of all Arctic navigation. These icebreakers can also be used in the wintertime during years of severe freezing in frozen, non-Arctic seas (Baltic, White, Okhotsk). The atomic ship, Lenin, (N = 44,000 hp) and Moscow-class icebreakers (N=26,000 hp) can be included in this class.

The medium icebreaker class or II-class, includes icebreakers with a capacity of 9,000 to 20,000 hp which are intended for making channels; conducting, breaking around and towing ships; and forcing ice dams and

Table 13  
Requirements of various shipping registries for ice strengthening of cargo ships

Shipping Registry	Year of issue of regulations.	Ice class.	Shell plating			Side framing			Sectional area	Notes		
			Width of Thickness of ice belt plates and length of strengthened area			Frames		Stringers				
			In fore body (from the stem).	In stern (from stern-post).	Midships	intermediate	Length of intermediate frames according to the height of the sides.	Area of installation (from stem) and distance between stringers, mm.				
Registry of Shipping of the USSR	1956	UL	0.5	1.0	1.60 to 1.15	1.20	1.15	1.20	1.50	1.25	F	Lower deck beams must have a section modulus with the attached flange 25% greater than that required for lower decks which are not ice strengthened.
			Above LML.	Below BML.	for a distance of 0.15L**	for a distance of 0.15L to 0.15L.	for a distance of 0.15L from stem, $W_{main} = 2.3W_i$ for a sector (0.15 - 0.25)L $W_{main} = (2.3 \text{ to } 1.5)W_i$ in after-peak, $W_{main} = 2.3 W_i$ for remainder	For engine tire length of ship $W_{int} > 0.50 W_{main}$ .	From deck For engine above LML tire length to upper edges of plate frames.	From deck For engine length (a system of web frames is recommended) $1 < 1.8$ to 2.0.		





									below LML), must extend entire length. Remaining stringers for a length of 1.5B; $t = 1.85m$ .			500 hp, but cannot exceed 25.5 mm.	
									Same, ice stringer must extend for length of 2.5B.	1.15 $F_0$	1.25 $F$	Same.	
								For a length of 2.5B or to widest section of the LML, $W_{int} = W_{main}$ .	Same.				
								For a length of 1.5B in accordance with table of Regulations.	Same.				
								For a length of 1.5B in accordance with table of Regulations.	Same.	1.10 $F_0$	1.075 $F$	Gradual reduction of shell plating thickness to thickness of mid-ship plating of a regular ship at LML.	
								For a length(0.15 deck - 0.20)L above ice where L = belt to -120 to plate 60m. Magnitude $W_{int}$ frames.	Same.				
French Bureau Veritas.	1563 Ice.	0.61	0.61	150									Remaining classes: ice I, Ice II, and ice III correspond to classes IA, IB and IC of the Regulations of the Finnish Shipping Council.

							is given depending on L.														
Finnish Shipping Council	1958	1A	0.5	0.5	1.50t <sub>0</sub> for a distance of 1.5B.	1.25 t <sub>0</sub>	1.25 t <sub>0</sub>	Same	For en-tire length $W_{int} = W_{main}$ .	From level 0.5m above winter LML and to flooring of the inner bottom or floors.	1.25 F <sub>0</sub>	1.15 F.									
											1B	0.5	0.5	1.25t <sub>0</sub> for a distance of B.	1.15 t <sub>0</sub>	1.15 t <sub>0</sub>	Same.	For a length 2B $W_{int} = W_{main}$ .	Same.	1.15 F <sub>0</sub>	1.10 F.
											1C	0.5	0.5	Same	-	-	Same.	Same.	For a length 2B when $W_{int} = 0.75W_{main}$ .	Same.	F <sub>0</sub>
American Bureau of Shipping.	1959	A1	0.915	0.915	For a distance 0.6L at least 15 mm for ships with L=76m and no greater than 25.5 mm for ships with L=152m.	t <sub>0</sub>	t <sub>0</sub>	Same.	For a distance 0.6L $W_{int} = 0.75 W_{bow}$ in fore-peak.	From deck above ice belt to plate frame.	F <sub>0</sub>	F.									

\* The following symbols are used in the table: L-ship's design length; B-ship's design breadth; EHP-power plant capacity (rated); t-shell plating thickness, t<sub>0</sub>-thickness of side shell plating in midsection of conventional (without ice strengthening) ship; W-section modulus of midship frames of conventional ship; W<sub>main</sub>-section modulus of main frames; W<sub>bow</sub>-section modulus of bow frames of conventional ship; W<sub>int</sub>-section modulus

of intermediate frames; F<sub>Q</sub>-sectional area of stem of conventional ship; F-sectional area of sternpost of conventional ship, LWL-load waterline; BWL-ballast waterline.

\*\* According to regulations of registries of shipping, thickness of the ice belt plating must be: minimum 10 to 12.5 mm, maximum 25 to 25.5 mm. The Registry of Shipping of the USSR and American Bureau of Shipping do not specify the minimum thickness of ice belt plating and Norwegian Veritas does not specify it for IsC class.

Table 14.

Strength of ice belt plating on a ship displacing 10,000 t, selected from regulations of various shipping registries.

Классификационное обозначение	Толщина листа	d		e		L	B
		И		II			
		335	335	216	216		
Первый Сухопутная Лодка (Американский Лодка)	I	335	266-160	111	111	156	156
	II	335	266-111	99	99	140	140
Норвежский Веритас	IaA	216	164-120	111	111	153	153
	IaB	216	164-106	99	99	140	140
Московский Первострой СССР	УЛ	206	216	216-106	106	163	163
	Жм	223	165	165-19	19	28	28

a-Shipping registry; b-ice class; c-strength of ice belt plating, t/m; d-forepeak; e-fore body sector; f-collision bulkhead-0.2L; g-midsection; h-after peak; i-Lloyd's Register of Shipping (Lloyd's Registry); j-Norwegian veritas; k-Registry of Shipping of the USSR; l-UL: k-L.

Table 15.

Strength of side framing (frames) of a ship displacing 10,000 t, selected from regulations of various shipping registries.

Классификационное обозначение	Толщина листа	d		e		L	B
		I		II			
		49.5	49.5	36.5	36.5		
Первый Сухопутная Лодка (Американский Лодка)	I	49.5	42.5	42.5	42.5	42.5	42.5
	II	42.5	42.5	42.5	42.5	21.2	21.2
Норвежский Веритас	IaA	36.5	36.5	36.5	36.5	36.5	36.5
	IaB	36.5	36.5	36.5	36.5	18.2	18.2
Московский Первострой СССР	УЛ	57.6	57.6	57.6-34.8	34.8	34.8	34.8
	Жк	34	34	34-17	17	17	17

a-Shipping registry; b-ice glass; c-strength of side framing (frames), t/m; d-fore body sector; e-collision bulkhead - 0.2L; f-midsection; g-Lloyd's Register of Shipping (Lloyd's Registry); h-Norwegian Veritas; i-Registry of Shipping of the USSR; j-UL: k-L.

hummocked formations in Arctic seas in the summer to autumn period and in frozen, non-Arctic seas in the winter period. These icebreakers work together with Polyarnyy icebreakers in conducting ships over difficult, iced sectors of the route. The icebreakers Sibir' and Krasin can be counted in this class.

The harbor icebreaker class or III-class, includes icebreakers intended to operate in ports, bays and roads of Arctic seas in the summer to autumn period and in frozen, non-Arctic seas in the winter period, as well as for conducting ships together with icebreakers of heavier classes. The power plant capacity of icebreakers of this class can fluctuate over a wide range; however, it is usually not greater than 5,000 to 6,000 hp. The icebreakers Il'ya Muromets (N = 3,700 hp) and Ledokol-1 (N = 5,400 hp) can be included in ships of this class.

Classification of ice cargo ships. UL (Arkt.)-class includes ships intended for systematic navigation in Arctic and Antarctic seas throughout the entire navigation period under icebreaker conduct, as well as for independent navigation in compact ice fields up to 0.5 m thick and in very compact, coarsely-broken ice. Ships of this class should be given icebreaker form hull lines, at least in the fore part. The strength of UL (Arkt.)-class ships must allow them to endure ice compression and roughly corresponds to the strength of Lena and Anguema-class ships. The power plant capacity must be chosen to allow independent navigation in ice.

The UL-class includes ships intended for navigation in Arctic and frozen non-Arctic seas throughout the navigation period conducted by icebreakers and in open pack ice independently. Ships of this class can be subjected to ice compression. The UL-class includes the largest numerical group of cargo ships intended for navigation in ice.

In view of the increased demands on modern ice ships occasioned by the commissioning of new, heavy, icebreakers and the extension of the navigation period in Arctic and non-Arctic frozen seas, the strength of ships of the class under consideration must be somewhat higher than the strength of constructed UL-class ships of the Registry of Shipping of the USSR (in accordance with regulations issued in 1956). It is advisable to give UL-class ships a semi-icebreaker form bow to improve their ice qualities.

The L-class includes ships destined to sail in frozen non-Arctic seas and in the summertime of years of moderate and light freezing in Arctic Seas, L-class ships conducted by icebreakers must not be subjected to ice compression. The hull strength of these ships roughly corresponds to the strength of ships constructed in accordance with the requirements for L-class of the Registry of Shipping of the USSR (in accordance with regulations issued in 1956).

Classification of tugboats. The UL-class tugboat includes tugboats destined to conduct and tow ships in frozen, non-Arctic seas and in Arctic seas in the summertime. The L-class tugboat includes tugboats destined

to conduct and tow ships in ice in the Black and Caspian Seas, as well as in the southern part of the Baltic Sea and Sea of Azov.

UL-class tugboats should be given icebreaker lines and L-class tugboats, semi-icebreaker lines. The hull strength of these tugboats, according to the new classification, must be somewhat increased over the requirements of effective regulations.

For example, Figure 46 presents design ice loads on side framing for cargo ships displacing 10,000 t in conformance with the classification proposed by the authors (see page 99).

## SECTION TWO

### CALCULATION OF THE RESISTANCE OF HULL STRUCTURES TO THE

#### EFFECT OF ICE LOADS

### CHAPTER V

#### STRENGTH OF SIDE PLATING AND FRAMING\*

---

\* Materials which Engineer, A. A. Bubyakin, helped develop were used when writing this chapter.

---

#### 18. Designating Scantlings and Determining Ice Belt Plating Thickness.

The side plating of ice ships is constantly subjected to hydrostatic loads when sailing in clear water and to the effect of contact stresses from ice cover. Under normal operating conditions, plating must withstand external loads without receiving non-elastic strains. Stresses caused by ice considerably exceed in intensity, hydrostatic pressures; therefore, hull structures in the area of interaction between the ship's hull and ice should be calculated exclusively for ice loads. A test of the plating's hydrostatic head strength and its part in overall bending can be required only in rare cases.

Ice load applications are usually local in nature, acting on a relatively small sector along the ship's side (mainly in the area of the effective waterline). The area of ice load application increases significantly only during ice compression of a ship.

An ice belt of increased strength to absorb ice loads is installed on all ice ships and icebreakers in the area of the side which is directly subjected to ice action. Side plating in the area of the ice belt is strengthened by means of increasing its thickness and decreasing the distance between frames. High tensile steel with a yield stress up to  $\sigma_y = 45$  to  $50 \text{ kg/cm}^2$  and more, often is used for the ice belt of the shell plating. This allows the weight of the ice strengthening to be reduced.

The ice belt length is designated depending on the operating conditions and type of ship and is regulated by regulations of the shipping registries for each ice class individually. Changes in the ship's draft

when sailing with cargo and in ballast, and possible trim and list angles, as well as pressing up of the hull and hummocking of ice at the ship's side during ice compression are considered.

The largest part of floating ice is below the water, i.e., below the effective waterline. Moreover, a substantial number of ice floes are submerged by the hull as a consequence of the flare. The numerous impacts against ice experienced by the underwater part of the hull testify to this. The underwater part of the hull can be encompassed by ice for a substantial distance from the stem to the midsection and from the waterline down. Therefore, the width of the ice belt below the effective waterline must be considerably greater than its width above the water.

Figure 47 presents diagrams of the location of the ice belt on sea cargo ships according to requirements of various shipping registries and indicates the increase in thickness of the ice belt plating (by percent) in comparison with the thickness of the plating in the midsection of ships which are not ice strengthened.

Recommendations of the authors for designating scantlings for the ice belt of ice ships and icebreakers, based on an analysis of experience in the design and operation of Soviet ships, are presented below. In making the recommendations, the above-cited considerations of the nature of the interaction between a ship's hull and the ice were taken into consideration and attention was given to lengthening the navigation periods in the Arctic and frozen, non-Arctic seas, extending areas of ice navigation, etc.

For I- and II-class icebreakers, displacement of which varies little, the lower edge of the ice belt amidships must extend at least 3,500 mm below the waterline corresponding to its load displacement. This lowering of the bottom edge of the ice belt corresponds to the thickness of compact ice in which these icebreakers can operate. At the same time, this lowering will be adequate when the icebreaker is required to operate at the minimum possible draft because of shallow water. The upper edge of the ice belt must remain at least 800 mm from the waterline corresponding to the icebreaker's maximum draft. Possible listing of the icebreaker and impacts against hummocks protruding above the water's surface were taken into consideration when designating these scantlings. For III-class icebreakers which sail under less severe conditions, the ice belt width can be taken as nearly 500 mm above water and on the order of 1000 mm underwater (from the waterline corresponding to full displacement). Considering that damages in the fore part of hulls of all classes of icebreakers are observed much lower than the ice belt, the authors suggest that the ice belt in that area be extended completely to the keel for a distance of  $0.2L$  astern from the forward perpendicular. The lessening of the height of the ice belt in the transition from the bow area to the midsection must be gradual. Through strakes must also be installed above and below the ice belt, the entire length of the ship.

On UL (Arkt.) and UL-class cargo ships, the ice belt must extend 650 mm above the summer load waterline and 1,200 mm below the summer load waterline amidships. On UL-class tugboats, the ice belt must be 300 mm

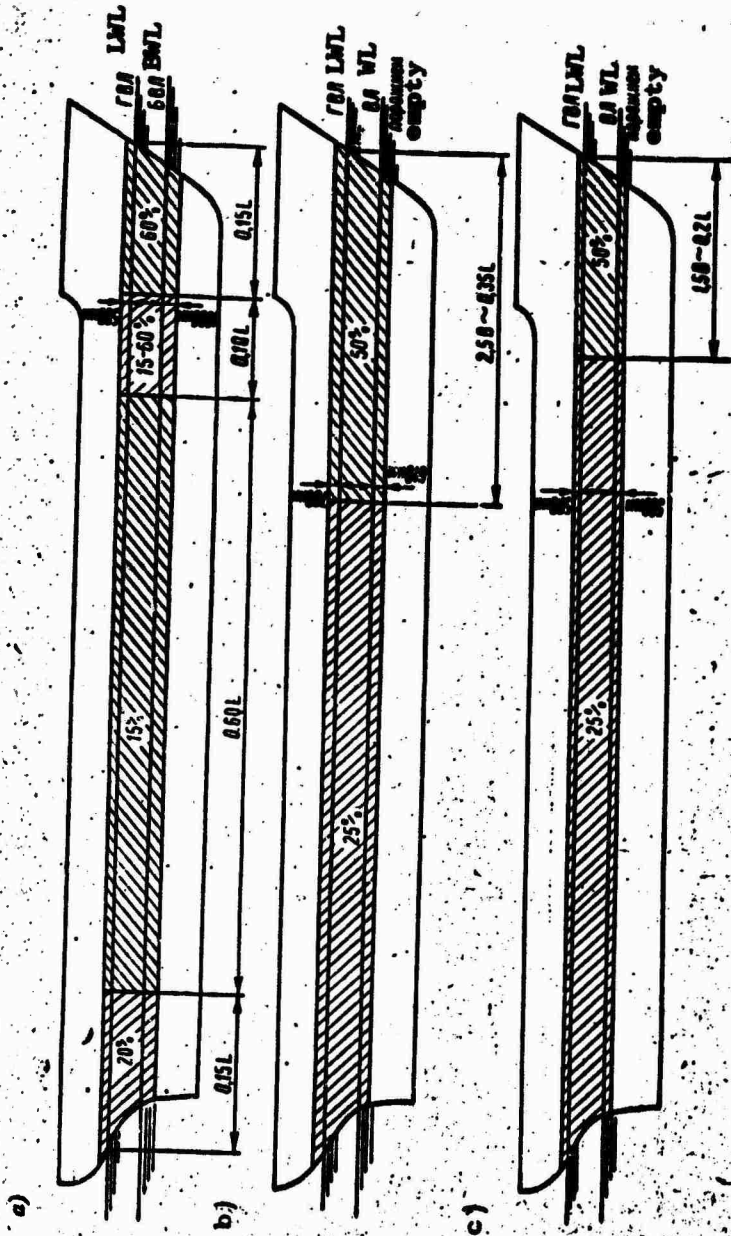


Figure 47. Area of ice strengthening in accordance with regulations of various shipping registries: a-Registry of Shipping of the USSR, UL-class; b-Lloyd's Registry, I-class; c-Finnish Shipping Council, IA-class.

above the waterline corresponding to the maximum draft and 800 mm below the waterline corresponding to the minimum operating draft. On L-class tugboats, these measurements are 300 and 600 mm respectively. Considering the possibility of impacts by ice floes against the underwater part of the hull, the ice belt on UL (Arkt.)-class ships and UL-class tugboats should go completely down to the keel for a distance of 0.2L astern from the forward perpendicular. This distance can be reduced to 0.1 L on UL-class ships and L-class tugboats. The requirements for transitional areas here are the same as those maintained for icebreakers.

On L-class ships, the ice belt is installed only in the bow for a distance of at least 0.2 L from the forward perpendicular\* and extends 400 mm above the winter load waterline and 900 mm below the ballast waterline.

---

\* It is advisable to extend the ice belt to the transition area between the fore part and the parallel middle body.

---

As indicated above, local strength of side plating in the area of the ice belt should be calculated for ice loads only. The side framing, decks and platforms serve as a rigid, index contour for the plating and divide it into a series of rectangular plates. Distance between the short sides of the index contour  $c$  is usually several times greater than the frame spacing  $s$ . The design ice load should be applied to the center of the plate span. In this case, with  $c/s > 2.0$ , the rectangular plate can be considered as an infinite band with a width of  $s$ . When  $c/s < 2.0$ , the effect of the short sides of the index contour should be considered. Such calculations can be required when there are frequently placed, bearer stringers installed to support the frames and increase the carrying capacity of the side plating.

The procedure for calculating bending of rectangular plates, in both the elastic and elasto-plastic areas, is sufficiently completely developed. Therefore, it is theoretically possible to calculate the shell plating for an ice load of a given intensity. The basic difficulty consists of a lack of a substantiated procedure for designating the magnitude of the design load on plating, as well as inadequate knowledge of the nature of load distribution. There have been various calculation methods. A. K. Osmolovskiy [35] and Yu. I. Voskresenskiy considered the work of plating in elasto-plastic and plastic zones, deducing all dependencies for plates bending along a cylindrical surface (for a strip). Along with this, an attempt was made to determine the ice loads acting on a hull by means of analyzing measured strains and to establish corresponding norms of strength. However, the procedure of calculating external loads by non-elastic strains remained practically unexploited. Therefore, at the present time, until it becomes possible to use the results of these works, direct calculation of actual external loads on plating by means of strain is extremely desirable.

A. A. Kurdyumov [28] proposes that the shell plating be calculated as a strip, rigidly constrained on frames. The intensity of external loads, in this case, is taken as equal to the temporary resistance of the ice to breaking up (crushing), which for local loads equals  $\sigma_c = 600 \text{ t/m}^2$ . In the fore part (0.25L), in connection with the dynamic action of the load, its magnitude grows by 50 to 100%. The admissible stress in a plate is assumed as equal to the yield stress of the material. Thus, the design load on plating turns out to be independent of the ship's velocity, hull lines and displacement. For most ships, calculation by this method leads to an increase in the thickness of the plating.

In N. F. Yershov's work [17], a calculation of the critical load on a ship's plating is made, allowing for inherent thrust. The plate is considered as being a simply supported strip and the critical load corresponds to the appearance of a plastic hinge in the center of the span. As should be expected, allowing for membrane tensions has an influence on the magnitude of the critical load, only for small thicknesses and large frame spacings which are not characteristic of ice ships.

A general defect of the above-cited calculating systems is the absence of a link between calculation of design external stresses for the framing and the plating. This cannot be considered correct inasmuch as the same external load is acting on the ship's hull. Moreover, no sharp delineation was made between ships by classes and the cited calculation systems were not analyzed from the point of view of actual ice navigating conditions from which, in the final analysis, requirements for framing and plating strength must originate.

In his work [53], Yu. A. Shimanskiy notes that the strengths of side framing and plating must be found in relation to each other. In order to establish the degree of this relationship, Yu. A. Shimanskiy introduces a conditional gauge -- the modulus of resistance of the hull side plating depending on plating thickness, frame spacing, critical load on framing and critical stress of the plating material. This coefficient makes it possible to judge only the relative strength of the framing and plating of various ships. The true dependence between these magnitudes actually remains unestablished.

Thus, the above-cited methods allowed the strength of a ship to be calculated according to the known strength of a corresponding ship-prototype. In other cases, they yielded satisfactory results for only a determined group of ships. Use of the design formulas for ships of other dimensions and classes led to either an overestimate or an unbased reduction in plating thickness. In essence, the external ice load actually acting on the plating was not determined. Whereas it is perfectly clear that ice belt plating is subjected to action of pressure developing in the zone of contact between the ship's side and ice, the zone of ice load application to plating takes the form of a patch stretching along the ship for several frame spacings. Therefore, when calculating strength, ice belt plating should be considered as a plate supported on a rigid contour and rigidly fixed on the frames. Shell plates must be considered as rigid

plates, disregarding membrane tensions as being negligible in comparison with flexural stresses.

Flexural elements of plating under the effect of a local load equally distributed over the area of the crushing zone (Figure 48), can be computed as the corresponding cylindrical bending elements of plates multiplied by correction factors  $k$ , as minor units [48]. The values of coefficient  $k_2$  as a function of the relationship  $c/s$  are presented in Table 16. As the table shows, when  $c/s > 1.4$ , a rectangular plate can be considered as infinite and calculated by the formula for a strip.

Table 16

Value of correction factor  $k_2$ .

$c/s$	0,2	0,4	0,6	0,8	1,0	1,2	1,4	1,6	1,8	2,0	2,2
$k_2$	0,338	0,578	0,744	0,854	0,923	0,965	0,990	0,996	-	-	1,0

We shall assume that the strength of side plating is assured if the maximum, normal, stresses in the extreme fiber acting on the center of the loaded edge of the index contour do not exceed the yield stress  $\sigma_y$  of the material. The design bending moment in the indicated section of the plate is calculated according to formula

$$M_2 = \frac{ps^2}{12} k_2. \quad (18.1)$$

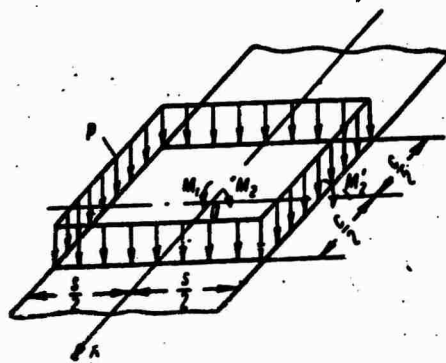


Figure 48. Design diagram of the load for ice belt plating.

Assuming bending to be cylindrical, for extreme fiber stresses of the plate we obtain

$$\sigma = \frac{p}{2} \left( \frac{s}{b} \right)^2, \quad (18.2)$$

where  $\rho$  - is the intensity of the ice load on the plating;  
 $s$  - is the frame spacing;  
 $\delta$  - is the plating thickness.

Assuming that fiber yield occurs, we obtain a final formula for calculating shell thickness

$$\delta = 225s \sqrt{\frac{\rho}{\sigma_y}} \text{ mm.} \quad (18.3)$$

where yield stress is assumed in  $\text{kg/cm}^2$ , pressure  $\rho$  in  $\text{t/m}^2$  and frame spacing  $s$ , in meters.

When stipulating plating thickness, its intensive wear in the process of the ship's operating under ice conditions, should be taken into consideration. It is especially important to consider the wear for small ships with relatively thin plating. Designating the period of the ship's service (in years) by  $t$ , and the annual wear of the plating (in mm) by  $\Delta\delta$ , we write the condition of the plating strength at the end of an operating period

$$\sigma_y = \frac{\rho}{2k} \left( \frac{s}{\delta_1 - t\Delta\delta} \right)^2, \quad (18.4)$$

where  $k$  - is a coefficient equal to the ratio of the section moduli in the elastic and plastic zones;  
 $\delta_1$  - is the plating thickness designated, taking its wear into consideration.

In accordance with data from operating experience of ships sailing in ice,  $\Delta\delta = 0.2$  mm can be assumed as average. The thickness of the side plating, taking its wear into consideration, should be calculated on the basis of attainment of a plastic hinge in the abutment sections of the plate ( $k = 1.5$ ), at the end of its service period which can be assumed as twenty years.

Then, substituting values  $k$  and  $t$  in formula (18.4), we obtain an expression for calculating plating thickness, taking wear into consideration

$$\delta_1 = 184s \sqrt{\frac{\rho}{\sigma_y} + 4} \text{ mm.} \quad (18.5)$$

As the calculations showed, formula (18.5) should be used when  $\delta < 22$  mm, i.e., when  $s \sqrt{\frac{\rho}{\sigma_y}} < 0.1$ ; in all other cases, formula

(18.3) should be used since the condition of plate strength at the end of the service period is also observed without correcting for wear.

For ships with a longitudinal framing system, the ratio  $l/a$  (where  $a$  is the distance between longitudinal strengthening ribs,  $l$  is the distance between the short sides of the index contour), usually exceeds 2.0. Therefore, formulas (18.3) and (18.5) can also be used, in this case, for designing the plates of ice belt plating.

**Example.** We shall calculate the thickness of side plating of a UL-class ship. Length of ship  $L = 120.6$  m. Frame spacing in the ends and amidships  $s = 362$  mm. Plating material is steel with a yield stress  $\sigma_y = 3,500$  kg/cm<sup>2</sup>. Design load on the bow plating is calculated by formula (13.4); a calculation of the thickness of plating for this area of the hull is presented in Table 17.

Intensity of the ice load on the ship's midship and stern plating are assumed to be the same and equal  $p = 76$  t/m<sup>2</sup>. Then, according to formula (18.5)

$$\delta_{mid} = 184 \cdot 0,302 \sqrt{\frac{76}{3500} + 4} = 13,8 \text{ mm.}$$

Thus, finally, for the midship and stern section, it should be assumed that  $\delta_{mid} = \delta_{st} = 14$  mm, and for the bow,  $\delta_{bow} = 20$  mm.

Table 17

Calculating bow plating thickness for a UL-class ship.

Parameters	Theoretical frame numbers					
	1	2	3	4	5	
s, frame numbers	16	16	14	11,5	8	
$s^{4/5}$	9,2	9,2	8,3	7,15	5,3	
$\beta$ , deg.	17	17	13,5	8	3,5	
$k_1$	0,98	1,05	1,07	1,29	1,39	
$k$	6,5	6,5	6,5	6,5	6,5	
$L^{4/5}$	306	306	306	306	306	
$p$	179,5	192,4	176,5	183,5	146,5	
$s \sqrt{\frac{p}{\sigma_y}}$	0,082	0,085	0,0812	0,0811	0,074	
$\delta$ , mm	specified	19,1	19,6	19,0	18,9	17,6
	actual	20	18	18	16	14
	а по Правилам Регистра СССР (изд. 1956 г.)	22,2	19,8	19,8	—	14,1

a- in accordance with regulations of the Registry of Shipping of the USSR (1956 ed.).

### 19. Types of Side Grillages.

As a rule, a transverse system of framing is used for side grillages of icebreakers and ice cargo ships. Along with this, a truss framing system is used in American shipbuilding practice. On Soviet, L-class tankers which have ice strengthening in the bow only, a longitudinal framing system is used amidships. Various types of ice ship side grillages have a number of common characteristic features, specifically including: reduced frame spacings, increased thickness of shell plating in the ice belt area and intermediate frames and side stringers, as well as single-cant framing in the extremities which provides stability to the frames.

The magnitude of the frame spacing along the side of icebreakers and ice-strengthened classes of cargo ships is 300 to 450 mm. This is a result of the facts that with frame spacing of less than 300 mm, it is difficult to perform high-quality welding of the shell plating to the side framing, and with frame spacing greater than 450 mm, plating thickness and weight of the side grillage noticeably increases.

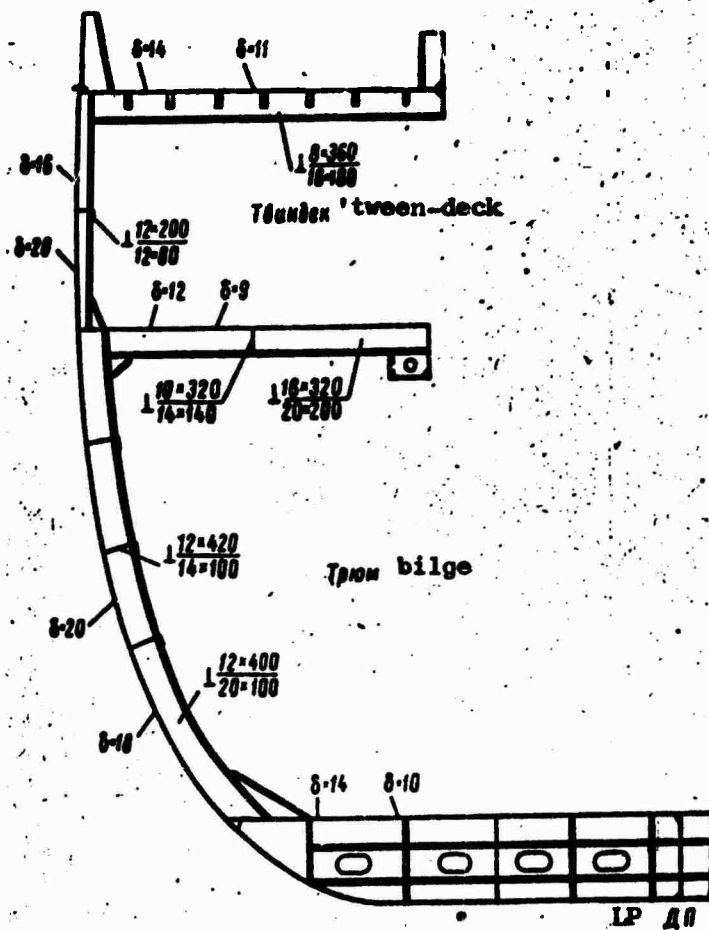


Figure 49. Cross section of the hull of an icebreaker-cargo ship used for active, ice navigation.

Selection of a certain framing system and type of grillage depends on the purpose and class of ship. The class of a ship, regulates either obviously or indirectly, the magnitude of the design ice loads and, to a certain degree, the form of hull lines.

Various side grillage structures of ships which sail in ice are considered below.

Side grillage with transverse framing system (Figure 49). In this case, the side framing consists of main and intermediate frames. Moreover, bearer stringers the same height as the main frames, can be installed. These transfer part of the load from frames under load to adjacent frames. Scantlings of intermediate frames are less than or the same as those of main frames. It was previously considered that the role of intermediate frames consisted only of strengthening the shell plating. Therefore, their section modulus usually did not exceed 50% of the section modulus of the main frames. Experience has shown that such frames are often damaged and strained along with the shell plating, when it is damaged. A framing system with different frame profiles provides no advantage in respect to weight characteristics or construction technology. Therefore, since the 1950's, a system of main and intermediate frames of the same profile has been used with increasing frequency. This tendency is reflected in the regulations of shipping registries (Lloyd's, Finnish Shipping Council). This type of grillage is widely used in the hold area of ice class, dry, cargo ships since it makes possible a gain in usable cargo spaces and has several technological advantages.

The side grillage of the Polish construction, Bobruyskies-class lumber carrier can be considered as a variant of a type of grillage with a transverse framing system. The framing consists of main frames, bearer stringers and intermediate frames of a smaller profile than the main frames. In addition, web frames (more precisely, reinforced) of the same height as the main frames but with a substantially increased free flange are installed through three or four frame spacings. However, even in this case, it is advisable to use intermediate frames with a reduced profile.

Another variant of side grillages with a transverse framing system is grillage with web frames and side stringers. This type of grillage, used when it is necessary to absorb large ice loads is a system of intersecting transverse (main, intermediate and web frames) and longitudinal (stringers) beams (Figure 50).

Intermediate frames installed the whole length of the ice belt often have the same profile as the main frames. When doing this, it is attempted to provide the same coefficient of constraint of the ends of the main and intermediate frames. This type of grillage has found wide use on icebreakers and icebreaker-cargo ships of the UL- and UL (Arkt.)-classes, as well as in the fore and after parts and engine room of many ships of other classes [Moskva, Voima (Finland)-class icebreakers and Lena, Dan (Denmark)-class icebreaker cargo ships].

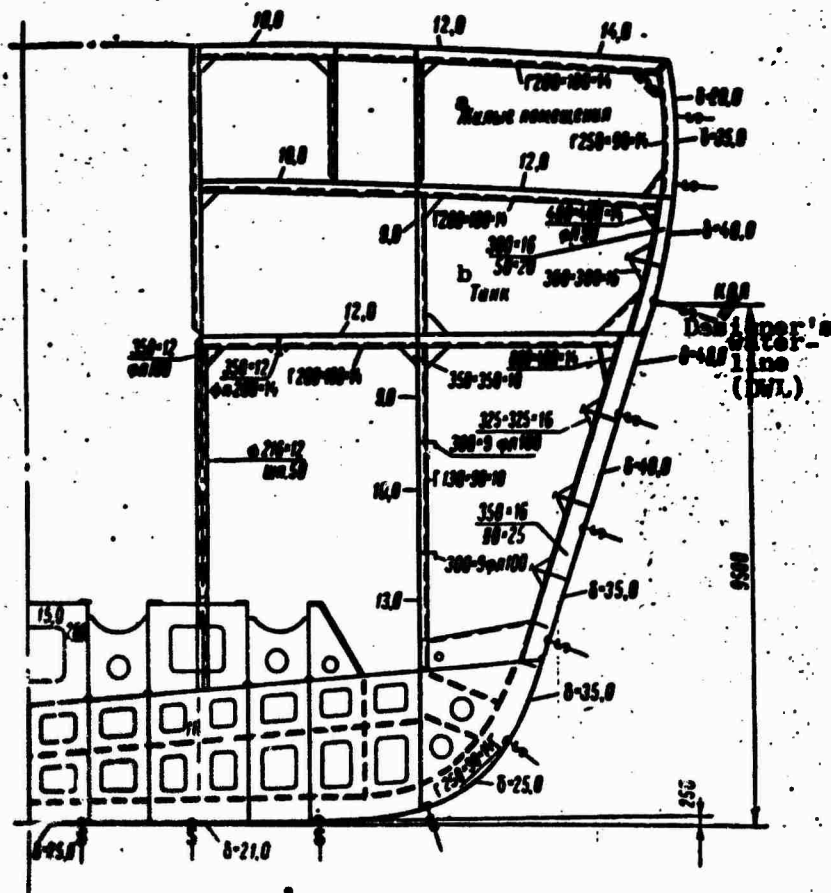


Figure 50. Diagram of main frame of a heavy icebreaker.  
 a-living compartments; b-tank; c-designer's waterline (DWL).

Side grillage with truss framing system (Figure 51). A truss framing system was used on American icebreakers of the "Wind" and "Glacier" class. The framing forms a single space truss consisting of side frames of the same profile and longitudinal bulkhead, vertical struts joined together by diagonal strut beams. A defect in the system is that the compartments are greatly encumbered and its technological design is difficult. In view of this, the truss framing system on "Wind-class" icebreakers is only used in the hull midsection which is nearly a true semicircle in profile. The framing is installed in a transverse system in the extremities.

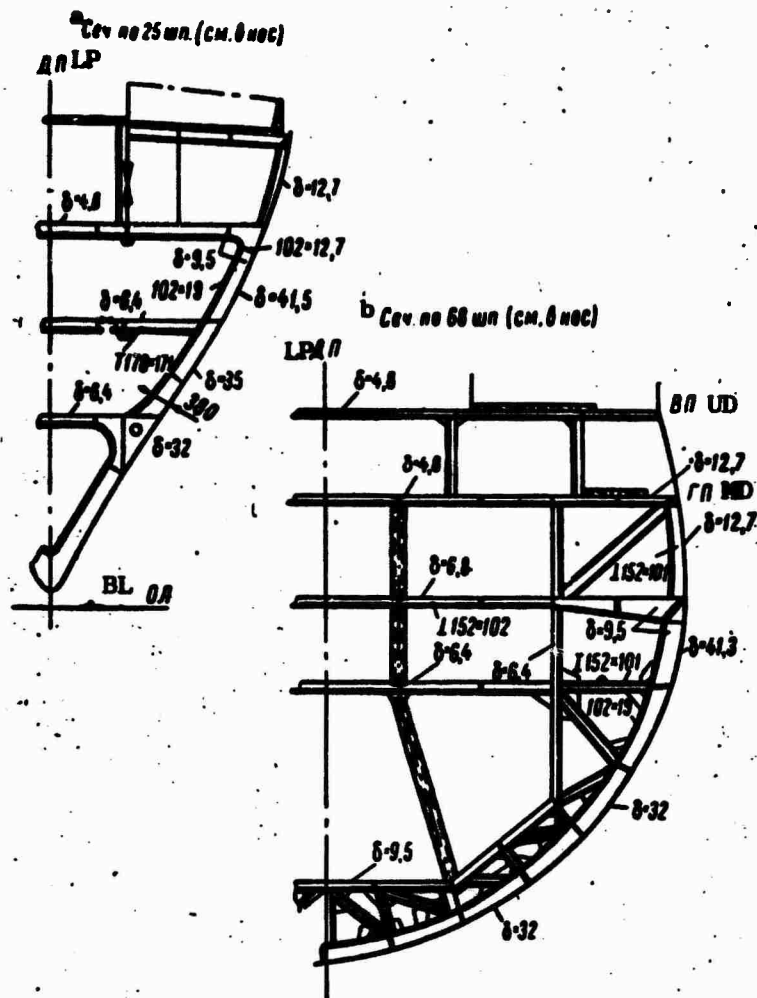


Figure 51. Hull framing system on "Wind-class" icebreakers. a-cross section at 25<sup>th</sup> frame (looking forward); b-cross section at 68<sup>th</sup> frame (looking forward).

## 20. Side framing without intersecting braces.

In this situation, the frames should be considered as isolated beams supported on non-sagging support-decks or platforms and undergoing an ice load  $Q = \rho s$  (Figure 52). The load intensity is calculated as shown in 12., depending on displacement, shape of hull lines and ship's velocity, as well as on the physical and mechanical characteristics of the ice. The load can also be directly set as a technical task for design of a ship. Since the width of the zone of contact between the side and the ice is usually small, in comparison with the frame span, the external load can be considered as being concentrated.

When determining side framing scantlings or checking the assumed dimensions of braces for ships which sail in ice loaded, as well as in ballast, the load should be applied to the center of the frame span in

the waterline area. For example, for a three-decker (see Figure 53), it is necessary to check the frame strength both in the bilge and in the 'tween deck, applying the load in each design situation to the center of the appropriate span.

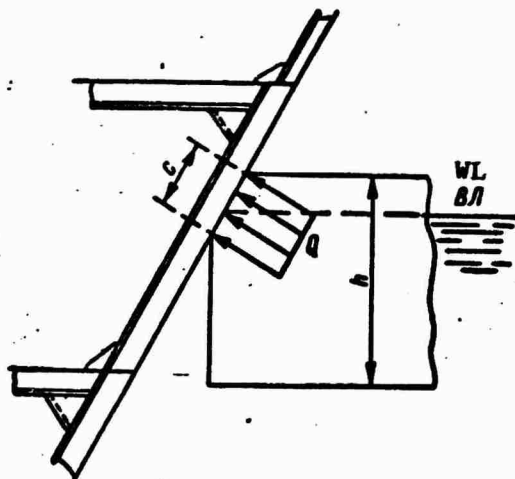


Figure 52. Design diagram for a frame with side grillage without intersecting braces.

The coefficients of yielding of the elastic constraint of the frame ends should be determined, calculating the entire frame web. However, they can be computed, approximately, by using the method of successive equilibration of connection points.

The method of constraining the ends of unloaded units of the web has small effect on the unknown magnitude of the coefficient of yielding and even a smaller effect on the magnitude of the bending moment at the joint. Therefore, for unloaded web units, it is possible to limit oneself to two forms of fastening (rigid fixing or simple support), selecting the form depending on the structural design of the joint.

The coefficient of yielding of the constraint  $\lambda_m$ , is equal to the joint rotation  $\alpha_m$  with the action of a single moment:

$$\lambda_m = -\alpha_m |_{m-1} = \frac{1}{\sum_{j=1}^n k_{jm}}, \quad (20.1)$$

where  $k_{jm}$  - is the stiffness factor of bar  $j$  which adjoins joint  $m$ ;  
 $n$  - is the number of bars converging at the joint.

For a bar, rigidly fixed on the opposite (not adjoining joint  $m$ ) end,

$$k_{jm} = \frac{4EI}{l};$$

for a bar simply supported on the opposite end,  $k_{jm} = \frac{3EI}{l}$ ,

where  $i$  - is the moment of inertia of a cross section of the bar;  
 $l$  - is the length of the bar.

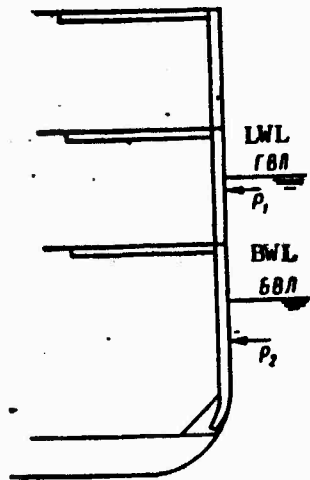


Figure 53. Areas of ice load application when ship is underway, loaded and in ballast.

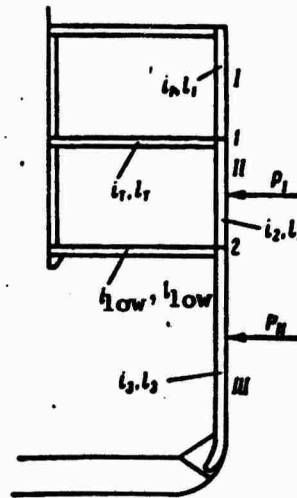


Figure 54. Symbols for calculating coefficients of constraint for side frame.

We shall discuss a method for calculating coefficients of constraint for a frame of a three decker (Figure 54), as an example. Sections II and III will be calculated.

We shall calculate the coefficient of yielding of joint I for section II according to the diagram presented in Figure 55a,

$$\alpha_1 = \frac{1}{3E \left( \frac{l_1}{i_1} + \frac{l_1}{i_1} \right)} \quad (20.2)$$

We shall calculate the coefficient of yielding of joint 2 of section II according to Figure 55b:

$$\alpha_2 = \frac{1}{3E \left( \frac{i_{low}}{l_{low}} + \frac{4}{3} \frac{i_3}{l_3} \right)} \quad (20.3)$$

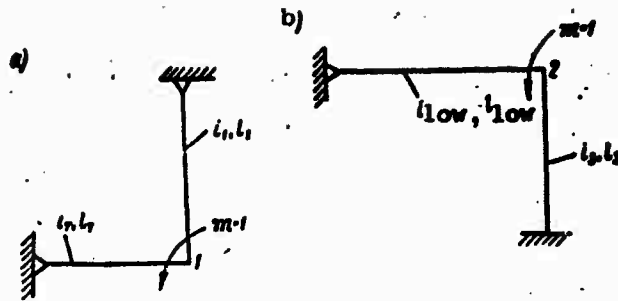


Figure 55. Diagram for calculating coefficients of yielding: a-in joint 1 for section II; b-in joint 2 for section II.

We shall determine the coefficient of yielding of joint 2 for section III by formula

$$\alpha_{2 \text{ III}} = \frac{1}{3E \left( \frac{i_2 + i_{1\text{ow}}}{2 + 1_{1\text{ow}}} \right)} \quad (20.4)$$

Coefficients of yielding for other structures can be calculated similarly.

It is advisable to reduce expressions for coefficients of yielding of elastic constraint to a dimension

$$\rho = \frac{6E\eta}{l} \quad (20.5)$$

where  $i, l$  - are the moment of inertia of a cross section and the length of the section being calculated respectively.

$$\text{For section II (Figure 54) } \left. \begin{aligned} \rho_1 &= \frac{2}{\frac{l_1}{l_2} \frac{l_2}{l_1} + \frac{l_1}{l_2} \frac{l_2}{l_1}}; \\ \rho_2 &= \frac{2}{\frac{i_{1\text{ow}}}{i_2} \frac{l_2}{l_{1\text{ow}}} + \frac{4}{3} \frac{l_2}{l_1} \frac{l_1}{l_2}} \end{aligned} \right\} \quad (20.6)$$

Taking the aforesaid into account, a frame is calculated according to the diagram depicted in Figure 56.

$$\left. \begin{aligned} M_1 &= \frac{\eta(1-\eta)[(2-\eta)(2+\rho_2)-(1+\eta)]}{(2+\rho_1)(2+\rho_2)-1} Pl, \\ M_2 &= \frac{\eta(1-\eta)[(1+\eta)(2+\rho_1)-(2-\eta)]}{(2+\rho_1)(2+\rho_2)-1} Pl, \end{aligned} \right\} \quad (20.7)$$

where  $\eta = c/l$ .

Curves of bending moments which act on a frame are most easily constructed graphically by superposition procedure (Figure 57).

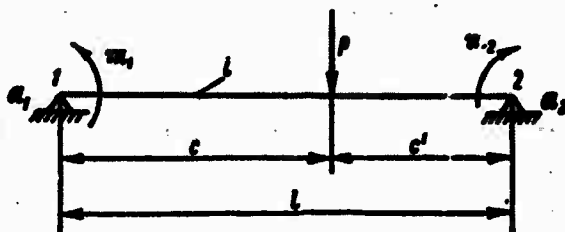


Figure 56. Design diagram for a frame.

Then, the maximum bending moment in the frame span is calculated by formula

$$M = \frac{qsc'}{l} \left[ M_2 + \frac{c'}{l} (M_1 - M_2) \right]. \quad (20.8)$$

Expression (20.8) can be written in the form

$$M = kqs l \cdot 10^3 \text{ (kg cm)},$$

where  $k$  - is a numeral coefficient depending on the number of decks, area of load application, and method of fastening the frame ends;

$s$  - is the frame spacing, m;

$l$  - is the frame span, measured along a chord between decks or platforms, m.

The condition of frame strength is expressed by formula

$$\sigma = \frac{M}{W_{\min}} \leq \sigma_y, \quad (20.9)$$

where  $\sigma_y$  - is the yield stress of the frame material,  $\text{kg/cm}^2$ .

The minimum section modulus of the frame with an attached flange of plating in the ice belt area:

$$W_{\min} > \frac{M}{\sigma_y} = k \frac{qsl}{\sigma_y} 10^3 \text{ cm}^3. \quad (20.10)$$

When calculating the magnitude of coefficient  $k$ , various cases of loading a frame with a concentrated tension  $P = qs$  for a single-deck, two-deck, and three-deck ship are considered. The lower frames are considered to be rigidly fastened in the inner bottom and the upper frames, elastically fastened at the upper deck (calculations have shown that for actual structures  $\rho_{\text{up}} = 3$ ) can be assumed as an average. The decks and platforms are considered to be rigid supports for the frame. The external load was applied

to the center of the frame span.

We cite values of coefficients  $k$  to be entered into formula (20.10): for bilge frames of single deck ships,  $k = 15$ ; for bilge frames of ships having two or more decks,  $k = 14$ ; for frames between decks and platforms,  $k = 16.5$  (if the ice belt covers no more than  $1/3$  of the frame span) and  $k = 19.0$  (if the ice belt covers more than  $1/3$  of the frame span).

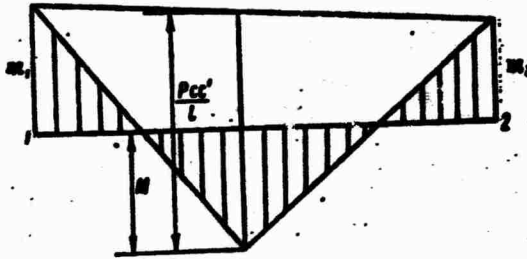


Figure 57. Bending moment diagram for a frame.

For intermediate positions on the edge of the ice belt, the values of coefficient  $k$  can be computed by linear interpolation. Formula (20.10) is used for calculating side framing consisting of identical frames with their ends constrained in the same manner.

In a situation when main and intermediate frames have the same profile but their ends are constrained differently, the frames should be calculated, taking into account their actual constraint and then, for a design moment, taking the mean arithmetical value from the moments calculated in the span for the main and intermediate frames.

If the intermediate frame profile is substantially smaller than the main frame profile ( $W$  of intermediate less than  $0.5$  of main), only the main frames are calculated. In this situation, the design load is assumed as equaling  $P = q s_0$ , where  $s_0$  is the main frame spacing. Intermediate frames are included as part of the attached flange when calculating the elements of the main frame profile.

Another case of practical interest is one in which the intermediate frames do not reach the deck and bottom, but terminate at horizontal shelves or bearer stringers (Figure 58). With this structural arrangement of side framing, an intermediate frame should be considered as a beam on elastic supports and the main frame as being additionally loaded with reactions from the shelves.

In addition to checking the bending strength of frames, it is necessary to check the resistance of abutment sections to action of shearing forces

$$\tau = \frac{Nsh}{\omega_{red}} \leq \tau_y = 0,57\sigma_y \approx 0,6\sigma_y \quad (20.11)$$

where  $N_{sh}$  - is shearing force;

$\sigma_{red}$  - is the reduced area of a normal section of the frame bulkhead; for an I-beam profile, its mean value  $\sigma_{red} = 0.85\sigma$  [28];

$\sigma$  - is the area of a normal section of the frame wall together with knees (if knees are installed);

$\sigma_y$  - is the shear yield stress of the material.

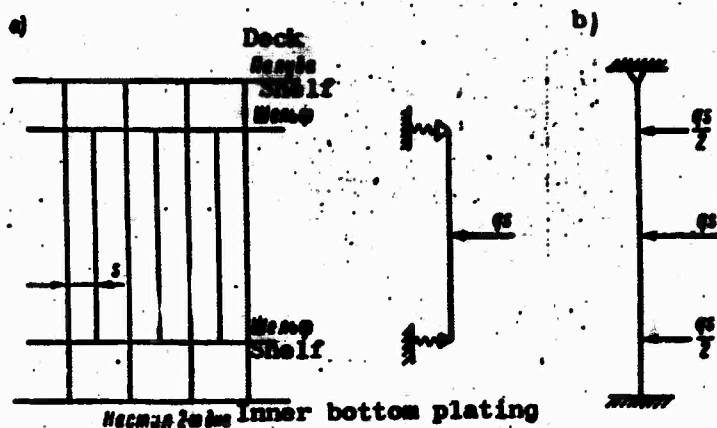


Figure 58. Diagram of side framing with intermediate frames terminating on shelves: a-intermediate frame; b-main frame.

Several examples of calculating scantlings of side framing, taken from the practice of designing ice ships, are considered below.

**First example.** Check the scantlings of the midship side framing of a two-deck ship with a load capacity of 10,000 t (Figure 59). The design load on the framing  $q = 100$  t/m. We assume the load to be applied a distance of  $c = 1.5$  m below the deck. When calculating, we shall allow for a different degree of constraint on the ends of the main and intermediate frames.

Design conditions:  $l = 7.0$  m,  $l_1 = 4.0$  m,  $l_2 = 1.9$  m;  
 $i = 17.0 \cdot 10^3$  cm<sup>4</sup>,  $i_1 = i$ ,  $i_2 = 4.73 \cdot 10^3$  cm<sup>4</sup>;  $W = W_1 = 775$  cm<sup>3</sup>,  
 $W_2 = 268$  cm<sup>3</sup>;  $s = 0.4$  m,  $c = 1.5$  m,  $l_c = 5.5$  m;  $P = q \cdot s = 40$  t.

1. Main frame calculation. We shall determine coefficients for  $\varrho$ :

$$\rho_1 = \frac{2}{1 \cdot \frac{7}{4} + \frac{4.73}{17.0} \cdot \frac{7}{1.9}} = 0.72,$$

$$\rho_2 = 0.$$

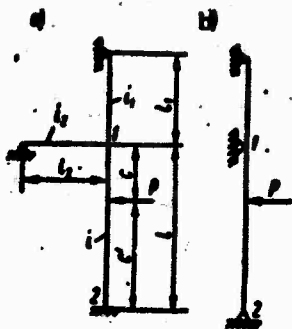


Figure 59. Design diagram for checking the strength of side framing of a ship with a load capacity of 10,000 t; a- main frame; b- intermediate frame.

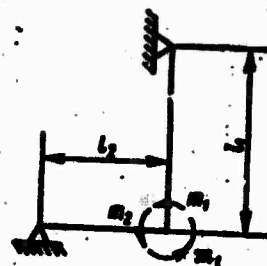


Figure 60. Design diagram for calculating bending moments in a 'tween deck beam and frame.

We calculate support moments:

$$\eta = \frac{c}{l} = \frac{1,5}{7} = 0,214, \quad 1 - \eta = 0,786;$$

$$\mathfrak{R}_1 = \frac{0,214 \cdot 0,786 (1,786 \cdot 2 - 1,214)}{2,72 \cdot 2 - 1} 7 \cdot 40 = 25 \text{ t.m.}$$

$$\mathfrak{R}_2 = \frac{0,214 \cdot 0,786 (1,214 \cdot 2,72 - 1,786)}{2,72 \cdot 2 - 1} 7 \cdot 40 = 16,1 \text{ t.m.}$$

Moment in the span

$$M_{\text{span}} = \frac{40 \cdot 1,5 \cdot 5,5}{7} - \left[ 16,1 + \frac{5,5}{7} (25 - 16,1) \right] = 24,1 \text{ t.m.}$$

Bending moments in 'tween deck beam and frame (Figure 60).

$$m_2 = \frac{\mathfrak{R}_1 \cdot l}{1 + \frac{l_2 \cdot l_1}{l_1 \cdot l_2}} = 25 \cdot \frac{1}{1 + \frac{4,73}{17,0} \cdot \frac{7,0}{1,9}} = 12,65 \text{ t.m.}$$

$$m_1 = \mathfrak{R}_1 - m_2 = 12,65 \text{ t.m.}$$

A curve of bending moments is presented in Figure 61.

2. Intermediate frame calculation. We determine coefficients for  $\rho$ :

$$\rho_1 = \frac{2}{1 \cdot \frac{7}{4}} = 1,143,$$

$$\rho_2 = \infty.$$

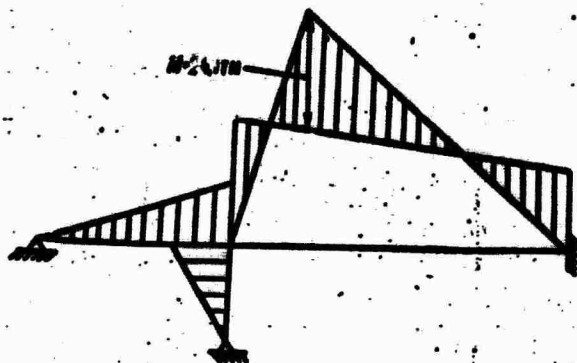


Figure 61. Curve of bending moments for main frames.

Support moments

$$M_0 = 0; M_1 = \frac{0,214 \cdot 0,788 \cdot 1,788}{3,143} \cdot 40,7 = 26,7 \text{ t.m.}$$

Moment in span

$$M_{\text{span}} = \frac{40 \cdot 1,5 \cdot 5,5}{7} - \left[ 0 + \frac{5,5}{7} (26,7 - 0) \right] = 26,1 \text{ t.m.}$$

As a design moment for the frame, we take its mean value from the values determined for the main and intermediate frames:

$$M_{\text{des}} = \frac{26,1 + 26,1}{2} = 26,1 \text{ t.m.}$$

The maximum tensions in the frame span

$$\sigma = \frac{M_{\text{des}}}{W} = \frac{26,1 \cdot 10^8}{775} = 3369 \text{ kg/cm}^2 < \sigma_y = 4000 \text{ kg/cm}^2.$$

We check the resistance of a half-beam to the action of end moment. The length of the beam knee  $l_k = 0,65 \text{ m}$ ;  $l_2 = 1,90 \text{ m}$ .

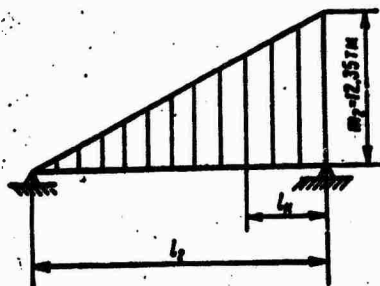


Figure 62. Curve of bending moments for a beam.

The design bending moment in a section at the end of the knee (Figure 62)

$$M_0 = 12,35 \cdot \frac{1,25}{1,90} = 8,12 \text{ t.m.}$$

Maximum bending stress in the beam

$$\sigma = \frac{M_0}{W_1} = \frac{8,12 \cdot 10^8}{268} = 3030 \text{ kg/cm}^2 < \sigma_y = 4000 \text{ kg/cm}^2.$$

**Second example.** Determine stresses in the side framing of an icebreaker tugboat. A design diagram is presented in Figure 63. Design load  $q = 40$  t/m applied to the center of span  $l_1$ .

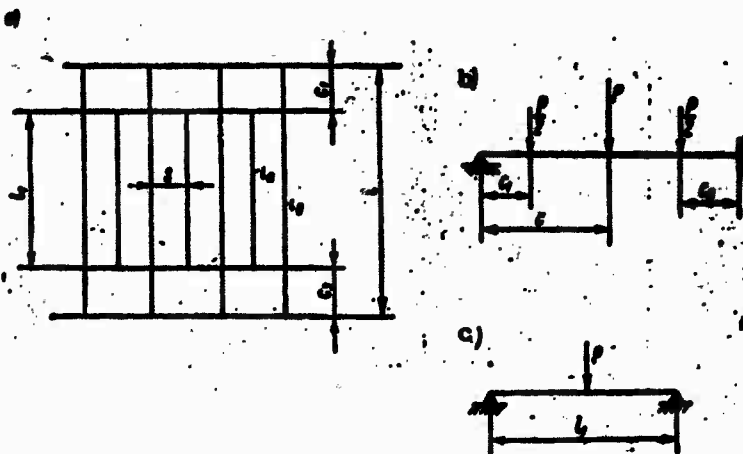


Figure 63. Diagram for calculating side framing of an icebreaker tugboat: a-grillage diagram; b-main frame; c-intermediate frame.

**Design data:**  $t = 4.0$  m,  $l_1 = 2.2$  m;  $c_2 = 1.9$  m,  $s = 0.3$  m;  $i_0 = 8720$  cm<sup>4</sup>,  $i_{red} = 5110$  cm<sup>4</sup>;  $W_0 = 434$  cm<sup>3</sup> (bulb flat bar 24a),  $w_{red} = 293$  cm<sup>3</sup> (bulb flat bar 20b);  $c_1 = 0.8$  m,  $c_3 = 1.0$  m;  $P = q \cdot s = 12$  t. Material is steel with  $\sigma_y = 2,400$  kg/cm<sup>2</sup>.

Maximum bending moment in the side frame corresponds to Figure 63, c

$$M_{span} = \frac{Pl_1}{4} = \frac{12 \cdot 2.2}{4} = 6.6 \text{ t} \cdot \text{m}$$

Maximum bending stresses

$$\sigma = \frac{6.6 \cdot 10^6}{293} = 2250 \text{ kg/cm}^2 < \sigma_y = 2400 \text{ kg/cm}^2$$

Bending moments in the main frame span are determined in accordance with Figure 63, b

$$M_{span} = \frac{6 \cdot 0.8 \cdot 3.2}{4} = 3.84 \text{ t} \cdot \text{m} \quad (\text{in the span from } P/2 = 6 \text{ m at } c_1);$$

$$M_{span} = \frac{6 \cdot 3 \cdot 1.0}{4} = 4.5 \text{ t} \cdot \text{m} \quad (\text{in the span from } P/2 = 6 \text{ m at } c_3)$$

$$M_{span} = \frac{12 \cdot 1.9 \cdot 2.1}{4} = 11.98 \text{ t} \cdot \text{m} \quad (\text{in the span from } P = 12 \text{ m}).$$

On the support

$$M_{10} = \frac{0.2 \cdot 0.2 \cdot 1.2}{2} \cdot 6.4 = 2.3 \text{ t.m.}$$

$$M_{20} = \frac{0.75 \cdot 0.25 \cdot 1.75}{2} \cdot 6.4 = 3.94 \text{ t.m.}$$

$$M_{30} = \frac{0.475 \cdot 0.525 \cdot 1.475}{2} \cdot 12.4 = 8.82 \text{ t.m.}$$

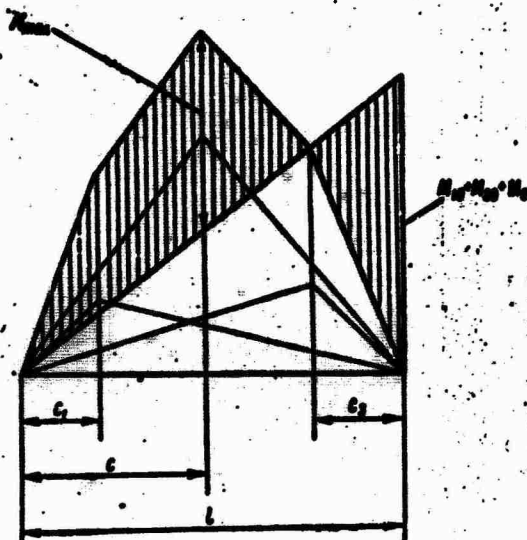


Figure 64. Curve of bending moments for main frame.

We shall determine the maximum bending moment in the span of the main frame graphically, constructing a curve of bending moments (Figure 74):  $M_{\max} = 10.3 \text{ t.m.}$

Bending stress

$$\sigma = \frac{10.3 \cdot 10^5}{434} = 2370 \text{ kg/cm}^2 < \sigma_y = 2400 \text{ kg/cm}^2.$$

### 21. Grillage with One Cross Bracing.

A ship's hull is an aggregate of a number of grillages -- sides, bottom, decks and platforms and longitudinal and transverse bulkheads -- joined together. We shall consider all these coverings as being two-dimensional. In most cases, known methods for calculating two-dimensional coverings can be used for calculating ships' grillages. Basic design premises are generally accepted and consist of the following:

1. the grillage is considered as a system of beams intersecting at right angles. When expanding the statistical indeterminate form of this system, it is assumed that there is only one bracing in the joints (points where beams intersect), causing a vertical reaction, normal to the plane of the grillage;

2. the plates of the shell fulfill two functions: first, they absorb the external load and transmit it to the grillage beams. Secondly, they take part in the bending of these beams as attached flanges.

We shall consider an ice load applied along a line on a sector between transverse bulkheads or between web frames. When necessary, the grillage can be calculated, taking the actual length of load distribution into consideration. We shall take as a design case, a situation in which the web frames can be considered as rigid supports for a stringer. A design diagram of the grillage is presented in Figure 65, where  $s$  is the frame spacing,  $L$  is the stringer span,  $l$  is the frame span,  $n$  is the number of frame spacings between web frames,  $i$  is the moment of inertia of the frame and  $I$  is the moment of inertia of the stringer.

When there is an adequately large number of frames (more than five or six), a stringer should be considered as a beam on an elastic foundation with inflexibility

$$k = \frac{El}{\gamma l^3}, \quad (21.1)$$

where  $\gamma$  - is the coefficient for the effect of the reaction of the stringer to the frame deflection in the joint determined for unit force according to the design diagram in Figure 66 ( $\gamma = \nu_1 \frac{El}{I}$ ).

Coefficients of yielding of the elastic constraint of the frame ends  $\nu$  are determined according to the procedure described in 20.

The given load for which the stringer is being calculated will have a varying form, depending on the type of load acting on the grillage. With load  $\rho$  equally distributed over the entire grillage surface, the stringer should be considered as a beam on an elastic foundation under the effect of an equally distributed load

$$\bar{q} = \frac{\rho}{\tau} pl, \quad (21.2)$$

where  $\beta$  - is a coefficient for the effect of the external load on the frame deflection in the joint, determined from design diagram (Figure 67).

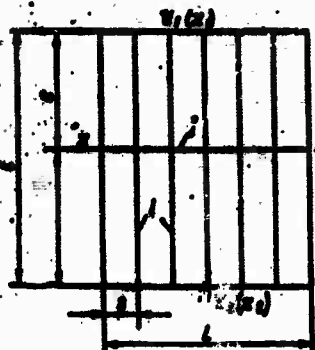


Figure 65. Schematic diagram of side span with one x-shaped tie.



Figure 66. Diagram for determining coefficient  $\gamma$ .

With load  $q$ , equally distributed along line  $y = b$  (Figure 68).

$$\bar{q} = \frac{b}{\gamma} q. \quad (21.3)$$

Coefficient  $\beta$  is determined according to the design diagram presented in Figure 69. If a load is applied directly to the stringer,  $b = c$ ,  $\gamma = \beta$  and  $\bar{q} = q$ .

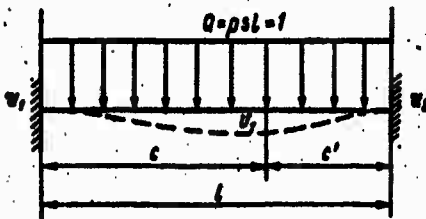


Figure 67. Diagram for calculating coefficient  $\beta$  in the case of an equally distributed external load.

With a concentrated load  $P$  applied to a frame at section  $x = \zeta L$  (Figure 70), the stringer should be calculated for action of the given concentrated force  $\bar{P} = \beta/\gamma P$ , applied to it at point  $x = \zeta L$ . Coefficient  $\beta$  for this situation will be determined according to the design diagram in Figure 69. When  $b = c$ , (force acts directly on the stringer),  $\beta = \gamma$  and  $\bar{P} = P$ .

Flexural elements of the grillage for an equally distributed load are expressed in Bubnov functions:  $x_0(u)$ ,  $x_1(u)$ ,  $x_2(u)$ ,  $\mu(u)$  and  $v(u)$ .

The bending moment in the center of a crossbeam span

$$M_{\text{span}} = \frac{\bar{q}L^3}{8} \left[ (1-x)\chi_0(u) + \frac{1}{8}x\chi_1(u) \right]. \quad (21.4)$$

Bending moment in abutment section

$$M_{\text{abut}} = \frac{\bar{q}L^3}{12} \chi_2(u). \quad (21.5)$$

Shearing force in abutment section

$$N_{\text{abut}} = \frac{\bar{q}L}{2} [(1-x)\mu + xv(u)]. \quad (21.6)$$

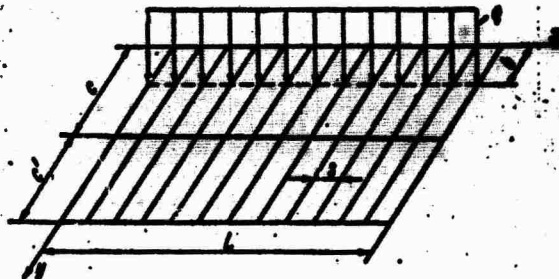


Figure 68. Diagram of grillage loaded along a line by an equally distributed external load.

For a concentrated load applied at point  $x = \zeta L$ , flexural grillage elements are expressed in functions  $M_0(u, \zeta)$ ,  $M_A(u, \zeta)$ ,  $v_A(u, \zeta)$ ,  $\psi_1(u, \zeta)$  and  $\psi_2(u, \zeta)$ , cited in [42].

The bending moment at the center of the span

$$M_{\text{span}} = \bar{P}L [(1-x)\psi_1(u, \zeta) + xM_0(u, \zeta)]. \quad (21.7)$$

Bending moment in abutment section

$$M_{\text{abut}} = \bar{P}L x M_A(u, \zeta). \quad (21.8)$$

Shearing force in abutment section

$$N_{\text{abut}} = \bar{P} [(1-x)\psi_2(u, \zeta) + xv_A(u, \zeta)]. \quad (21.9)$$

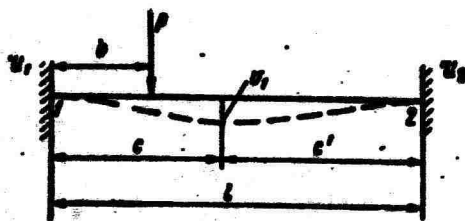


Figure 69. Diagram for determining coefficient  $\beta$  when there is an equally distributed load along a line.

For a load distributed over part of the length of the grillage, we can write

$$M_{\text{пан}} = \bar{q}L \left[ (1-x) \int_0^x \phi_1(u, \zeta) d\zeta + x \int_x^L M_0(u, \zeta) d\zeta \right]. \quad (21.10)$$

Analogous expressions can be obtained for all other flexural elements. Integrals appearing in expression (21.10) are computed by any method of numerical integration in tabular form.

When calculating grillage for ice load action, it is necessary to check the strength of stringers by applying a load directly to them and the strength of the frames, by applying a load in the frame span between a stringer and deck or in the span between stringers. Bending stresses in the span center and in the abutment sections of the stringer are calculated. They must not exceed the yield stress of the material

$$\sigma = \frac{M}{W_{\text{min}}} \leq \sigma_y, \quad (21.11)$$

where  $W_{\text{min}}$  - is the minimum section modulus of the stringer with the attached flange of the plating.

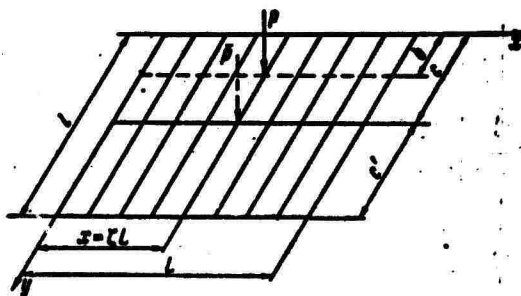


Figure 70. Diagram of grillage loaded with a concentrated force.

Moreover, stringer abutment sections should be checked for action of shearing forces

$$\tau = \frac{N_{\text{shear}}}{0.85\omega} \leq \tau_y = 0.6\sigma_y, \quad (21.12)$$

where  $\omega$  - is the total cross-sectional area of the stringer wall and knee.

The strength is calculated for an extreme frame, if the stringer is considered as a rigid support and for a middle frame as for a beam with a displaced support (Figure 71, where  $Q = P$  with action of a concentrated force and  $Q = qs$  with action of a load equally distributed along a line).

The linear reaction of a stringer on a middle frame

$$r = \bar{q}[1 - (1-x)\varphi_0 - x\varphi_1(u)]. \quad (21.13)$$

Deflection of the stringer in the span center

$$v = \frac{\bar{q}}{k}[1 - (1-x)\varphi_0 - x\varphi_1(u)]. \quad (21.14)$$

The values of functions  $\varphi_0$ ,  $\varphi_1$  are cited in [45, volume 1]. Coefficients of yielding of the elastic constraint of the frame ends  $\alpha_1$  and  $\alpha_2$  (or  $e_1$  and  $e_2$  respectively) are calculated by formulas in 20.

Computing reference couple coefficients for a stringer. Coefficient  $x$  for stringers should be calculated by considering the stringer as a multi-span, continuous, beam resting on an elastic foundation. However, for practical purposes, we can rest confine ourselves to approximation methods.

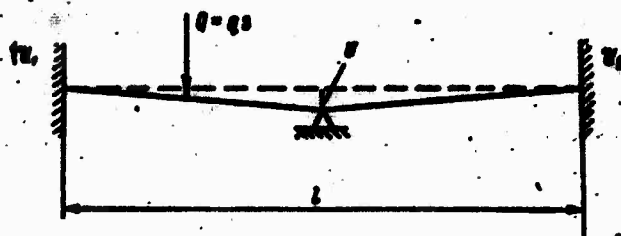


Figure 71. Design drawing for middle frame (along the length of the span).

Web frame yielding can be disregarded in most cases. Therefore, for a homogeneous side structure and load which is symmetric relative to the stringer, we shall calculate the coefficient of the reference couple according to the design diagram presented in Figure 72:

$$x = \frac{\psi_1(u) + 2\psi_0(u)}{\psi_1(u) + 4\psi_0(u)}, \quad (21.15)$$

where  $\psi_0(u)$  and  $\psi_1(u)$  are Bubnov functions.

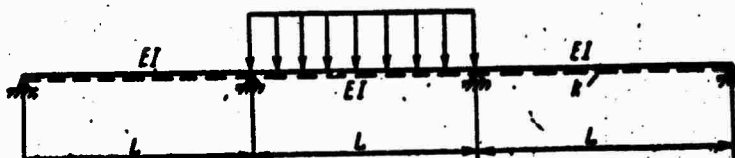


Figure 72. Design diagram for determining the coefficient of support for the stringer couple.

The elastic foundation argument is

$$s = \frac{L}{2} \sqrt{\frac{k}{4EI}} = \sqrt{\frac{s}{64\gamma} \left(\frac{L}{i}\right)^2 \frac{k}{I}} \quad (21.16)$$

In practice, values of the reference couple coefficient for a stringer lie within the range 0.5 to 0.6 (Table 18).

Table 18

Coefficients  $\alpha$  for a stringer.

$s$	0	0.5	1.0	1.5	2.0
$\alpha$	0.610	0.598	0.574	0.538	0.499

Calculating grillage, taking web frame yielding into consideration. Web frame yielding is computed by loading the cross bracing with a supplementary, concentrated force

$$\Delta P = \left( \frac{k_{wf}}{I} - \frac{\beta}{I} \right) q s \quad (21.17)$$

and introducing a supplementary support with rigidity

$$k_{sup} = \left( \frac{I}{I_{wf}} n_0 - 1 \right) \frac{EI}{\gamma^2} \quad (21.18)$$

at the intersection of the stringer and web frame.

In formulas (21.17) and (21.18), it is specified:

$$n_0 = \frac{k_{sup}}{I}$$

$I_{wf}$  - is the moment of inertia of the web frame;

$i$  - is the moment of inertia of a standard frame;

$\gamma, \gamma_{wf}$  - are influence coefficients of unit resistance to deflection of standard and web frames in the joint of intersection with the stringer;

$\beta, \beta_{wf}$  - are influence coefficients of the external load.

Influence coefficients, when there is a stringer located at the center of the span, are computed by formula

$$\gamma = \frac{1}{48} \frac{3}{128} \frac{2 + p_1 + p_2}{(2 + p_1)(2 + p_2) - 1} \quad (21.19)$$

When constraint of standard and web frames is the same, the latter can be split in two with moments of inertia  $i$  and  $(n_0 - 1) i$  respectively.

The beam with moment of inertia  $i$  becomes part of the elastic foundation, the other forms, an elastic support. When there is different constraint of web, main and intermediate frames, rigidity of the elastic foundation is calculated by formula

$$k_{\text{elas}} = k_{\text{wf}} - k, \quad (21.20)$$

where  $k_{\text{wf}} = \frac{1}{v_{\text{wf}}}$  - is the stiffness factor of the web frame;  
 $v_{\text{wf}}$  - is the deflection of the web frame under the effect of unit resistance  $R$ .

Stiffness factor  $k$  is determined by formula (21.22).

The stringer is considered as a beam resting on an elastic foundation and supported at the ends on elastic supports, the web frames. Flexural elements of the stringer are expressed in Bubnov functions. For example, bending moment in the center of the span

$$M_{\text{span}} = \frac{qL^2}{8} \left[ \frac{(1-\mu) \gamma_0(u)}{1+R} + \frac{\mu}{3} \frac{\gamma_1(u)}{1+R_1} \right], \quad (21.21)$$

where  $R = \frac{AkL}{2} \mu(u)$ ,

$R_1 = \frac{AkL}{2} \gamma(u)$ ,

$A = \frac{1}{k_{\text{elas}}}$ .

Tables of functions  $x_0$ ,  $x_1$ ,  $\mu$  and  $v$  are presented in [45, volume 1].

Calculating grillage including main and intermediate frames of unlike profiles with different constraint on their ends. A case in which intermediate frames have a span of the same length as the main frames is of great interest. We will assume that deflections of adjacent main and intermediate frames in the joint of intersection with the stringer are equal. Then, the stiffness factor of the elastic foundation will be

$$k = \frac{1 + \frac{\gamma_{\text{main}}}{\gamma_{\text{int}}} \frac{i_{\text{int}}}{i_{\text{main}}}}{2} \frac{Ei_{\text{main}}}{\gamma_{\text{main}}}, \quad (21.22)$$

where  $\gamma_{\text{main}}$  and  $\gamma_{\text{int}}$  - are influence coefficients of stringer resistance to deflection of the main and intermediate frames in the joint;

$i_{\text{main}}$ ,  $i_{\text{int}}$  - are moments of inertia of a cross section of the main and intermediate frames.

The given load on the stringer

$$\bar{q} = q \left( \frac{\beta_{\text{main}}}{\gamma_{\text{main}}} + \frac{\beta_{\text{int}}}{\gamma_{\text{int}}} \right) \cdot \frac{1}{2} \quad (21.23)$$

where  $\beta_{\text{main}}$ ,  $\beta_{\text{int}}$  are influence coefficients of the external load on deflection of the main and intermediate frames respectively, in the joint.

The parameter of the elastic foundation

$$u = \sqrt[4]{\frac{n}{64 \gamma_{\text{main}}} \frac{i}{I} \left( \frac{L}{l} \right)^3 \left( 1 + \frac{\gamma_{\text{main}}}{\gamma_{\text{int}}} \frac{i_{\text{int}}}{i_{\text{main}}} \right)} \quad (21.24)$$

Strength of extreme frames should be calculated by assuming the stringer as a rigid support and the strength of middle frames is calculated as the strength of a beam with a displaced support, taking the actual constraint of the ends into consideration. The magnitude of the displaced support for middle (main and intermediate) frames is calculated as deflection of a stringer in the center of a span (allowing for yielding of web frames)

$$v = \frac{\bar{q}}{k} \left[ 1 - \frac{(1-\alpha) \varphi_2(u)}{1+R} - \frac{\alpha \varphi_1(u)}{1+R_1} \right] \quad (21.25)$$

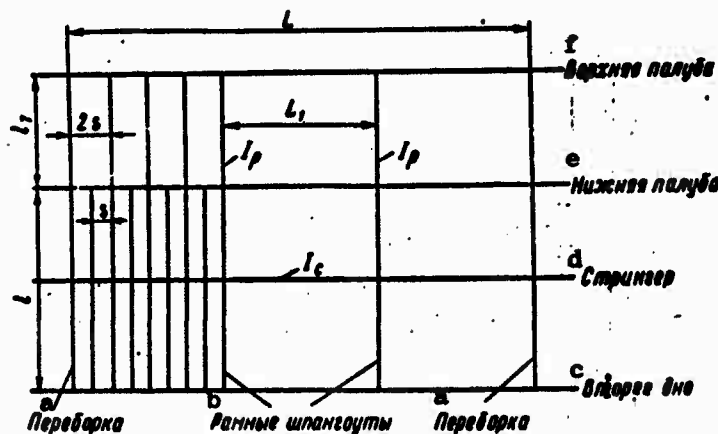


Figure 73. Diagram of side grillage with one cross bracing. a-bulkhead; b-web frames; c-inner bottom; d-stringer; e-lower deck; f-upper deck.

**Example.** It is required to calculate the strength of grillage with one cross bracing (Figure 73) with the following initial data:  $L = 9.6$  m,  $L_1 = 3.2$  m,  $2s = 0.8$  m,  $l = 4.0$  m,  $l_1 = 2.5$  m,  $i_1 = i_{\text{main}}$ ,

$$\begin{aligned}
 l_b &= 2.0 \text{ m}, i_b = 3530 \text{ cm}^4, W_b = 218 \text{ cm}^3, I_{str} = 57,760 \text{ cm}^4, I_{vf} = \\
 &= 57,760 \text{ cm}^4, i_{main} = 8870 \text{ cm}^4, i_{int} = 4585 \text{ cm}^4; W_{str} = 1,890 \text{ cm}^3, \\
 W_{vf} &= 1,890 \text{ cm}^3, W_{main} = 463 \text{ cm}^3, W_{int} = 267 \text{ cm}^3; F_{str} = 56 \text{ cm}^2, \\
 F_{vf} &= 56 \text{ cm}^2.
 \end{aligned}$$

We shall perform calculations for two classes of application of external load  $q = 50 \text{ t/m}$ . Specifically, when it is applied directly to a stringer or to the center of a frame span between a stringer and the lower deck.

We shall determine the influence coefficient  $\gamma$ . This stage of calculation will apply to both cases of external load application.

Assuming the intermediate frame to be simply supported at both ends (Figure 74), we obtain  $\gamma_{int} = \frac{1}{48} = 0.0208$ . When de-

termining influence coefficients for the main frame, we shall consider its constraint at its upper and lower ends. We find dimensionless coefficients of yielding of elastic constraints for the main frame. At the lower deck [formula 20.6]

$$\rho_4 = \frac{2}{\frac{4}{2.5} + \frac{3530}{8870} \cdot \frac{4}{2}} = 0.835.$$

At the inner bottom, we consider the main frame as being rigidly constrained to the plate frame:  $\rho_4 = 0$ .

We determine the influence coefficient  $\gamma_{main}$  according to the design diagram in (Figure 74). For  $\eta = 0.5$ , we find according to formula (20.7)

$$\begin{aligned}
 \eta_1 &= \frac{\frac{3}{8} qsl}{2,835 \cdot 2 - 1} = 0,0803 qsl, \\
 \eta_2 &= \frac{\frac{3}{8} \cdot 1,835 qsl}{2,835 \cdot 2 - 1} = 0,1474 qsl.
 \end{aligned}$$

Then

$$\gamma_{main} = \frac{1}{48} - \frac{1}{16} (0,1474 + 0,0803) = 0,0066.$$

We calculate the stiffness coefficient of the elastic foundation for the stringer. According to formula (21.22), we obtain

$$k = \left(1 + \frac{0,0066}{0,0208} \cdot \frac{4585}{8870}\right) \frac{Ei_{\text{main}}}{2\gamma_{\text{main}}^2 l^3} = 0,582 \frac{Ei_{\text{main}}}{\gamma_{\text{main}}^2 l^3} = 641 \text{ kg/cm}^2 = 6410 \text{ t/m}^2.$$

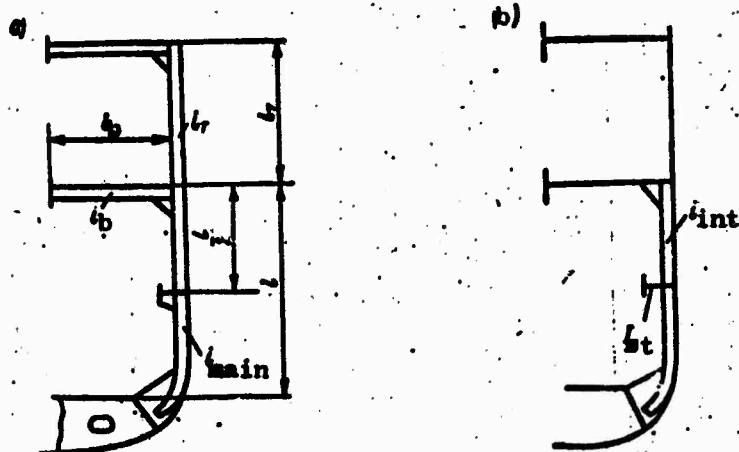


Figure 74. Diagram of frame fastenings: a-main frame; b-intermediate frame.

We find the parameter of elastic foundation  $u$  by formula (21.24), assuming the stringer span to be equal to the distance between web frames

$$u = \sqrt[4]{\frac{0,582 \cdot 8}{64 \cdot 0,0066} \cdot \frac{8870}{57760} \left(\frac{3,2}{4,0}\right)^3} = 0,96.$$

We determine according to [45] the functions of parameter  $u = 0.96$  which are necessary for further calculation (Table 19).

We shall consider a case in which a load is applied directly to a stringer. We shall assume that the web frames are a rigid support for the stringer. We determine the reference couple coefficient for the stringer according to Table 18 for  $u = 0.96$ ;  $x = 0.576$ . Since the load is applied directly to the stringer,  $\xi = \eta = 50 \text{ t/m}$ .

Table 19

Numerical values of parameter  $u$  functions.

$u$	$\chi_0$	$\chi_1$	$\chi_2$	$\mu$	$\nu$	$\eta_0$	$\eta_1$
0,96	0,630	0,894	0,912	0,709	0,931	0,516	0,871

Bending moment in the stringer abutment section (at the web frame) is determined by formula (21.5)

$$M_{abut} = 0,576q \cdot \frac{3,2^2}{12} \cdot 0,912 = 0,440q = 22,5t \cdot m.$$

Bending moment in the span center, according to formula (21.4)

$$M_{span} = \frac{3,2^2}{8} q \left( 0,424 \cdot 0,630 + \frac{0,576}{3} \cdot 0,894 \right) = 0,602q = 28,1t \cdot m.$$

Shearing force in abutment section at the web frame, according to formula (21.3)

$$N_{abut} = \frac{3,2}{2} q (0,424 \cdot 0,700 + 0,576 \cdot 0,894) = 1,34q = 67t.$$

Maximum bending stresses of stringer in span center

$$\sigma = \frac{M_{span}}{W_{str}} = \frac{28,1 \cdot 10^6}{1080} = 1400 \text{ kg/cm}^2.$$

Maximum tangential shearing stress of stringer in abutment section

$$\tau = \frac{N_{abut}}{0,85F_{str}} = \frac{67 \cdot 10^3}{0,85 \cdot 56} = 1400 \text{ kg/cm}^2.$$

Reaction of stringer on main frame [see formula (21.13)]

$$R_{main} = \frac{50 \cdot 0,4}{0,562} (1 - 0,424 \cdot 0,516 - 0,576 \cdot 0,871) = 0,192q = 9,56t;$$

reaction of stringer on the intermediate frame

$$R_{int} = \frac{2 \cdot 0,4 \cdot 50}{1 + \frac{4585}{8870} \cdot \frac{0,0208}{0,0066}} \cdot 0,279 = 4,25t.$$

Bending moment in center of intermediate frame span under the influence of reaction  $R_{int}$

$$M_{span} = \frac{R_{int} \cdot l}{4} = \frac{4,25 \cdot 4}{4} = 4,25t \cdot m.$$

Maximum bending stresses of frame

$$\sigma = \frac{M_{span}}{W_{int}} = \frac{4,25 \cdot 10^6}{267} = 1590 \text{ kg/cm}^2.$$

Bending moments on the main frame supports

$$M_2 = 0,0803R_{main} \cdot l = 3,08t \cdot m,$$

$$M_4 = 0,1474R_{main} \cdot l = 5,64t \cdot m.$$

Bending moment in center of main frame span is determined by formula (20.8)

$$M_{\text{span}} = 5.20 \text{ t.m.}$$

Maximum bending stresses of frame

$$\sigma = \frac{M_{\text{span}}}{W_{\text{main}}} = 1120 \text{ kg/cm}^2.$$

We shall compute yielding of the web frame, assuming it to be constrained the same as the main frames ( $\gamma_{\text{wf}} = \gamma_{\text{main}} = 0.0066$ ).

The yielding of the web frame as an elastic support

$$\lambda = 0.0066 \frac{l^3}{E (I_{\text{wf}} - I_{\text{main}})}.$$

We calculate magnitudes  $R$  and  $R_1$  by formula (21.21):

$$R = \frac{\lambda L_1}{2} \mu(u) = \frac{0.582}{2} \frac{\pi l}{4l_1 - 4a_{\text{main}}} \mu(u) = 0.422 \cdot 0.709 = 0.303,$$

$$R_1 = \frac{\lambda L_1}{2} \nu(u) = 0.422 \cdot 0.931 = 0.393.$$

When calculating yielding of web frames, stress in the stringer is decreased and load of the frames is increased. For example, bending moment in the abutment section of a stringer

$$M_{\text{abut}} = \frac{qL_1^2}{12} \cdot \frac{\gamma_2(u)}{1 + R_1} = \frac{0.576 \cdot 50 \cdot 3.2^2}{12} \cdot \frac{0.912}{1.393} = 16.12 \text{ t.m.}$$

Shearing force at the support, equal to reaction of the stringer to the web frame,

$$N_{\text{abut}} = \frac{50 \cdot 3.2}{2} \left( 0.424 \frac{0.709}{1.393} + 0.576 \cdot \frac{0.931}{1.393} \right) = 49.3 \text{ t.}$$

Considering that the web frame is constrained the same as the main frame, maximum bending moment in its span is determined by formula

$$M_{\text{span}}^{\text{wf}} = M_{\text{span}}^{\text{main}} \frac{N_{\text{abut}}}{R_{\text{main}}} = 5.20 \cdot \frac{49.3}{9.56} = 26.8 \text{ t.m.}$$

where  $M_{\text{span}}^{\text{main}} = 5.20 \text{ t.m.}$  is the bending moment in the main frame span

under the influence of reaction span  $R_{\text{main}} = 9.56 \text{ t.}$

Maximum bending stresses in the web frame span

$$\sigma = \frac{M_{wf}}{W_{wf}} = \frac{26.8 \cdot 10^6}{1890} = 1420 \text{ kg/cm}^2$$

Reaction of the stringer on the main frame, allowing for yielding of the web frame

$$R'_{\text{main}} = \frac{50 \cdot 0.4}{0.582} \left( 1 - \frac{0.424 \cdot 0.516}{1.303} - \frac{0.567 \cdot 0.871}{1.303} \right) = 16.2 \text{ t}$$

reaction on the intermediate frame

$$R'_{\text{int}} = \frac{4.25}{9.56} \cdot 16.2 = 7.2 \text{ t}$$

Maximum bending stress in the intermediate frame span

$$\sigma_{\text{int}} = 1590 \cdot \frac{7.2}{4.24} = 2690 \text{ kg/cm}^2$$

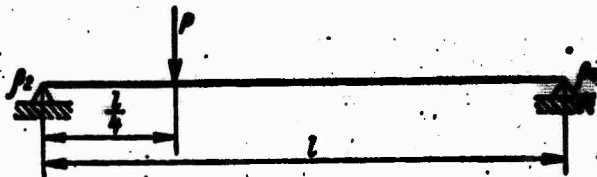


Figure 75. Design diagram for calculating influence coefficient  $\beta$  for main and intermediate frames.

Maximum bending stress in main frame span

$$\sigma_{\text{main}} = 1120 \cdot \frac{16.2}{9.56} = 1890 \text{ kg/cm}^2$$

Thus, it is obvious that the end rigidity of web frames exerts a substantial influence on the work of the frames as part of the side grillage and must necessarily be taken into consideration when calculating.

Now, we shall consider a second situation in which a load is applied to the center of a frame span between a stringer and lower deck. We shall determine influence coefficient  $\beta$  for the main frame (Figure 75) when  $\eta = 1/4$ .

We find the support moments by formula (20.7):

$$M_3 = \frac{0,25 \cdot 0,75 (1,75 \cdot 2 - 1,25)}{2,835 \cdot 2 - 1} P l = 0,0903 P l,$$

$$M_4 = \frac{0,25 \cdot 0,75 (1,25 \cdot 2,835 - 1,75)}{2,835 \cdot 2 - 1} P l = 0,0718 P l,$$

$$\beta_{\text{main}} = \frac{11}{6 \cdot 128} - \frac{1}{16} (0,0903 + 0,0718) = 0,0042.$$

For an intermediate frame

$$P_3 = P_4 = \infty; M_3 = M_4 = 0; \beta_{\text{int}} = \frac{11}{6 \cdot 128} = 0,01433.$$

We shall determine the reduced load on the stringer

$$\bar{q} = 80 \left( \frac{0,0042}{0,0066} + \frac{0,01433}{0,0206} \right) \frac{1}{2} = 33,1 \text{ t/m.}$$

All flexural elements of the stringer are decreased in comparison with the foregoing case  $\frac{q}{\bar{q}} = \frac{50}{33,1} = 1,51$  times.

Deflection of the stringer in the span center with allowing for yielding of the web frame

$$v = \frac{331}{341} (1 - 0,424 \cdot 0,516 - 0,576 \cdot 0,571) = 0,144 \text{ cm.}$$

allowing for web frame yielding

$$v = \frac{331}{641} \left( 1 - \frac{0,424 \cdot 0,516}{1,303} - \frac{0,576 \cdot 0,571}{1,303} \right) = 0,244 \text{ cm.}$$

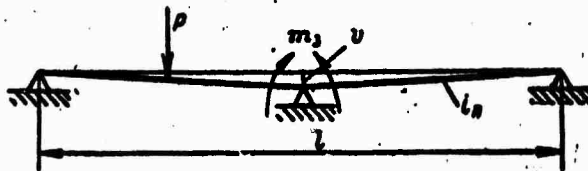


Figure 76. Diagram for calculating middle frames, considered as beams with displaced support.

We shall calculate middle frames, considering them as beams with displaced (on the stringer) supports (Figure 76):

$$P = q_s = 50 \cdot 0,4 = 20 \text{ t,}$$

$$M_3 = \frac{3}{64} P l - 12 \frac{Ei \int v}{2} = 3,75 - 1,04 = 2,71 \text{ tm,}$$

Moment in center of span

$$M_{\text{span}} = \frac{Pl}{2.4} = 1.36 = 8.64 \text{ ts.}$$

Maximum bending stresses of intermediate frame in center of span

$$\sigma = \frac{M_{\text{span}}}{W_{\text{int}}} = \frac{8.64 \cdot 10^6}{267} = 3230 \text{ kg/cm}^2$$

Allowing for web frame yielding

$$M_3 = 3.75 = 1.04 \cdot \frac{0.244}{0.144} = 1.82 \text{ ts}$$

moment in center of the span

$$M_{\text{span}} = 10 = 0.76 = 9.24 \text{ ts.}$$

maximum stresses

$$\sigma = \frac{M_{\text{span}}}{W_{\text{int}}} = \frac{9.24 \cdot 10^6}{267} = 3460 \text{ kg/cm}^2$$

Curves of bending moments, with and without allowing for web frame yielding, are presented in Figure 77. It is obvious that in this case, yielding of the web frame has little influence on the bending of frames in the center span of the grillage.

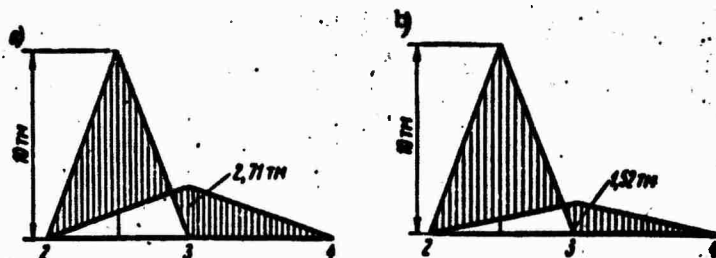


Figure 77. Diagrams of bending moments  $M_2$ ,  $M_3$  and  $M_4$  in the main frame (Figure 78), we compile a system of three moment equations

$$\frac{1}{2} M_2 = -\frac{M_2^i}{6Ei_{\text{main}}} - \frac{M_3^i}{12Ei_{\text{main}}} + \frac{2v}{l} + \frac{Pl^2}{64Ei_{\text{main}}}$$

$$\frac{M_2^i}{12Ei_{\text{main}}} - \frac{M_3^i}{6Ei_{\text{main}}} + \frac{2v}{l} - \frac{Pl^2}{64Ei_{\text{main}}} = -\frac{2v}{l} - \frac{M_3^i}{6Ei_{\text{main}}} - \frac{M_4^i}{12Ei_{\text{main}}}$$

$$\frac{M_3^i}{12Ei_{\text{main}}} - \frac{M_4^i}{6Ei_{\text{main}}} - \frac{2v}{l} = 0,$$



Figure 78. Design diagram for determining support moments.

or after multiplying by  $\frac{6Ei_{\text{main}}}{l}$

$$(1 + \mu) M_1 + \frac{1}{2} M_2 = \frac{6}{64} Pl + \frac{12Ei_{\text{main}} \Delta}{l^3}$$

$$\frac{1}{2} M_1 + 2M_2 + \frac{1}{2} M_3 = \frac{6}{64} Pl - \frac{24Ei_{\text{main}} \Delta}{l^3}$$

$$\frac{1}{2} M_1 + M_3 = \frac{12Ei_{\text{main}} \Delta}{l^3}$$

Without allowing for yielding of web frames  $M_2 = 5.2 \text{ tm}$ ,  $M_3 = -0.06 \text{ tm}$ ,  $M_1 = 2.04 \text{ tm}$ .

The maximum bending moment in the span (see diagram in Figure 79)  $M_{\text{span}} = 7.4 \text{ tm}$ ; maximum bending stress

$$\sigma = \frac{M_{\text{span}}}{W_{\text{main}}} = \frac{7.4 \cdot 10^6}{463} = 1600 \text{ kg/cm}^2$$

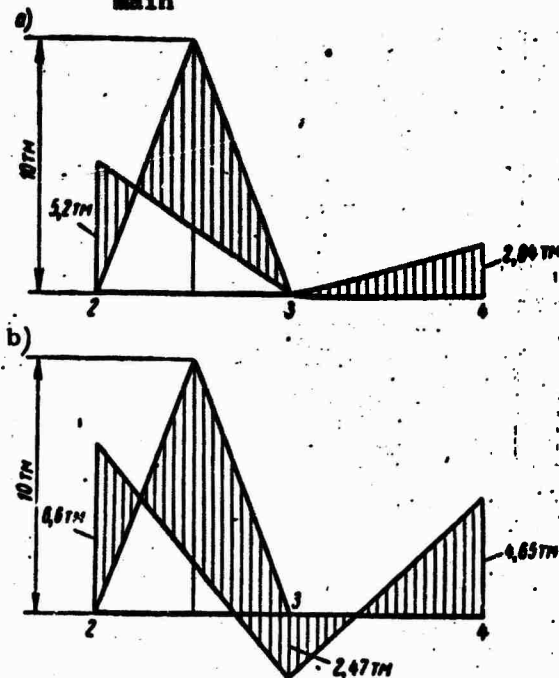


Figure 79. Diagram of bending moments for main frame, without allowing (a) and allowing (b) for yielding of frames.

Allowing for yielding of web frames  $M_2 = 6.62 \text{ tm}$ ,  $M_3 =$   
 $= 2.47 \text{ tm}$ ;  $M_4 = 4.65 \text{ tm}$ .

Maximum bending moment in the span (Figure 79)  $M_{\text{span}} =$   
 $= 8.00 \text{ tm}$ . Maximum bending stress

$$\sigma = \frac{M_{\text{span}}}{W_{\text{main}}} = \frac{8 \cdot 10^6}{463} = 1730 \text{ kg/cm}^2.$$

## 22. Grillages With Several Cross Bracings. Method of Elastic Supports.

Grillage with two stringers can easily be calculated by the method of principal bends. However, when the number of cross bracings is increased, calculations become significantly more time-consuming and its use is irrational. In 1959, D. Ye. Kheysinyy and A. A. Bubyakinyy proposed an approximation method for calculating grillages with several cross bracings for ice load action.

The essence of this method, called the method of "elastic supports," consists of determining the rigidity of the elastic foundation under any cross bracing, allowing for the influence of the rigidities and position of other cross beams. According to a method proposed by A. I. Segal' [43], an arbitrary, external load is reduced to nodal form, i.e., to a load directly applied to the cross bracings. This is achieved by determining the reaction of the beams running in the main direction, which are supported on cross beams, as on absolutely rigid supports. False reactions taken with the opposite sign are called a nodal load.

According to the principle of superposition, the problem of calculating a grillage with  $n$  stringers, where each cross beam is loaded with a corresponding nodal load, can be divided into  $n$  problems, in each of which there is only one loaded cross bracing. In any individual problem, the elastic line of each of the unloaded bracings is taken according to the first free vibrational mode of a prismatic beam constrained in corresponding manner. Then, each unloaded cross bracing can be substituted with a series of independent elastic supports for the beams running in the main direction. Rigidity  $k$  of these supports will be constant over the length of the grillage according to the selected elastic line. After this substitution, the problem is reduced to calculating the cross bracing for the action of a nodal load under the conditions that the bracing is resting on beams running in the main direction which, in turn, are supported on intermediate elastic supports -- cross beams which are unloaded in the given problem. When there is a large number of beams running in the main direction (more than five), the problem under consideration reduces to a calculation of a stringer as a beam on an elastic, riser-type foundation with constant rigidity. For an equally distributed load,

design formulas can be expressed in I. G. Babnov's functions and for a concentrated force, it is possible to apply it in case of an external load of any type, making appropriate integrations.

Comparisons of calculations in the method of principal bends and the method of elastic supports have given good correspondence of results. Basic calculation dependencies and steps according to the method of elastic supports are set forth in detail below.

Reducing a load to nodal form. In the first calculation stage, all beams running in the main direction are considered to be supported on false, rigid supports installed at the joints (intersection points of the stringers and frames). Reactions of these supports  $P_1, P_2, \dots, P_n$ , taken with the opposite sign, represent a nodal load.

With  $n$  cross bracings and an external load in the form of a concentrated force  $P$ , applied on the span of the frame, reactions  $P_j$  are found by the Navier method, i.e.,

$$\sum_{j=1}^n \gamma_{ij} \frac{P_j P}{EI} - \beta_i \frac{PP}{EI} = 0,$$

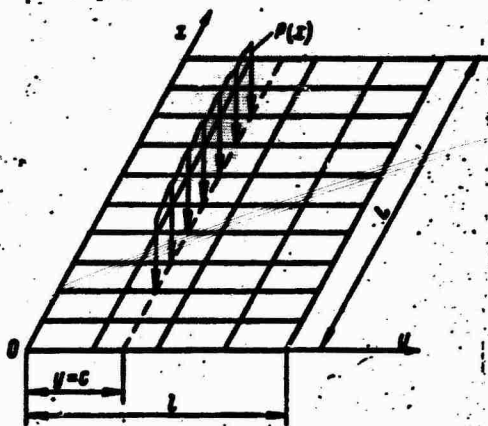


Figure 80. Diagram for determining nodal reactions.

or

$$\sum_{j=1}^n \gamma_{ij} P_j - \beta_i P = 0. \quad (22.1)$$

Assuming  $P_j = \alpha_j P$ , we have

$$\sum_{j=1}^n \gamma_{ij} \alpha_j - \beta_i = 0, \quad i = 1, 2, \dots, n, \quad (22.2)$$

where

$\gamma_{ij}$  - is the influence coefficient of the reaction of the  $j$ -th cross bracing to deflection of the beam running in the main direction at joint  $i$ ;

$\beta_i$  - is the influence coefficient of the external load to deflection of the beam running in the main direction at joint  $i$ ;

$\alpha_j$  - is the coefficient of reduction of the external load to a nodal load for the  $j$ -th cross bracing.

With identical, equally spaced beams running in the main direction and a load distributed along a line (Figure 80), nodal reactions are calculated by formula

$$P_i(x) = \alpha_j P(x), \quad (22.3)$$

where  $\alpha_j = \text{const}$ , and is found from system of equations (22.2).

If an external load is applied directly to a cross bracing, this stage of the calculation is omitted.

Calculating rigidity of elastic supports (unloaded stringers) for frames. If  $R_j$  is the reaction of the  $j$ -th stringer supporting a frame, a differential equation for bending of the stringer can be written in the form

$$EI \rho_j^{IV}(x) = \frac{R_j}{s}. \quad (22.4)$$

Assuming

$$v_j(x) = A_j f(x), \quad (22.5)$$

where  $f(x)$  - is the first form of free vibrations by the corresponding form of constrained prismatic beam which satisfies the differential equation

$$f^{IV}(x) = \left(\frac{\mu}{L}\right)^4 f(x), \quad (22.6)$$

and using these dependencies, we can obtain

$$v_j^{IV}(x) = \left(\frac{\mu}{L}\right)^4 v_j(x). \quad (22.7)$$

Substituting (22.7) in (22.4), we shall have

$$R_j = EI_1 \left(\frac{\mu}{L}\right)^4 v_j(x), \quad (22.8)$$

or

$$R_j = k \rho_j(x), \quad (22.9)$$

i.e., reaction of the stringer is equal to reaction of an elastic foundation with rigidity

$$k_j = \left(\frac{\mu}{L}\right)^4 EI \rho, \quad (22.10)$$

where  $\mu$  is a multiple root of the characteristic equation for the differential equation for bending of the cross bracing, depending only on the method of fastening its ends [24]. Values of  $\mu$  are presented in Table 20.

Table 20

Values of  $\mu$  depending on reference couple coefficients\*.

$\alpha_2$	$\alpha_1$				
	0.00	0.25	0.50	0.75	1.00
0.00	3.142	3.235	3.367	3.569	3.927
0.25	3.235	3.334	3.454	3.657	4.005
0.50	3.367	3.454	3.577	3.776	4.130
0.75	3.569	3.657	3.776	3.967	4.321
1.00	3.927	4.005	4.130	4.321	4.730

\* The table is borrowed from P. F. Papkovich' book, Strength of Ships, part 2, State All-Union Publishing House of the Shipbuilding Industry, 1941.

Calculating the rigidity of an elastic foundation for a loaded stringer. Substituting each unloaded stringer with a series of elastic supports of corresponding rigidity, a loaded stringer can be considered as a beam on a riser-type, elastic foundation with rigidity  $k_j^{**}$ . The coefficient of rigidity of an elastic foundation for the  $j$ -th stringer

$$k_j = \frac{1}{v_j}, \quad (22.11)$$

where  $v_j$  - is the deflection at joint  $j$  of a beam running in the main direction, caused by unit stress  $P_j = 1$  applied at that same joint.

\* Reactions of a riser-type foundation are proportional to the deflection at the given point and do not depend on deflections of adjacent points.

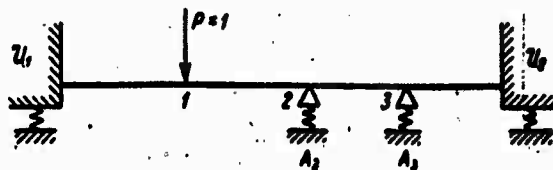


Figure 81. Diagram for determining the rigidity of an elastic foundation for a loaded stringer.

We shall show the procedure for determining the coefficient of rigidity of elastic foundation  $k$  below the first stringer in an example of grillage with three cross bracings (Figure 81).

The coefficient of yielding of the elastic supports

$$A_1 = \frac{1}{k_1} = \frac{L^4}{r_1^4 EI_1^3}$$

$$A_2 = \frac{1}{k_2} = \frac{L^4}{r_2^4 EI_2^3} \quad (22.12)$$

Redundancy of the frame is most easily expanded by the Navier method, determining the unknown reactions of supports  $R_2$  and  $R_3$ . The amount of deflection in joint 1 from action of unit stress is calculated by formula

$$v_1 = \frac{1P}{EI} \gamma_{11} - \frac{R_2 P}{EI} \gamma_{12} - \frac{R_3 P}{EI} \gamma_{13}$$

Then

$$k_1 = \frac{1}{v_1} = \frac{EI}{\lambda_1 P}$$

where

$$\lambda_1 = 1 \cdot \gamma_{11} - R_2 \gamma_{12} - R_3 \gamma_{13}$$

The parameter of elastic foundation

$$u_1 = \frac{L}{2} \sqrt[4]{\frac{k_1}{4EI_1}} = \sqrt[4]{\frac{\pi}{64\lambda_1} \left(\frac{L}{l}\right)^3 \frac{l}{I_1}} = \sqrt[4]{\frac{\sigma_1^4}{60_1}} \quad (22.13)$$

where

$$\sigma_1^4 = A_1 \frac{EI}{P} = \frac{\pi}{\mu^4} \left(\frac{L}{l}\right)^3 \cdot \frac{l}{I_1}$$

Bending of the stringer will subsequently be calculated by known formulas as for a beam on an elastic foundation.

General comments for a design plan. The following should be kept in mind when using the proposed method. Beams running in all directions are considered as prismatic, frames are considered to be equally spaced and identical and cross bracings equally constrained at both ends. Coefficients of restraint can differ for different stringers.

Strength of stringers should be checked by applying a load directly to the stringer. When calculating frames, the load is applied between stringers in the center of frame spans. In the first situation, all stringers except the one being calculated should be replaced by elastic supports. In the second situation, all stringers except the two adjacent to the span where the load is applied, should be replaced by elastic supports.

When calculating a middle section, reactions to elastic supports are determined and then a bending-moment diagram is constructed. An extreme frame is considered as a single-span, continuous, beam supported on rigid supports. If yielding of web frames is not taken into consideration, it is possible to proceed in two ways. First, it is possible to disregard the web frame when calculating the coefficients of yielding  $A$  of elastic supports. In this case, the stringer span  $L$  will be measured from bulkhead to bulkhead in formulas for coefficients of  $A$ . The remaining (loaded) stringer should be considered taking the web frame into account as was shown in the foregoing paragraph for grillage with one cross bracing. In this, an error is made on the side of providing a margin of safety. In the second method, when calculating coefficients of yielding of elastic supports, the web frames are considered as rigid supports for the stringers and the stringer spans are measured between web frames. Subsequent calculations are performed the same as in the first case (with error on the side of providing a margin of safety). For more accurate calculation of the yielding of web frames, it is necessary to calculate the grillage according to the method of principal bends. When calculating coefficients of the yielding of constraint of the frames  $U_1$  and  $U_2$ , as well as reference couple coefficients for stringers, formulas of the preceding paragraph should be used.

**Example.** Check the strength of the side grillage (Figure 82) for two situations of application of external load  $q = 120$  t/m, specifically: directly to the second stringer and along a line in the center of the span between the first and second stringers. In both cases, the design load is considered to be applied over the entire length of the grillage.

Initial data:  $L = 2.8$  m,  $s = 0.35$  m,  $F_1 = F_2 = 86.4$  cm<sup>2</sup>,  
 $I_1 = I_2 = 269300$  cm<sup>4</sup>,  $W_1 = W_2 = 4380$  cm<sup>3</sup>,  $I_3 = 144600$  cm<sup>4</sup>,  $W_3 = 42840$  cm<sup>3</sup>,  $V = 597$  cm<sup>3</sup>,  $i_1 = 5.4$  m,  $i_2 = 12690$  cm<sup>4</sup>,  $i_3 = 2.6$  m,  
 $i_4 = 2380$  cm<sup>4</sup>,  $i_{int} = 2.65$  m,  $i_{int} = 2,600$  cm<sup>4</sup>,  $i_b = 5.5$  m,  $i_b = 2600$  cm<sup>4</sup>,  $i_{btm} = 3.00$  m,  $i_{btm} = 12690$  cm<sup>4</sup>,  $i_{main} = 1.0$  m,  $i_{main} = 1.7$  m,  $i_2 = 1.5$  m,  $i_3 = 1.2$  m,  $x = 0$ ;  $\mu = 3.14$ ;  $\sigma_y = 3000$  kg/cm<sup>2</sup>,  
 $\tau_y = 0.6$ .  $\sigma_y = 1,800$  kg/cm<sup>2</sup>.

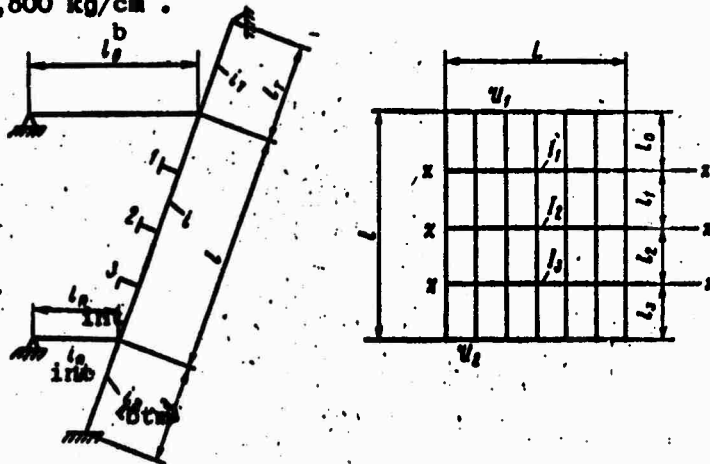


Figure 82. Diagram of side grillage with three stringers.

We calculate influence coefficient  $\gamma$ . Dimensionless coefficients of yielding of the plastic constraint of the frame ends are found by formula (20.6):

$$\gamma_1 = \frac{2}{\frac{2,6}{12,00} \cdot \frac{5,4}{5,5} + \frac{2,38}{12,00} \cdot \frac{5,4}{2,6}} = 3,39,$$

$$\gamma_2 = \frac{2}{\frac{2,6}{12,00} \cdot \frac{5,4}{2,65} + \frac{4}{3} \cdot \frac{12,00}{12,00} \cdot \frac{5,4}{3,0}} = 0,71.$$

We determine the magnitude of support moments from unit stress applied to the joints according to formula (20.7). For load  $P = 1$ , applied at joint 1, we obtain

$$\eta_1 = \frac{l_0}{l} = 0,185,$$

$$\mathfrak{M}_{11} = \frac{0,185 \cdot 0,815 (1,815 \cdot 2,71 - 1,185)}{5,39 \cdot 2,71 - 1} l = 0,0413l,$$

$$\mathfrak{M}_{21} = \frac{0,185 \cdot 0,815 (1,185 \cdot 5,39 - 1,815)}{5,39 \cdot 2,71 - 1} l = 0,0507l.$$

For load  $P = 1$  applied at joint 2:  $\eta_2 = 0,5$ ,

$$\mathfrak{M}_{12} = \frac{\frac{3}{8} \cdot 1,71}{5,39 \cdot 2,71 - 1} l = 0,0471l,$$

$$\mathfrak{M}_{22} = \frac{\frac{3}{8} \cdot 4,39}{5,39 \cdot 2,71 - 1} l = 0,1211l.$$

For load  $P = 1$ , applied at joint 3:

$$\eta_3 = 0,778,$$

$$\mathfrak{M}_{13} = \frac{0,778 \cdot 0,222 (1,222 \cdot 2,71 - 1,778)}{5,39 \cdot 2,71 - 1} l = 0,0196l,$$

$$\mathfrak{M}_{23} = \frac{0,778 \cdot 0,222 (1,778 \cdot 5,39 - 1,222)}{5,39 \cdot 2,71 - 1} l = 0,1062l.$$

Influence coefficient

$$\gamma_{11} = \frac{1}{6} \gamma_1 (1 - \gamma_1) \left\{ \left[ 1 - (1 - \gamma_1)^3 - \gamma_1^3 \right] - \left[ \mathfrak{M}_{11} (2 - \gamma_1) + \mathfrak{M}_{21} (1 + \gamma_1) \right] \frac{1}{l} \right\} = \frac{1}{6} \cdot 0,185 \cdot 0,815 \left\{ (1 - 0,185^3 - 0,185^3) - (0,0413 \cdot 1,815 + 0,0507 \cdot 1,185) \right\} = 0,00418.$$

Using analogous formulas, we obtain  $\gamma_{22} = 0.01032$ ,  
 $\gamma_{12} = \gamma_{21} = 0.00530$ ,  $\gamma_{23} = \gamma_{32} = 0.00510$ ,  $\gamma_{33} = 0.00381$ ,  
 $\gamma_{13} = \gamma_{31} = 0.00222$ .

We calculate coefficients of yielding of elastic supports. The dimensionless coefficient of yielding of support is determined, taking formula (22.13) into account

$$a_i^0 = \left(\frac{L}{l}\right)^3 \frac{l}{l_i} \frac{R}{R^0},$$

$$a_1^0 = a_2^0 = \frac{8}{3,14^2} \cdot \left(\frac{2,8}{5,4}\right)^3 \cdot \frac{12600}{269300} = 0,000541,$$

$$a_3^0 = \frac{8}{97,1} \cdot \left(\frac{2,8}{5,4}\right)^3 \cdot \frac{12600}{144600} = 0,001007.$$

Load applied directly to the second stringer.

We determine parameter  $u$  of elastic foundation for stringer 2. The magnitude of deflection  $v_{P=1}$  and coefficient  $k_2$  are found according to the design diagram in Figure 83.

After solving the system of equations

$$R_1(a_1^0 + \gamma_{11}) + R_2\gamma_{12} = P\gamma_{12},$$

$$R_1\gamma_{12} + R_2(a_2^0 + \gamma_{22}) = P\gamma_{22},$$

we obtain  $R_1 = 0.7976$ ;  $R_2 = 0.6912$ .

Deflection under the influence of unit force  $P = L$

$$v_{P=1} = \gamma_2 \frac{P}{EI} = \frac{P}{EI} (\gamma_{22} - \gamma_{21}R_1 - \gamma_{23}R_2) = 0,00267 \frac{P}{EI}.$$

The parameter of elastic foundation according to formula (22.13)

$$u_2 = \sqrt[4]{\frac{12,69}{269,3} \cdot \left(\frac{2,8}{5,4}\right)^3 \cdot \frac{8}{0,165}} = 0,76.$$

Values of parameter  $u$  functions which are necessary for subsequent calculations are presented in Table 21.

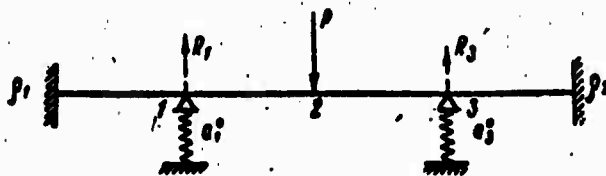


Figure 83. Design diagram for calculating coefficient  $k_2$  for the second stringer.

Table 21

Numerical values for elastic foundation parameter  $u$  functions.

$u$	$\gamma_0$	$\gamma_1$	$\gamma_2$	$\gamma_3$	$\gamma_4$	$\mu$	$\nu$
0,75	0,770	0,948	0,836	0,968	0,984	0,985	0,972

We determine flexural elements of the stringer: bending moment in the center of the span

$$M_{\text{span}} = \frac{qL^3}{8} \left[ (1-u)\gamma_0 + \frac{u}{3}\gamma_3 \right] = -0,921q = -98,6 \text{ t} \cdot \text{m}$$

bending stress

$$\sigma = \frac{M_{\text{span}}}{W_s} = \frac{98,6 \cdot 10^6}{4300} = 2293 \text{ kg/cm}^2 < \sigma_y = 3000 \text{ kg/cm}^2$$

shearing force in the abutment section of the stringer

$$N_{\text{abut}} = \frac{qL}{2} [(1-u)\mu + \nu] = 1,197q = 143,6 \text{ t}$$

shearing stress in the stringer wall

$$\tau = \frac{N_{\text{abut}}}{F_s} = \frac{143,6 \cdot 10^6}{86,4} = 1662 \text{ kg/cm}^2 < 0,6\sigma_y = 1800 \text{ kg/cm}^2$$

stringer reaction to the middle section

$$R_{22} = qL(1-0,770) = 0,221 \cdot 120 \cdot 0,35 = 9,27 \text{ t}$$

We determine bending moments in the middle section. Reactions of the first and third stringers when stress action  $R_{22} = 9,27 \text{ t}$ :

$$R_{12} = R_{22}R_1 = 0,7976 \cdot 9,27 = 7,4 \text{ t}$$

$$R_{32} = R_{22}R_3 = 9,27 \cdot 0,6612 = 6,11 \text{ t}$$

Bending moment from stress  $R_{22}$  in the span

$$M_2 = R_{22}\gamma_2(1-\gamma_0)l = \frac{9,27}{4} \cdot 5,4 = 12,5 \text{ t} \cdot \text{m}$$

on the supports

$$M_{12} = \mathfrak{R}_{12}R_{22} = 0,0471 \cdot 9,27 \cdot 5,4 = 2,36 \text{ t} \cdot \text{m}$$

$$M_{32} = \mathfrak{R}_{32}R_{22} = 0,1211 \cdot 9,27 \cdot 5,4 = 6,05 \text{ t} \cdot \text{m}$$

Bending moments from stress  $R_{12}$  in the span

$$M_1 = 7,4 \cdot 0,185 \cdot 0,815 \cdot 5,4 = 6,02 \text{ t} \cdot \text{m}$$

on the supports

$$M_{11} = \mathfrak{R}_{11}R_{12} = 0,0413 \cdot 7,4 \cdot 5,4 = 1,65 \text{ t} \cdot \text{m}$$

$$M_{31} = \mathfrak{R}_{31}R_{12} = 0,0507 \cdot 7,4 \cdot 5,4 = 2,03 \text{ t} \cdot \text{m}$$

Bending moments from stress  $R_{13}$  in the span

$$M_0 = 0,778 \cdot 0,222 \cdot 6,41 \cdot 5,4 = 5,98 \text{ tm.}$$

on the supports

$$M_{13} = 2R_{13}R_{13} = 0,0196 \cdot 6,41 \cdot 5,4 = 0,67 \text{ tm.}$$

$$M_{23} = 2R_{23}R_{23} = 0,1082 \cdot 6,41 \cdot 5,4 = 3,68 \text{ tm.}$$

The design bending moment in the frame span is determined graphically by constructing a bending-moment diagram:

$$M_{\text{span}} = 4,7 \text{ tm.}$$

Maximum bending stress

$$\sigma = \frac{M_{\text{span}}}{W} = \frac{4,7 \cdot 10^6}{667} = 700 \text{ kg/cm}^2.$$

Load applied to the center of the frame span between the first and second stringers (Figure 84).

We determine influence coefficients of the external load

$$\eta_p = \frac{c_p}{l} = \frac{1,85}{5,4} = 0,343.$$

Support moments from load P:

$$2R_{P1} = \frac{0,343 \cdot 0,657 (1,657 \cdot 2,71 - 1,343)}{5,30 \cdot 2,71 - 1} P_l = 0,0622 P_l.$$

$$2R_{P2} = \frac{0,343 \cdot 0,657 (1,343 \cdot 5,30 - 1,657)}{13,6} P_l = 0,0024 P_l.$$

Then

$$\beta_1 = \frac{\eta_1 (1 - \eta_p)}{6} [1 - (1 - \eta_p)^2 - \eta_1^2] - \frac{\eta_1 (1 - \eta_1)}{6} \left[ \frac{2R_{P1}}{l} (2 - \eta_1) + \frac{2R_{P2}}{l} (1 - \eta_1) \right] = 5,00 \cdot 10^{-3},$$

$$\beta_2 = 6,12 \cdot 10^{-3}, \quad \beta_3 = 4,0 \cdot 10^{-3}.$$

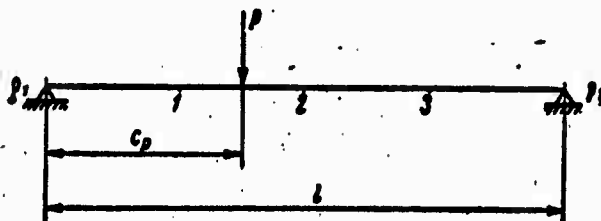


Figure 84. For determining influence coefficients  $\beta_1$ ,  $\beta_2$  and  $\beta_3$ .

The middle section is calculated according to the diagram in Figure 85.

Unknown reactions of elastic supports are calculated from the system of equations:

$$\begin{aligned} R_{1P}(\gamma_{11} + a_1^0) + R_{2P}\gamma_{12} + R_{3P}\gamma_{13} &= q_1 \\ R_{1P}\gamma_{21} + R_{2P}(\gamma_{22} + a_2^0) + R_{3P}\gamma_{23} &= q_2 \\ R_{1P}\gamma_{31} + R_{2P}\gamma_{32} + R_{3P}(\gamma_{33} + a_3^0) &= q_3 \end{aligned}$$

from which  $R_{1P} = 0.60 q_3$ ;  $R_{2P} = 0.552 q_3$ ;  $R_{3P} = 0.030 q_3$ .

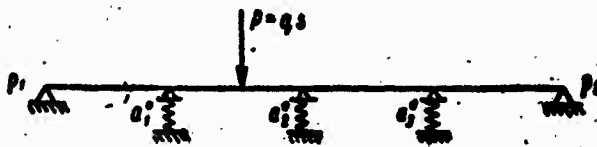


Figure 85. Design diagram for middle section.

Maximum bending moment at the point of force application

$$M = -0.022 q_1 = 14.26 \text{ tm,}$$

bending stress

$$\sigma = \frac{M}{W} = \frac{14.26 \cdot 10^6}{597} = 2390 \text{ kg/cm}^2 < \sigma_y = 3000 \text{ kg/cm}^2.$$

Stringers for the extreme frame should be considered as rigid supports. The unknown reactions of these supports are calculated by the cited system of equations, assuming that  $a_1 = a_2 = a_3 = 0$ ; then,  $R_{1P} = 0.684 q_3$ ;  $R_{2P} = 0.593 q_3$ ;  $R_{3P} = -0.142 q_3$ .

Maximum bending moment at the point of force application:

$$M_p = 0.0175 q_1 = 11.33 \text{ tm,}$$

bending stress in the extreme frame

$$\sigma = \frac{M}{W} = \frac{11.33 \cdot 10^6}{597} = 1890 \text{ kg/cm}^2 < \sigma_y = 3000 \text{ kg/cm}^2.$$

Calculating scantlings of web frames. Web frames which are being installed as intermediate supports for side stringers should be calculated for reaction from these stringers.

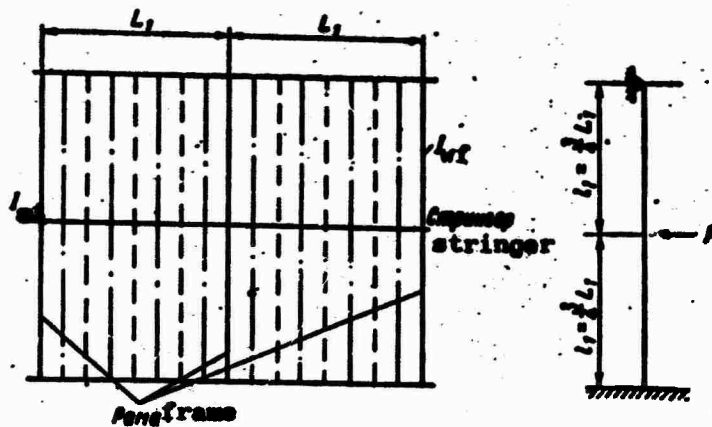


Figure 86. Diagram of side grillage with one stringer and web frames.

We shall consider the case of a grillage with one stringer (Figure 86), where  $L_1 = 8 \cdot 8 \cdot 0.4 = 3.2$  m. The space between the stringer and platform (deck)  $l_1$  must not exceed 2.5m. We shall assume  $l_1 = 6 \cdot 0.4 = 2.4$  m, i.e.,  $l_1 = 3/4 L_1$ .

We assume the stringer to be rigidly constrained on the web frames. The maximum bending stress of the stringer when there is uniform load action  $q$  applied directly to the stringer,

$$\sigma = \frac{qL_1^2}{12W_{st}}, \quad (22.14)$$

where  $W_{st}$  is the section modulus of the stringer.

Disregarding the part of the load which is transmitted to the deck and bottom by the frames, we obtain for the reaction to the frame when a load is applied to the span of a stringer between frames

$$P = \frac{qL_1}{2},$$

and for a load applied along the entire span of the grillage,

$$P = qL_1.$$

We adopt the latter as a design case. Then, bending stress of the web frame, considering it to be rigidly constrained below and simply supported above, is calculated according to the formula

$$\sigma = \frac{5qL_1}{32} \cdot \frac{3}{2} \cdot \frac{L_1}{W_{wf}} = \frac{15}{4} \cdot \frac{qL_1^2}{16W_{wf}}$$

Assuming the admissible stresses in the stringer and web frames to be equal, we obtain:

$$\frac{W_{wf}}{W_{st}} = \frac{15}{4} \cdot \frac{12}{16} = 2.8 \approx 3.$$

Taking the unloading effect of the frames into consideration, we can write

$$W_{wf} = 2 (1.5W_{st} - W_{main}) = 3 (W_{st} - \frac{2}{3}W_{main}).$$

When  $W_{st} = 3W_{main}$ , we obtain  $W_{wf} = 7W_{main}$ . Thus,  $W_{main} : W_{st} : W_{wf} = 1 : 3 : 7$ .

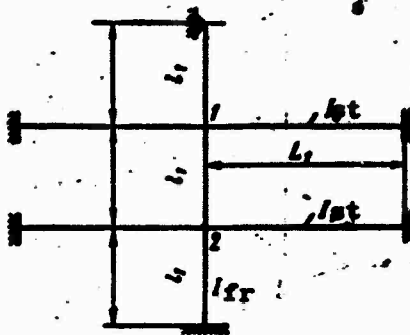


Figure 87. Diagram of grillage with two stringers.

Calculations show that such a relationship between profiles is nearly optimum.

If bearer stringers are installed

$$W_{st} = W_{main} \text{ and } W_{wf} = W_{main},$$

where  $W_{main}$  is the section modulus of the main frames.

We shall consider a section of grillage with two stringers (Figure 87). We assume the stringers to be identical and on the strength of symmetry of the load, to be rigidly constrained to the adjacent web frames - rigid supports. Let the first stringer be loaded with a uniform load. Then, the maximum stresses in the stringer are calculated by formula (22.14). We find stresses in the web frame, taking the unloaded stringer into consideration, which is an elastic support.

Reaction of the loaded stringer on the web frame, allowing a safety factor, will be

$$R_1 = qL_1.$$

Deflection of the second stringer at joint 2 (Figure 87)

$$v_2 = \frac{1}{24} \cdot \frac{R_2 L_1^3}{E I_{bt}}$$

Deflection of the web frame in this joint is determined from the design diagram in (Figure 88).

Influence coefficients of stringer reaction to frame deflection is determined according to handbook [14]:

$$v_{11} = 0,00914 \frac{R_1 (2l_1)^3}{E I_{rf}}; \quad v_{21} = -0,00503 \frac{R_1 (2l_1)^3}{E I_{rf}}$$

$$v_{12} = -0,00526 \frac{R_2 (2l_1)^3}{E I_{rf}}; \quad v_{22} = 0,00526 \frac{R_2 (2l_1)^3}{E I_{rf}}$$

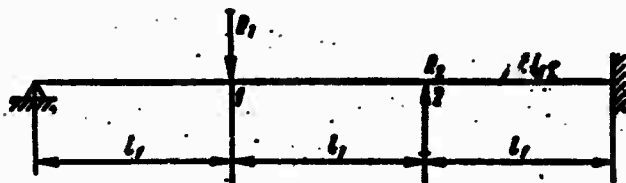


Figure 88. Design diagram for determining reactions in grillage joints.

Equating deflections of the frame and stringers in joints 1 and 2, we obtain

$$\frac{1}{24} \cdot \frac{q l_1^4}{E I_{bt}} - \frac{1}{24} \cdot \frac{R_1 L_1^3}{E I_{bt}} = 0,00914 \frac{R_1 (2l_1)^3}{E I_{rf}} - 0,00526 \cdot \frac{R_2 (2l_1)^3}{E I_{rf}}$$

$$\frac{1}{24} \cdot \frac{R_2 L_1^3}{E I_{bt}} - 0,00526 \cdot \frac{R_1 (2l_1)^3}{E I_{rf}} - 0,00503 \cdot \frac{R_2 (2l_1)^3}{E I_{rf}}$$

or

$$R_1 \left( 0,247 + 0,0416 \frac{l_{rf}}{l_1} \right) - 0,142 R_2 = 0,0416 q l_1 \frac{l_{rf}}{I_{bt}}$$

$$0,142 R_1 - \left( 0,136 + 0,0416 \frac{l_{rf}}{l_1} \right) R_2 = 0,$$

from which

$$R_1 = \frac{0,136 + 0,0416 \frac{l_{rf}}{l_1}}{0,142} R_2$$

When  $I_{wf}/I_{st} = 6.4$  (normal ratio for grillage with two cross bracings, must be within the range of 6 to 7),  $R_1 = 2.83 R_2$  or  $R_2 = 0.353 R_1$ .

We shall determine bending moments in the span of the web frame:

in joint 1 with effect of reaction  $R_1$ :

$$M_{R_1} = \frac{R_1(2L_1)^2 L_1 (6L_1 + l_1)}{2 \cdot 27 l_1^3} = qL_1^3 \frac{4.7}{2.27} = 0.518 qL_1^3$$

in joint 1 with effect of reaction  $R_2$ :

$$M_{R_2} = R_2 3L_1 \left( \frac{1}{2} \cdot \frac{2}{9} \left( 1 + \frac{2}{3} \right) - \left[ 1 - \frac{1}{2} \cdot \frac{1}{9} \left( 3 - \frac{1}{3} \right) \right] \frac{2}{3} + \frac{1}{3} \right) = 0.053 qL_1^3$$

Design bending moment in joint 1

$$M = M_{R_1} - M_{R_2} = (0.518 - 0.053) qL_1^3 = 0.465 qL_1^3$$

Bending stress of web frame

$$\sigma = \frac{M}{W_{wf}} = \frac{0.465 qL_1^3}{W_{wf}}$$

Assuming the admissible stresses in the stringer and frame to be equal, we obtain  $W_{wf}/W_{st} = 3.15$ . Allowing for the unloading effect of the frames and satisfying condition  $W_{wf} = W_{main}$  where  $W_{main} = W_{st}$ , as was done for grillage with one stringer, we obtain  $W_{wf} = 4 \left( W_{st} - \frac{3}{4} W_{main} \right)$ . When  $W_{st} = 3W_{main}$ , we have  $W_{main} : W_{st} : W_{wf} = 1 : 3 : 9$ .

We can write in general form for any number of stringers

$$W_{wf} = (m+2) \cdot \left( W_{st} - \frac{m+1}{m+2} W_0 \right), \quad (22.15)$$

where  $m$  is the number of stringers.

**Example.** Calculate the necessary section moduli of beams of a grillage with three cross bracings with the following initial data: frame spacings  $s=0.4$  m; distance between webs  $L_1 = 3.2$  m; frame span  $l = 8.0$  m; ice load intensity  $q = 200$  t/m; yield stress of the metal  $\sigma_y = 4,000$  kg/cm<sup>2</sup>.

We calculate the section modulus of a standard frame

$$W_{main} = k \frac{qsl}{\sigma_y} \cdot 10^6$$

Coefficient  $k$  is determined, depending on characteristic

$$a^* = 2 \left( \frac{L_1}{l} \right)^2 \cdot s = 2 \left( \frac{3.2}{8} \right)^2 \cdot 8 = 1.02,$$

where  $n = L_1 / s$  is the number of frame spacings in the stringer span.

For  $a^* = 1.02$   $k = 0.057$  and then

$$W_{\text{main}} = \frac{0.057 \cdot 200 \cdot 0.4 \cdot 8}{4000} 10^6 = 911 \text{ cm}^3.$$

We calculate the section modulus of the stringer. The elastic foundation parameter  $\gamma$  for the stringer is found depending on the characteristic  $a_1 = a / 2 = 0.51$ . Then  $u = 0.95$ . Bubnov functions which are necessary for subsequent calculations are determined depending on parameter  $u$  from Tables [45]:  $x_0(0.95) = 0.640$ ;  $x_1(0.95) = 0.898$ ;  $x_2(0.95) = 0.915$ .

The reference couple coefficient for stringers can be taken as equal to  $x = 0.5$  (see Table 18). Then, bending moment in the abutment section of the stringer is calculated by formula

$$M_{\text{abut}} = \frac{qL_1^2}{12} \chi_0(u) = \frac{0.918}{24} qL_1^2 = 0.038 qL_1^2.$$

bending moment in the span

$$M_{\text{span}} = \frac{qL_1^2}{8} \left[ \frac{1}{2} \chi_0(u) + \frac{1}{6} \chi_1(u) \right] = 0.059 qL_1^2.$$

The necessary section modulus of the stringer is determined from a condition of the maximum standard stresses reaching the yield stress of the material

$$W_{\text{st}} = \frac{M_{\text{span}}}{\sigma_y} = \frac{0.059 \cdot 200 \cdot 3.2^2}{4000} 10^6 = 2870 \text{ cm}^3.$$

$$\frac{W_{\text{st}}}{W_{\text{main}}} = \frac{2870}{911} = 3.14.$$

We determine the section modulus of the web frame by formula (22.15)

$$W_f = 5 \left( 2870 - \frac{4}{5} 911 \right) = 10700 \text{ cm}^3.$$

$$\frac{W_{\text{wf}}}{W_{\text{st}}} = \frac{10700}{2870} = 3.72.$$

### 23. Grillage with Bearer Stringers.

On UL (Arkt.) and UL-class cargo ships, it is advisable to install bearer stringers the same height as the main frames to strengthen the shell plating and side framing in the area of holds where use of increased profile stringers is often impossible because of the considerable decrease in cargo space. It is recommended that main and intermediate frames have the same profile. It is advisable to install bearer side stringers in the area of possible ice load application, i.e., at the height of the ice belt. Distance between stringers must not exceed 1.2 to 1.5 m. These stringers spread concentrated loads over several frame spaces along the length of the ship, increase the carrying capacity of the plating by dividing the panel between frames into parts and finally, increase stability of the two-dimensional form of frame bending.

The strength of bearer stringers is calculated in the following manner. For a grillage with a large number of frames, a bearer stringer can be considered as a beam on an elastic foundation with rigidity  $k_i$  (see 21.):

$$k_i = \frac{1}{\gamma_i s} = \frac{Ei}{\gamma_i s^3},$$

where  $i$  - is the moment of inertia of the frame;  
 $l$  - is the span of the frame;  
 $s$  - is the frame spacing;  
 $\gamma_i$  - is the influence coefficient of force  $P = 1$ , applied at the point where the stringer being considered intersects the frame, on deflection of that joint.

The procedure for determining influence coefficient  $\gamma$  was shown above.

When there are main and intermediate frames of different profiles with different end constraints, values of the coefficient of rigidity of the elastic foundation  $k$  should be calculated by formula (21.22).

The reduced length on which a concentrated load acting on a stringer is dispersed is calculated by an approximation formula [24]:

$$l_{\text{span}} = 2 \sqrt[4]{\frac{4EI_{st}}{k}} = 2l \sqrt[4]{4 \frac{I_{st}s}{l^3 \gamma_i}} \quad (23.1)$$

where  $I_{st}$  is the moment of inertia of the stringer.

Maximum bending moment acting on the stringer,

$$M_{\text{max}} = -\frac{Pl_{\text{span}}}{8}$$

which corresponds to the value of the greatest moment for a simple, supported, beam loaded with a uniformly distributed load with an intensity of  $q = P/l_{\text{span}}$ . Then

$$M_{\text{max}} = - \frac{q l_{\text{span}}^2}{8} .$$

Substituting the value  $l_{\text{span}}$ , we obtain

$$M_{\text{max}} = - q^2 \sqrt{\frac{2t}{l}} \quad (23.2)$$

Thus, the following strength condition must be met at the center of the span of a bearer stringer

$$\sigma = \frac{M_{\text{max}}}{W} = - \frac{q^2}{W} \sqrt{\frac{2t}{l}} \gamma_1 \leq \sigma . \quad (23.3)$$

In addition, the strength of a bearer stringer in the section by transverse bulkheads should be checked according to the diagram given in Figure 89. We assume the stringer to be rigidly constrained to the bulkhead. For ease of calculation, we shall consider the stringer as a semi-infinite beam loaded with uniform load  $q$ . It is possible to permit an increase in the yield stress for the normal bending stresses in the stringer abutment section. Only a transfer of shearing force to the transverse bulkhead should be provided, not permitting an increase in ultimate shearing stress of the stringer wall material.

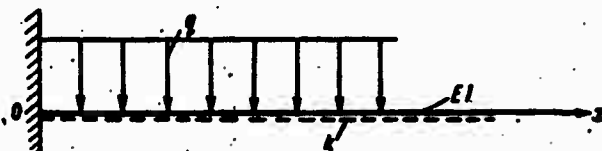


Figure 89. Design drawing for checking the strength of a bearer stringer in the cross section at the transverse bulkhead.

Deflection of a beam, depicted in Figure 89,

$$v = \frac{q}{k} [1 - e^{-\alpha x} (\cos \alpha x + \sin \alpha x)] ,$$

where  $\alpha = \sqrt{\frac{k}{4EI_{st}}}$ ;

the maximum bending moment occurring in the constraint,

$$M_{\text{max}} = 2\alpha^2 \frac{q}{k} EI_{st} = q \sqrt{\frac{EI_{st}}{k}} \quad (23.4)$$

shearing force in the abutment section

$$N_{\text{shear}} \frac{q}{\sigma} = q \sqrt{\frac{4EI_{\text{st}}}{h}} \quad (23.5)$$

The shearing strength condition of a stringer in an abutment section can be written in the form

$$\frac{N_{\text{shear}}}{F} \tau_y = 0.6\sigma_y \quad (23.6)$$

where  $\sigma_y$  is the yield stress of the stringer material;

$F$  is the total sectional area of the stringer wall and the knee.

Calculations have shown that the height of the knee cannot exceed the stringer height and its length cannot exceed two heights (Figure 90). Knees are usually made with same thickness as the stringer wall and have a wide flange, equal to ten knee thicknesses but no larger than 100 mm.

When designing the joint between a bearer stringer and a transverse bulkhead, it should be stipulated that the stringer be fastened to a horizontal rib installed on the bulkhead. Other construction of this joint is possible. However, the strength condition (23.6) must be observed in all cases.

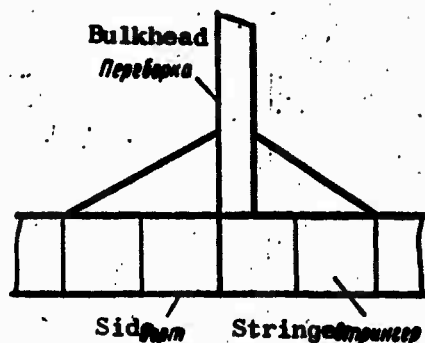


Figure 90. Strengthening of a bearer stringer with knees at a transverse bulkhead.

Mathematical calculations have shown that the influence coefficient can be calculated from the diagram given in Figure 91,

$$\gamma_1 = \frac{1}{48} - \frac{1}{16} \left( \frac{1}{24} + \frac{1}{6} \right) = \frac{1}{128}$$



Figure 91. Design diagram for determining influence coefficient.

Assuming the moments of inertia of the bearer stringer and the frame to be equal in the first approximation, taking (23.3) into consideration, we obtain for the stringer

$$W_{st} = 0,045 \frac{q^p}{\gamma} \sqrt{\frac{s}{l}}$$

We calculate the section modulus of the frame (Figure 91), by formula (20.10)

$$W = 0,140 \frac{q^p}{\gamma} = 0,140 \frac{q^p}{\gamma} \frac{s}{l}$$

Assuming section moduli of the bearer stringer and frame to be equal and equating the right member of the above-cited expression, we obtain  $l/s \approx 8$ . When  $l/s < 8$ , the section modulus of the bearer stringer is smaller than the section modulus of the frame. In this situation, it is not expedient to install bearer stringers.

As an example, we present a calculation of the strength of a lower stringer (Figure 92). The main and intermediate frames have identical profiles but different methods of end constraint (see the first example, presented in 20). When calculating the moment of inertia and section modulus of a bearer stringer, the width of the attached flange is taken as equal to the distance between stringers, i.e., equal to one meter. The profile of a bearer stringer  $\perp \frac{12 \times 300}{12 \times 150}$ ,  $I = 24,120 \text{ cm}^4$  and  $W = 886 \text{ cm}^3$ .

We shall calculate influence coefficients for the main and intermediate frames using the design diagram shown in Figure 93. We assume the following data for calculating: distance of stringer from the deck  $c = 2.0 \text{ m}$ , span of the frame  $l = 7.0 \text{ m}$ , frame spacing  $s = 0.4 \text{ m}$ , moment of inertia of the frame,  $i = 17,000 \text{ cm}^4$ .

The influence coefficient of unit force applied to the joint where the bearer stringer intersects the frame on deflection in the joint

$$\gamma_{11} = \frac{c^2(l-c)^2}{3i^2} = \frac{4 \cdot 25}{3 \cdot 7^2} = 0,0139.$$

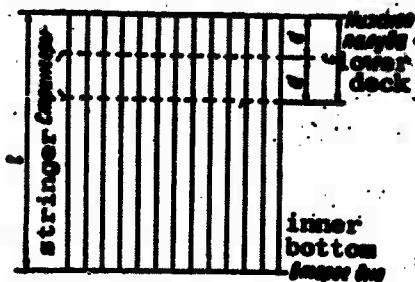


Figure 92. Diagram for calculating bearer stringer strength.

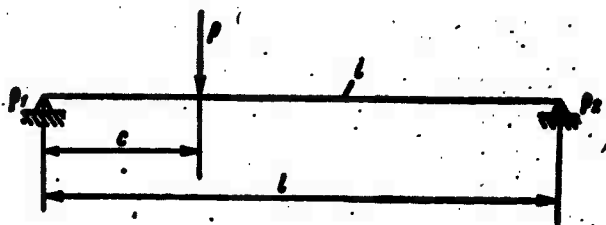


Figure 93. For calculating influence coefficients for main and intermediate frames.

We shall determine support moments for the intermediate frame, assuming the dimensionless reference couple coefficients to equal  $\rho_1 = 1,143$  and  $\rho_2 = 0$  (simple support). We shall designate  $\eta = c/l = 2/7 = 0,286$  and  $1 - \eta = l - c/l = 0,714$ .

Support moments are, respectively

$$M_{int} = \frac{\eta(1-\eta)(2-\eta)}{2+\rho_1} Pl = \frac{0,286 \cdot 0,714 \cdot 1,714}{3,143} Pl = 0,1115Pl$$

$$M_{sint} = 0$$

The influence coefficient from moment  $M_{int}$  (when  $P = 1$ ) on deflection of the intermediate frame at the joint with bearer stringer 2

$$\gamma_{M_{int}} = \frac{M_{int}}{6l} \eta(1-\eta)(1+\eta) = \frac{0,1115}{6} \cdot 0,286 \cdot 0,714 \cdot 1,286 = 0,0049$$

Thus, the influence coefficient for the intermediate frame

$$\gamma_{int} \gamma_{11} = \gamma_{M_{int}} = 0,0139 - 0,0049 = 0,0090$$

Support moments for the main frame are computed by formula (20.7) when  $\rho_1 = 0,72$ ,  $\rho_2 = 0$ :

$$R_1 = \frac{0,286 \cdot 0,714 \cdot (1,714 \cdot 2 - 1,286)}{2,72 \cdot 2 - 1} P_l = 0,0986 P_l,$$

$$R_2 = \frac{0,286 \cdot 0,714 \cdot (1,286 \cdot 2,72 - 1,714)}{2,72 \cdot 2 - 1} P_l = 0,0789 P_l,$$

$$\gamma_{\text{str}} = \frac{1}{6} \nu (1 - \nu) [R_1 (2 - \nu) + R_2 (1 + \nu)] =$$

$$= \frac{0,286 \cdot 0,714}{6} (0,0986 \cdot 1,714 + 0,0789 \cdot 1,286) = 0,0089.$$

The influence coefficient on deflection in the joint for the main frame  $\gamma_0 = 0.0139$  to  $0.0089 = 0.0050$ . The coefficient of rigidity of the elastic foundation for the stringer is calculated by formula (21.22):

$$k = \frac{1 + \frac{0,0050}{0,0089}}{2} \frac{2,1 \cdot 10^6 \cdot 17\,000}{0,0050 \cdot 40 \cdot 700^3} = 405.$$

Then, the reduced length

$$l_{\text{red}} = 2 \sqrt[4]{\frac{4 \cdot 2,1 \cdot 10^6 \cdot 24\,120}{405}} = 3,0 \text{ m.}$$

Width of the attached flange in the second approximation

$$b = \frac{l_{\text{red}}}{4} = 750 \text{ mm.}$$

Distance of the neutral axis of the stringer profile from the neutral axis of the attached flange

$$e = \frac{1139}{189} = 6,0 \text{ cm;}$$

$$I = 29\,660 - 1139 \cdot 6,0 = 22\,800 \text{ cm}^4;$$

$$W = \frac{22\,800}{26,2} = 878 \text{ cm}^3.$$

Reduced length in second approximation

$$l_{\text{red}} = 3,0 \sqrt[4]{\frac{22\,800}{24\,120}} = 2,96 \text{ m.}$$

We shall calculate maximum stresses in the stringer for external load  $q = 30 \text{ t/m}$ :

$$\sigma = \frac{q l_{\text{red}}^2}{8W} = \frac{30 \cdot 2,96^2 \cdot 10^3}{8 \cdot 878} = 3750 \text{ kg/cm}^2 < \sigma_y = 4000 \text{ kg/cm}^2.$$

The stringer is made of steel with yield stress  $\sigma_y = 4000 \text{ kg/cm}^2$ .

We shall determine stresses in the stringer by the transverse

bulkhead, allowing for the knee. Shearing force in the abutment section of the stringer (formula 23.5) is

$$N_{\text{shear}} = 30 \sqrt{\frac{4 \cdot 2,1 \cdot 10^6 \cdot 22800}{405} 10^{-9}} = 43,4 \text{ t.}$$

Maximum shear stress in wall

$$\tau = \frac{N_{\text{shear}}}{0,85 \cdot 72} = \frac{43,4 \cdot 10^3}{0,85 \cdot 72} = 710 \text{ kg/cm}^2 < \tau_y = 0,8 \tau_y = 2400 \text{ kg/cm}^2.$$

Moment of inertia of the abutment section of the bearer stringer together with the knee

$$I_K = 60800 \text{ cm}^4;$$

Section modulus

$$W_K = 1448 \text{ cm}^3;$$

Maximum bending moment in the constraint (formula 23.4)

$$M_{\text{max}} = 30 \sqrt{\frac{2,1 \cdot 10^6 \cdot 22800}{405} 10^{-9}} = 32,0 \text{ t m.}$$

Bending stress

$$\sigma = \frac{M_{\text{max}}}{W_K} = \frac{32,0 \cdot 10^6}{1448} = 2200 \text{ kg/cm}^2.$$

Normal bending stresses in the abutment section of a bearer stringer do not exceed the yield stress of the material.

#### 24. Side Framing with a Longitudinal System.

We shall consider the working plan of individual, side grillage braces arranged in a longitudinal system when there is ice load action.

Longitudinally disposed beams. Longitudinal strengthening ribs are multi-spanned, continuous beams supported on intermediate elastic supports, the web frames. However, in practice, the relationship between rigidity of longitudinal ribs and web frames is such that the latter can be considered as rigid supports.

We shall assume that ice load  $q$  is applied simultaneously to two adjacent beams (main and supplementary) and consequently, load  $q/2$  acts on one beam running in the main direction. Distance between frames is usually  $l = 2$  to  $3$  m; at the same time, the area of impact stress application in the fore part does not, as a rule, exceed  $3$  to  $4$  m. Therefore, to calculate longitudinal, strengthening ribs in the fore part, load  $q/2$  should be considered as uniformly distributed on one span of the beam

between frames (Figure 94). In this case, the loaded span can be considered as an isolated beam, elastically constrained on supports, with a reference couple coefficient  $\alpha = 0.63$  [24].

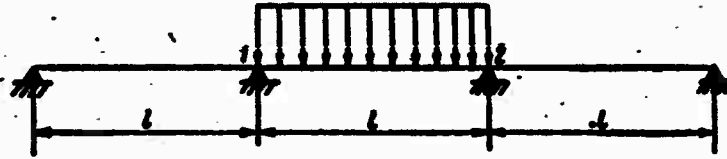


Figure 94. Schematic diagram for the application designed ice load for a longitudinal stiffener.

Then, bending moment in the center of the beam span will be

$$M_{span} = \frac{q l^2}{2.24} \alpha + \frac{q l^2}{2.8} (1 - \alpha) = 0.036 q l^2. \quad (24.1)$$

bending moment in the abutment section

$$M_{abut} = \frac{q l^2}{2.12} \alpha = 0.026 q l^2. \quad (24.2)$$

shearing force in the abutment section

$$N_{abut} = \frac{q l}{2.2} = \frac{q l}{4}. \quad (24.3)$$

Assuming the occurrence of stresses in the center of the beam span equal to yield stress in the extreme fiber, we find the magnitude of the minimum, necessary section modulus of a longitudinal strengthening rib

$$W = 0.036 \frac{q l^2}{\sigma_y}. \quad (24.4)$$

Assuming that shearing force in the abutment section is experienced by the section wall and tangential stresses are equally distributed along its height, we assume the magnitude of the minimum necessary sectional area of the section wall at the frame

$$F = \frac{q l \sqrt{3}}{2.2 \cdot \sigma_y} = 0.43 \frac{q l}{\sigma_y}. \quad (24.5)$$

Longitudinal strengthening ribs are usually relatively low beams. Therefore, when satisfying ultimate bending strength conditions of the beam, shearing strength conditions are also met as a rule. When there are relatively short, longitudinal, disposed beams, their strength should be calculated, taking shearing strain into consideration.

During compression, the midsection of a ship's side is usually subjected to ice pressure for a substantial length. In this case, a longitudinal strengthening rib can be calculated by assuming it to be rigidly constrained on the frames. Then, bending moment in the span will be

$$M_{\text{span}} = \frac{q^2 l^2}{2.94} = 0.021 q^2 l^2, \quad (24.6)$$

bending moment in the abutment section

$$M_{\text{abut}} = \frac{q^2 l^2}{2.12} = 0.041 q^2 l^2, \quad (24.7)$$

shearing force in the abutment section

$$N_{\text{abut}} = \frac{q l}{2.2} = \frac{q l}{4}. \quad (24.8)$$

It is obvious from the above-cited formulas, that design bending moments and shearing forces are close in magnitude for longitudinally disposed beams in the extremities and amidships. Therefore, for longitudinally disposed beams in the ice belt area, for the entire length of the ship, we can finally assume

$$W_{\text{min}} = 0.041 \frac{q l^2}{\sigma_y}, \quad (24.9)$$

$$F_{\text{min}} = 0.43 \frac{q l}{\sigma_y}. \quad (24.10)$$

Loads  $q$  in expressions (24.9) and (24.10) are taken for the fore part and midsection respectively.

Rib frames. Rib frames on ships having a longitudinal system, assembled according to regulations of shipping registries, usually have great strength and rigidity. However, on small ships of the highest ice classes, the strength of web frames calculated for the hydrostatic pressure of water can sometimes be inadequate to stand up under an ice load. It is evident that maximum stress acts on a web frame when an ice load is applied along the side of a ship over a distance of several adjacent spans of a longitudinally disposed beam. Inasmuch as all frames between transverse bulkheads have the same profile, as a rule, their yielding will also be equal. The greatest load on a web frame

$$Q = q l.$$

The maximum bending moment acting on a frame cross section under load is,

$$M_{\text{max}} = k q l l_1, \quad (24.11)$$

where  $q$  is the intensity of the ice load;

$l$  is the span of a beam running in the main direction between web frames;

$l_1$  is the design span of the web frame in which the ice load is applied;

$k$  is a numeral coefficient, the magnitude of which depends on the arrangement of the decks and platforms, as well as on coordinates of the load application and rigidity relationship of individual web frame sectors.

Values of coefficient  $k$  are calculated for various arrangements of web frame loading (Figure 95 and Table 22).

Table 22

Values of coefficient  $k$ .

a № расчет- ной схемы (рис. 95)	1	2	3	4	5	6	7	8	9	10
$k$	0,146	0,124	0,138	0,128	0,192	0,165	0,188	0,163	0,161	0,165

$a$ -number of design diagram (Figure 95).

Design bending moment in a web frame section must not exceed

$$M = W_{wf} \sigma_y,$$

where  $W_{wf}$  is the section modulus of a web frame cross section;

$\sigma_y$  is the yielding stress of the web frame material.

Then, considering (24.11), we obtain an expression for the section modulus of the web frame profile

$$W_{wf} = k \frac{ql_1}{\sigma_y}. \quad (24.12)$$

Keeping in mind that tankers which have one deck, are assembled in a longitudinal system, we can assume coefficient  $k = 0.135$ .

**Example.** Determine the ice belt, shell plating thickness and scantlings of midship side bracings of a tanker assembled in a longitudinal system with the following initial data: load on the plating  $p = 0.05 \text{ t/m}^2$ , load on framing  $q = 70 \text{ t/m}$ ; longitudinal

strengthening rib span  $l = 3.6$  m; distance between longitudinally disposed beams  $a = 0.45$  m; span of web frames  $l_1 = 11.0$  m; hull material - steel with yield stress  $\sigma_y = 3,000$  kg/cm<sup>2</sup>.

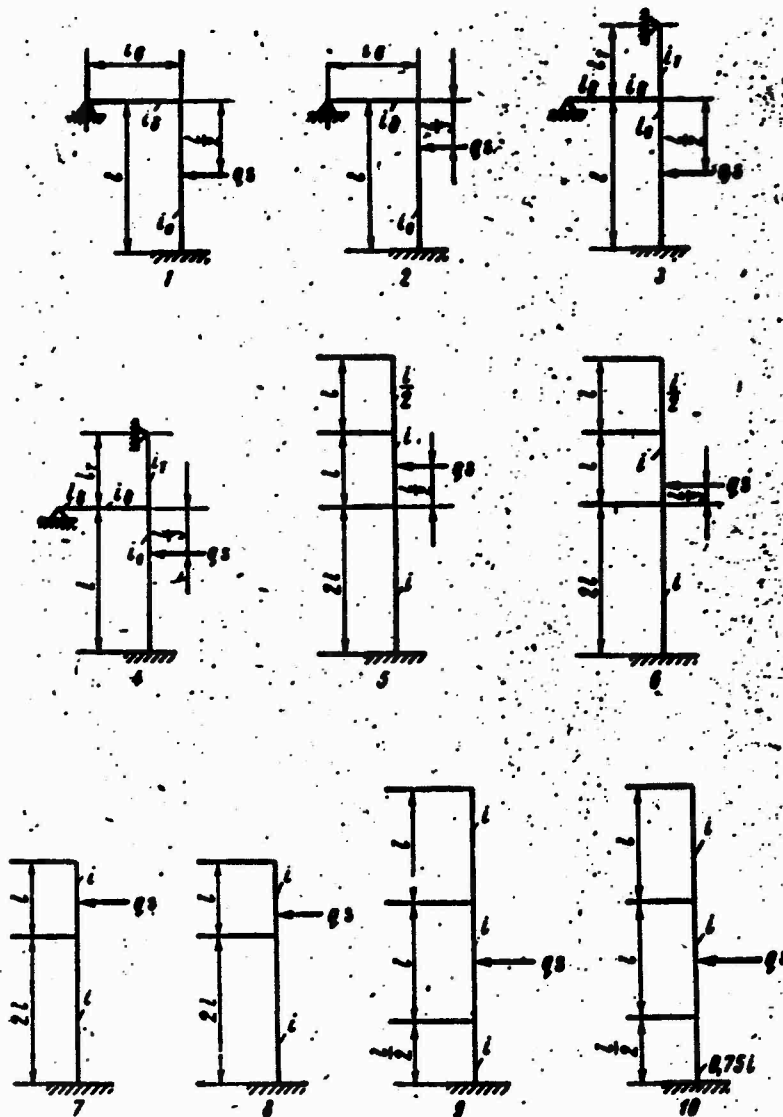


Figure 95. Diagram of loading of web frame.

We determine plating thickness of the ice belt by formula (18.5)

$$\delta = 184 \cdot 0.45 \sqrt{\frac{105}{3000} + 4} = 19.5 \text{ mm.}$$

Based on the existing assortment of rolled plate, we should assume  $\delta = 20$  mm.

The minimum necessary section modulus and sectional area of longitudinal strengthening ribs, according to formulas (24.9) and (24.10) will be, respectively,

$$W_{\min} = 0,041 \frac{70 \cdot 3,6 \cdot 10^6}{3000} = 1240 \text{ cm}^3,$$

$$F_{\min} = 0,43 \frac{70 \cdot 3,6 \cdot 10^6}{3000} = 36,1 \text{ cm}^2.$$

In the case under consideration, we assume a T-section profile  $\frac{12 \times 400}{18 \times 100}$  with cross-sectional area  $F = 66 \text{ cm}^2$ ,  $W = 1,260 \text{ cm}^3$ .

The necessary section modulus of the web frame, calculated by formula (24.12) with coefficient  $k$  assumed according to diagram 1 (Figure 95):

$$W_{\text{wf}} = 0,146 \frac{70 \cdot 3,6 \cdot 11,0 \cdot 10^6}{3000} = 13480 \text{ cm}^3,$$

is too large. Therefore, to reduce the profile, crossbars, joining web frames with frames of the longitudinal bulkheads should be installed and the former should be calculated as continuous beams on elastic, intermediate supports.

## CHAPTER VI

### STRENGTH OF DECKS AND PLATFORMS

#### 25. General Requirements for the Design of Decks and Platforms Located in the Area of Ice Load Action.

Decks and platforms of ships which sail in ice are subjected to action of substantial ice loads. In some cases, these stresses cause warping and breaking of the deck covering, loss of stability and failure of beams and beam brackets, etc. When designating scantlings of these structures, it is necessary to take ice loads into consideration, besides the usual design loads (overall bending, deck cargo, hydrostatic head). In doing this, the heaviest combination of external loads should be assumed. Simultaneous action of loads in the plane of the grillage and lateral loads cause unsymmetric bending of the deck grillage which should be allowed for in calculations. Stresses from overall bending in ice decks are relatively small inasmuch as they are near to the neutral axis, as a rule.

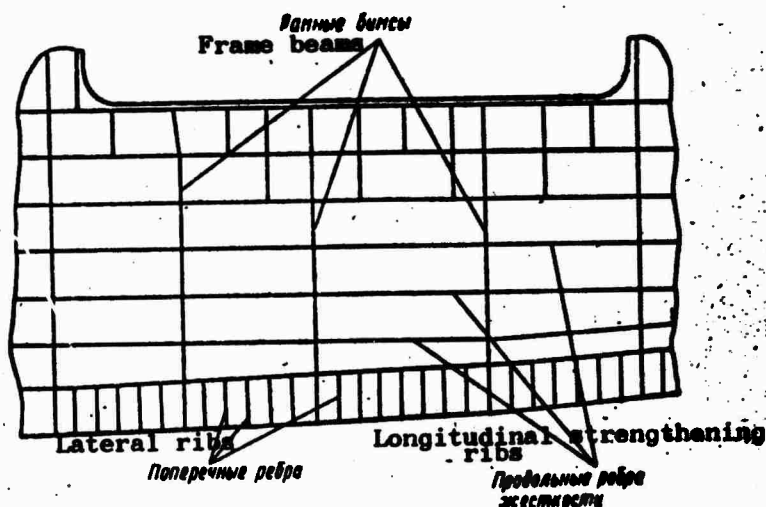


Figure 96. Diagram of deck framing of diesel-electric ship, Lena.

Ice loads can act directly on deck and platform planes or can be transmitted to them in the form of reactions from frames. In the latter case, the decks and platforms play the role of a rigid contour to which the frames transmit pressure from the ice. Ice loads applied directly to a deck are the greatest and should be considered as design loads. Decks and platforms, on the planes of which an ice load can directly act, shall arbitrarily be called ice decks and platforms, in the future. On all

classes of icebreakers and UL (Arkt.) and UL-class cargo ships having two or more decks, one of the decks must be located in the area of the load waterline, as a rule, i.e., in the area which most often comes into contact with the ice. Installation of a platform in this area is also not excluded. In any case, continuity of longitudinal bracings adjacent to the side should be provided over the entire length of the ship in this area. The placement of a deck on the load waterline level is explained as an attempt to transmit the greatest part of the ice load directly to a very strong structure to which it is relatively easy to provide rigidity.

Ice decks are usually made without bends and saddle backing. A transverse framing system is the most expedient for them. If a longitudinal framing system is used, the section of the deck adjacent to the side must be strengthened by installing lateral, strengthening, ribs at least two or three frame spacings long, on each frame (Figure 96).

Particular attention should be given to the proper structural design of the joint between the intermediate frames and the ice deck. Inasmuch as beams are not usually installed on intermediate frames, reactive stresses can be reliably transmitted to the deck by knees (Figure 97a) or supplementary half-beams (Figure 97b), running to the nearest deck girder.

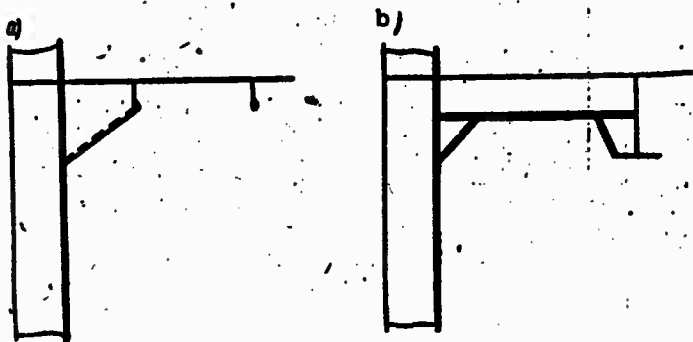


Figure 97. End constraint of intermediate frames: a-by means of knees; b-by means of supplementary half-beams.

As a rule, ice damage to decks and platforms is of a local nature and is usually a consequence of loss of stability of individual elements of the deck structure. Cases of warping of the entire deck grillage are observed less often. Therefore, when calculating decks and platforms for ice load action, stability of the deck covering between beams and stability of beams and the entire deck grillage between transverse bulkheads or its individual sectors (for example, between frames), must be checked. In addition, the resistance of the deck to action of compressive and shearing stresses must be checked. Besides that, the resistance of decks adjacent to the ice decks, to action of reactive stresses from the frames should be checked. These reactions are calculated when calculating side framing for the most adverse case of ice load application.

The magnitude of an ice load on ice decks is assumed to be no less than the design load for side framing in the corresponding hull section. The ice load amidships, caused by compression of the ship, can be distributed for a considerable length. Therefore, the design load should be assumed as being applied to the plane of the deck for the length from bulkhead to bulkhead. The zone of ice load application in the extremities does not usually exceed 2.5 to 3.0 m in length and the design load here should be considered as being applied to a sector of no more than three or four frame spacings along the side. Since the period of impact ice load action is 0.2 to 1.0 seconds, the design load on the deck can be considered as being static. The ice load caused by compression of a ship in ice is bilateral and deck grillage experiences pressure on both sides, simultaneously. The load on the extremities is unilateral and is equalized by shearing stresses in the transverse bulkheads.

## 26. Calculating the Strength and Stability of Deck and Platform Coverings.

The purpose of calculating the strength of ice decks and platforms is to determine the thickness of deck-covering plates, distribute material rationally and check the strength and stability of deck bracings. When checking the strength of ice decks and platforms, the deck sector between bulkheads which is under consideration, should be considered as a deep, short beam with a length-height relationship on the order of one (Figure 98). Along with this, the side grillages play the role of flanges of this beam. An ice load acting in the plane of the beam wall, causes it to bend and causes shearing strain in its plane. As Yu. N. Raskin [39] indicates, longitudinal stresses  $\sigma_x$  and strains  $\epsilon_x$  caused by the bending are relatively small and only lateral, normal and shear stresses  $\sigma_y$  and  $\tau_{xy}$ , are of interest when evaluating deck strength.

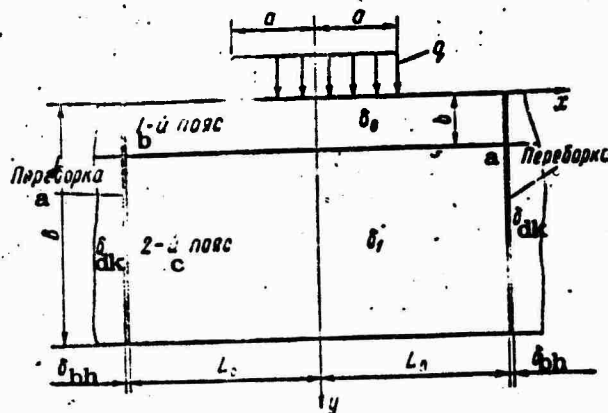


Figure 98. Diagram of local compression of a deck located in the ice belt area. a-bulkhead; b-first strake; c-second strake.

Following the previously-assumed design diagram, we shall consider the work of deck structures in the elastic range, limiting allowed stresses to the yield stress. Then, all design dependencies for checking the strength of ice decks can be obtained on the basis of solutions of linear problems of the theory of elasticity. Absolute solutions evidently cannot be used in actual calculations because of their unyieldiness. A rough solution to the problem of calculating the strength of ships' ice decks, closely matching the exact solution, was obtained by Yu. N. Raskiny [39]. The results of this solution will be used subsequently.

We shall consider a deck grillage without large openings as being a thin plate of gradually changing thickness loaded with stress  $q$ , equally distributed along its edge (Figure 98). The small magnitude of longitudinal stresses and strains in such a plate, make it possible for their influence on lateral, normal and shear stresses to be disregarded. Thus, individual, longitudinal, deck strakes can be assumed to be functioning only during shearing effect of an ice load.

Strain of a deck, considered as the aggregate of the individual, longitudinal, strakes joined together by elastic seams, is described by a system of  $n$ -second order, linear, differential equations, where  $n$  is the number of strakes. For practical calculations, stresses in a given deck section can be calculated if the grillage is considered to consist of two strakes when there is a uniaxial load or of three symmetrically arranged strakes, when there is a biaxial load. The conditional junction line of these strakes coincides with a design section of the deck.

The greatest normal and shear stresses acting in section  $y = b$  when there is a uniaxial load, are calculated by formulas

$$\sigma_y(0, b) = \sigma_0 \frac{\omega_2 \omega_1}{\omega_1 \omega_2} \left[ 1 - \frac{\text{ch } r_1(L_0 - b)}{\text{ch } r_1 L_0} \right], \quad (26.1)$$

$$\tau_{xy}(a, b) = \frac{b_0}{b_1} \tau_0 \left\{ 1 + \frac{1}{2} \left[ \frac{1 - e^{-2r_1 a}}{2r_1 a} \times \right. \right. \\ \left. \left. \times \left( \frac{a}{a_1} - 4 \right) - e^{-2r_1 a} \left( \frac{a}{a_1} - 2 \right) \right] \right\}, \quad (26.2)$$

where  $\sigma_0 = -q/\delta_0$  is the compressive stress in the deck stringer;

$\tau_0 = qa/\omega$  are the mean shear stresses along the width of the deck;

$\omega = \omega_1 + \omega_2$  is the cross section plane of the deck;

$\omega_1 = b\delta_0$  is the sectional area of the first strake;

$\omega_2 = (B - b)\delta_1$  is the sectional area of the second strake;

$\delta_0$  and  $\delta_1$  are the reduced thicknesses of the first and second

deck strakes, computed allowing for the cross section plane of the deck framing.

An ice load, equally distributed for length  $2a$  along the side, is considered to be applied to the center of the length of the deck grillage between bulkheads. In this case, normal stresses in the strakes are small.

Magnitude  $r_1$ , depending on the rigidity of the deck strakes under compression, is entered in formulas (26.1) and (26.2),

$$r_1 = \left[ \frac{k_1}{G\omega_1} \left( 1 + \frac{\omega_1}{\omega_2} \right) \right]^{1/2},$$

where  $G$  is the module of rigidity;

$k_1$  is the coefficient of rigidity of the elastic bracing between the first and second deck strakes under uniaxial compression.

Mean, shear, stresses along the width of the first strake (deck stringer) are determined by the formula

$$\tau_{xy}^{\text{mean}}(a, b) = \tau_0 \left[ 1 + \frac{1}{r_1^2} \cdot \frac{\omega_2}{\omega_1} \cdot \frac{\text{sh } r_1 a \text{ ch } r_1 (L_0 - a)}{\text{ch } r_1 L_0} \right]; \quad (26.3)$$

When there is a biaxial load, stresses are calculated by formulas

$$\sigma_y(0, b) = \sigma_0 \frac{\delta_0}{b} \left[ 1 - \frac{\text{ch } r_2 (L_0 - a)}{\text{ch } r_2 L_0} \right]; \quad (26.4)$$

$$\tau_{xy}^{\text{mean}}(a, b) = \tau_0 \frac{\omega_2}{\omega_1} \frac{\text{sh } r_2 a \text{ ch } r_2 (L_0 - a)}{r_2 a \text{ ch } r_2 L_0}; \quad (26.5)$$

where  $r_2 = \sqrt{\frac{k_2}{G\omega_1}}$ ,

$k_2$  is a coefficient of rigidity of the elastic bracing between the first and second strakes, under biaxial compression.

When making actual calculations in the case of uniaxial compression, it should be assumed that

$$\left. \begin{aligned} r_1 &= \frac{1,61}{B} \sqrt{\frac{B}{b} \left( 1 + \frac{\omega_1}{\omega_2} \right) k_1}, \\ k_1 &= \frac{2,937 \frac{\delta_0}{b_0}}{\frac{b}{B} + \frac{\delta_0}{b_1} \left( 1 - \frac{b}{B} \right)}, \end{aligned} \right\} \quad (26.6)$$

where B is the breadth of the ship;

$\varphi$  is a coefficient determined from the graph in Figure 99, depending on the ratio B/a.

When there is biaxial compression

$$r_2 = \frac{1.61}{B} \sqrt{\frac{B}{b} k_2},$$

$$k_2 = \frac{2.27 \frac{\delta_0}{b_0}}{\frac{b}{B} + \frac{\delta_0}{\delta_1} \left(1 - \frac{2b}{B}\right)}.$$

If a deck consists of several strakes of various thicknesses, the strakes between the side and section under consideration are considered as one strake, equal to the strakes in area.

All these formulas [39] do not allow for the effect of yielding of the lateral edge of the grillage, i.e., the bulkheads. If the distance between bulkheads is great and the condition  $L_0 - a/B \geq 1/2$  is observed, yielding of bulkheads and adjoining segments of the deck does not exert a noticeable influence on the magnitude and nature of stress distribution in the deck. If the load is distributed for a substantial length and  $L_0 - a/B < 1/2$ , the coefficient  $m$ , allowing for the influence of the ultimate rigidity of the index contour, should be introduced:

$$t = 1 + \frac{\delta_1}{\delta^*} \left(1 - 2 \frac{L_0 - a}{B}\right), \quad (26.7)$$

where

$$\delta^* = 2\delta_{bh} + \delta_{dk},$$

$\delta_{bh}$  - being the thickness of bulkhead plates;

$\delta_{dk}$  - being the thickness of the deck beyond the bulkhead.

Allowing for correction, design values of normal and shear stresses when there is uniaxial load action are calculated by formulas

$$\bar{\sigma}_y(0, b) = \frac{\delta_0}{\delta_1} \left\{ \sigma_0 \left(1 - \frac{b}{B}\right) + \left[ \frac{\delta_1}{\delta_0} \sigma_y(0, b) - \sigma_0 \left(1 - \frac{b}{B}\right) \right] \frac{1}{t} \right\}, \quad (26.8)$$

$$\bar{\tau}_{xy}(a, b) = \frac{\delta_0}{\delta_1} \left\{ \tau_0 + \left[ \frac{\delta_1}{\delta_0} \tau_{xy}(a, b) - \tau_0 \right] \frac{1}{t} \right\}, \quad (26.9)$$

where  $\delta_y(0, b)$  and  $\tau_{xy}(a, b)$  are stresses computed by formulas (26.1) and (26.2), without allowing for yielding of grillage edges.

In case of biaxial compression, even if the load is equally distributed over the entire length between bulkheads, the influence of yielding

of the lateral edges is very small. This provides basis for using formulas (26.4) and (26.5) which, when  $a = L_0$ , take the form

$$\sigma = \sigma_0 \frac{E_0}{E} \left( 1 - \frac{1}{\operatorname{ch} r_0 L_0} \right),$$

$$\tau_{\text{mean}} = \tau_0 \frac{\sigma}{\sigma_1} \cdot \frac{\operatorname{th} r_0 L_0}{r_0 L_0}.$$

Design normal stresses in deck strakes must not exceed the yield stress of the material  $\sigma_y$ , and shear stresses, the magnitude  $\tau = 0.57 \sigma_y$ . At the same time, design shear stresses at the boundary of application of a uniformly distributed load become infinitely large. Thus, the sector of the deck located near the side passes into a yield state and stresses in it maintain a constant magnitude.

We note that shear stresses exceeding  $\tau_y$  can be permitted in these sections. In this situation, the presence of yielding should be roughly allowed for by introducing a reduced sectional area of the extreme deck strake

$$\sigma_1^{\text{red}} = \sigma_1 - \mu_y \delta_0 \left[ 1 - \frac{\tau_T}{\tau_{\text{mean}}(a, y_T)} \right], \quad (26.10)$$

where  $y_T$  is the width of the reduced strake;

$\tau_{\text{mean}}$  is the mean magnitude of shear stresses occurring at that strake.

The reduced area, according to formula (26.10), should be calculated by a method of successive approximations using expression (26.3) or (26.5). In this case, it is usually adequate to make one approximation. The remaining deck strakes are calculated as shown above (without allowing for reduction).

When designing, it is advisable to distribute material throughout the breadth of the deck so that compressive stresses under ice load action will be uniformly distributed in the entire section. For this purpose, it is proposed in work [39] that the following approximate dependence be used when assigning thickness of deck covering strakes

$$\delta_n = \delta_0 e^{-\frac{y}{b}}, \quad (26.11)$$

where  $\delta_n$  is the thickness of the  $n$ -th covering strake.

It is necessary to check the stability of the deck covering as well as its strength. When there is a lateral system, Euler stresses in plates of the covering are calculated by the formula

$$\sigma_E = 800 \left( \frac{1000}{s} \right)^2,$$

where  $\delta$  is the thickness of the deck covering;

$s$  is the distance between beams.

Normal stresses in the deck covering strakes, calculated by above-cited formulas, must not exceed corresponding Euler stresses, i.e., they must fulfill the condition

$$\sigma < 800 \left( \frac{1000}{s} \right)^2. \quad (26.12)$$

Moving from stresses to loads, we write the condition of deck stability in the form

$$q < q_E + q_{fmg}. \quad (26.13)$$

where  $q$  is a load on the deck equal to the load on the side framing;

$q_E$  is the Euler load for the deck covering;

$q_{fmg}$  is the load absorbed by the framing:

$$q_{fmg} = \frac{f}{s} 800 \left( \frac{1000}{s} \right)^2.$$

$f$  is the beam, cross-sectional area.

If the thickness of the covering is designated from the above-cited condition, the structure will practically have no margin of stability. To provide one, it would be necessary to assume a higher Euler load. However, it is impossible to select an increased Euler load so that a thickness of deck and platform coverings simultaneously acceptable for ships of various types and ice classes is obtained. Therefore, instead of increasing the Euler load, the design load should be increased. Taking designing and operating experience into consideration, the design load on the deck is increased by 50 t/m and amounts to  $q_{des} = q + 50$ . In this situation, the minimum necessary thickness of the deck stringer, in millimeters, is calculated by the formula

$$\delta = 10 \sqrt[3]{\frac{q+50}{80} s^3}. \quad (26.14)$$

where  $s$  is the distance between beams m;

$q$  is the intensity of the ice load, t/m.

The thickness of a deck stringer should be determined by this formula for cargo ships only. On icebreakers, ice decks are strengthened by supplementary beams and there is no point in checking the stability of the deck stringer. Its thickness should be determined from a condition of strength

$$\frac{q}{\delta} < q_0.$$

The transition from deck stringer thickness to thicknesses of other strakes must be gradual in all cases and the selected value of the thickness must be no less than that indicated in Table 23. The width of the deck stringer must be at least three frame spacings.

Table 23

Minimum thicknesses of deck covering.

Тип судна а	Класс б	Толщина налубного стрингера, с мм	Толщина настила налубы, д мм
е Ледокол	I	14	10
»	II	12	8
г »	III	8	8
Буксир	УЛ UL	8	6

a-ship type; b- class; c-deck stringer thickness, mm; d-deck covering thickness, mm; e-icebreaker; f-tugboat.

Additional requirements are imposed on the upper deck and fore-castle deck covering of icebreakers and ice-strengthened classes of ships. For a length of  $0.05L$  from the stem in the bow and in the area of the sternpost in the stern, the thickness of the main deck covering over its entire width must be at least the thickness of the deck stringer. When there is a forecastle, the thickness of the upper deck stringer, in this area can be decreased by 2 mm and the thickness of the remaining deck covering strakes by 1 mm in comparison with the corresponding magnitudes. for an ice deck (Table 23). The thickness of the forecastle stringer and deck flooring is assumed the same as for the upper deck situated below the forecastle.

Example. Make a check calculation of a sector of the lower deck of an icebreaker bow. Breadth of deck  $B = 19.4$  m, length of grillage  $2L_0 = 10.4$  m, frame spacing  $s = 0.4$  m; width of deck stringer  $b = 3.5$  m, thickness  $\delta_0 = 14$  mm; all other plates have a thickness of  $\delta_1 = 12$  mm. Cross-sectional area of the beam  $f = 40$  cm<sup>2</sup>; yield stress<sub>2</sub> of the framing material and covering plates  $\sigma = 2,600$  kg/cm<sup>2</sup>; intensity of the design ice load  $q = 450$  t/m. Load is unilateral, applied for a length of  $2a = 3.2$  m in the center of the grillage span.

Cross-sectional area of deck

$$w = 2 \cdot 350 \cdot 1,4 + 1240 \cdot 1,2 = 2470 \text{ cm}^2;$$

sectional area of first and second design strakes

$$w_1 = 350 \cdot 1,4 = 490 \text{ cm}^2; \quad w_2 = w - w_1 = 1980 \text{ cm}^2.$$

Reduced thickness

$$\xi_1 = t_0 + \frac{2f}{2s} = 1,4 + \frac{80}{80} = 2,4 \text{ cm};$$

$$\xi_2 = \frac{a_2}{B-b} + \frac{f}{2s} = \frac{1900}{1940-250} + \frac{40}{80} = 1,74 \text{ cm}.$$

Compressive stresses in the deck stringer

$$\sigma_1 = \frac{450 \cdot 10}{2,4} = 1875 \text{ kg/cm}^2 < \sigma_2 = 800 \left( \frac{100 \cdot 1,4}{80} \right)^2 = 3400 \text{ kg/cm}^2;$$

shear stresses

$$\tau_1 = \frac{q_2}{s} = \frac{4500 \cdot 160}{2470} = 290 \text{ kg/cm}^2.$$

Coefficient of rigidity (26.6)

$$k_1 = \frac{2,93 \cdot 2,23 \cdot \frac{2,4}{1,4}}{\frac{3,5}{19,4} + \frac{2,4}{1,74} \left( 1 - \frac{3,5}{19,4} \right)} = 8,53.$$

where coefficient  $\varphi$  is taken by means of extrapolation from the graph in Figure 99 for the relationship

$$\frac{B}{a} = \frac{19,4}{1,6} = 12,1; \quad \varphi = 2,23.$$

$$r_1 = \frac{1,61}{19,4} \sqrt{\frac{19,4}{3,5} \left( 1 + \frac{490}{1900} \right) 8,53} = 0,637.$$

Compressive stress in the second strake ( $\delta_1 = 12 \text{ mm}$ );

$$\sigma_2 = \sigma_1 \frac{2,4}{1,74} \cdot \frac{1900}{2470} \left( 1 + \frac{\text{ch } 5,60}{\text{ch } 6,63} \right) = 0,71 \sigma_1 = 1330 \text{ kg/cm}^2 < \sigma_2;$$

Euler stresses for the second strake

$$\sigma_E = 800 \left( \frac{100 \cdot 1,2}{80} \right)^2 = 1800 \text{ kg/cm}^2 > \sigma_2;$$

Mean shear stresses along the width of the deck stringer

$$\text{med } \tau_1 = \left( 1 + \frac{1}{1,02} \cdot \frac{1900}{2470} \cdot \frac{\text{sh } 1,02 \text{ ch } 5,6}{\text{ch } 6,63} \right) = 1,34 \tau_1 = 390 \text{ kg/cm}^2.$$

Yielding of bulkheads, in this case, influences the magnitude of stresses in the deck covering, inasmuch as

$$\frac{L_2 - a}{B} = \frac{5,2 - 1,6}{19,4} < \frac{1}{2}$$

We consider the influence of the ultimate rigidity of the index contour using formulas (26.7), (26.8) and (26.9). Then, we obtain for the deck stringer

$$\begin{aligned}
 s^* &= 2 \cdot 1,6 + 1,4 = 4,6 \text{ cm}; \\
 t &= 1 + \frac{1,2}{4,6} \left( 1 - 2 \frac{5,2 - 1,6}{19,4} \right) = 1,164; \\
 \bar{\sigma}_0 &= \frac{1,4}{1,2} \left[ 290 + \left( \frac{1,2}{1,4} 300 - 290 \right) \frac{1}{1,164} \right] = 394 \text{ kg/cm}^2.
 \end{aligned}$$

for the second deck strake

$$\begin{aligned}
 s^* &= 2 \cdot 0,9 + 1,2 = 3,0 \text{ cm}; \\
 m &= 1 + \frac{1,2}{3,0} \left( 1 - 2 \frac{5,2 - 1,6}{19,4} \right) = 1,252; \\
 \bar{\sigma}_0 &= \frac{2,4}{1,74} \left\{ 2450 \left( 1 - \frac{3,5}{19,4} \right) + \left[ \frac{1,74}{2,4} 1330 - 2450 \left( 1 - \frac{3,5}{19,4} \right) \right] \frac{1}{1,252} \right\} = 1638 \text{ kg/cm}^2.
 \end{aligned}$$

## 27. Designing Decks in the Area of Large Openings.

The design dependencies of the preceding paragraph relate to solid decks not having significant openings which is characteristic for ice-breakers. On ice cargo ships, the decks are weakened by large, hatch openings. When calculating ice decks in the area of large openings, the sector of the deck between the side and the opening and the sector between the hatch end coaming and transverse bulkhead, should be considered separately. When calculating the deck between the side and hatch opening, this sector should be considered as a high beam working in bending and shearing strain. The flanges of this beam are the hatch side coaming and the side plating. Therefore, the strength and stability of the side coaming should be checked while it is functioning as the flange of the beam under consideration.

The section coinciding with the hatch end coaming, where largest shear stresses act, is the most dangerous. In section A-A (Figure 100), there is shearing force action

$$Q = \frac{ql}{2},$$

where  $l$  is the length of the hatch opening.

Assuming the acting shear stresses to be equally distributed over the width of deck sector  $c$ , for section A - A, we obtain

$$\tau = \frac{ql}{2 \Sigma c_i \delta_i}, \quad (27.1)$$

where  $\sum c_i \delta_i$  is the total, cross-sectional area of the deck sector under consideration.

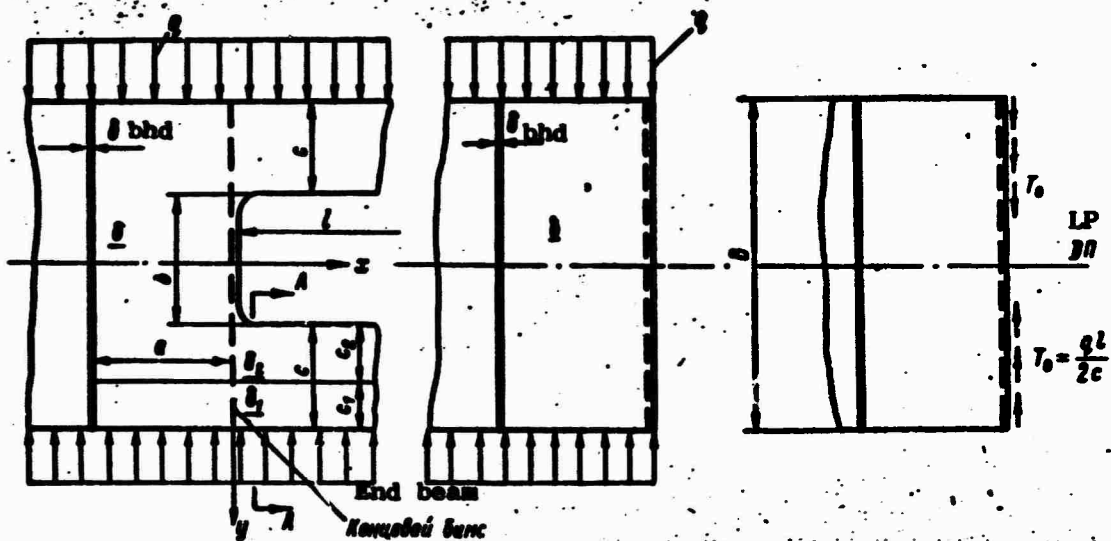


Figure 100. Design diagram for deck in cargo hatch area.

Actually, because of the nonuniform distribution of these stresses over the section, the minimum necessary sectional area of the deck should be calculated by the expression

$$\omega = \frac{ql}{2\tau_{ad}}$$

where  $\tau_{ad} = \frac{\tau_y}{k_3}$  is the admissible stress;

$k_3 = 1.5$  is a safety factor allowing for nonuniform distribution of shear stresses;

$\tau_y$  is shear yield stress.

Considering that  $\omega = \sum c_i \delta_i$ , we obtain the condition which, when satisfied, will assure the strength of the given deck sector

$$\sum c_i \delta_i \geq \frac{k_3 ql}{2\tau_y} \quad (27.2)$$

In addition to shearing strength, it is necessary to check the stability of the deck plates against shear stress action. The ultimate shearing force absorbed by the deck in section A - A and determined from

the condition of stability is

$$Q_s = 1140 \sum c_i \delta_i \left( \frac{100\delta_i}{s} \right)^3 \quad (27.3)$$

where  $s$  is frame spacing.

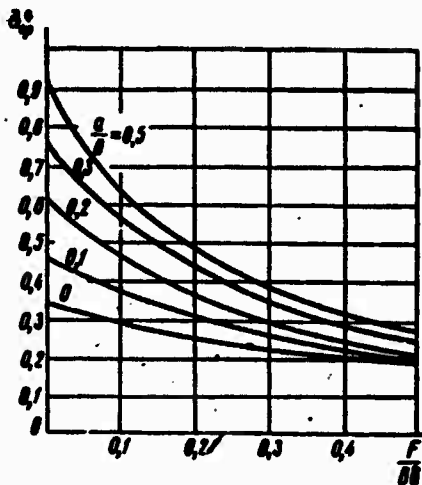


Figure 101. Values of the relative component of normal stress.

This formula was obtained under an assumption of uniformly distributed shear stresses for width  $c$ . Allowing for the actual nonuniformity of stress distribution, safety factor  $k_s = 1.5$  should be introduced. Then, the stability condition of the deck covering in this area is written in the form

$$1140 \sum c_i \delta_i \left( \frac{100\delta_i}{s} \right)^3 > 0.75ql. \quad (27.4)$$

Design diagram (Figure 100), can be used to calculate stresses in the deck covering between the bulkhead and hatch end coaming. Normal stresses in this area of the deck are calculated as a sum of stresses caused by external normal load  $q$  and load  $T_0$  (Figure 100):

$$\bar{\sigma}_{\text{mean}} = \frac{\bar{\sigma}_q + \bar{\sigma}_T}{2} = \frac{1}{b} \left[ \int_{-b/2}^{b/2} \sigma_y^q(0, y) dy + \int_{-b/2}^{b/2} \sigma_y^T(0, y) dy \right] \quad (27.5)$$

The mean, normal, stresses acting in a section coinciding with the hatch end coaming are design stresses. The concentration of stresses in the hatch joints can be lowered to safe limits by appropriate construction measures. Using the solution to the two-dimensional problem of the

theory of elasticity, Yu. N. Raskin [39] calculated both components of normal stress (27.5), depending on the dimensionless relationships  $a/B$ ,  $F/B\delta$  and  $b/B$ , where  $F$  is the cross-sectional area of the end beam,  $\delta$  is the thickness of the deck covering.

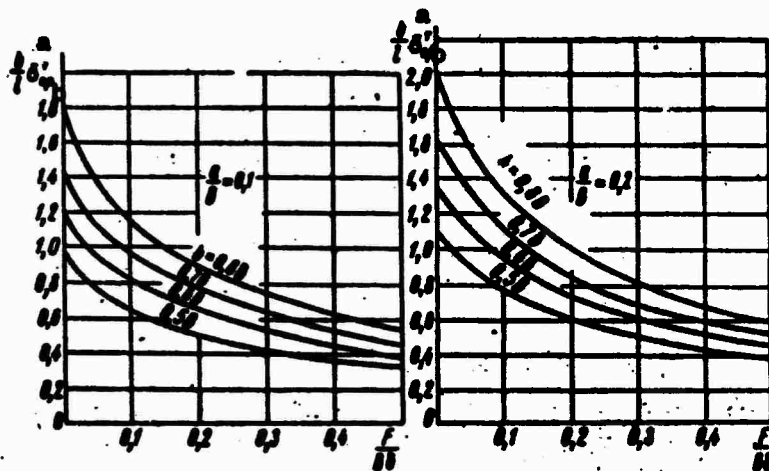


Figure 102. Values of  $\frac{b}{y} \sigma_{\text{mean}}$  - a-y; b-mean.

The first component  $\bar{\sigma}_{\text{mean}}^q$  is practically independent of the width of the hatch opening and is determined according to the graphs in Figure 101 for various relationships of  $a/B$  and  $F/B\delta$ . The second component  $\bar{\sigma}_{\text{mean}}$  depends on the hatch width and is determined from the graphs in Figure 102 depending on parameters  $b/B$  and  $F/B\delta$  for various relationships of  $a/B$ . Interpolation can be used for intermediate values of  $a/B$ . Both normal stress components are presented in Figures 101 and 102 as fractions of the compressive stress in the deck stringer  $\sigma_0 = q/\delta$ , where  $\delta$  is the reduced deck covering thickness in the area under consideration. The strength condition of the covering is written in the form  $\bar{\sigma}_{\text{mean}} < \sigma_y$ .

In addition to checking the resistance of the deck covering to action of normal stresses, the strength and stability of the covering in the extreme frame space adjoining the transverse bulkhead should be checked. Assuming the load to be bilateral and applied along the entire length of the deck grillage from bulkhead to bulkhead, we write the stability condition of the extreme panel in the following form:

$$1140 \sum_{i=1}^{B/2} c_i \delta_i \left( \frac{1000 \delta_i}{s} \right)^2 > k_3 \frac{qL}{2},$$

where safety factor  $k_3 = 1.5$ , as was assumed above.

**Example.** We shall check the strength and stability of the deck depicted in Figure 100, with the following initial data:  $L = 15.2$  m is the distance between bulkheads;  $B = 14.4$  m is the breadth of the ship along the deck in the area of load application;  $l = 10.4$  m is the hatch length;  $b = 8.0$  m is the hatch width;  $a = 2.4$  m is the distance between the hatch opening and the transverse bulkhead;  $s = 0.8$  m is the frame spacing,  $c_1 = 1.2$  m;  $\delta_1 = 12$  mm;  $c_2 = 2.0$  m;  $\delta_2 = 10$  mm;  $\delta = 8$  mm;  $F = 21.2$  cm<sup>2</sup> is the sectional area of the beams, less flanges;  $q = 100$  t/m is the ice load. Deck covering and beam material is steel with a yield stress  $\delta_y = 3,000$  kg/cm<sup>2</sup>,  $\tau_y = 0.57 \sigma_y = 0.57 \cdot 3,000 = 1,710$  kg/cm<sup>2</sup>.

$$\text{Parameter } \frac{F}{B\delta} = \frac{21.2}{14.4 \times 0.8 \times 10^2} = 0.0184.$$

According to the graph in Figure 101, for  $\frac{a}{B} = \frac{2.4}{14.4} = 0.167$ , we find  $\bar{\sigma}_{\text{mean}}^q = 0.53 \sigma_0$ .

According to the graph in Figure 102, we find the second component  $\bar{\sigma}_{\text{mean}}^y$  for  $b/B = \frac{8}{14.4} = 0.55$ :

$$\frac{b}{l} \bar{\sigma}_{\text{mean}}^{y, 1.05 \sigma_0}$$

or, considering that  $\frac{b}{l} = \frac{8.0}{10.4} = 0.77$ ,

$$\bar{\sigma}_{\text{mean}}^{y, 0.77} = \frac{1.05}{0.77} \sigma_0 = 1.36 \sigma_0.$$

Design mean compressive stresses

$$\sigma_{\text{mean}} = \bar{\sigma}_{\text{mean}}^q + \bar{\sigma}_{\text{mean}}^y = 0.53 \sigma_0 + 1.36 \sigma_0 = 1.89 \sigma_0 = 1780 \text{ kg/cm}^2;$$

$$\sigma_0 = \frac{q}{\delta} = \frac{100 \cdot 10}{1.08} = 950 \text{ kg/cm}^2.$$

where  $\bar{\delta} = \delta + \frac{F}{s} = 0.8 + \frac{21.2}{80} = 1.06$  cm.

Area of deck in section A - A

$$f = c_1 \delta_1 + c_2 \delta_2 = 120 \cdot 1.2 + 200 \cdot 1.0 = 344 \text{ cm}^2.$$

Shear stresses in this section

$$\tau = \frac{ql}{2f} = \frac{100 \cdot 10.4 \cdot 10^3}{2 \cdot 344} = 1510 \text{ kg/cm}^2 < \tau_y$$

We check stability of the deck covering by formula (27.3):

$$Q_g = 1140 \left[ 144 \left( \frac{130}{80} \right)^3 + 200 \left( \frac{100}{80} \right)^3 \right] \cdot 10^{-3} = 725 \text{ t.}$$

$$Q = 0,75ql = 0,75 \cdot 100 \cdot 10,4 = 780 \text{ t} > Q_g.$$

Thus, the stability condition (27.4) is not satisfied in the section coinciding with the lateral edge of the hatch. This forces the thickness of the plate adjoining the opening to be increased.

#### 28. Calculating Ice Deck Beams.

Scantlings of beams of ships not having an ice classification are assigned according to Shipping Registry regulations on the basis of a certain lateral design load on the decks, keeping in mind the participation of the beam in bending of the web frame. Ice deck beams of ice ships are also subjected to the effect of longitudinal loads from the ice. When calculating ice decks not bearing a lateral load which takes place on icebreakers, for example, the stability of beams compressed by the ice load should be checked. Beams of ice decks on cargo ships which are usually the cargo decks, as well as beams of ice decks and platforms which confine tanks, should be designed for simultaneous, longitudinal and lateral load action.

Let us consider the latter case, from the beginning. We shall consider the beam as being a simply supported, prismatic beam, loaded with a lateral load and longitudinal, compressive forces (Figure 103). Let  $q_0$  be a design, lateral load on the beam caused by cargoes present in the 'tween deck space. Then, we determine the maximum stress in the center of the span of the beam by formula

$$\sigma_0 = \frac{M}{W_0} = \frac{q_0 l^2}{8W_0},$$

where  $l$  is the span of the beam, m;

$W_0$  is the section modulus of the section of the beam with attached flange for a ship of a non-ice class, calculated in accordance with chapter 6, section II of the Regulations of the Registry of Shipping of the USSR (1956 edition).

If, in addition to load  $q_0$ , compressive force  $T = qs$  acts on the beam, the maximum stress in the center of the beam span is determined by formula

$$\sigma_1 = \frac{M_1}{W_1} = \frac{qs^2}{8W_1} \chi^*(u^*),$$

where  $\chi^*(u^*)$  is a Bubnov function;

$u^* = \frac{l}{2} \sqrt{\frac{qs}{EI}}$  is the parameter of unsymmetrical bending;

$q$  is the ice load intensity, t/m;

$s$  is the distance between beams, m;

$I$  is the moment of inertia of the sectional area of the beam,  $\text{cm}^4$ ;

$W_1$  is the section modulus of the beam,  $\text{cm}^3$ .

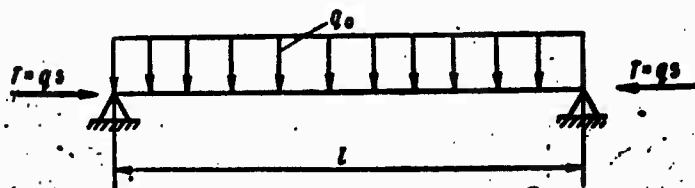


Figure 103. Design diagram for calculating scantlings of cargo deck beams.

Assuming the modulus of elasticity  $E = 2.1 \times 10^6 \text{ kg/cm}^2$ , we obtain a design formula for  $u^*$ :

$$u^* = 1.11 \sqrt{\frac{qs}{l}}$$

Assuming admissible stresses in both cases to be equal, we obtain an equation relating to  $W_0$  to  $W_1$ :

$$W_1 = k_{\text{stress}} W_0, \quad (28.1)$$

where  $k_{\text{stress}} = \chi^*(u^*)$  determined from Table 24.

Table 24

Values of stress coefficients  $k_{\text{stress}}$  for a beam, as a function of the parameter of unsymmetrical bending  $u^*$

$u^*$	0,0	0,2	0,4	0,6	0,8	1,0	1,2	1,4
$k_{\text{stress}}^a$ (точное решение)	1,0	1,016	1,073	1,176	1,361	1,704	2,441	4,938
$k_{\text{stress}}^b$ (приближенное)	1,0	1,016	1,079	1,171	1,362	1,684	2,404	4,930

a-exact solution; b-approximation.

When  $u^* = \frac{\pi}{2}$ , function  $x^*(u^*) \rightarrow \infty$  which corresponds to loss of stability of the beam.

$W_1$  should be computed according to formula (28.1) by the method of successive approximations inasmuch as coefficient  $k_{\text{stress}}$  depends on the unknown magnitude  $I$ . In the first approximation in the formula for  $u^*$ , it should be assumed that  $I = I_0$  with a corresponding  $W_0$ . We can limit ourselves to the first approximation only when the value of parameter  $u^*$  is small ( $u^* < 0.2$ ). When parameter  $u^*$  has large values, use of one approximation will lead to unacceptable results. In this case, several approximations must be made, taking into consideration the slow convergence of the process.

**Example.** For a beam of standard (non-ice) deck, take bulb flat bar 14a with  $W_0 = 100 \text{ cm}^3$  and  $I_0 = 1,274 \text{ cm}^4$ ;  $l = 2.5 \text{ m}$  is the beam span;  $s = 0.8 \text{ m}$  is the distance between beams;  $q = 200 \text{ t/m}$  is the design ice load.

We shall calculate  $u^*$  in a first approximation, assuming  $I = 1,274 \text{ cm}^4$ :

$$u_1^* = 1,1 \cdot 2,5 \sqrt{\frac{200 \cdot 0,8}{1274}} = 0,973.$$

According to table 24, we find  $k_{\text{stress}} = 1,37$ . Then, in the first approximation  $W_1 = 1,37 \times 100 = 137 \text{ cm}^3$ .

Let us assume bulb flat bar 16b with  $W = 165 \text{ cm}^3$  and  $I = 2,434 \text{ cm}^4$ . We determine  $u^*$  in a second approximation:

$$u_2^* = 1,1 \cdot 2,5 \sqrt{\frac{160}{2434}} = 0,705.$$

According to table 24, we find  $k_{\text{stress}} = 1,26$ . Then, in the second approximation,  $W_2 = 1,26 \times 100 = 126 \text{ cm}^3$ .

We assume bulb flat bar 16a with  $W = 147 \text{ cm}^3$  and  $I = 2,200 \text{ cm}^4$ . Then

$$a_3 = 1,1 \cdot 2,5 \sqrt{\frac{160}{2200}} = 0,74; \quad \text{to cross}$$

Thus, in the third approximation  $W_3 = 1,3 \times 100 = 130 \text{ cm}^3$ .

We stop on bulb flat bar 16a.

We shall adduce an approximate solution to the problem of unsymmetrical bending of a simply supported prismatic beam, based on the energy method. An expression of the total energy of a beam is written in the following manner

$$\mathcal{J} = \int_0^l \left[ \frac{EI}{2} \left( \frac{d^2v}{dx^2} \right)^2 - \frac{qs}{2} \left( \frac{dv}{dx} \right)^2 - q_0 v \right] dx = \text{min.}$$

The Euler-Poisson equation for function  $\mathcal{J}$  is a well-known expression for unsymmetrical bending of a beam:

$$EIv^{IV} + qsv'' - q_0 = 0.$$

We look for the deflection line in the form  $v = v_0 \sin \frac{\pi x}{l}$  ( $v_0$  is an unknown parameter) which satisfies the conditions at the beam ends.

Substituting the obtained solution for  $v$  into functional  $\mathcal{J}$  and carrying out integration, we obtain

$$\frac{EI}{2} v_0^2 \left( \frac{\pi}{l} \right)^4 \frac{l}{2} - \frac{qs}{2} \left( \frac{\pi}{l} \right)^2 v_0^2 \frac{l}{2} - q_0 v_0 \cdot 2 \frac{l}{\pi} = \text{min.}$$

Taking the derivative for  $v_0$  and equating it to zero, we find

$$v_0 \left[ EI \left( \frac{\pi}{l} \right)^4 - qs \right] \left( \frac{\pi}{l} \right)^2 \frac{l}{2} = 2q_0 \frac{l}{\pi},$$

from which

$$v_0 = \frac{4q_0 l^3}{\pi^3 \left[ EI \left( \frac{\pi}{l} \right)^4 - qs \right]}.$$

When  $qs = T_E = EI \left( \frac{\pi}{2} \right)^2$ , the magnitude  $v_0 \rightarrow \infty$  which should be expected.

The maximum bending moment in the center of the span is determined by the formula

$$M = EIv'' \Big|_{x = \frac{l}{2}} = \frac{4q_0 EI}{\pi \left[ EI \left( \frac{\pi}{l} \right)^4 - qs \right]}.$$

When  $qs = 0$ , this expression differs little from the exact solution:

$$M = \frac{q_0 l^2}{7.76} \text{ (instead of } M = \frac{q_0 l^2}{8} \text{ )}.$$

We rearrange the obtained expression for bending moment:

$$M = \frac{q_0 l^2}{8} \cdot \frac{1}{1 - \frac{q_0 l^2}{EI \left(\frac{\pi}{l}\right)^2}}$$

assuming  $\frac{\pi^2}{4} \approx 8$ .

Assuming the permissible stresses for a beam in a state of unsymmetric bending and for a beam loaded with a single, lateral load,  $q_0$  to be equal, we obtain:

$$W_1 = W_0 \cdot \frac{1}{1 - \frac{q_0 l^2}{EI \left(\frac{\pi}{l}\right)^2}} \quad (28.2)$$

We also calculate the profile of the beams in this formula by the method of successive approximations with which  $I = I_0$  should be taken as the first approximation ( $I_0$  corresponds to the section modulus of  $W_0$ ).

To compare the exact and approximate solutions, we consider the numerical example cited above (see page 191). In the first approximation, we take  $I = 1,274 \text{ cm}^4$ . Then

$$W_1 = \frac{100}{1 - \frac{200 \cdot 10 \cdot 80}{2,1 \cdot 10^6 \cdot 1,274 \cdot \left(\frac{\pi}{250}\right)^2}} = \frac{100}{1 - 0,378} = 161 \text{ cm}^3.$$

We take bulb flat bar 16b with  $W = 165 \text{ cm}^3$  and  $I = 2,434 \text{ cm}^4$ . Then, in the second approximation

$$W_2 = \frac{100}{1 - 0,378 \cdot \frac{1274}{2434}} = 125 \text{ cm}^3.$$

We take bulb flat bar 16a with  $W = 147 \text{ cm}^3$  and  $I = 2,200 \text{ cm}^4$ . Then, in the third approximation

$$W_3 = \frac{100}{1 - 0,378 \cdot \frac{1274}{2200}} = 128 \text{ cm}^3.$$

We stop on bulb flat bar 16a.

Thus, convergence of the process of successive approximations, in both cases, is equal. Therefore, it is difficult to give preference to one method or the other.

We present the formula for  $W_1$ , as was done earlier, in the form

$$W_1 = k_{\text{stress}} W_0,$$

where

$$k_{\text{stress}} = \frac{1}{1 - \left(\frac{\pi}{2} u^0\right)^2}.$$

Values of coefficient  $k_{\text{stress}}$  determined by the approximation formula, are presented in Table 24. When  $u^* = \pi/2$ , coefficient  $k_{\text{stress}} \rightarrow \infty$ . A comparison of the values of coefficients  $k_{\text{stress}}$  convinces that the approximation formula for  $W_1$  gives results which practically coincide with the exact solution (see Table 24). This makes it possible to use it for further computations.

The process of computing  $W_1$  and  $k_{\text{stress}}$  can be simplified if the moment of inertia is set in the function of the unknown section modulus.

The dependence  $I = f(W)$  for bulb flat bars with attached flanges constructed according to data in table "B" of part II of the Regulations of the Registry of Shipping of the USSR, 1956 edition, is presented in figure 104. It is not difficult to see that curve  $I = f(W)$  can be approximated, sufficiently close by the analytic dependence  $I = W^{3/2}$ .

In practical calculations, the discrepancy between the approximate and actual curve  $I = f(W)$  does not have a substantial influence on the final result. Then, the formula for  $W_1$  can be given in the form

$$W_1 = W_0 \cdot \frac{1}{1 - \frac{qs}{W_1^{3/2} \cdot E \left(\frac{\pi}{l}\right)^2}}.$$

Substituting  $W_1 = k_{\text{stress}} W_0$  here, we obtain

$$k_{\text{stress}} \frac{1}{\sqrt{k_{\text{stress}}}} \cdot \frac{qs}{E \left(\frac{\pi}{l}\right)^2 \cdot W_0^{3/2}} = 1.$$

Designating

$$N = \frac{qs}{E \left(\frac{\pi}{l}\right)^2 W_0^{3/2}},$$

we obtain an equation for calculating coefficient  $k_{\text{stress}}$ :

$$k_{\text{stress}} = \frac{N}{\sqrt{k_{\text{stress}}}} + 1.$$

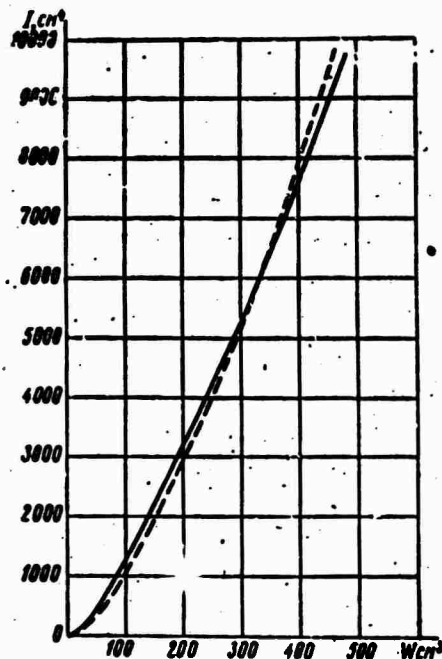


Figure 104. Dependencies  $I = f(W)$ .  
 according to Regulations of the Registry of Shipping of the  
 USSR, - - - - -  $I = W^3/2$ .

Taking  $q$  in t/m,  $s$  and  $l$  in meters,  $W_0$  in  $\text{cm}^3$ , and assuming  $E = 2.1 \times 10^6$  kg/cm<sup>2</sup>, we finally obtain

$$N = \frac{qsl^3 \cdot 10^7}{2.1 \cdot 10^6 \cdot W_0^{3/2}} = 0,483 \frac{qsl^3}{W_0^{3/2}}. \quad (28.3)$$

In practice, values of characteristic  $N$  are located within the range of zero to one.

Thus, the necessary section modulus  $W_1 = k_{\text{stress}} W_0$ , using data of Table 25 to calculate coefficient  $k_{\text{stress}}$  depending on characteristic  $N$ .

As calculations have shown, the thickness of ice deck covering, calculated for the frame spacing designated by Regulations of the Registry of Shipping, are extremely large. For example, with frame spacing  $s = 800$  mm, the minimum thickness of the lower deck according to Regulations of the Registry of Shipping is  $\delta = 9.5$  mm. Then, for a UL (Arkt.)-class ice ship, where  $q = 200$  t/m, we obtain [formula (26.14)]

$$\delta = 10 \sqrt[3]{\frac{q+50}{80} s^3} = 10 \sqrt[3]{\frac{250 \cdot 0,8^3}{80}} = 13 \text{ mm.}$$

The overall increase in the deck section for the frame spacing is  $\Delta F = (13 \text{ to } 9.5) \times 80 = 28 \text{ cm}^2$  [sic], which corresponds to bulb flat bar 20a. In this case, it is better to install intermediate beams, dividing the frame spacings in half. Then, the required deck covering thickness for the example under consideration will be

$$\delta = 10 \sqrt[3]{\frac{250 \cdot 0,4^3}{80}} = 8,2 \text{ mm.}$$

It is most expedient to install intermediate beams on icebreakers where ice loads are large. When doing this, the thickness of the deck covering should not be decreased from the requirements of the Regulations of the Registry of Shipping of the USSR. For I and II-class icebreakers, intermediate beams of the same profile as the main beams should be installed throughout the entire length of the ice deck in the area of the effective waterline and in the extremities on the lower decks and platforms. On III-class icebreakers, UL (Arkt.)-class ice ships, and UL class tugboats, intermediate beams should be installed only in the beam and stern. The section modulus of the beams can be taken as equal to 50% of the main beams, inasmuch as the purpose of intermediate beams, in this case, consists mainly of increasing the stability of deck plates.

In view of the fact that stresses in deck covering attenuate relatively quickly, in relation to the distance from the side, there is no need to install intermediate beams more than 1.5 to 2 m long. In practice, they should run up to the nearest deck girder (carling, hatch side coaming) or longitudinal side bulkheads.

Table 25.

Values of coefficient  $k_{\text{stress}}$

$N$ stress	0	0,1	0,2	0,3	0,4	0,5
	1,00	1,10	1,18	1,27	1,34	1,42
$N$ stress	0,6	0,7	0,8	0,9	1,0	1,1
	1,49	1,56	1,63	1,69	1,77	1,82

If a lateral load is not acting on the ice deck, then only stability of the beams should be checked. In this case, the beam is considered as a prismatic beam simply supported on the nearest carling (hatch coaming) and simply supported or rigidly constrained at the side. The beam is compressed by force  $P$  acting on one side (Figure 105). In this case, the problem of stability of the beam during compressive force action which varies along the length of the beam should be considered. As was shown in work [9], the Euler stress for this case will be

$$P_e = \eta \frac{\pi^2 EI}{l^2}, \quad (28.4)$$

where  $I$  is the moment of inertia of the beam with attached flange;  
 $l$  is the span of the beam;  
 $\eta$  is a coefficient derived from the graph in Figure 106, depending on the magnitude of parameter  $\alpha^*$ .

This parameter is determined, in turn, from the graph in Figure 107, depending on characteristic

$$b = \frac{R}{F},$$

where  $b$  is the thickness of the deck stringer;  
 $F$  is the cross-sectional area of the beam, less attached flange.

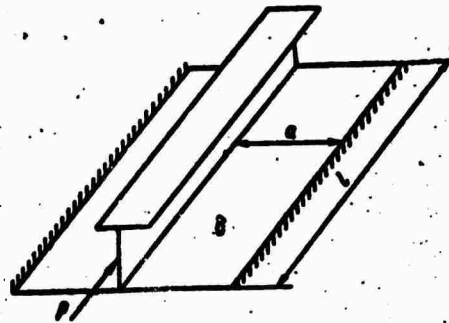


Figure 105. Diagram of unilateral compression of a beam.

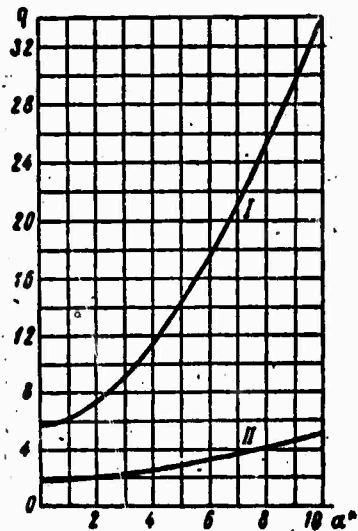


Figure 106. Values of coefficient  $\eta$ . I-One end rigidly constrained, other, simply supported; II-both ends, simply supported.

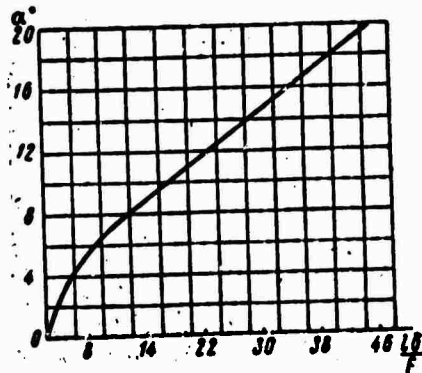


Figure 107. Values of coefficient  $\alpha^*$ .

The value of critical stress  $P_{cr}$  for the beam must be found, allowing for deviations from Hooke's law. For this, we calculate Euler stresses in the beam

$$\sigma_E = \frac{R_E}{F}$$

Subsequently, we find the corresponding value  $\sigma_{cr}$  from the well-known tables of Yu. A. Shimanskiy [45, Vol. 3], and then, the magnitude of  $P_{cr}$  by formula

$$P_{cr} = \eta_{cr} R_b$$

where  $F_b$  is the cross section area of the beam with attached flange.

The stability condition of the beam has the form  $qs < P_{cr}$ , where  $s$  is the distance between beams.

### 29. Checking Stability of Deck Grillages.

Detailed instructions for checking stability of deck grillages are presented in the Handbook on the Strength of Ships [45, Vol. 2, Section III; Vol. 3, Section III]. When checking stability of deck grillages in ice load action, it should be kept in mind that compressive stresses act on the hull laterally here, and not lengthwise as occurs in the case of overall bending. Therefore, all dependencies cited in [45] for a longitudinal framing system should be related to a lateral system and vice versa.

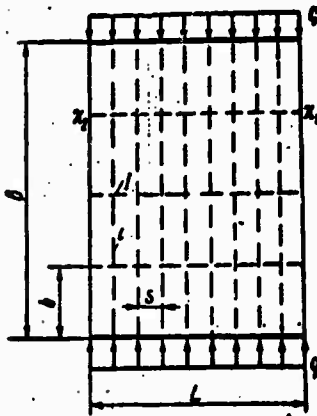


Figure 108. Diagram of ice compression of a deck constructed with a lateral framing system.

Let us consider a grillage consisting of beams having an identical profile and evenly spaced carlings, also having an identical profile, elastically constrained on rigid supports - transverse bulkheads or web beams (Figure 108). Here

- l** is the width of the grillage, in the given case, equal to the ship's breadth **B**;  
**s** is the distance between beams;  
**L** is the length of the grillage, equal to the distance between transverse bulkheads of web beams, if the latter have great rigidity;  
**b** is the distance between carlings;  
**i** is the moment of inertia of the beam (with attached flange);  
**I** is the moment of inertia of the carling (with attached flange);  
 $x_1, x_2$  are conditional, reference couple, coefficients of the end fastenings of the carlings:

$$x_1 = \frac{1}{1 + \frac{2M_1 EI}{L}}; \quad x_2 = \frac{1}{1 + \frac{2M_2 EI}{L}}$$

$\mu_1, \mu_2$  are coefficients of yielding of the elastic constraint of the beams on the supports;

$n - 1$  is the number of carlings ( $n = \frac{l}{b}$ ).

We find the necessary section modulus of the carlings by formula

$$I = \left(\frac{\pi}{\mu}\right)^4 \left(\frac{L}{B}\right)^3 \frac{L}{s} l \varphi \chi_{jmax}(\lambda),$$

where  $\mu$  is a coefficient determined from Table 6 of Section III of Handbook [45], depending on the conditional reference couple coefficients  $x_1$  and  $x_2$ ;

$\varphi$  is a coefficient allowing for deviation from Hooke's law, determined from a graph [45, Vol. 2, p. 95].

$\chi_{jmax}(\lambda)$  is a coefficient determined from Handbook [45, Vol. 3, p. 164].

Euler stress of the web beam

$$\sigma_E = \frac{\pi^2 EI_b}{l^2 (f_b + f_a)} \left( m^2 + \frac{\beta}{m^2} \right),$$

where  $I_b$  is the moment of inertia of the web beam with attached flange;

$l$  is the span of the web beam;

$f_b$  is the cross section of the web beam;

$f_a$  is the area of the attached flange of the web beam;

$m$  is the number of half waves of stability loss, determined from a condition of minimum  $\sigma_E$ ,

$$\beta = \frac{A l^4}{\pi^2 E I_b};$$

$k = \frac{EI}{\lambda bL^3}$  is the coefficient of rigidity of the elastic foundation created by the carlings;

$\lambda$  is the influence coefficient of the concentrated force on deflection of the carling at the point of intersection with the web beam.

A detailed calculation of the stability of a web beam is presented in [45, Vol. 3].

With a longitudinal system of framing (Figure 109), stability of deck grillage is checked as the stability of a plate strengthened by lateral strengthening ribs [45, Vol. 3, Section III, #7].

We will use the following symbols:  $I$  is the moment of inertia of the longitudinal deck rib;  $a$  is the distance between ribs;  $B_1$  is the span of the rib, measured from bulkhead to the web beam or between web beams. Erring slightly on the side of providing a margin of stability, we will assume the strengthening ribs to be simply supported on the web beams, i.e.,  $x_1 = x_2 = 0$ .

Euler stress of the deck plate

$$\sigma_E = 200\lambda \left( \frac{100\delta}{a} \right)^3 \left( 1 + \frac{a^2}{B_1^2} \right)^3.$$

The value of parameter  $\lambda$  is taken from the graph in Figure 4 [45, Vol. 3, Section III], depending on the magnitude of  $\chi$ , which is determined by formula

$$\chi = 100 \left( \frac{\mu}{\pi} \right)^4 \left( \frac{a}{B_1} \right)^3 \frac{I}{B_1 \delta^3},$$

where  $\delta$  is the thickness of the deck covering.

For  $x_1 = x_2 = 0$   $\mu = \pi$ .

The  $\lambda \geq 3.67$  rigidity of the longitudinal ribs exceeds the critical rigidity and stability of the plate is determined by the stability of one of its fields between ribs. The critical moment of inertia of longitudinal

$$I_{cr} = 0,0367 \left( \frac{\pi}{\mu} \right)^4 \cdot \left( \frac{B_1}{a} \right)^3 B_1 \delta^3.$$

Euler stresses in the deck covering calculated in this way that it correspond to a case in which web beams can be considered as an adequately rigid support for the longitudinal ribs.

We find the Euler stress for a web beam, as for a simply supported bar on an elastic foundation, according to the formula

$$\sigma_E = \frac{\pi^2 E I_b}{l^2 (l_b + l_a)} \left( m^2 + \frac{\beta}{m^2} \right),$$

where

$$f_{\sigma} \approx 0.15B_2(1 + \varphi)\beta;$$

$B_2$  is the sum of the distances from the web beam under consideration to the bulkhead and nearest web beam;

$$\varphi = \frac{\sigma_p}{\sigma_{E,p}}$$

( $\sigma_{E,p}$  is the Euler stress for a plate of the deck covering).

The magnitude  $\beta$  is determined depending on the coefficient of rigidity

$$k = \frac{EI}{\gamma L_{1b}^3}$$

$L_{1b}$  is the distance between the side and longitudinal bulkhead;

$\gamma$  is the influence coefficient of the concentrated force, applied at the point of intersection of the rib with the web beam, on deflection of the longitudinal rib.

## CHAPTER VII

### TRANSVERSE BULKHEADS, STEMS AND STERNPOSTS

#### 30. Design Loads on Transverse Bulkheads.

Transverse bulkheads of icebreakers and ice cargo ships are subjected to substantial ice loads. Loads acting in the planes of bulkheads, in some cases, cause damage and loss of stability in the bulkheads. Thus, in contrast to transverse bulkheads of ships not having an ice classification, bulkheads of ice ships must be designed for action of longitudinal, compressive stresses, as well as for lateral, hydrostatic load. Deep-tank bulkheads, as well as all main, watertight bulkheads, should be designed for such a load variant, keeping in mind the assurance of unsinkability in case of shipwreck.

Ice loads can be directly applied to a bulkhead or as reactions from the loaded, side stringers and ice decks (platforms). In both cases, the compressive load has a local nature. Therefore, primary attention should be given to providing strength and stability to sectors of the bulkhead nearest the side.

The load transmitted to the bulkhead by the side stringers and ice decks is balanced by a system of shear stresses acting along the line of their intersection. The most difficult situation is one in which an ice load occurs directly on a bulkhead and acts in the span between decks or between a deck and the inner bottom. The value of a design ice load acting on a bulkhead can be calculated on a basis of the design load on the side structures. The magnitude of the ice load when a ship strikes against an ice field is determined by the formula

$$P = 1,26 \sqrt{\frac{D}{gC'} v_{\text{red}}^2 \frac{b\sigma_c}{\sin 2\beta}} \quad (30.1)$$

where  $D$  is the ship's displacement;  
 $C'$  is the reduced mass coefficient;  
 $v_{\text{red}}$  is the velocity reduced toward the line of impact;  
 $\sigma_c$  is the ultimate crushing strength of the ice;  
 $\beta$  is the vertical slope of the frame at the point of impact;  
 $b$  is the length of load distribution.

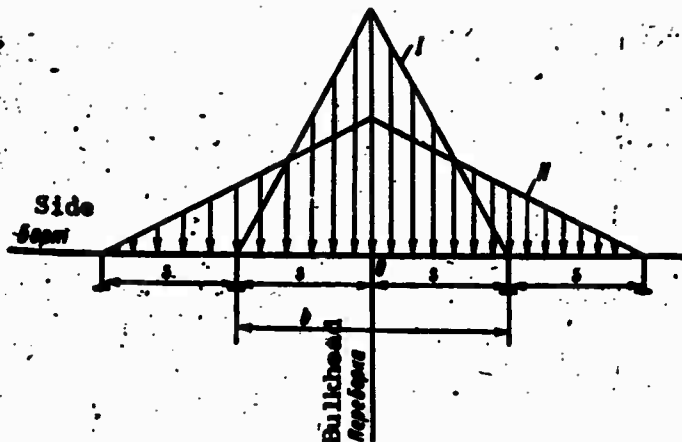


Figure 110. Diagram of ice stress action on a transverse bulkhead. I - Load limited to two frame spacings; II - Load limited to four frame spacings.

In formula (30.1), the length of the load distribution is an unknown parameter. To calculate this parameter as applied to a case in which an impact is applied to an area where a transverse bulkhead is installed, we use the following considerations. When the length of the distribution  $b$ , is increased, magnitude of the total ice load is somewhat increased. However, the part of the load experienced by the bulkhead is decreased, inasmuch as the intensity of the linear load decreases in this case (Figure 110). As a consequence of the crushing of the edge of the ice field in the impact process, the different degree of rigidity of the bulkhead and frames has practically no effect on the distribution of the ice load along the ship's side. Thus, it is assumed that the frames and bulkhead experience that part of the ice load which arrives at them directly. Based on this, the most dangerous case is an impact against a projection of the edge of a field, so that the contact stress is distributed within the limit of two frame spaces (diagram I in Figure 110) adjoining a bulkhead, i.e., when  $b = 2s$ .

We shall transfer a small part of the load occurring on the adjacent frames to the bulkhead (erring on the side of safety in so doing). Then, the stress acting on the bulkhead will be [see (9.7) and (9.8)]

$$P = 1.26v_{\text{red}} \sqrt{\frac{D}{gC'} \frac{2s_c}{\sin 2\beta}} \quad (30.2)$$

This stress is distributed on a comparatively small sector along the height of the side, giving basis to consider an ice load as a concentrated force applied in the area of the effective waterline when calculating the strength of a transverse bulkhead.

The load on a bulkhead located amidships is calculated from conditions of ice compression of ships. For ships with sloping sides ( $\beta \geq 8^\circ$ ),

we have the following expression for total stress experienced by the bulkhead, from the two, adjacent, frame spacings [see (12.8) where  $2R = 50$  m]:

$$P = \frac{0.233s}{\sin \beta} \sqrt[3]{\sigma_c \sigma_b^2 h^4}, \quad (30.3)$$

where  $s$  is the frame spacing;  
 $\sigma_c$  is the ultimate crushing strength of the ice;  
 $\sigma_b$  is the ultimate bending strength of the ice;  
 $h$  is the ice thickness;  
 $\beta$  is the slope amidships.

For ships with vertical sides, the maximum load is calculated from a condition of crack formations in the ice (Figure 110). In the sector adjacent to point O, the ice is in a plane state of stress; the largest primary compressive stress in this case being

$$\sigma = \frac{\sigma_x + \sigma_y}{\sqrt{2}}.$$

For ice  $\sigma_x = \sigma_y = \frac{q}{h}$ , consequently

$$\sigma = \sqrt{2} \frac{q}{h},$$

where  $q$  is the intensity of the load.

Assuming that failure begins when the static, compressive, stress reaches the ultimate crushing strength of the ice ( $\sigma_c = 200 \text{ t/m}^2$ ), for the critical load we obtain

$$q_{\text{fail}} \sqrt{2} = \frac{h \sigma_c}{\sqrt{2}} = 141h.$$

The stress transmitted to the bulkhead from the two, adjoining, frame spaces

$$P = 2sq_{\text{fail}} = 282hs. \quad (30.4)$$

Design diagrams for flat and corrugated transverse bulkheads are presented below.

### 31. Flat, Transverse, Bulkheads.

The strength of transverse bulkheads which are subjected to ice loads, as well as hydrostatic loads, is assured first of all, by structural measures directed toward increasing their rigidity. For this reason, all main, transverse, bulkheads on heavy and medium icebreakers must have horizontal, strengthening ribs. In the sector between the side and longitudinal bulkheads or vertical web stiffeners, these ribs should be installed normal to the side (Figure 111).

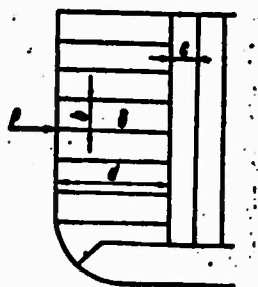


Figure 111. Diagram of a bulkhead sector strengthened next to the side by horizontal ribs.

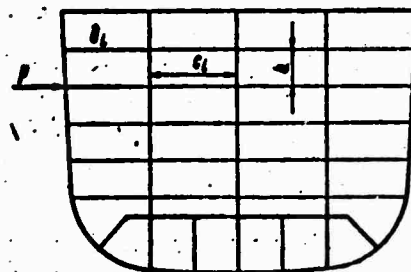


Figure 112. Diagram of strengthening of a transverse bulkhead amidships.

On all icebreakers, UL (Arkt)-and UL-class cargo ships and UL-class tugboats, it is desirable to install transverse bulkheads in the forepeak and afterpeak, perpendicular to the side and the strengthening ribs for them should also be installed perpendicular to the side. In doing this, the strengthening ribs must be structurally linked in the longitudinal plane with the longitudinal bulkheads (partial bulkheads), located in the fore- and afterpeaks, or supported on docking stiffeners. On all other transverse bulkheads, strengthening ribs normal to the side should lead to the nearest, vertical, web stiffener of the bulkhead. The midsection of bulkheads in the parallel, middle body area, can be strengthened either by horizontal or vertical, stiffening ribs (Figure 112).

On L-class cargo ships and tugboats, lateral bulkheads in the bow must have horizontal strengthening ribs leading to the nearest, vertical stiffener. These ribs are installed over the entire height of the bulkhead, from the flooring of the inner bottom to the deck located in the load, waterline, area. Midship bulkheads of these ships can be of standard structure with vertical stiffeners. The distance between the horizontal ribs which are subjected to ice loads must not exceed 600 to 700 mm for structural considerations. So that extreme plates of the bulkhead panel can stand up under shearing stresses, their thickness must be at least the

thickness of the side stringer wall or the thickness of the deck stringer. The width of these thickened plates must be no less than the height of the side stringer or width of the deck stringer, and in any case, must be at least 1,000 to 1,200 mm. Experience in construction and operation of ice ships shows that the minimum permissible thickness of extreme, bulkhead plates, should also be regulated (Table 26).

Table 26

Minimum values for the thickness of extreme plates of transverse bulkheads.

a Тип судна	b Класс судна	Г Толщина листов, мм	
		в носовой оконечности	в остальных районах
f Ледоколы	I	16	14
	II	14	12
	III	10	9
g Судя ледового плавания	УЛ (Аркт.)	9	8
	Л	8	8
	Л	8	8
i Буксиры	j УЛ	8	7
	Л	7	6

a-ship type; b-ship class; c-plate thickness, mm; d-forepart; e-remaining areas; f-icebreakers; g-ice ships; h-UL (Arkt.) UL,L; i-tugboats; j-UL,L.

It is necessary to pay particular attention to the quality of welding and the rational distribution of welded joints in the area where decks join transverse bulkheads. Analysis of shipwreck cases has shown that ice damage to bulkheads usually begins with breakdown of welded joints under the effect of shearing stresses.

Transverse bulkheads with horizontal strengthening ribs should be calculated for ice load action, similarly to calculations of ice deck strength. In this case, all the design dependencies of the previous chapter can be used.

If an ice load on a bulkhead is nearly a concentrated load (Figure 112), the bulkhead can be calculated similarly to the way in which strength of local bulkheads with vertical stiffeners is calculated when a ship is docked [28; 45, Vol. 3]. Let P be an external load on a bulkhead. Assuming admissible shearing stresses to be  $\tau_{ad} = 0.25\tau_y$ , we shall

find the minimum, necessary, cross-sectional area of the bulkhead:

$$a = \frac{4P}{\sigma_y}$$

The ultimate shearing force which can be endured by a bulkhead from a condition of stability of its plating

$$N_{\text{stress}} = 1140 \sum c_i \delta_i \left( \frac{1000}{b} \right)^3$$

where  $\delta_i$  is the plate thickness;

$b$  is the distance between horizontal ribs;

$c_i$  is the distance between vertical stiffeners.

With this, the condition  $N_{\text{shear}} \geq (1.5 \text{ to } 2)P$  can be fulfilled. Moreover, it is necessary to check the stability of the sector of the plate between horizontal ribs for action of normal stresses

$$q_E = 8008 \left( \frac{1000}{b} \right)^3 > q_{\text{des}} = \frac{q}{s} \quad (31.1)$$

where  $q_{\text{des}}$  is the design ice load on the bulkhead;

$q$  is the design ice load on the side framing;

$s$  is the frame spacing;

$b$  is the distance between horizontal ribs.

Scantlings of the bulkhead ribs and stiffeners are determined from a condition of assuring lateral strength, allowing for unsymmetrical bending, as was previously done for ice deck beams. When horizontal ribs are installed on transverse bulkheads, amidships only at the side and the midsection of the bulkhead is strengthened by vertical stiffeners (Figure 111), the stability of bulkhead plates between horizontal ribs should be checked for action of normal stresses according to expression (31.1). Moreover, it is necessary to check the stability of that sector of the bulkhead leaf for action of shear stresses

$$11408 \left( \frac{1000}{b} \right)^3 d \geq qs \quad (31.2)$$

where  $d$  is the length of the horizontal, strengthening, rib.

This formula was obtained assuming uniform distribution of shear stresses along the length of the horizontal, strengthening, rib. In view of the difficulty of establishing the nature of the distribution of shear stresses along the length, the safety factor  $k_3 = 1.5 \text{ to } 2$ , should be introduced.

The stability of a horizontal rib is checked by formula

$$P_E = \frac{\pi^2 EI}{d^3} > q_s.$$

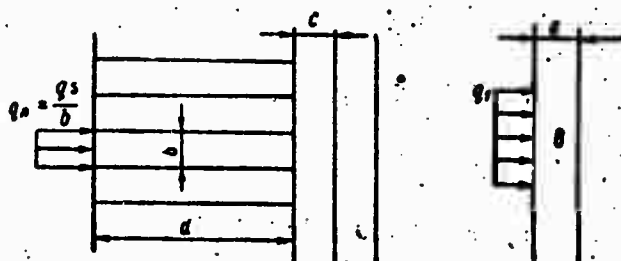


Figure 113. Design diagram for calculating the length of horizontal, strengthening, ribs.

The necessary length  $d$ , of horizontal ribs is determined in the following manner. The Euler load on the first sector of a bulkhead with vertical ribs (Figure 113), is computed by the formula

$$q_E = 200 \left( \frac{100\delta}{c} \right)^2 \delta.$$

Assuming that the design ice load on the bulkhead  $q_{bh}$  is distributed on sector  $b$  (Figure 113), and disregarding the presence of horizontal ribs, we obtain an expression for stresses transmitted to the sector of the bulkhead strengthened by vertical stiffeners\*

$$q_1 = q_{bh} \frac{2}{\pi} \left\{ \operatorname{arctg} \frac{b}{2d} + \frac{b}{2d \left[ 1 + \left( \frac{b}{2d} \right)^2 \right]} \right\}.$$

---

\* See the solution to the two-dimensional problem of the theory of elasticity in N. I. Bezukhov's book, The Theory of Elasticity and Plasticity, GITTL, 1953, for example.

---

Let  $\frac{d}{b} = n$ . Assuming  $n > 3$ , we can write

$$q_1 = q_{bh} \frac{2}{\pi n}.$$

From a condition providing stability of a vertical segment of the bulkhead plating, we obtain

$$n = \frac{d}{b} \geq \frac{qs}{100\pi\delta \left(\frac{100\delta}{c}\right)^2 b}$$

where  $q$  is the design load on the framing.

Calculations have shown that usually  $n > 3$  to 5, i.e., the length of horizontal ribs adjoining the side must be three-to-five times greater than the distance between them.

Let us consider a bulkhead with vertical, strengthening, ribs. The segment of the bulkhead between the side and the nearest, vertical, stiffener has the greatest load (Figure 114). The magnitude of critical stress for the extreme plate (in tons), is determined according to work [30, p. 304]:

$$P_{cr} = \frac{4\pi D}{b} = 2420 \frac{\delta^3}{b}, \quad (31.3)$$

where  $\delta$  is the bulkhead thickness, cm;

$b$  is the distance between vertical stiffeners, cm;

$D = \frac{E\delta^3}{12(1-\mu^2)}$  is the flexural stiffness of the plate.

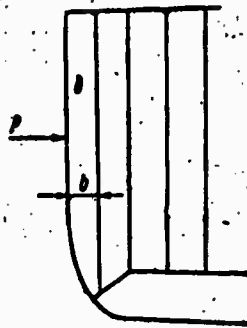


Figure 114. Diagram of a bulkhead with vertical stiffeners.

Then, the condition providing stability to bulkhead plating against action of an external ice load is written in the form:

$$P < P_{cr},$$

or

$$P < 2420 \frac{\delta^3}{b},$$

where  $P$  is the external load on the bulkhead, calculated according to formulas of the preceding paragraph.

It is permissible to install bulkheads with vertical stiffeners only amidships of UL- and L-class, ice cargo ships. The midship load of UL-class ships is calculated from conditions of ice compression (30.4). Then, for ships with a vertical side, we obtain the condition

$$0,282hs < 24200 \frac{b^3}{s}$$

where all dimensions are assumed in centimeters. This inequality can be presented in dimensionless form

$$\left(\frac{b}{s}\right)^3 \cdot \frac{s}{b} \cdot \frac{h}{b} < 3,6 \cdot 10^4.$$

The relationship  $\frac{h}{b}$  for these ships, usually does not exceed 1.6 to 1.7, and the relationship  $\frac{b}{s} \leq 1.5$ . Then, the following inequality must occur

$$\frac{b}{s} < 45.$$

This condition can be obtained for ships with sloped sides, in similar manner. Using formula (30.3) of the previous paragraph and substituting  $\sigma_c = 200 \text{ t/m}^2$ ,  $\sigma_{\text{frac}} = 100 \text{ t/m}^2$  and  $h = 0.9 \text{ m}$ . Therein, we obtain

$$\frac{35,6}{s \sin \beta} < 2,42 \cdot 10^4 \left(\frac{b}{s}\right)^3 \cdot \left(\frac{b}{s}\right)^3.$$

Usually, the vertical slope of the side of cargo ship midsections does not exceed 8 to 10° and frame spacing (main and intermediate)  $s = 0.35$  to 0.40 m. Then, we obtain  $\frac{b}{s} < 50$ .

Thus, when strengthening ribs are placed vertically, the distance between them must be no greater than 45 to 50 thicknesses of the transverse bulkhead plates.

When there are side stringers, stability of the bulkhead against action of reactive stress from the stringer should be checked. This stress is usually absorbed by a horizontal, strengthening, rib (shelf) mounted on the bulkhead. In this case, calculation of shelf stability should be performed similarly to calculation of a docking stiffener when a ship is placed in dock [45, Vol. 3].

The Euler load for a shelf is calculated by the formula

$$R_E = 10,3 \frac{\pi^2 EI}{l^2}$$

where  $I$  is the moment of inertia of the shelf;  
 $l$  is the span of the shelf.

The shelf elements must be selected in such a manner that  $R_E \geq R$  and compressive stress in any section, will not surpass yield stress. The magnitude of reaction  $R$ , is determined from a calculation of side grillage for ice load action  $q$ .

### 32. Corrugated Bulkheads.

Corrugated bulkheads can be installed in the midsection of ice cargo ships, with the corrugation axes being either vertically or horizontally oriented. The strength of such bulkheads is primarily assured by structural measures.

Structural requirements of transverse, corrugated, bulkheads consist of forming a flat sector of the bulkhead adjoining the side. This sector must be strengthened by horizontal, strengthening, ribs installed normal to the side. In certain cases, it is permissible to use vertical, strengthening, ribs. The thickness of the plates in this sector of the bulkhead must be at least the minimum, permissible, thickness (see Table 26). The minimum thickness of the flat sector of the bulkhead must be at least 8 mm for L-class cargo ships. The width of the flat sector of the bulkhead  $C$ , (Figure 115), is designated on the basis of a condition of strength under ice load action. Moreover, the stability of flat sectors under shearing strain, should be checked. It is recommended that strength and stability of these sectors be calculated according to the formulas of the preceding paragraph as for flat, transverse, bulkheads.

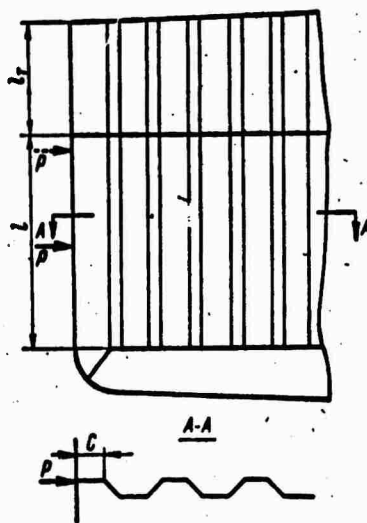


Figure 115. Diagram for calculating the resistance of a transverse bulkhead to ice load action.

The minimum width of the flat sector of a corrugated bulkhead can be calculated on a basis of the following considerations. Assuming design

loads on the side framing amidships to equal 100 t/m for a UL (Arkt.)-class ice ship, 50 t/m for UL-class ice ships and 22 t/m for L\*-class ice ships, and assuming the permissible, shear stresses in sections of the flat sectors to equal  $0.25 \sigma_y$  for frame spacing  $s = 0.4m$  on UL-(Arkt.) and UL-class ships and  $s = 0.75 m$  on L-class ships, we obtain the following values for the minimum width of the flat sector of a corrugated bulkhead with vertically-oriented corrugation axes (for transverse, side framing system) respectively: 1,200, 600 and 400 mm.

---

\* Loads for UL-(Arkt.) and UL-class ships are calculated on the basis of a condition of ice compression; for L-class ships, load  $q = 22$  t/m corresponds to the average magnitude of side framing strength of these ships assembled according to Regulations of the Registry of Shipping of the USSR.

---

With a longitudinal system of side frame, which is usually permissible for L-class ice ships, the minimum width of the flat sector must be increased to 1,200 mm. When frame spacing of the transverse framing is increased over the above-indicated values, as well as on ships displacing more than 10,000 t, the width of the flat sector should be increased in corresponding fashion (10 mm for each subsequent 1,000 t displacement). This is called for by the increase in the design ice load.

The stability of flat, bulkhead sectors under compression and shearing strain is assured when the distance between horizontal ribs on L-class ice ships does not exceed 70 to 80 plate thicknesses. In this case, when standard carbon steel is used

$$\tau_E = 1140 \left( \frac{100}{80} \right)^2 = 1780 \text{ kg/cm}^2 > 0,57 \sigma_y.$$

The stability of a flat sector under compression will be assured if

$$R_E = \frac{4\pi D}{b} = \frac{4\pi E \delta^3}{10,9 \frac{b}{\delta}} = 18,4m > P, \quad (32.1)$$

where  $\delta$  is the thickness of the flat sector of the bulkhead;  
 $b$  is the distance between horizontal ribs;

$$P = qs = 22 \cdot 0,75 = 16,5 m.$$

The obtained margin of stability ( $k_3 = 1.1$ ) can be considered adequate inasmuch as an ice load actually acts on one side and has no sharply-expressed, local nature which is not allowed for in formula (32.1). For UL-class ice ships, distance between horizontal, strengthening, ribs must not exceed 60 plate thicknesses.

Besides checking the strength of the flat sector, the strength of the corrugation should also be checked, determining normal stresses in the area of its first bend. It is easy to be convinced that these stresses will attenuate when the width of the flat sector is increased. The corrugated sector of the bulkhead should be calculated in accordance with recommendations worked out for calculating bulkheads when placing a ship in dock. It is recommended that the admissible stresses, in this case, be taken as equal to  $0.8 \sigma_y$  [45, Vol. 3]\*. If horizontal corrugations are used, their stability should be brought up to yield stress. Such stability, as a rule, is assured when the inequality  $\frac{l}{h} < 20$  is fulfilled, where  $l$  is the corrugation span and  $h$  is its height.

---

\* See also the monograph by A. L. Vasil'yev, M. K. Glozman, Ye. A. Pavlinova, M. V. Filippov titled "The Strength of Ships' Corrugated Bulkheads," Sudpromgiz, 1964.

---

Stability of the entire bulkhead, as a whole, under ice load action will evidently be assured by a condition fulfilling the above-cited requirements. A design in which the corrugations are cut at web stiffeners is more complex. Overall stability of a bulkhead, in this case, needs experimental and theoretical examination.

### 33. Calculating Scantlings of the Stem and Sternpost.

The stem of ice ships is most subject to ice load action during impacts against ice. Calculating the strength of stem structures is extremely complex. Therefore, when calculating their scantlings, ice-operating experience of ships is considered, first of all.

The stem structure of an icebreaker with strengthening is shown in Figure 116. The stem of all classes of icebreakers and of UL-(Arkt.) and UL-class ice ships must be forged or cast. On L-class ships, the stem can be welded. The thickness of plates of welded stems must be at least 30% greater than the thickness of shell plating of the ice belt adjacent to the stem.

On all classes of icebreakers and on UL-(Arkt.) and UL-class ships, the stem should be strengthened in the area of the ice belt by horizontal brackets at least 500 mm high and of the same thickness as the vertical keel, installing them approximately 600 mm from each other. A longitudinal bulkhead or vertical keel 400 to 600 mm high, stretching from the forepeak bulkhead to the deck above the ice belt is installed on the longitudinal plane in the forepeak.

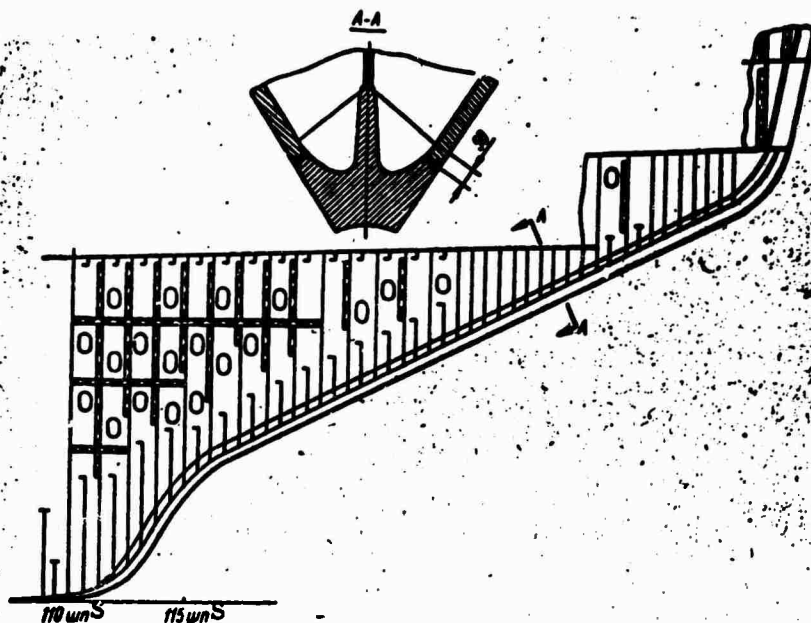


Figure 116. Stem structure and bow framing of a heavy icebreaker.

The stem of an ice ship can be considered as a curved beam with non-uniform rigidity, supported on a series of elastic supports formed by decks, platforms, stringers and breast hooks. Academic research shows that the ship's displacement, rake of the stem, ship's speed at the moment of impact and strength of the ice, influence the magnitude of the contact stress occurring when the stem impacts against ice. A detailed, academic analysis of the impact of a ship's stem against ice was conducted in work [48].

The cross-sectional area of the stem  $F$ , must be proportional to the magnitude of contact stress  $P$ , acting on the stem during impact, i.e.,  $P/P_0 = F/F_0$ . Subscript "0" relates to a prototype ship, the stem structure of which has proven itself in operation.

The component of contact stress normal to the stem is calculated by formula:

$$P_N = 1.3 \sqrt[3]{\frac{(M_{red} v_{red}^2)^2 \sigma_c \operatorname{tg} \alpha}{\cos \varphi \sin^2 \varphi}}, \quad (33.1)$$

where  $\sigma_c$  is the crushing strength of the ice;  
 $\varphi$  is the horizontal slope of the stem;  
 $\alpha$  is the entry angle of the bow waterline;

$v_{red} = v \sin \varphi$  is the reduced velocity of the ship;

$M_{red} = \frac{D}{gC'}$  is the reduced mass of the ship;

$D$  is the displacement;

$C'$  is the coefficient of the ship's reduced mass.

For ships having similar structural and operational elements, the cross-sectional areas of their stems are related as follows:

$$\frac{F}{F_0} = \sqrt[3]{\left(\frac{D}{D_0}\right)^2 \left(\frac{C'}{C'_0}\right)^2 \left(\frac{v}{v_0}\right)^4 \frac{e_c \operatorname{tg} \alpha \sin^3 \varphi \cos \varphi_0}{e_{c0} \operatorname{tg} \alpha_0 \sin^3 \varphi_0 \cos \varphi}} \quad (33.2)$$

Assuming, for ships of the same ice class

$$\frac{C'_0}{C'} = \frac{v}{v_0} = \frac{e_c}{e_{c0}} = 1,$$

we obtain an expression for determining the stem, cross-sectional area by means of a prototype ship

$$F = k \sqrt[3]{\frac{D^2 \operatorname{tg} \alpha \sin^3 \varphi}{\cos \varphi}}, \quad (33.3)$$

where

$$k = F_0 \sqrt[3]{\frac{\cos \varphi_0}{D_0^2 \operatorname{tg} \alpha_0 \sin^3 \varphi_0}}$$

Considering that angle  $\alpha$ , for various ice ships, changes within a relatively narrow range (20 to 26°), we can write

$$k = F_0 \sqrt[3]{\frac{\cos \varphi_0}{D_0^2 \sin^3 \varphi_0}}$$

and

$$F = k \sqrt[3]{\frac{D^2 \sin^3 \varphi}{\cos \varphi}}. \quad (33.4)$$

The following mean values of coefficient  $k$  were obtained as a result of calculations made for ships and icebreakers which have been constructed for I-class icebreakers,  $k = 3.6$ ; for II-class icebreakers,  $k = 2.5$ ; for III-class icebreakers and UL-(Arkt)-class, cargo ships,  $k = 1.9$ ; for UL-class cargo ships,  $k = 1.4$ ; for L-class ships,  $k = 0.6$

Instead of formula (33.4), we can write:

$$F = a + bD, \quad (33.5)$$

where empirical coefficients a and b are selected so that this expression well approximates formula (33.4). Such approximation is easily achieved if dependence (33.5) is sorted into two sectors of argument variation for D, with various values of coefficients a and b:  $D \leq 3500$  t and  $D > 2,500$  t. Moreover, parameters a and b depend on the ice class and type of ship and are chosen so that actual, cross-sectional areas of stems of a series of ships which have been constructed and proven themselves agree with formula (33.5).

Calculations were made, allowing for these considerations, and a graph for determining the cross-sectional area of stems of icebreakers and ice cargo ships was constructed (Figure 117). Stem, cross-sectional areas of L- and UL-class ships, regulated by Regulations of the Registry of Shipping of the USSR (1956 ed.), are shown by dotted lines. The figure also presents actual, stem, sectional areas of various types of ships presently operating in the Arctic. Table 27 gives numeral values for coefficients a and b, corresponding to the following form of formula (33.5)

$$F = a + bD \cdot 10^{-2} \text{ cm}^2, \quad (33.6)$$

where D is displacement, full-load for icebreakers and tugboats and according to the summer load waterline for ice ships, t.

Table 27

Values of coefficients a and b

Тип судна a	Ледовый класс b	Форма форштевя c	a		b	
			при $D < 2500$ т	при $D > 2500$ т	при $D < 2500$ т	при $D > 2500$ т
Ледоколы	I	f Ледокольная	—	700	—	3,0
	II		—	590	—	3,0
	III		135	250	9,0	4,0
Суда ледового плавания g	UL (Аркт.)	Ледокольная f	110	210	7,5	3,6
	UL	„	75	120	3,75	1,85
	UL	Полуледокольная h	85	150	5,0	2,3
	UL	Неледокольная i	100	180	6,0	2,8
	L	Полуледокольная h	65	100	3,0	1,6
L	Неледокольная i	75	120	3,75	1,85	
Буксыры	UL	f Ледокольная	135	—	9,0	—
	L		75	—	3,75	—

a-ship type; b-ice class; c-stem form; d-when; e-Icebreakers; f-Icebreaker; g-Ice ships; h-Semi-icebreaker; i-Non-icebreaker; j-Tugboat.

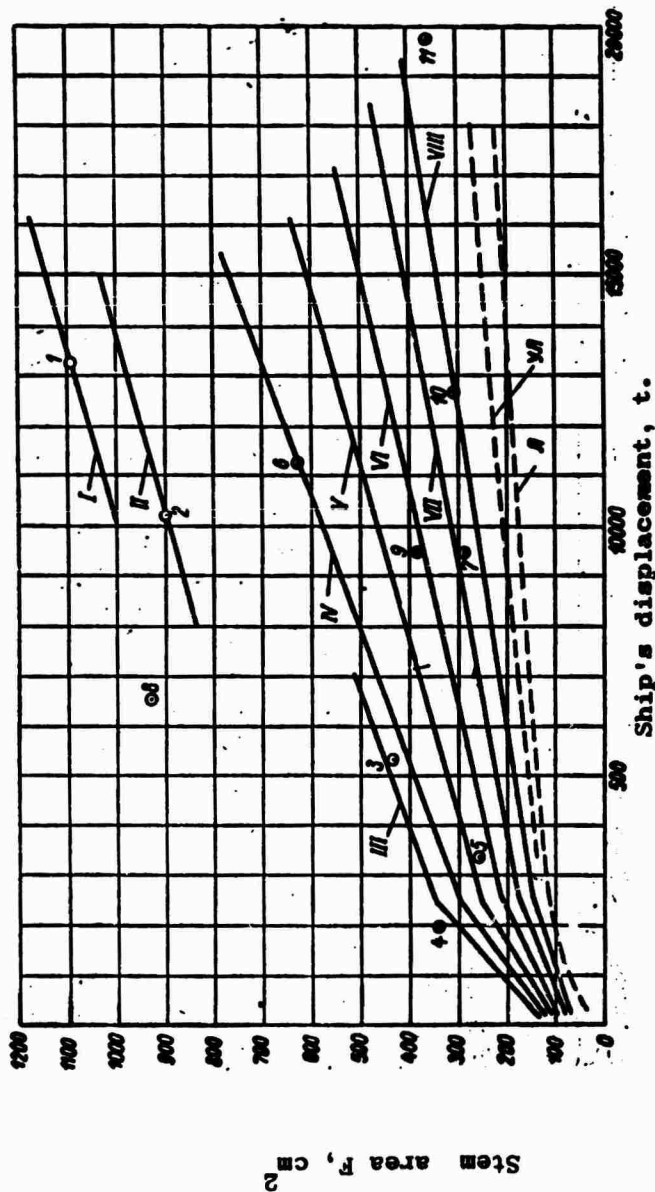


Figure 117. Areas of stems of ships of various ice classes [arabic numerals indicate stem areas of ships which are in operation, roman numerals indicate design areas determined by formula (33.6)].

1, I - I-class icebreakers; 2, 3, II to II class icebreakers; 4, 5, 6, III, IV to III-class icebreakers and UL-class tugboats; 7, 8, 9, V, VI, VII - UL-class ships (with various hull shapes) and L-class tugboats; 10, 11, VIII - L-class ships.

When stern frame scantlings are being designated, they should be based on designing experience of ships which have been constructed and are operating. When doing this, it is necessary to remember that the distribution of material between the sternpost and rudder-post of ships which sail in ice must differ substantially from standard, inasmuch as the rudder-post is subjected to larger ice loads than the sternpost under all conditions of ice navigation. A smooth boss is usually stipulated in the upper part of the stern frame above the rudder blade to protect the blade from ice damage when the ship moves astern (Figure 118). Such protection is mandatory on icebreakers and UL-(Arkt.)-class ships. In addition, the slope of the lower edge of the heel brace in relation to the base line, must be at least  $1/8$ , starting from the sternpost.

There are no requirements for strengthening the stern frame of icebreakers and UL-(Arkt.)-class ships in Regulations of the Registry of Shipping of the USSR (1956 ed.). The requirements relating to L-class and UL-class ships are inadequate. Moreover, strengthening of the sternpost and rudder-post are not considered individually, in the Regulations. As Table 28 shows, the increase coefficients of the cross-sectional area of the sternpost  $k_2$  and rudder-post  $k_1$ , in relation to the sectional area of the stern frame  $F_0$ , for a non-strengthening ship, vary over a very wide range, even for ships of the same ice class. However, it is obvious that coefficients  $k_1$  and  $k_2$  increase for ships and icebreakers of higher ice classes. In this case, the rudder-post is strengthened more than the sternpost.

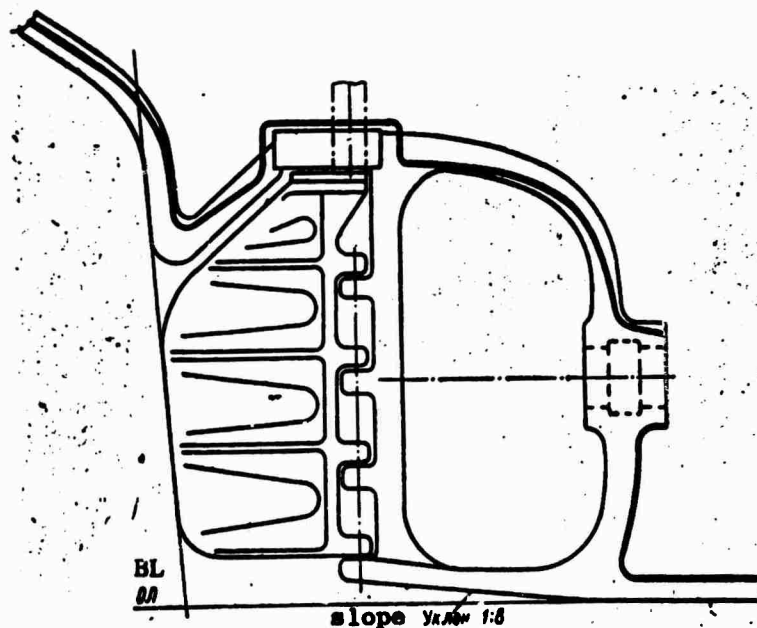


Figure 118. Stern frame of a heavy icebreaker.

Calculations performed for a large number of ice cargo ships and icebreakers, have made it possible to determine mean, empirical, values for coefficients  $k_1$  and  $k_2$ .

Table 28

Values of coefficients  $k_1$  and  $k_2$  for various ships in operation.

а Тип судна	б Ледовый класс	с L по КВЛ, м	д F <sub>0</sub> по Регистру, см <sup>3</sup>	е F <sub>g</sub> , см <sup>3</sup>	ж F <sub>r</sub> , см <sup>3</sup>	з $\frac{F_r}{F_g}$	и $\frac{F_r}{F_0}$	к $\frac{F_g}{F_0}$
Ледоколы	I	112,4	(440)*	964	1830	1,92	4,15	2,17
	II	100,8	(372)*	894	1015	1,13	2,72	2,40
		80,4	(268)*	—	581	—	2,17	—
	III	62,0	(185)*	—	360	—	1,94	—
Транспортные суда	UL (Аркт.)	123,0	(490)*	1086	1223	1,12	2,50	2,22
	UL	102,0	378	—	875	—	2,31	—
	UL	120,6	474	446	—	—	—	0,94
	UL	115,0	444	526	750	1,42	1,69	1,18
	L	156,0	704	813	—	—	—	1,15
	L	130,0	537	610	990	1,62	1,84	1,14
	L	95,8	348	380	608	1,60	1,75	1,09

З. \* Для обычного судна, не имеющего ледовых подкреплений.

a-ship type; b-ice class; c-L at designer's waterline, m; d-F<sub>0</sub> according to Register, cm<sup>3</sup>; e-Icebreakers; f-Cargo ships; g-\* for standard ships, not ice-strengthened.

Table 29

Values of coefficients  $k_1$  and  $k_2$  for icebreakers and ships of various classes.

Коэффициенты б	а Тип судна и ледовый класс								
	с Ледоколы			д Транспортные суда			е Буксиры		
	I	II	III	UL (Аркт.)	UL	Л	UL	Л	
$k_1$	4,0	3,0	2,5	2,5*	1,5	1,3	2,5	1,5	
$k_2$	2,5	2,0	1,75	1,75	1,25	1,15	1,75	1,25	

a-ship type and ice class; б-coefficients; с-Icebreakers; д-Cargo ships; е-Tugboats.

Thus, the cross-sectional area of the rudder-post and sternpost of ice-breakers and ice ships can be calculated by formulas

$$F_r = k_1 F_0, \quad (33.7)$$

$$F_s = k_2 F_0, \quad (33.8)$$

where  $F_0$  is the cross-sectional area of the stern frame, calculated according to Regulations of the Registry of Shipping of the USSR (1956 ed), for a ship which is not ice-strengthened;

$k_1$  and  $k_2$  are coefficients, numerical values of which are given in Table 29, depending on the ship type and ice class.

### Literature

1. Arnol'd-Alyab'yev, V. I. Ice strength in the Barents and Kara seas. Transactions of the VAI, vol. 121, 1938.
2. Afanas'yev, V. I. Materials concerned with ship movement study. Part III. Icebreakers. St. Petersburg, 1899.
3. Blagoveshchenskiy, S. N. Handbook on Ship Theory. Sudpromgiz, 1950.
4. Bogorodskiy, V. V. Elastic moduli of ice crystals. Acoustic Journal of the AN SSSR, 1964, vol. X, Issue 2.
5. Budnevich, S. S. and Deryagin, B. V. Slipping of solid bodies on ice. Journal of Technical Physics. 1952, vol. XXII, Issue 12.
6. Butyagin, I. P. The strength of the ice cover in the ice loads on hydraulic engineering installations. Transactions of the Transportation and Energetics Institute of the Siberian Branch of the AN SSSR. Novosibirsk, 1961, Issue XI.
7. Butyagin, I. P. Ice strength and ice cover strength. "Nauka" Publishing House (Siberian Division). Novosibirsk, 1966.
8. Bureau Veritas. Rules for the Classification and Building of Steel Ships. 1958. "Morskoy Transport" Publishing House. Leningrad, 1962.
9. Veynberg, B. P. Ice. Properties, Formation and Disappearance of Ice. Gostekhteorizdat, Moscow-Leningrad, 1940.
10. Vinogradov, I. V. Ships for Sailing in Ice. Oborongiz, Moscow, 1946.
11. Voytkovskiy, K. F. Plastic bending of ice beams. DAN SSSR, 1956, vol. 110, Issue 3.
12. Davydov, V. V. Theoretical research on the impact of a ship on ice. Collection "Problems of the Arctic," No. 5-6, 1938.
13. Davydov, V. V. Strength of icebreaking ships. Sudostroyeniye, No. 2, 1937.
14. Davydov, V. V., Mattes, N. V., Sivertsev, N. N. Textbook on the strength of internal waterway ships. "Rechnoy Transport" Publishing House, Moscow, 1958.
15. Deyvis, R. M. Stress waves in solid bodies. IL, 1961.
16. Yershov, N. F. Questions of the strength of cargo ships in ice. Abstracts from a Candidate Dissertation. GIIVT, 1958.
17. Yershov, N. F. Determination of the limiting load on a ship's skin. Scientific Transactions of the OIIMF, 1955, Issue XI.
18. Zhemochkin, B. N. Theory of elasticity. State Publishing House for Literature on Construction and Architecture. Moscow, 1957.
19. Zabolkin, N. A. Impact of an icebreaker on an ice field and its creeping through the ice. Transactions of the LKI, 1951, Issue 9.
20. Zylev, B. V. Ice pressure on sloping ice cutters. Transactions of the MIIT, 1950, Issue 74.
21. Kashtelyan, V. I. Approximate determination of the forces which destroy the ice cover. Collection "Problems of the Arctic," No. 5, 1960.

22. Korzhavin, K. N. Ice effect on engineering installations. SO AN SSSR Publishing House, Novosibirsk, 1962.
23. Korzhavin, K. N., Butyagin, I. P. Investigation of deformations and strength of ice fields under natural conditions. Transactions of the TEI SO AN SSSR, Novosibirsk, 1961, Issue XI.
24. Korotkin, Ya. I., Lokshin, A. Z., Siviers, N. L. Bending and Strength of Rods and Rod Systems. Mashgiz, 1958.
25. Kragel'skiy, I. V. Friction and wear. Mashgiz, 1962.
26. Krasil'nikov, V. N. The refraction of bent waves. Acoustic Journal of the AN SSSR, 1962, vol. VIII, 1st Issue.
27. Kuznetsov, P. A. Ice loads on hydraulic engineering installations. Collection of Transactions of the LONITOV, Leningrad, 1948.
28. Kurdyumov, A. A. The strength of ships. Sudpromgiz, 1956.
29. Lavrov, V. V. Questions of the physics and the mechanics of ice. Transactions of the AANII, vol. 247. "Morskoy Transport" Publishing House, 1962.
30. Lekhnitskiy, S. G. Anisotropic plates. Gostekhizdat, 1947.
31. Makarov, S. O. Yermak in the ice. St. Petersburg, 1901.
32. Maslov, A. I. Experience in computing external forces acting on a ship's hull in ice conditions. Transactions of the VNITOSS, 1937, Vol. II, Issue 3.
33. Nogid, L. M. Impact of a ship on ice. Transactions of the LKI, 1959, Issue 26.
34. Norwegian Veritas. Rules for the Building and Classification of Steel Ships. 1962. "Morskoy Transport" Publishing House, 1964.
35. Osmolovskiy, A. K. The establishment of a standard for the strength of ships hulls when sailing in ice. Transactions of the TsNIIVT, 1934, Issue 95, 1935, Issue 154.
36. Papkovich, P. F. Transactions on ship's strength. Sudpromgiz, 1956.
37. Peschanskiy, I. S. Glaciology and Ice Engineering. "Morskoy Transport" Publishing House, 1963.
38. Popov, Yu. N. The question of ship impact on ice. Transactions of the LKI, 1955, Issue XV.
39. Raskin, Yu. N. Investigation of the working of ships coverings subjected to the effects of local forces in their plane. Summary of a dissertation, LKI, 1963.
40. Register of the USSR. Rules for the Classification and Building of Seagoing Steel Ships. "Morskoy Transport" Publishing House, 1956.
41. Lloyds Register of Shipping. Rules for the Building and Classification of Steel Ships. 1963. "Transport" Publishing House, 1964.
42. Reznitskiy, L. Ya. Transporting ore in cargo ships. "Morskoy Transport" Publishing House, 1956.
43. Segal', A. I. The strength and stability of ships coverings. Rechtransizdat, 1955.

44. Slezkin, N. A. Dynamics of a viscous incompressible liquid. Gostekh-teoretizdat, 1955.
45. Handbook on the construction mechanics of ships. Vols. 1-3, Sudpromgiz, 1958-1960.
46. Freyental', A., Geyringer, Kh. Mathematical theory of an inelastic unbroken medium. Fizmatgiz, 1962.
47. Kheysin, D. Ye. Bending of an infinite plate with rectangular edges acted on by a local load. "Sudostroyeniye," No. 4, 1962.
48. Kheysin, D. Ye. Determination of contact forces when a ship's stem impacts on ice. Collection "Problems of the Arctic and Antarctic," No. 8, 1961.
49. Kheysin, D. Ye. The non-stationary problem of the oscillations of a finite plate floating on the surface of an ideal liquid. Mechanics and Machine-building. AN SSSR Publishing House, No. 1, 1962.
50. Kheysin, D. Ye. The problem of elastic-plastic bending of ice cover. Collection of Transactions of the AANII, vol. 267. "Transport" Publishing House, 1964.
51. Khoff, N. Longitudinal bending and stability. IL, 1955.
52. Shapiro, G. S. Semi-finite plate on an elastic foundation. PMM, 1949, vol. VII, No. 4.
53. Shimanskiy, Yu. A. Conditional measurements of the ice qualities of ships. Transactions of the ANII, 1938, vol. 130.
54. Shimanskiy, Yu. A. Bending of plates. ONTI, 1934.
55. Shchapov, N. M. The impact of ice floes on installations. Hydraulic Engineering Construction, No. 2, 1933.
56. Jansson, I. E. Icebreakers and their design. European Shipbuilding, No. 5, 6, 1956.
57. Milano, V. Notes on Icebreaker Design. Journal of the American Society of Naval Engineers, 74, No. 1, 1962.
58. Simpson, D. Bow characteristics for icebreaking. Journal of the American Society of Naval Engineers, 48, No. 2, 1936.

TABLE OF CONTENTS

Author's Forward . . . . . 1

SECTION ONE

DETERMINING ICE LOADS WHICH ACT ON A SHIP'S HULL

Chapter I. Navigational Conditions and an Analysis of Interaction between a Ship's Hull and the Ice. . . . . . 5

    1. Classification of Sea Ice and Its Physical and Mechanical Properties . . . . . 5

    2. Sailing Conditions for Ships in Ice. . . . . 9

    3. Interaction between a Ship's Hull and the Ice. . . . . 11

    4. Nature of Ice Cover Strains. . . . . 18

Chapter II. Calculating the Magnitude of Stresses Occurring When A Ship Strikes Ice and During Ice Compression. . . . . . 22

    5. Calculating Momentum and Reduced Masses When a Ship Strikes the Ice. . . . . 22

    6. Contact Stresses When a Ship Strikes a Floating Ice Floe . . . 29

    7. Contact Stresses During Impact of a Ship Against an Ice Floe With a Rounded and an Angular Edge . . . . . 36

    8. Impact of a Ship Against the Edge of an Ice Field. . . . . 40

    9. Relationship of the Magnitude of Contact Stresses to the Length of the Crushing Zone of the Ice . . . . . 50

    10. Impact of a Ship Against Ice, Accompanied by Wedging and a Reverberated Impact. . . . . 53

    11. Magnitude of Stresses Occurring During Ice Compression of a Ship . . . . . 57

Chapter III. Calculating Magnitudes of Design Ice Loads for Main Hull Bracings. . . . . . 64

    12. Loads on Side Framing . . . . . 64

    13. Loads on Shell Plating. . . . . 79

    14. Effect of Hull Shape on the Magnitude of Ice Loads. . . . . 86

Chapter IV. Data on Operational Experience of Ships Under Ice Conditions. Classification of Ships Sailing in Ice. . . . . . 91

    15. Ice Damage to Hull Structures of Icebreakers and Cargo Ships. .91

    16. Comparison of Construction Strength of Ships with Design Ice Loads . . . . . 92

    17. Requirements of Various Shipping Registries for Ice Strengthening of Ships. Proposals for Classifying Ice Ships. . . . . 100

SECTION TWO

CALCULATION OF THE RESISTANCE OF HULL STRUCTURES TO THE  
EFFECT OF ICE LOADS

Chapter V. Strength of Side Plating and Framing. . . . . . 111

18. Designating Scantlings and Determining Ice Belt Plating Thickness. . . . . 111

19. Types of Side Grillages. . . . . 119

20. Side Framing without intersecting braces . . . . . 122

21. Grillage with One Cross Bracing. . . . . 133

22. Grillages With Several Cross Bracings. Method of Elastic Supports. . . . . 149

23. Grillage with Bearer Stringers. . . . . 165

24. Side Framing with a Longitudinal System . . . . . 171

Chapter VI. Strength of Decks and Platforms. . . . . . 177

25. General Requirements for the Design of Decks and Platforms Located in the Area of Ice Load Action. . . . . 177

26. Calculating the Strength and Stability of Deck and Platform Coverings . . . . . 179

27. Designing Decks in the Area of Large Openings . . . . . 187

28. Calculating Ice Deck Beams. . . . . 192

29. Checking Stability of Deck Grillages. . . . . 201

Chapter VII. Transverse Bulkheads, Stems and Sternposts. . . . . . 205

30. Design Loads on Transverse Bulkheads. . . . . 205

31. Flat, Transverse, Bulkheads. . . . . 208

32. Corrugated Bulkheads. . . . . 214

33. Calculating Scantlings of the Stem and Sternpost. . . . . 216

Literature . . . . . 224

UNCLASSIFIED

Security Classification

DOCUMENT CONTROL DATA - R & D

(Security classification of title, body of abstract and indexing annotation must be entered when the overall report is classified)

1. ORIGINATING ACTIVITY (Corporate author) Foreign Science and Technology Center US Army Materiel Command Department of the Army		2a. REPORT SECURITY CLASSIFICATION UNCLASSIFIED	
2b. GROUP			
3. REPORT TITLE STRENGTH OF SHIPS SAILING IN ICE			
4. DESCRIPTIVE NOTES (Type of report and inclusive dates) Translation			
5. AUTHOR(S) (First name, middle initial, last name) Yu. N. Popov, O. V. Faddeyev, D. Ye. Kheysin, A. A. Yakovlev			
6. REPORT DATE 5 February 1969		7a. TOTAL NO. OF PAGES 228	7b. NO. OF REFS N/A
8a. CONTRACT OR GRANT NO. A. PROJECT NO. G. 9223628 2301 4.		9a. ORIGINATOR'S REPORT NUMBER(S) FSTC-HI-23-96-68 9b. OTHER REPORT NUMBER (Any other numbers that may be assigned this report) ACSI Control Number J-4623	
10. DISTRIBUTION STATEMENT Distribution of this document is unlimited.			
11. SUPPLEMENTARY NOTES		12. SPONSORING MILITARY ACTIVITY US Army Foreign Science and Technology Center	
13. ABSTRACT <p>Questions concerned with the theory and calculation of the strength of hull structures of ships sailing in ice are considered. A method for determining the ice loads which act on a ship's hull as a result of navigation conditions, ice strength and characteristics, ship's hull lines, displacement, and speed in the ice, is presented.</p> <p>Basic methods for calculating internal stresses occurring in hull structure elements as a result of ice loads are presented. Questions concerned with rational designs for these structures are considered.</p> <p>The book is intended for design engineers and scientific workers concerned with questions of the strength and design of ships. It can also be used by students and graduate students in the shipbuilding specialties.</p>			

DD FORM 1473

REPLACES DD FORM 1473, 1 JAN 64, WHICH IS OBSOLETE FOR ARMY USE.

UNCLASSIFIED

Security Classification

14. KEY WORDS	LINK A		LINK B		LINK C	
	ROLE	WT	ROLE	WT	ROLE	WT
Ice Sea ice Icebreaker Cargo ship Merchant ship Ship component Ship navigation Marine engineering Shipbuilding engineering Electrical measurement Scientific research Metallurgic research Oceanographic research facility						